AD-A245 055

①

A PRIORI CALCULATION OF THERMODYNAMIC FUNCTIONS

N00123-89-G-0531

DTIC
ELECTE
JAN 24 1992
S B D

DISTRIBUTION STATEMENT A
Approved for public release;
Distribution Unlimited

APPROVED BY
DISSERTATION COMMITTEE:

James E. Boggs

Raymond E Davis

92-01533

92 1 16 117

To
Navy Wives

and
Intruder Crews Who Have Not Returned

DTIC
COPY
INSPECTED
6

Accession For
NTIS GRA&I ☑
DTIC TAB ☐
Unannounced ☐
Justification

By per form 50
Distribution/
Availability Codes
Dist | Avail and/or Special
A-1

A PRIORI CALCULATION OF THERMODYNAMIC FUNCTIONS

by

FLOYD RICHARD CORDELL, B.S., M.A.

DISSERTATION
Presented to the Faculty of the Graduate School of
The University of Texas at Austin
in Partial Fulfillment
for the Degree of
Doctor of Philosophy

THE UNIVERSITY OF TEXAS AT AUSTIN
December 1991

ACKNOWLEDGMENT

This Dissertation has been a constant theme during the last four turbulent years of my life. It was written in diverse places ranging from a stateroom onboard USS Ranger (CV-61) in the Gulf of Oman to an office at the University of Texas. The writing has been interrupted by five aircraft accidents involving friends and one involving me. During the course of these four years, I have received support and encouragement from more friends than I can possibly thank on this page. A constant question from these people has been "What does chemistry have to do with flying airplanes for the Navy?" I have found that despite all their differences, the basics of the two fields are quite similar. In both disciplines, one must first define the problem, develop a hypothesis to solve the problem, and then test the hypothesis. The major difference between chemistry and flying airplanes is in testing the hypothesis. In chemistry, if the hypothesis is wrong, one returns to the laboratory and develops a new hypothesis. In Naval Aviation, if the hypothesis is wrong, one does not have a guaranteed second chance.

This work has been supported by the Robert A. Welch Foundation. A few individuals have contributed greatly to this work. Vickie Sanders is responsible for solving the intricacies of Navy bureaucracy. She found a way to change my orders in August 1985 from Kansas to Texas, without her help this work would have never been started. Jeff Wieringa earns a special thanks for granting me thirty days of leave for final formatting of the Dissertation and preparing for the Oral Defense. In accordance with Murphy's Law, my leave request came in the middle of a paperwork nightmare as we worked to launch the AX aircraft program. The members of my Dissertation Committee deserve a special thanks for their consideration and time. They accepted a very short timeline for the review of a very large Dissertation. My wife, Sandi, and daughters, Rebecca and Elizabeth, have given me all the support I have needed through the last four years. They have been understanding when Dad said, "No, we can't go camping this weekend." They are a source of reassurance whenever I need it.

Dr. Boggs has the heart and soul of a Naval Aviator. He has found solutions to problems during the course of this work that have appeared insurmountable. Without his help and guidance, I would not have been able to start this work, much less finish it. I will miss my close relationship with him and hope he will always experience "Fair Winds and Following Seas."

A PRIORI CALCULATION OF THERMODYNAMIC FUNCTIONS

Publication No. __________

Floyd Richard Cordell, Ph. D.
The University of Texas at Austin, 1991

Supervisor: James E. Boggs

A method for calculating a priori thermodynamic functions (specific heat, entropy, free energy, and enthalpy) from a combination of single determinant ab initio calculations employing the 4-21NO* basis and experimental data is developed and validated. An estimate of the $\hat{r}_e$ geometry is determined by empirically correcting the optimized 4-21NO* ab initio geometry with formulae derived from carefully selected experimental $\hat{r}_e$, $\hat{r}_s$, and $\hat{r}_g$ geometries for errors caused by basis set truncation and neglect of electron correlation. The $\hat{r}_e$ geometry is then used as the reference geometry for the calculation of the ab initio force field by the finite difference method. The Scaled Quantum Mechanical force field is calculated from the ab initio force field using a standard set of scale factors. Fundamental vibration frequencies derived from the Scaled Quantum Mechanical force field usually agree to within 15 cm^{-1} of the corresponding experimental fundamental vibration frequencies. Rotational constants derived from the $\hat{r}_e$ geometry, Scaled Quantum Mechanical fundamental vibration frequencies, and molecular weight are used as inputs for calculating thermodynamic functions via standard statistical mechanic methods, invoking the Born-Oppenheimer and rigid rotor harmonic oscillator approximations. The heat of formation at 0 K, $\hat{E}_0$, is calculated either via a method based on atomic equivalents or a method based on isodesmic reactions. (25) * Thermodynamics,

Test calculations completed for water, benzene, and naphthalene show the a priori thermodynamic functions are similar in accuracy to experimentally derived thermodynamic functions that invoke the Born-Oppenheimer and rigid rotor harmonic oscillator approximations. Optimum ab initio geometries, estimated r_e geometries, rotational potential surfaces, fundamental vibration frequencies and intensities, and a priori thermodynamic functions are determined for the hypothetical molecules (hydroxy-methyl-amino)nitro-methanol, 2,4,6,8-tetraazabicyclo-[3.3.0]octane, and 1,2,3-oxadiazolo-1,2,3-oxadiazole-1,1-dioxide.

* Geometries, * Finite difference theory

Table of Contents

Acknowledgment........iv
Abstract........v
Table of Contents........vi
Chapter One........1
Chapter Two........5
Chapter Three........27
Chapter Four........41
Chapter Five........75
Chapter Six........84
Chapter Seven........99
Chapter Eight........146
Chapter Nine........195
Chapter Ten........207
Bibliography........210
Vita........216

CHAPTER ONE

INTRODUCTION

The United States Navy supports an active energetic materials research program with the basic goals of developing a better understanding of detonation processes and of developing explosives that are more efficient and more stable than current explosives. Warhead size, magazine storage limitations, survivability, and aircraft performance are the driving factors behind this development of improved explosives. Existing warheads can be improved only by developing more energetic explosives or explosives that are higher in density than current explosives.

Improving warhead performance by simply increasing the size of the warhead is not feasible for several reasons. First, the cost of replacing every existing warhead with a new larger warhead is prohibitive. Second, ships and many shore bases have limited magazine storage and, consequently, they could only store a smaller number of the larger warheads limiting their ability to sustain the fight in combat. Additionally, the magazines would be storing the same total amount of explosive power, even though each individual warhead is larger and more effective. Third, in some weapon systems, most notably guns, physical constraints prohibit increasing warhead size without an expensive rework of the entire weapon system. As a result of these factors, improvements in warhead performance are being sought through improvements in the efficiency of the explosive or by increasing the density of the explosive.

A second goal of the Navy's program is the development of insensitive or "safe" munitions to improve a ship's chances of surviving combat damage or a fire in a weapon's magazine. Experiences in the Falklands Campaign, the Persian Gulf, and numerous shipboard fires have shown that enemy weapons are not always the major cause of damage to a ship. Weapons stored in a ship's magazine occasionally detonate if they are hit by an enemy weapon or if they are involved in a fire. Both situations are bad; one does not want to successfully survive the wounds inflicted by the enemy or by a fire only to have his ship sink because his own weapons detonate. The Navy is addressing these problems through a combination of technological improvements, e.g. a thermal fuse that detects the temperature rise associated with a fire and destroys the integrity of the warhead to prevent a high order detonation, and the development of shock insensitive and heat tolerant explosives.

The third goal of the Navy's research program is to improve aircraft and ship survivability by developing more efficient explosives. Fewer weapons are required to destroy any given target if the warhead is more efficient. As a result, fewer aircraft need be exposed to hostile fire or each aircraft may be loaded with fewer weapons which results in improved aerodynamic performance and improved ability to avoid enemy fire. Additionally, ships will spend less time in the range of a hostile force while engaging any given target. All of these situations result in an increased probability of mission survival.

Unfortunately, the development of new explosives is a long and demanding process with no guarantee of success. This study develops a formalism for the calculation of a priori molecular thermodynamic functions to help experimentalists more carefully evaluate potential explosive compounds.

Thermodynamic functions provide a variety of useful data about a substance including its entropy, specific heat, heat of formation and free energy of formation [1,2]. By combining the thermodynamic functions of substances involved in a reaction, we may determine the reaction's equilibrium constant, change in entropy (ΔS), heat of reaction (ΔH) and free energy of reaction (ΔG or ΔA). If we determine molecular thermodynamic functions over a temperature range, we may easily calculate the effect temperature changes have on a given reaction. The usefulness of thermodynamic functions is limited, however, because they apply only to equilibrium processes and give no data concerning a reaction's kinetics [1].

Thermodynamic functions are usually determined by experiment or calculated from statistical mechanics. Experimentally determining a complete set of thermodynamic functions over a wide temperature range is a difficult and time-consuming task. By invoking the Born-Oppenheimer and rigid-rotor harmonic oscillator approximations, statistical mechanics reduces the effort required to determine a complete set of thermodynamic functions for many substances [2]. For temperatures less than 1500 K, statistical mechanic thermodynamic functions usually agree with experimentally derived thermodynamic functions to an accuracy of 5 per cent .

The statistical mechanical calculation of molecular thermodynamic functions requires the following data [2]:

(1) The molecular weight.

(2) The molecular rotational constants.

(3) The molecular fundamental vibration frequencies.

(4) The molecular electronic energy levels.

For relatively small, stable molecules experimentally determining the above data is a manageable task. For molecules larger than about 12 atoms or for unstable molecules, accurately determining the above data, particularly the vibrational frequencies and rotational constants, becomes increasingly difficult. For hypothetical molecules, it is, quite obviously, impossible to determine the above data experimentally.

In this dissertation we examine the feasibility of calculating the data required to determine statistical mechanic thermodynamic functions from single determinant ab initio calculations combined with limited experimental data. This study places emphasis on the calculation of the rotational and vibrational partition functions from the rotational constants and fundamental vibration frequencies because of their large contribution to the molecular partition function and due to the difficulty encountered in determining these quantities experimentally. The goal of this study is the calculation of a priori thermodynamic functions that agree within 2 per cent of current tabulations of thermodynamic functions that employ the rigid rotor harmonic oscillator approximations; see for example the JANAF tables [3].

Chapter Two opens with a review of statistical mechanic partition functions and then describes transformation of the partition function into a set of equations that determine the entropy, specific heat, enthalpy, and free energy. The second half of Chapter Two describes how one may calculate the data required by the statistical mechanic formalism from a careful combination of limited experimental data and ab initio theory and reviews methods of accurately calculating molecular rotation constants and fundamental vibration frequencies. Chapter Two closes with a description of how one may change the theoretical energy zero point, isolated nuclei and electrons, to the more common experimental definition, an element in its standard state at a given temperature.

Chapters Three and Four develop the basis set scaling factors required for the accurate calculation of bond lengths and vibrational frequencies. Scale factors are developed for two versions of the 4-21NO* basis set, described in Chapter Two. Chapter Three presents the equations required to convert ab initio bond lengths to an approximation of the equilibrium, r_e, bond length. Chapter Four presents the scale factors required by the Scaled Quantum Mechanical Force Field formalism [4] for the 4-21NO* basis set. Chapter

Five describes a set of empirical atomic energy equivalents for the 4-21NO* basis set that may be used to calculate the heat of formation at 298 K from the calculated ab initio energy.

Chapter Six puts all the pieces together and tests the method for the molecules; water, benzene, and naphthalene. Fortunately, the test calculations are successful and Chapters Seven, Eight, and Nine apply the method to the hypothetical molecules (hydroxy, methyl, amino)nitro-methanol, 2,4,6,8-tetraaza-bicyclo[3.3.0]octane and 1,2,3-dioxy-1,2,3-dioxane. These molecules were suggested for study by researchers at the Naval Surface Weapons Center, White Oak in support of the United States Navy's energetic materials research program. Chapter Ten closes this work with a brief summary and offers suggestions for improving the model and for future research.

CHAPTER TWO

In this chapter, we develop a formalism for the a priori calculation of statistical mechanic thermodynamic functions. The method is not an ab initio method because carefully chosen, limited experimental data are combined with results from ab initio calculations to produce the final answer. The method described below provides results that are compatible with existing tabulations of thermodynamic functions [3,5,6] and that agree with experimentally derived values to within two per cent over the temperature range 300 K to 1500 K.

This chapter starts with a review of the statistical mechanic partition function. This review emphasizes the approximations used to obtain a working equation for the partition function and the limitations caused by invoking these approximations. More comprehensive and complete derivations of the equations presented later in this chapter are available in most statistical mechanic textbooks, see for example references 2, 7, and 8. Next we derive relatively simple expressions for the enthalpy, free energy, entropy and specific heat of a molecule and find that these equations require only a few molecular constants [2]. In the second section of this chapter we transform the equations derived in section one into more useful forms. The partition function is split into two parts; one part is defined entirely by our choice of zero energy and the other part defined by terms independent of the definition of zero energy.

The third section of this chapter reviews ab initio calculations. It is purposely not a review of ab initio theory. Our primary interest is not the derivation of the Hartree-Fock equations or the efficient implementation of these equations in a modern program, but rather what limitations we must accept at a chosen level of theory. A complete derivation of the Hartree-Fock equations is given by Szabo and Ostlund [9]. A description of the efficient implementation of the Hartree-Fock equations has been provided by Pople [10].

The fourth section of this chapter describes a method for obtaining an estimate of the equilibrium geometry from the ab initio geometry. The equilibrium geometry is used to calculate molecular rotational constants and is required as part of the Scaled Quantum Mechanical Force Field formalism [4,11], the subject of section five.

Throughout this work we encounter several different definitions of zero energy. The heat of formation at 0 K is the usual definition used in tables of thermodynamic functions [3,5,6] and Chapter Two closes with a discussion of two methods that may be used to calculate the heat of formation at 0 K from ab initio energies.

REVIEW OF STATISTICAL MECHANICS

The statistical mechanic partition function provides a simple but powerful method for calculating thermodynamic functions. This review of the equations and approximations used to obtain a working set of mathematical formulae for various thermodynamic quantities is taken primarily from McQuarrie's text [2]. We start by reviewing the partition function and then invoke a series of approximations to derive workable equations defining free energy, enthalpy, entropy and specific heat.

The partition function is similar to the quantum mechanical wave function in many respects. It is the basic entity of statistical thermodynamics and contains all of the information we can determine about any given system. One may define several different partition functions by fixing different external variables and one usually chooses to work with a particular partition function for mathematical convenience [2]. For example, the grand canonical partition function is defined by fixing the volume, temperature and chemical potential of the system. In this study we deal with the canonical partition function which fixes the number of molecules in the system, the volume of the system and the temperature of the system.

The canonical partition function is defined either by equation 2-1 or equation 2-2. In the following discussion "Q" refers to the partition function for the entire system, or ensemble, while "q" refers to the partition function for a single molecule or single element of the ensemble. The sum in equation 2-1 runs over all quantum states available to the system. Equation 2-2, the classical definition of the partition function, is derived assuming the particles are identical and indistinguishable. We will apply this assumption to equation 2-1 after we transform it to a more manageable form. Equation 2-1 is the usual starting point for the derivations described below.

$$Q(N,V,T)=\Sigma_j \exp(-E_j\,(N,V)/kT) \tag{2-1}$$

$$Q=1/N!h^{SN} \iint \exp(-H(p,q)/kT)\, dp\, dq \tag{2-2}$$

E_j the eigenvalue associated with quantum state j

N the number of molecules in the system.

$H(p,q)$ the classical hamiltonian for the system.

s the number of degrees of freedom

p the generalized momenta for the system.

q the generalized coordinates, conjugate to q, for the system.

k Boltzmann constant.

T temperature

We begin transforming equation 2-1 by finding the probability that the system occupies any arbitrary eigenstate, j, as shown in equation 2-3 and then invoke the Gibbs postulate, which states that the observed, or mechanical, value of some parameter equals the sum over all states of the probability that an eigenstate is occupied times the eigenvalue, as shown in equation 2-4 for the energy of an ensemble. Applying the Gibbs postulate and some mathematical manipulation leads to the following equations for energy (2-5), Helmholtz free energy (2-6), pressure (2-7) and entropy (2-8). Readers interested in a complete derivation of these equations should refer to Chapter 2 of reference [2].

$$P_j=\exp(E_j/kT)/Q \tag{2-3}$$

$$<E>=\Sigma_j E_j \exp(-E_j /kT)/Q=\Sigma_j E_j P_j \tag{2-4}$$

$$E=kT^2(\partial \ln(Q)/\partial T)_{N,V} \tag{2-5}$$

$$A=-kT \ln(Q) \tag{2-6}$$

$$p=kT(\partial \ln(Q)/\partial V)_{N,T} \tag{2-7}$$

$$S=kT(\partial \ln(Q)/\partial T)_{N,V} + k \ln(Q) \tag{2-8}$$

E_j the eigenvalue associated with eigenstate j.

Q the partition function.

k Boltzmann constant.

T the temperature.

Conceptually, equations (2-5) through (2-8) offer an easy method for calculating thermodynamic data. One simply determines Q, performs some relatively easy math and out pops a useful result. Unfortunately determining Q is rather difficult. The sum in equation (2-1) runs over all quantum states available to the system and, as a result, the sum is normally open ended and can not be solved analytically. At this point we are forced to leave the well defined world of mathematical theory and enter the more interesting world of chemically meaningful approximations.

The first two approximations we invoke are the ideal gas [2] and Born-Oppenheimer [12] approximations, which allow us to make several simplifying assumptions. The ideal gas approximation assumes the molecules do not interact with one another and is very accurate for gas phase monomers above room temperature and at pressures below 1 atmosphere. We may write the partition function as shown in equation 2-9, assuming the molecules are independent and identical. The system partition function is now written as a product of single molecule partition functions divided by a factor that compensates for overcounting identical states. Equation 2-9 represents a great reduction in our work, we now need only calculate the partition function for a single molecule instead of the entire ensemble.

$$Q(N,V,T)=q(N,V,T)^N/N! \qquad (2\text{-}9)$$

Q the system partition function.

q the partition function for a single molecule.

N the number of molecules in the system.

The Born-Oppenheimer, or adiabatic, approximation [12] allows separation of the molecular partition function and Hamiltonian into smaller, easier to solve parts and assumes the electrons move much faster than nuclei. Within this approximation the Hamiltonian separates into two parts; one part describes the motion of the electrons in the field generated by fixed nuclei, while the other part describes the motion of the nuclei over the electronic potential surface. The electronic potential surface is calculated by fixing the nuclei at several different positions, solving the electronic Schrodinger equation at each point and fitting the resulting table of values to a mathematical equation [12].

The equations describing the motion of the nuclei are further simplified by dividing the motion into two parts, the translational motion of the center of mass and the internal motion of the molecule [2]. The molecular partition function then can be separated into the two products shown in equation 2-10. The translational energy levels of the molecule define the first term, q(trans), while the rotational, vibrational, electronic and nuclear energy levels of the molecule define the second product, q(int).

$$q=q(trans)^{*}q(int) \tag{2-10}$$

Calculating q(trans) is easily completed assuming the translational energy levels are equal to the energy levels defined by a particle in a box [2]. These energy levels are very closely spaced and the partition function sum may be converted to an integral without loss of accuracy. The resulting integral may be solved analytically with the result shown as equation 2-11, which shows that q(trans) depends only on the molecular mass, volume and temperature.

$$q(trans)=(2\pi kMT/h^2)^{3/2}V \tag{2-11}$$

M the molecular mass.
T the temperature.
V the volume.

We have taken the ideal gas and Born-Oppenheimer approximations as far as we can and must use several more approximations to obtain a more tractable form of q(int). The next approximation assumes the electronic and nuclear partition functions are separable from the rotation-vibration partition function to give equation 2-12. For most molecules this is an excellent approximation.

$$q=q(trans)^{*}q(elec)^{*}q(nuc)^{*}q(rot\text{-}vib) \tag{2-12}$$

The electronic, q(elec), and nuclear, q(nuc), partition functions are easily calculated by modifying equation 2-1 from a sum over energy levels to a sum over energy states as shown in equation 2-13. The spacing of electronic energy levels is usually very large [2], 1 electron volt or more, and as a result the excited electronic states do not make a significant contribution to the molecular partition function. In this case, the sum defined in equation 2-13 converges rapidly. Defining the dissociation energy, D_e, of the ground state equal to zero and expanding the sum in equation 2-13 yields equation 2-14. If the energy difference between the ground state and the first excited state is greater than 15 kcal/mol (0.65 eV.), the contribution of the second term is less than 0.65% and equation 2-14 may be truncated after the first term. The electronic partition then reduces to the degeneracy of the ground state; if the molecule is a ground state singlet q(elec) equals one.

$$q(elec)=\Sigma_i d_i \exp(-E_i/kT) \qquad (2\text{-}13)$$

$$q(elec)=d_1+d_2\exp(F_2/kT)+ d_3\exp(F_3/kT)+ \cdots \qquad (2\text{-}14)$$

d_i the degeneracy of state i

E_i the energy of state i

F_i the energy difference between level i and the ground state.

Calculating q(nuc) is exactly analogous to calculating q(elec). The spacing of nuclear energy levels is much larger than the spacing of electronic energy levels, on the order of several million electron volts [2]. From the discussion just presented on the electronic partition function, one may quickly conclude that only the first term of equation 2-14, the degeneracy of the nuclear ground state, is important. We can simplify the nuclear partition function further by recognizing that the nature of the nuclear states is not changed in most chemical reactions. The nuclear partition function thus only contributes a constant term to the system partition function that cancels during the calculation of thermodynamic properties. For convenience, the nuclear partition function is traditionally assigned a value of one.

Although the above paragraph indicates the nuclear partition function is benign, in some cases it couples with the rotational partition function and the symmetry of the nuclear wave function must be considered. Readers interested in a thorough discussion of the coupling between the rotational and nuclear partition functions are referred to section 6-5 of reference 2.

The molecular partition function is now completely separated except for the rotation-vibration partition function. Solving the coupled rotation-vibration hamiltonian or partition function is extremely difficult [12,13,14]. The rigid-rotor harmonic oscillator approximation [13] allows complete separation of the molecular partition function [2]. The rigid-rotor harmonic oscillator approximation assumes that the rotational constants do not change as the molecule vibrates in a quadratic vibrational potential well and leads to simple expressions for the rotational and vibrational partition functions.

The rotational energy levels are determined by the molecular moments of inertia. Although the energy levels for linear, symmetric and spherical rotors are defined by simple equations, the energy levels for an asymmetric rotor are more complex [13,14]. The equations defining the energy levels of the various types of rotors are not given here and readers interested in these equations should see references 13 and 14. Defining tne rotational partition function with equation 2-14, assuming high temperature and converting the sum to an integral leads to equation 2-15 as the high temperature limit for the asymmetric rotor partition function. The spherical and symmetric rotor partition functions are obtained from equation 2-15 by recognizing that all three rotational constants are equal for the spherical rotor and that two rotational constants are equal for the symmetric rotor. The high temperature linear rotor partition function is defined by equation 2-16. Group theory gives the rotational symmetry number as the sum of the characters of the pure rotational sub-group of the molecular point group. The rotational partition function is determined by molecular rotational constants, or equivalently by the moments of inertia, which may be determined experimentally from the microwave spectrum or calculated from the molecular structure.

$$q(rot)=\pi^{1/2}/s(T^3/\theta_a\theta_b\theta_c) \tag{2-15}$$

$$q(lin)=T/(s\theta_r) \tag{2-16}$$

$q(rot)$ the non-linear rotational partition function.

$q(lin)$ the linear rotor partition function

s the rotational symmetry number.

θ_i the characteristic temperature of rotation about axis i

$= h^2/(8\pi^2 I_i k) = Z_i ch/(\pi k)$.

I_i the moment of inertia about axis i

Z_i the observed rotational constant in cm^{-1}

Equations 2-15 and 2-16 are those given in most references on statistical mechanics, see for example [2,7,8], and in the JANAF tables [3]. Levine has recently pointed out that these two equations contain a small error [16] and lead to rotational energies that are incorrect by a small constant factor. For simplicity, we will examine this problem for the linear rotor. The definition of the linear rotor partition function is given by equation 2-17. By converting the sum in equation 2-17 to an integral, one obtains equation 2-16. Applying the Euler-MacLaurin summation formula to equation 2-17 yields a more accurate rotational partition function [2,16], equation 2-18. The high temperature limit of equation 2-18 is the same as equation 2-16 except for the addition of the constant term $\theta_r/3$.

$$q(\text{lin})=\Sigma_J(2J+1)\exp(-BJ(J+1)/kT) \qquad (2\text{-}17)$$

J the rotational quantum number

B the rotational constant

$$q(\text{lin})=T/(s\theta_r)(1+\theta_r/3T+\theta_r^2/15T^2+4\theta_r^3/315T^3+\cdots) \qquad (2\text{-}18)$$

We are now at the crux of the problem pointed out by Levine. If we calculate the high temperature limit of equation 2-18 and then calculate the rotational energy according to equation 2-5, the equipartition value, RT, is obtained. If, however, we calculate the rotational energy by substituting equation 2-18 into equation 2-5, obtaining equation 2-19, and then calculate the high temperature limit, we obtain equation 2-20 as a better approximation to the rotational energy [2,16]. This improved estimate of the high temperature limit of the rotational energy differs from the traditionally given equipartition value by $-\theta_r{}^*R/3$. For light molecules this value may be significant, it is 30 cal/mole for $\theta_r=45$. The molecules studied in this work have θ_r less than 5 and the error induced by using equation 2-16 instead of asymmetric rotor equivalent to equation 2-20 is less than 3 cal/mole.

$$E(\text{lin})=R(T-\theta_r/3-\theta_r^2/45T-\cdots) \qquad (2\text{-}19)$$

$$\lim_{T\to\infty} E(\text{lin})=R(T-\theta_r/3) \qquad (2\text{-}20)$$

The vibrational partition function may be evaluated analytically under the harmonic oscillator approximation. Equation 2-21 defines the vibration partition function which depends only on the fundamental vibrational frequencies. Experimentally determining a complete set of fundamental frequencies is a difficult and time consuming task for many molecules and is impossible for hypothetical molecules. The harmonic oscillator approximation breaks down above about 1500 K because anharmonic effects begin to make significant contributions to the vibrational energy.

$$q(vib)=\exp\left(-\sum_{j=1}^{3N-6}(n_j+1/2)h\nu_j/kT\right) \qquad (2\text{-}21)$$

$$=\prod_{j=1}^{3N-6}\exp(-h\nu_j/2kT)/(1-\exp(-h\nu_j/kT))$$

n_j the vibrational quantum number

ν_j the fundamental vibration frequency for the jth mode.

We have defined all of the contributions to the molecular partition function. The system partition function is given by equation 2-9 and the individual parts of the molecular partition function are given by equations 2-11 (translation), 2-14 (electronic), 2-15 (rotation) and 2-21 (vibration). In this work the nuclear partition function is assumed equal to 1 and the electronic partition function is truncated after the first term. Substituting these definitions into equations 2-5, 2-6 and 2-8 gives equations for energy (equation 2-22), Helmholtz free energy (equation 2-23) and entropy (equation 2-24). The specific heat is calculated by taking the derivative of the energy with respect to temperature, as shown in equation 2-25. Equations 2-22 through 2-25 assume the molecule is not linear and is an asymmetric rotor.

$$E=RT\{3/2+3/2+\sum_{j=1}^{3N-6}[(\theta_{vj}/2T+(\theta_{vj}/T)/(\exp(\theta_{vj}/T)-1)]-D_e/kT\} \qquad (2\text{-}22)$$

$$-A=RT\{\ln[(2\pi MkT/h^2)^{3/2}Ve/N]+\ln[\pi^{1/2}/s(T^3/\theta_a\theta_b\theta_c)^{1/2}]$$

$$-\sum_{j=1}^{3N-6}[\theta_{vj}/2T+\ln(1-\exp(-\theta_{vj}/T)]+D_e/kT+\ln(w_{e1})\} \qquad (2\text{-}23)$$

$$S=R\{\ln[(2\pi MkT/h^2]^{3/2}Ve^{5/2}/N] + \ln[\, pi^{1/2}e^{3/2}/s(T^3/\theta_a\theta_b\theta_c)^{1/2}] + \sum_{j=1}^{3N-6}[(\theta_{vj}/T)/(\exp(-\theta_{vj}/T)-1)-\ln(1-\exp(-\theta_{vj}/T))]+\ln(w_{e1})\} \tag{2-24}$$

$$C_v=R\{3/2+3/2+\sum_{j=1}^{3N-6}[(\theta_{vj}/T)^2(\exp(\theta_{vj}/T)/(\exp(\theta_{vj}/T)-1)^2]\} \tag{2-25}$$

R	the gas constant.
T	the temperature in Kelvin.
k	Boltzmann constant.
h	Plank constant.
M	the molecular weight.
D_e	the dissociation energy.
w_{e1}	the degeneracy of the electronic ground state.
θ_{vj}	vibration characteristic temperature.
$= h\nu_j/k$	ν_j the fundamental vibration frequency.
θ_i	i=a,b,c the rotation characteristic temperature defined in equation 2-15.
s	the rotational symmetry number.
V	the volume.

Equations 2-22 through 2-25 provide an easy method for calculating the energy, free energy, entropy and specific heat of a molecule from its molecular weight, electronic ground state degeneracy, moments of inertia and fundamental vibrational frequencies.

TRANSFORMING THE PARTITION FUNCTION

In the preceding section we derived the system partition function and equations for various thermodynamic quantities using the ideal gas, Born-Oppenheimer, rigid rotor and harmonic oscillator approximations. This derivation assumed zero energy occurs at the bottom of the electronic potential surface, as shown in Figure 2-1. While this is a convenient choice for deriving equations 2-22 through 2-25, different definitions of zero energy are more appropriate for experimental and theoretical studies. Transforming equations 2-22 through 2-25 to forms compatible with any arbitrary definition of zero energy permits the selection of any energy frame of reference.

The first step in transforming the partition function is separating the terms in the electronic and vibrational partition functions that are dependent on the definition of zero energy, the "external" terms, from the terms that are independent of zero energy, the "internal" terms. In the above derivation the electronic energy of the ground state was zero by definition, allowing us to simplify equation 2-14. Equation 2-26 is a more correct version of equation 2-14, the E_0 term is defined by the selection of zero energy and "scales" the electronic partition function to any arbitrary reference point.

$$q(elec)=\exp(-E_0/kT)(d_1 + d_2 \exp(E_2/kT)+ \cdots) \qquad (2\text{-}26)$$

E_0 an energy scaling factor.
d_i the degeneracy of state i.
E_i the energy difference between the ground state and state i.

$$q(molecule)=q^0 \exp(-E_0/kT) \qquad (2\text{-}27)$$

q^0 the "internal" molecular partition function to be defined later.
E^0 the energy scaling term.

For the vibrational partition function, the vibrational zero point energy, $\Sigma_i hg_i v_i/2$ (g_i is the degeneracy of state i), is calculated relative to the bottom of the electronic potential well. This constant term will always be present and it is normally factored out of the vibrational partition function and combined with the electronic scaling term [2]. Equation 2-27 is an alternative definition of the system partition function incorporating the energy scaling term. Figure 2-1 shows two common definitions for the energy scaling term. D_e is the usual theoretical definition; zero energy occurs when the nuclei are separated by an infinite distance. D_0, equal to D_e plus the vibrational zero point energy, is the usual experimental definition of zero energy. D_0 may be measured directly in an electronic dissociation experiment.

Combining equation 2-27 with the definition of chemical potential leads to the equations that are commonly used to determine thermodynamic tables [2]. Readers interested in complete derivations of the following equations should refer to Chapter 9 of reference [2]. The quantities normally presented in thermodynamic tables are free energy ($(G_0\text{-}E_0)/T$), enthalpy ($(H_0\text{-}E_0)/T$), entropy (S), and specific heat (C_v or C_p). In this work the pressure is restricted to one atmosphere. E_0 refers to any definition of the zero energy, but it is conventionally defined to be zero for the elements at 0 K when they are in their 298 K standard states. $(G_0\text{-}E_0)/T$, equation 2-28, and $(H_0\text{-}E_0)/T$, equation 2-29, are usually tabulated instead of $G_0\text{-}E_0$ and $H_0\text{-}E_0$ to give a "smoother" function for interpolation. Entropy is calculated via equation 2-24 and specific heat is calculated via equation 2-25.

$$(G_0\text{-}E_0)/T = R\ln\{(q^0/V)kT/1.01 * 10^6\} \qquad (2\text{-}28)$$

$$q^0 = (2\pi mkT/h^2)^{1.5}(T^3/\theta_a\theta_b\theta_c)^{0.5}[\sum_{j=1}^{3N-6}(1-\exp(-\theta_{vj}/T)^{-1}]$$

$$(H_0\text{-}E_0)/T = (G_0\text{-}E_0)/T+S \qquad (2\text{-}29)$$

S = the entropy calculated in equation 2-24.

REVIEW OF AB INITIO CALCULATIONS

Quantum chemistry has grown rapidly over the past 25 years. Theoretical chemists have developed a vast array of methods ranging from simple semi-empirical methods to complex multi-reference state configuration interaction methods that may be used to solve any given problem. Advances in computer technology, compilers and hardware, have complemented algorithm development and allow us to either use advanced methods on small molecules or to perform simpler calculations on "large" molecules, 15 to 20 non-hydrogen atoms.

As a result of these developments, the first step in any modern theoretical calculation is selecting the appropriate method for the problem. A compromise between the computational cost and the desired accuracy must be achieved. Before discussing the relative merits of different theoretical methods, we should closely examine what data we want to determine and the desired level of accuracy; remembering that the goal of this study is the calculation of a priori thermodynamic functions to an accuracy within two per cent of experimentally derived values.

The electronic partition function is calculated from the energy differences between the molecular ground state and various excited states. Advanced theoretical methods that include electron correlation effects can accurately determine these energy differences, but usually require at least two times the CPU time used in a closed shell Restricted Hartree-Fock calculation. In this study the electronic partition function is assumed equal to the degeneracy of the ground state, as discussed earlier, for the following reasons:

1. The advanced theoretical methods required to calculate excited state energies are too costly for the molecules of the size studied in Chapters 7, 8 and 9.

2. The contribution of excited electronic states to the system partition function is usually much less than one per cent.

The rotational partition function is inversely proportional to the molecular rotational constants. For the experimental ground state microwave spectroscopy easily determines these values to an accuracy of 1 part in 10^9 [13,14]. Expecting this level of accuracy from any theoretical calculation is unrealistic. Fortunately, an accuracy of one per cent is quite acceptable and this accuracy may be achieved at a modest theoretical level using an empirical correction technique described later in this Chapter.

The vibrational partition function is directly proportional to the fundamental frequencies of vibration. The accurate theoretical calculation of vibration frequencies is the subject of an intensive research effort. For small molecules one may calculate ab initio frequencies that are within 20 cm^{-1} of experimental frequencies by optimizing the geometry with a method that includes electron correlation effects calculated at a minimum level of fourth order perturbation theory, MP4, and by performing eighth order fits to the potential energy surface [17,18]. The size of the molecules examined in this study precludes using this very sophisticated and costly theoretical method. Fortunately the Scaled Quantum Mechanical Force Field method [4,11,19], which combines theoretical and experimental data, determines vibrational frequencies that are accurate enough for the calculation of thermodynamic data.

Before describing exactly how the above data are calculated in this work, we must first define the theoretical model. The molecules studied in this work contain up to 10 non-hydrogen atoms and, in general, are not symmetric. Configuration interaction methods are too costly for use on molecules of this size and, therefore, we must choose between Hartree-Fock and semi-empirical methods. Semi-empirical and Hartree-Fock calculations do not accurately determine absolute values for structural parameters, such as bond lengths, or molecular energies. They do, however, determine accurate relative values for many structural parameters and molecular energies.

CNDO calculations [20], the least expensive method considered in this work, are very sensitive to the selection of parameterization criteria. Generally, CNDO calculations determine qualitative, but not quantitative, relative values. The CNDO method is not accurate enough for our purposes.

The next step up in sophistication is the MNDO methods [21]. Again these calculations are sensitive to the selection of parameterization criteria. If the molecules selected for parameterization are chemically "close" to the molecules under study, the various MNDO methods usually determine reasonable values for relative bond lengths and molecular energies. The MNDO method does not determine relative values for vibration frequencies to the accuracy required for this work [23] and this is a fatal flaw.

We have now eliminated all methods except closed shell Restricted Hartree-Fock theory [9]. In earlier work, our group has developed the concept of the basis set offset [23,24], the difference between the calculated value of some molecular parameter and its experimental value, which is assumed to be very close to the equilibrium value. If we select a basis set that produces results with a constant basis set offset, then it is a simple matter to correct the calculated values and obtain an estimate of the experimental value. Experience indicates that split valence shell basis sets, for example Pople's 3-21G [25] or Pang's 4-21 [24], produce a constant basis set offset for most bond lengths, many bond angles and determine accurate relative energies [26]. Recent work has shown that polarization functions, commonly referred to as d functions, should be added to the basis set to accurately describe bond angles around oxygen and nitrogen and to obtain accurate torsion angles [27,28].

In this work the single determinant ab initio gradient program TEXAS [29] is used with the 4-21NO* basis set unless specifically stated otherwise. Although this basis set is not balanced, for most molecules it offers performance comparable to the 6-31G* [30] basis set at about one-third the cost. The 4-21NO* basis set is Pang's 4-21 basis set [24] augmented with polarization functions on nitrogen and oxygen. A thorough review of the strengths and weaknesses of this basis set has been previously presented [27]. Two versions of the TEXAS program were used while completing this work. The original version defines d functions as linear combinations of displaced p functions, as suggested by Pulay [29]. The newer version of TEXAS uses true d functions. The d orbital exponent is fixed at 0.8 in all cases.

The gradient method [31] was used to optimize all structures reported in this work. A structure is considered optimized when the following criteria are met:

1. Internal forces are less than 0.005 mdyne for "stiff" modes, bond lengths and most bond angles.
2. Bond lengths change by less than 0.002 Å.
3. Bond angles change by less than 0.2°.
4. Internal forces are less than 0.001 mdyne for "loose" modes, torsions and out-of-plane deformation angles.
5. Torsion and out-of-plane angles change by less than 2°.
6. "Loose" mode forces have changed sign.

Optimizing the "stiff" modes past the above points is often a waste of computer time because the structure is not changing in a significant manner. Failing to optimize the "loose" modes as described above may produce an "optimized" structure that is qualitatively incorrect. Small changes in the force of a loose mode may cause unexpectedly large changes in other coordinates.

A PRIORI CALCULATION OF ROTATIONAL CONSTANTS

Rotational constants are easily calculated with the traditional principal axis coordinate method after correcting the ab initio structure for the basis set offset. In Chapter Four the 4-21NO* basis set offset correction factors are derived for CC, CN, CO, NO, NN, CH, OH, and NH bond lengths. Correcting the ab initio structure is a controversial step and many theoreticians argue against it. The basis set offset, however, is an inherent error caused by using a particular basis set and is similar to the instrument error encountered during an experiment. Calculating an accurate estimate of the equilibrium structure is absolutely critical if we are to have any hope of calculating rotational constants to an accuracy of 1 or 2 per cent. For this work a modified version of Møllendal's MB06 program [32] was used to determine the principal axis coordinates, the moments of inertia, and the rotational constants.

A PRIORI CALCULATION OF VIBRATION FREQUENCIES

Ab initio calculations generally overestimate diagonal force constants by 10-30 per cent resulting in fundamental frequencies that are 5-15 per cent higher than the corresponding experimental frequencies [4]. The off-diagonal elements are usually as accurate as experimental values with the basis sets used in this study. Blom [11] and Pulay [4,19] noted that the error in the calculated vibration frequencies and diagonal force constants is reasonably constant and proposed scaling the ab initio force field to give a Scaled Quantum Mechanical Force Field which accurately reproduces experimental fundamental vibration frequencies. Accurate theoretical calculation of vibration frequencies without reference to experimental data is possible, but the cost is prohibitively high as previously discussed. The following review of the Scaled Quantum Mechanical Force Field formalism parallels Pulay's review of the method [4].

The Scaled Quantum Mechanical (SQM) Force Field formalism is conveniently divided into a series of steps each of which is discussed below:

1. Determine a reference geometry, usually an estimate of the *equilibrium* structure.
2. Determine the ab initio force field.
3. Scale the ab initio force field.
4. Calculate the fundamental vibration frequencies and, if desired, IR and Raman intensities.

The choice of the reference geometry for calculation of the force field is the most controversial step in the SQM formalism. One may choose to use either the optimized ab initio geometry or the optimized ab initio geometry corrected for the basis set offset. The proponents of using the ab initio structure point out that the first derivative of the energy, the second term in equation 2-30, is zero by calculation at this geometry [10].

$$V=V_0 +(r-R_{eq})d/dx_i + 1/2(r-R_{eq})^2d^2/dx_idx_j +1/6(r-R_{eq})d^3/dx_idx_j\,dx_k + \cdots \qquad (2\text{-}30)$$

R_{eq} the equilibrium position of some coordinate.

r the instantaneous position of some coordinate.

$$f_2(r)-F_2(R)=f_2(R)-F_2(R)+(r-R)F_3(R)+\cdots \qquad (2\text{-}31)$$

f_2 and F_2 are quadratic force constants at bond lengths of r and R.

F_3 is the cubic force constant at R.

The problem with this argument is simply that our goal is not to calculate ab initio frequencies, but rather to calculate frequencies that are directly comparable to experimentally derived frequencies. At the true equilibrium geometry the first derivative of the energy, the second term in equation (2-30), is zero by definition. Additionally we want to minimize the error in the second derivative, the harmonic force constant, and desire transferable scale factors. Pulay has shown the difference in the stretching force constant [4] of a diatomic molecule is given by equation (2-31) for two different geometries or two different theoretical models. Equation (2-31) shows the error in the force constant has two major components. The first two terms describe the error in the force constant, or the curvature of the potential surface, a scale factor corrects this error. The third term is the error due to expanding the potential surface about a non-equilibrium geometry. The presence of the linear r-R factor makes the scale factor dependent on bond length and limits the transferability of the scale factor.

Throughout this study the force field is defined with Pulay's recommended internal coordinates [4,24]. These coordinates have two important advantages over other definitions of the internal coordinates. First Pulay's internal coordinates tend to minimize the off-diagonal elements in the force field matrix reducing the numerical error in the calculated frequencies [5]. Second Pulay's internal coordinates are chemically meaningful, i.e. bond lengths, bending and wagging deformations, torsions, etc., allowing clear definition of the scale factors, which improves the transferability of the scale factors. Symmetry adapted internal coordinates, a common definition of internal coordinates, do not share the transferability property because the definitions of the coordinates may change if the symmetry of the molecule changes [4].

Force constants may be calculated either analytically [10] or numerically [24,33]. For molecules of the size considered in this study, analytical calculation of the force constants is about an order of magnitude faster than numeric differentiation of the gradient. Numeric differentiation, however, permits determination of the diagonal and semi-diagonal cubic and diagonal quartic force constants [24]. The TEXAS program does not currently support analytical evaluation of the quadratic force constants, thus, in this work the ab initio force field is determined by numerical differentiation.

The procedures for determining the force constants numerically are well established [24,33]. The gradient is calculated at displaced geometries and then numerically differentiated to give the force constants. Equal positive and negative displacements are used to reduce cubic anharmonicity in the harmonic force constants [24]. The displacement step size should be large enough to ensure numerical stability and small enough to reduce the contribution of cubic and higher order terms to the force constant. In this study, bond lengths are displaced by ±0.02 Å, bond angles are displaced by ±2° and torsion and out of plane angles are displaced by ±5°.

The ab initio force field is scaled according to equation (2-32) [4,19]. A small number of scale factors, corresponding to similar types of internal coordinates, are transferred from related molecules, providing an a priori determination of the force field, or are calculated from a least squares fit to available experimental frequencies. Calculating the scale factors in this manner includes some anharmonic effects because observed experimental frequencies and not corrected "harmonic" frequencies are used in the fitting procedure. This approximate treatment of anharmonicity has the undesirable side effect of producing different scale factors for different isotopic species and this leads, incorrectly, to slightly different force fields for different isotopic species. By weighting different isotopic species equally in the least squares fitting procedure, one obtains scale factors that average the anharmonicity effects of different isotopic species, that tend to minimize random errors in the experimental frequencies, and that produce symmetrical force fields.

$$F_{SQM} = C^{1/2} F_{AB} C^{1/2} \tag{2-32}$$

F_{SQM} = the Scaled Quantum Mechanical Force Field.
C = the diagonal matrix of scale factors.
F_{AB} = the ab initio force matrix.

Fundamental vibration frequencies are calculated from the scaled force field using Wilson's FG matrix method [34]. The scaled theoretical frequencies are usually within 20 cm^{-1} of the corresponding experimental frequencies [4]. Theoretical assignment of fundamental frequencies is accurate enough to identify experimental misassignment of fundamental vibration frequencies, see for example studies on cyclobutane [35] and oxetane [36]. In highly symmetric molecules, for example naphthalene [37], theory is the only method that can provide accurate frequencies for transitions that are symmetry forbidden in the both the infrared and Raman spectra. Theoretical infrared and Raman intensities, which provide semi-quantitative agreement with experimental intensities, may be calculated if Cartesian dipole moment and polarizability derivatives are calculated. In previous studies, the stronger theoretical transitions have corresponded to experimental transitions that were characterized as strong or very strong, while the weaker theoretical transitions have corresponded to experimental transitions that were characterized as weak, very weak, or were not observed.

The accuracy of the scaled force field may be checked by comparing the theoretical vibrational frequencies with available experimental frequencies or by comparing theoretical centrifugal distortion constants with experimental centrifugal distortion constants. Both comparisons should be completed, if possible, because the vibration frequencies are primarily determined by the diagonal force constants while the distortion constants are primarily determined by the off-diagonal force constants.

CALCULATION OF POTENTIAL SURFACES

Theoretical potential surfaces may be calculated by holding the internal coordinate defining the motion over the potential surface fixed at several different values. At each point the remaining 3N-7 internal coordinates are optimized to obtain the best estimate of the energy. The resulting table of energies and displacements is numerically fit to an appropriate function to give the theoretical potential surface. Potential surfaces calculated in this manner may not be precisely correct, because they implicitly assume the internal motion occurs over a single coordinate path.

ESTIMATING E_0

We now have discussed methods for calculating all of the terms that comprise q(int), but do not have a method for calculating q(ext), or equivalently E_0. E_0 is conventionally defined to be the heat of formation at 0 K [3], although some thermodynamic tables use the heat of formation at 298 K [5]. To comply with this convention we need a method for converting ab initio energies to the heats of formation at 0 K. We may use isodesmic reactions or empirically correct the ab initio energy to complete this conversion.

Pople developed the concept of isodesmic reactions to improve the accuracy of theoretical reaction energies [39]. An isodesmic reaction conserves the number and type of non-hydrogen bonds in a given molecule. Pople has shown that for isodesmic reactions theoretical and experimental reaction energies agree to within 2 to 5 kcal/mol if the experimental energies are corrected to 0 K and for vibrational zero point energy. This level of accuracy is probably the best we can expect from an ab initio method that ignores the effects of electron correlation.

We may use isodesmic reactions to calculate the heat of formation at 0 K in the following manner:

1. Calculate ab initio energies for all of the molecules involved in the isodesmic reaction.
2. Calculate zero point vibrational energies for all of the molecules involved in the isodesmic reaction.
3. Using the data from steps 1 and 2, calculate the heat of reaction at 0 K.
4. Look up E_0 energies for all of the molecules involved in the isodesmic reaction, except for the unknown molecule.
5. Calculate E_0 for the unknown molecule using the data from steps 3 and 4 and standard thermodynamic formulae [1].

Examining the five above steps points out the most serious disadvantage of the isodesmic reaction method: it requires a large amount of known data. If any one piece of data is missing, the method fails.

Wiberg [40] and Ibrahim and Schleyer [41] have calculated empirical corrections for the 6-31G basis set that correct ab initio energies to heats of formation at 298 K. Wiberg calculated theoretical energies that agreed to within 2 kcal/mol of experimental energies for a series of hydrocarbons. Ibrahim and Schleyer calculated theoretical energies that agreed to within 5 kcal/mol of experimental energies for a large number of small heteroatomic organic molecules. In Chapter Five a similar set of empirical correction factors are derived for the 4-21NO*(P) and 4-21NO*(D6) basis sets. The calculated heat of formation at 298 K may be corrected to 0 K by subtracting the contributions of the vibrational and rotational energy. This empirical correction scheme offers several advantages:

1. It is easy to use.
2. It immediately gives a very useful energy, the heat of formation at 298 K.
3. Once a set of correction factors is determined, they may be applied to any molecule.

When possible, E_0 will be calculated by both the isodesmic reaction method and the empirical correction method to help eliminate random numerical errors.

Thermodynamic functions calculated with the method outlined in this Chapter should have an accuracy similar to thermodynamic functions derived by experimental methods if they employ the same assumptions and approximations. The E_0 energy should agree with experimentally derived values to within 5 kcal/mol and, as a result, the free energy and enthalpy values derived by this method should be accurate to 5 kcal/mol. The entropy and specific heat do not depend on E_0 and they should be accurate within two per cent.

FIGURE 2-1

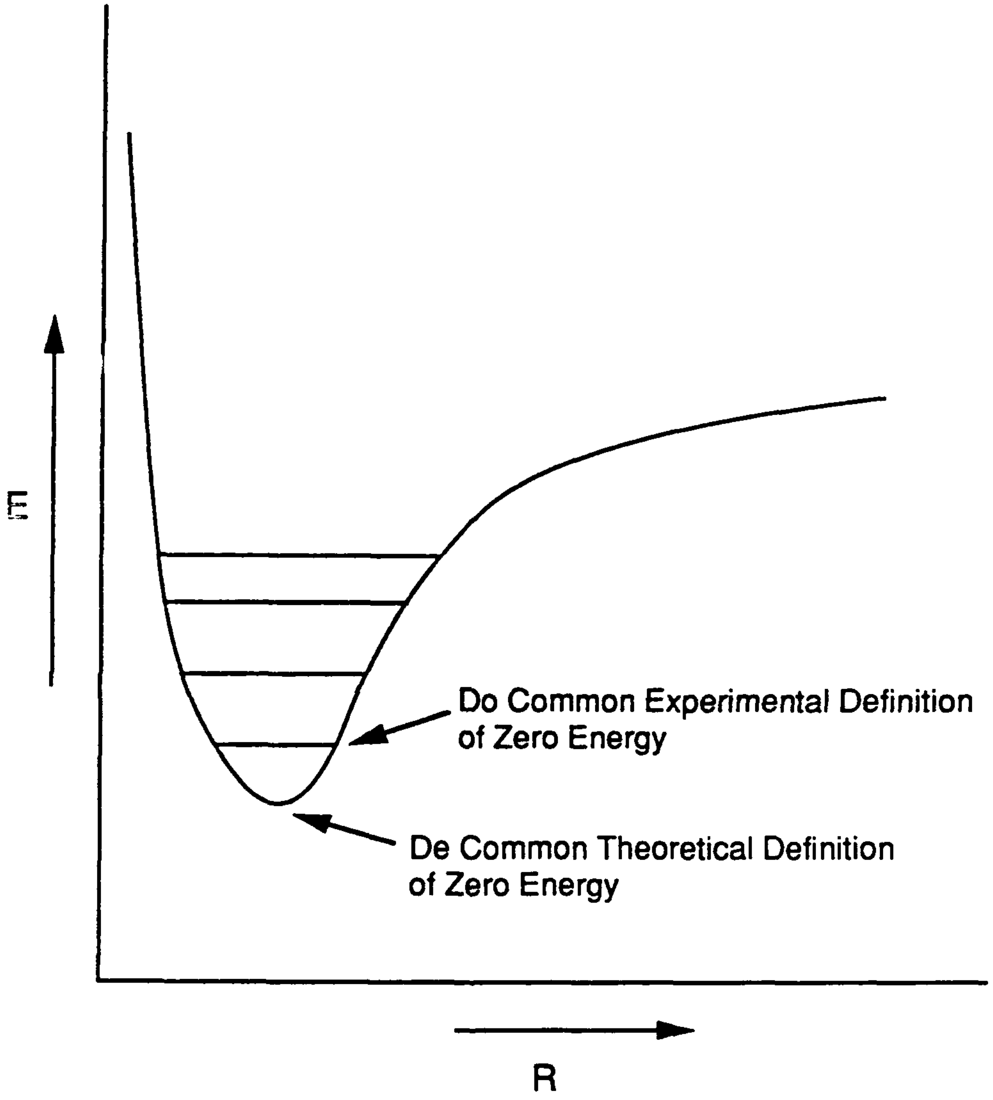
E
Do Common Experimental Definition of Zero Energy
De Common Theoretical Definition of Zero Energy
R

CHAPTER THREE

INTRODUCTION

In this work the Scaled Quantum Mechanical Force Field method [24] is used to calculate a priori fundamental vibration frequencies and vibrational partition functions. The first step in the Scaled Quantum Mechanical Force Field method is correcting the ab initio geometry for the basis set offset, which is caused by incomplete expansion of the basis set and neglect of electron correlation, to obtain an estimate of the equilibrium geometry, usually denoted r_e. We can directly calculate an r_e geometry with large basis sets, 6-31G** or better, and including electron correlation in the calculation at a minimum level of MP4 with single, double and quadruple excitations [17,18]. In Chapter Two, we showed that failing to correct the ab initio geometry for the basis set offset introduces a linear term in the potential energy expansion and limits transferability of force field scale factors from molecule to molecule. Additionally the molecular rotational constants are calculated directly from the estimated equilibrium geometry and any errors in this geometry will be reflected in the rotational partition function.

Previous work has shown that Pang's 4-21 basis set [24] calculates bond lengths with a predictable basis set offset [23,42], but calculates bond angles around oxygen and nitrogen with a random basis set offset. Adding d functions to the oxygen and nitrogen basis sets, forming the 4-21NO* basis set, corrects this defect while keeping the calculation cost at a modest level [23], about half of the cost associated with the 6-31G* basis set [30]. In this chapter we determine correction formulae for C-C, C-O, C-N, N-O, N-N, C-H, N-H and O-H bond lengths calculated with the 4-21NO* basis set offset. Previous work strongly suggests the basis set offset for bond angles calculated with the 4-21NO* basis set is zero [23].

STRUCTURE DEFINITIONS

The primary problem encountered during the development of basis set offset correction formulae is the different structure definitions used in theoretical and experimental work. A theoretical structure is derived from an exact mathematical definition while an experimental structure is derived from an operational definition. A theoretical structure is derived by locating the minimum of the molecular potential energy surface. Neglect of electron correlation and incomplete expansion of the basis set causes errors in this potential energy surface and as a result the structure may differ from the r_e structure. The magnitude of the structural errors depends on the size of the basis set and the degree of electron correlation included in the calculation.

The best gas phase experimental structures are microwave substitution structures, calculated from the observed molecular rotational constants of several isotopes and commonly denoted as r_s, and electron diffraction structures, calculated from the radial electron diffraction pattern and commonly denoted r_g. Zero point vibration and contribution of excited vibrational and rotational states cause these structures to differ from the r_e structure in a complicated manner. The r_s and r_g bond lengths are usually 0.002 to 0.005 angstroms longer than the corresponding r_e bond length [43]. The complete molecular force field is required to derive an r_e structure from its corresponding r_s or r_g structure. Experimentally determining the complete molecular force field is difficult and, as a result, few experimental r_e structures have been reported.

Ideally we want to compare an ab initio structure with the corresponding r_e structure. The difficulties encountered in deriving a theoretical or experimental r_e structure have prevented the establishment of base of reference molecules from which correction formulae may be derived. One is forced, therefore, to derive basis set correction formulae by comparing selected ab initio structures with the corresponding experimental r_s and r_g structures.

REVIEW OF PREVIOUS WORK

At least two different methods of correcting ab initio structures for the inherent basis set offset have been developed. Pulay proposed linear correction formulae [24], derived from a comparison of a small number of experimental r_e and ab initio bond lengths, for C-C and C-H bond lengths calculated with the 4-21 basis set. His correction formulae have been tested on larger molecules and give good agreement with experimental bond lengths [37,44].

Schäfer and coworkers developed empirical basis set offset correction values for C-C, C-O, C-N and C-H bond lengths calculated with the 4-21 basis set [45]. Their correction values are determined by the total energy difference between a pair of molecules that are related by simple substitution of one bond. For example, the correction value for the C-C bond length in ethane would be determined by the energy difference between ethane and methane. These correction values were derived by comparing r_s and r_g bond lengths with their corresponding ab initio bond lengths. Their work includes a wide range of small molecules and their corrected ab initio bond lengths generally agree with the respective experimental bond lengths to within 0.006 Å. Schäfer's method is not suitable for this work because it requires optimized energies for a series of molecules to obtain the energy increment and the associated basis set offset for each bond in the target molecule.

DERIVATION OF BOND LENGTH CORRECTIONS

The basis set offset correction formulae given below were derived by performing a least squares fit between selected high quality experimental r_s and r_g bond lengths and the corresponding ab initio bond lengths. The corrected ab initio bond lengths are an estimate of the r_e bond length, but because the formulae are derived from experimental data, one should expect the corrected values to be .002 to .005 Å longer than the true r_e bond lengths. Until additional r_e structures are reported, this method provides the best estimate of the r_e structure from a single determinant ab initio calculation.

BOND LENGTH CORRECTION FORMULAE

The bond length data used to determine correction formulae for the C-C, C-O, C-N, N-O, and N-N bond lengths are shown in Tables 3-1 through 3-5. The corresponding bond length correction formulae are shown as equations 3-1 through 3-5 and were derived from a linear least squares fit to the appropriate data. Figures 3-1 through 3-5 are plots of the bond length data and the corresponding correction formula. The apparently good agreement between the correction formulae and the corresponding bond length data is misleading because the residual errors, on the order of 0.005 Å, are less than one per cent of the bond length.

$$r(CC)=0.83699*r(\text{ab initio})+0.23848 \qquad (3\text{-}1)$$

r(CC)=the corrected C-C bond length

r(ab initio)=the ab initio C-C bond length calculated with the 4-21NO* basis set r(CO)=0.92535*r(ab initio)+0.10564 (3-2)

r(CO)=corrected C-O bond length

r(ab initio)=C-O bond length calculated with the 4-21NO* basis set.

r(CN)=0.90988*r(ab initio)+0.12767 (3-3)

r(CN)=corrected C-N bond length

r(ab initio)=C-N bond length calculated with the 4-21NO* basis set

r(NO)=1.1679*r(ab initio)-0.17256 (3-4)

r(NO)=corrected N-O bond length

r(ab initio)=N-O bond length calculated with the 4-21NO* basis set.

r(NN)=0.90929*r(ab initio)+0.13271 (3-5)

r(NN)=corrected N-N bond length

r(ab initio)=N-N bond length calculated with the 4-21NO* basis set.

We can more closely examine the linear dependance between the ab initio and experimental bond lengths by plotting difference between the experimental and ab initio bond lengths, r(exp)-r(ab initio), as a function of the ab initio bond length, as shown in Figures 3-6 through 3-10. The difference plots for the C-C, C-O, and N-O bond lengths are reasonably linear, the standard deviation is less than 0.006 Å. The CN and NN difference plots exhibit significantly more scatter, the standard deviation for both data sets is 0.009 Å. The causes of the scatter in the CN data are not obvious, but may be caused by the limitations of single determinant calculations or by contributions from low lying excited vibrational states to the experimental structures. The causes of the scatter in the NN data are the small number of data points and the poor agreement between the experimental and corrected bond lengths for 1,3,4 thiadiazol and hydrazine.

Figures 3-1 and 3-6 also show Pulay's C-C bond length correction formula [24], given as equation 3-6. As expected, corrected bond lengths derived from equation 3-6 are 0.002 to 0.003 Å shorter than corrected bond lengths derived from equation 3-1. Pulay's correction formula for C-C bond lengths is used throughout the remainder of this work because it was derived from r_e bond lengths instead of r_s or r_g bond lengths and should, therefore, provide a better estimate of the r_e bond length.

$$r(CC)=0.84*r(ab\ initio)+0.232 \qquad (3\text{-}6)$$

see equation 3-1 for definitions

Determining corrections for C-H, O-H and N-H bond lengths completes the set of basis set offset correction formulae required for this work. For C-H bond lengths we will use Pulay's correction formula determined from the r_e and ab initio structures of methane and formaldehyde [24]. The O-H bond length correction is a constant -0.004 Å and was derived by comparing the water r_e O-H bond length, 0.957 angstroms [46], with the ab initio O-H bond length, 0.961 angstroms. The N-H bond length correction of 0.000 angstroms was derived by comparing the ammonia r_e N-H bond length, 1.011 angstroms [47], with the ab initio N-H bond length, 1.011 angstroms.

Equations 3-2 through 3-6 along with the constant corrections for C-H and O-H bond lengths are used to obtain an estimate of the r_e structure from an optimized ab initio geometry determined with the 4-21NO* basis set. This corrected geometry is then used as the reference structure for calculating fundamental vibration frequencies and rotational constants.

TABLE 3-1

C-C BOND LENGTHS[a]

Molecule	r_{th}[b]	r_{exp}[c]	r_{exp}-r_{th}	TYPE[d]
Ethane	1.541	1.533	-0.008	r_g
Isobutane	1.542	1.535	-0.007	r_g
Isobutane	1.542	1.525	-0.017	r_s
Cyclobutane	1.567	1.551	-0.016	r_g
Acetaldehyde	1.519[e]	1.515	-0.004	r_g
Acetone	1.527[e]	1.520	-0.007	r_g
Acetone	1.527[e]	1.507	-0.020	r_s
Bicyclo(2.1.0)pentane	1.581	1.565	-0.016	r_s
Bicyclo(2.1.0)pentane	1.545	1.528	-0.017	r_s
Ethylmethyl ether	1.531[e]	1.520	-0.011	r_s/r_g
Ethanol	1.536[e]	1.512	-0.024	r_s
Isobutene	1.516	1.508	-0.008	r_g
Isobutene	1.317	1.342	0.025	r_g
Ethylene	1.312	1.337	0.025	r_g
Propene	1.314	1.342	0.028	r_g
Propene	1.314	1.336	0.022	r_s
Propene	1.512	1.506	-0.006	r_g
Propene	1.512	1.501	-0.011	r_s
Benzene	1.385	1.399	0.014	r_g
Pyrazole	1.363[e]	1.380[f]	0.017	r_e
Pyrazole	1.416[e]	1.415[f]	-0.001	r_e
Cyclopropane	1.515	1.511	-0.004	r_g
Cyclopropane	1.515	1.512	-0.003	r_g

a. Unless otherwise noted all data taken from L. Schafer, C. Van Alsenoy and J. N. Scarsdale, J. Mol. Struct., 86 (1982) 349.

b. Bond length calculated with the 4-21NO* basis set.

c. Experimental bond length.

d. Type of experment used to determine the experimental bond length.

e. This work.

f. L. Nygaard, D. Christen, J. T. Nielsen, E. J. Pedersen, O. Snerling, E. Vestergaard and G. O. Sorensen, J. Mol. Struct., 22 (1974) 401.

TABLE 3-2

C-O BOND LENGTHS

MOLECULE	r_{th}^{a}	r_{exp}^{b}	$r_{exp}-r_{th}$	TYPE^{c}
Carbon Dioxide	1.1450	1.1600^{d}	.0150	r_e
Ketene	1.1490	1.1614^{e}	.0124	r_s
Formic Acid	1.1860	1.2040^{f}	.0180	r_s
Methyl Formate	1.1880	1.2000^{g}	.0120	r_s
Acetic Acid	1.1900	1.2130^{f}	.0230	r_g
trans Glyoxal	1.1910	1.2120^{h}	.0210	r_g
Formaldehyde	1.1920	1.2090^{f}	.0170	r_g
trans Acrolein	1.1950	1.2170^{h}	.0220	r_g
trans Acrolein	1.1950	1.2190^{i}	.0240	r_s
Acetone	1.1960	1.2140^{f}	.0180	r_g
Formamide	1.1980j	1.2120^{k}	.0140	r_s
Methyl Formate	1.3360	1.3340^{g}	-.0020	r_s
Formic Acid	1.3420	1.3420^{f}	.0000	r_s
Acetic Acid	1.3500	1.3620^{f}	.0120	r_g
Furan	1.3650	1.3620^{l}	-.0030	r_s
Dimethyl Ether	1.4150	1.4100^{f}	-.0050	r_s
Dimethyl Ether	1.4150	1.4160^{f}	.0010	r_g
Ethyl Methyl Ether	1.4160	1.4130^{f}	-.0030	r_g
Ethyl Methyl Ether	1.4190	1.4220^{f}	.0030	r_g
Methanol	1.4210	1.4280^{f}	.0070	r_g
Ethanol	1.4240	1.4310^{f}	.0070	r_s
Methyl Nitrite	1.4410	1.4370^{m}	-.0040	r_s
Methyl Formate	1.4420	1.4370^{g}	-.0050	r_s

a. Bond length calculated with the 4-21NO* basis set.

b. Experimental bond length.

c. Type of experiment used to determine the experimental bond length.

d. C. P. Courtoy, Ann. Soc. Sci. Bruxelles, 73 (1959) 5.

e. J. W. C. Johns, J. M. R. Stone, G. Winnewisser, J. Mol. Spectros., 42 (1972) 523.

f. L. Schafer, C. Van Alsenoy and J. N. Scarsdale, J. Mol. Struct., 86 (1982) 349.

g. R. F. Curl, J. Chem. Phys., 30 (1959) 1529.

h. K. Kuchitsu, T. Fukuyama and Y. Morino, J. Mol. Struct., 4 (1969) 41. and J. Mol. Struct., 1 (1968) 463.

i. A. E. Cherniak and C. C. Coastain, J. Chem. Phys. 45 (1966) 104.

j. F. R. Cordell, Masters Thesis, The University of Texas at Austin, August 1987.

k. E. Hirota, R. Sugisake, C. J. Nielsen and O. Sorensen, J. Mol. Spectrosc., 49 (1974) 251.

l. P. Nosberger, A. Bauder and Hs. H. Gunthard, Chem. Phys. 1 (1973) 418.

m. M. J. Corkill, A. P. Cox and P. H. Turner, Seventh Austin Symposium on Molecular Structure, Austin, Texas, 1978, Paper TA6.

TABLE 3-3

C-N BOND LENGTHS

MOLECULE	r_{th}^a	r_{exp}^b	$r_{exp}-r_{th}$	TYPE^c
Hydrogen Cyanide	1.131	1.153^d	0.022	r_e
Cyanogen	1.131	1.163^e	0.032	r_g
Acetonitrile	1.132	1.157^f	0.025	r_s
Hydrogenisocyanide	1.155	1.169^g	0.014	r_e
Acetoisonitrile	1.156	1.166^f	0.010	r_s
1,3,4 Oxadiazole	1.267	1.297^h	0.030	r_s
1,3,4 Thiadiazole	1.277	1.302^i	0.025	r_s
Diazomethane	1.288	1.300^j	0.012	r_s
Pyrazole	1.309	1.331^k	0.022	r_s
Pyrazole	1.353	1.359^g	0.006	r_s
Formamide	1.373^l	1.368^j	- 0.005	r_g
Acetoisonitrile	1.436	1.424^f	-0.012	
Methyl amine	1.474	1.465^m	-0.009	r_g
Methyl amine	1.474	1.471^n	-0.003	r_s
Nitromethane	1.496	1.489^o	-0.007	r_s

a. Bond length calculated with the 4-21NO* basis set.

b. Experimental bond length.

c. Type of experiment used to determine the experimental bond length.

d. A. E. Douglas and E. Sharma, J. Chem. Phys., 21 (1953) 448.

e. Y. Morino, K.Kuchitsu, Y. Hori and M. Tanimoto. Bull. Chem. Soc. Japan, 41 (1968) 2349.

f. C. C. Costain. J. Chem. Phys. 29 (1958) 864.

g. A. Creswell and A. G. Robiette, Mol. Phys., 36 (1978) 869.

h. L. Nygaard, R. L. Hansen, J. T. Nielson, J. Rastrup-Anderson, G. O. Sorensen and P. A. Steiner. J. Mol. Struct. 12 (1972) 59.

i. L. Nygaard, L. Hansen and G. O. Sorensen. J. Mol. Struct. 9 (1971) 163.

j. C. B. Moore, J. Chem. Phys. 39 (1963) 1884.

k. L. Nygaard, D. Christen, J T. Nielsen, E. J. Pedersen, O. Snerling, E. Vestergarrd and G. O. Sorensen. J. Mol. Struct, 22 (1974) 401.

l. F. R. Cordell, Masters Thesis, The University of Texas, 1987.

m. J. H. Callomon, E. Hirota, K. Kuchitsu, W. J. Lafferty, A. G. Maki and C. S. Pote in K. H. Hellwege and A. M. Helwege (Eds), Landolt-Bornstein, Vol. 7, Springer Verlag, Berlin, 1976.

n. K. Takagi and T. Kojima, J. Phys. Soc. Japan 30 (1971) 1145.

o. A. P. Cox and S. Waring, J. Chem. Soc. Farad. Trans. II 68 (1972) 1060.

TABLE 3-4

N-O BOND LENGTHS

MOLECULE	r_{th}[a]	r_{exp}[b]	$r_{exp}-r_{th}$	TYPE[c]
trans Nitrous acid	1.154	1.170[d]	0.016	r_s
cis Methyl nitrite	1.162	1.182[e]	0.020	r_s
Nitric acid	1.174	1.199[f]	0.025	r_s
Nitroso methane	1.177	1.211[g]	0.031	r_s
Methyl nitrate	1.178	1.211[h]	0.033	r_s
Methyl nitrate	1.186	1.205[h]	0.019	r_s
Nitric acid	1.188	1.211[f]	0.023	r_s
Nitromethane	1.193	1.224[i]	0.031	r_s
cis Methyl nitrite	1.346	1.394[e]	0.048	r_s
Methyl nitrate	1.348	1.402[h]	0.054	r_s
Nitric acid	1.351	1.406[f]	0.055	r_s
trans Nitrous acid	1.371	1.432[d]	0.061	r_s

a. Bond length calculated with the 4-21NO* basis set.

b. Experimental bond length.

c. Type of experiment used to determine the experimental bond length.

d. A. P. Cox, A. H. Brittain and D. J. Finnigan, Trans. Farad. Soc. 67 (1971) 2179.

e. M. J. Corkill, A. P. Cox and P. H. Turner, Seventh Austin Symposium on Molecular Structure, Austin, Texas, 1978, Paper TA6.

f. P. N. Ghosh, C. E. Blom and A. Bauder, J. Mol. Spectrosc. 89 (1981) 159-173.

g. P. H. Turner and A. P. Cox, J. Chem. Soc. Farad. Trans. II 75 (1978) 533.

h. A. P. Cox and S. Waring, Trans, Faraday Soc., 67 (1971) 3441.

i. L. V. Vilkov, B. S. Mustryukov and N. I. Sadova, Determination of the Geometrical Structure of Free Molecules, Khimiya, Leningrad (1978).

TABLE 3-5

N-N BOND LENGTHS

MOLECULE	r_{th}[a]	r_{exp}[b]	$r_{exp}-r_{th}$	TYPE[c]
Dinitrogen oxide	1.091	1.128[d]	0.037	r_e
Diazomethane	1.112	1.139[e]	0.027	r_s
Pyridazine	1.312	1.330[f]	0.018	r_a
Pyrazole	1.335	1.351[g]	0.016	r_s
Dimethyl Nitramine	1.365[h]	1.383[i]	0.018	r_z
1,3,4 Thiadiazole	1.378	1.371[j]	-0.007	r_s
1,3,4 Oxadiazole	1.402	1.399[k]	-0.003	r_s
Dimethylhydrazine	1.420	1.417[l]	-0.003	r_z
Hydrazine	1.430	1.447[m]	0.017	r_s

a. Bond length calculated with the 4-21NO* basis set.

b. Experimental bond length.

c. Type of experiment used to determine the experimental bond length.

d. R. K. Narahari, Ann. Nwe York Acad. Sci., 220 (1973) 15.

e. C. B. Moore, J. Chem. Phys. 39 (1963) 1884.

f. A. Almenningen, G. Bjornsen, T. Ottersen, R. Seip and T. G. Strand, Acta Chem. Scand. A31 (1977) 63.

g. L. Nygaard, D. Christen, J. T. Nielsen, E. J. Pedersen, O. Snerling, E. Vestergaard and G. O. Sorensen, J. Mol. Struct. 22 (1974) 401.

h. F. R. Cordell, Masters Thesis, The University of Texas at Austin, 1987.

i. R. Stolevik and P. Rademacher, Acta Chem. Scand., 23 (1969) 672.

j. L. Nygaard, L. Hansen and G. O. Sorensen, J. Mol. Struct., 9 (1971) 163.

k. L. Nygaard, R. L. Hansen, J. T. Nielson, J. Rastrup-Anderson, G. O. Sorensen and P. A. Steiner, J. Mol. Struct., 12 (1972) 59.

l. M. Nakata, H. Takeo, C. Matsumura, K. Yamanouchi, K. Kuchitsu and T. Fukuyama, Chem. Phys. Lett. 83 (1981) 246.

m. S. Tsunekawa, J. Phys. Soc. Japan, 41 (1976) 2077.

FIGURE 3-1

C-C Bond Lengths

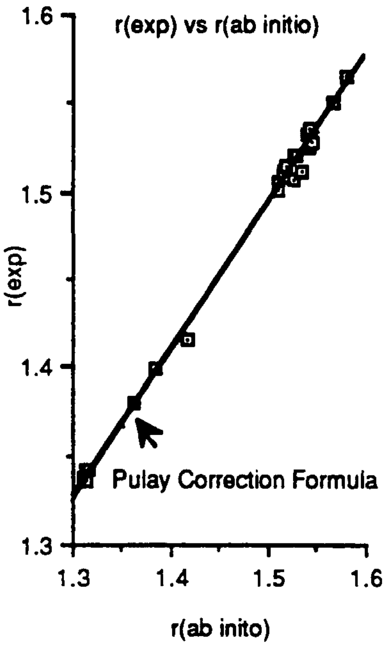

FIGURE 3-2

C-O Bond Lengths

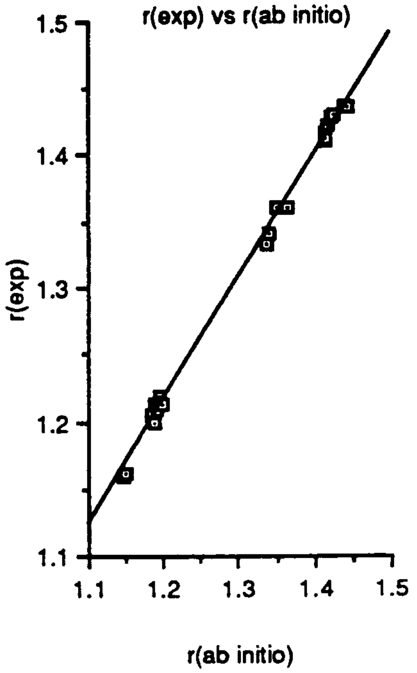

FIGURE 3-3

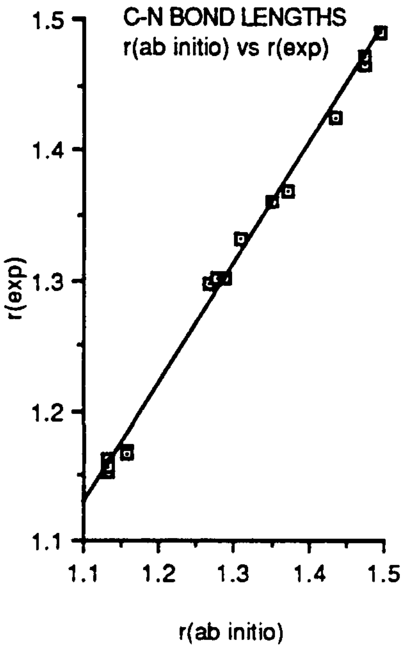

FIGURE 3-4

N-O Bond Lengths

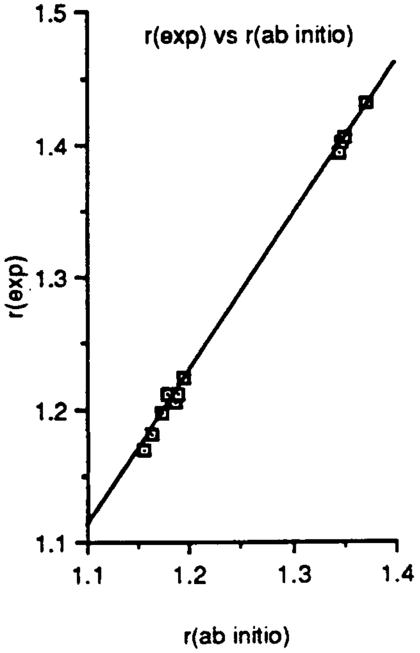

FIGURE 3-5

N-N Bond Lengths

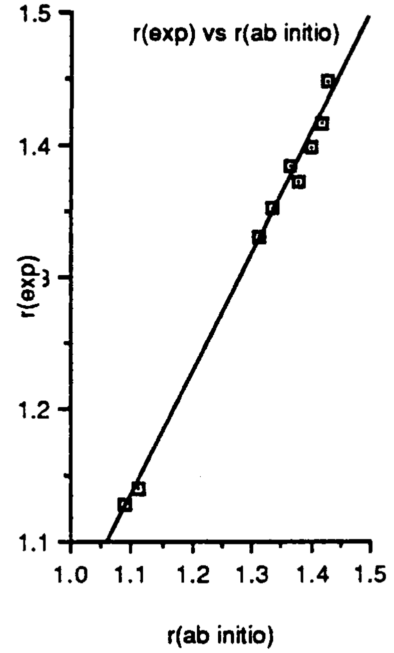

FIGURE 3-6

C-C Bond Lengths

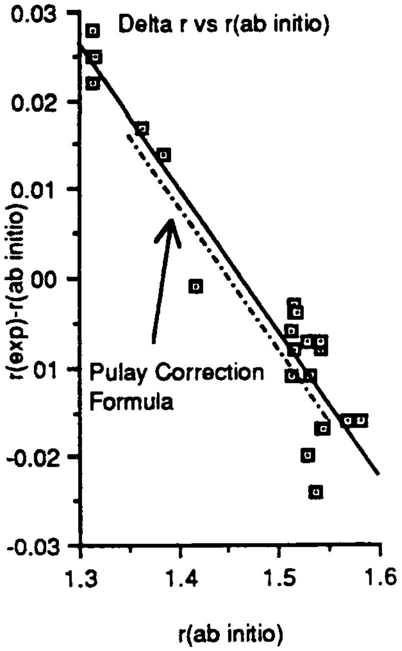

FIGURE 3-7

C-O Bond Lengths

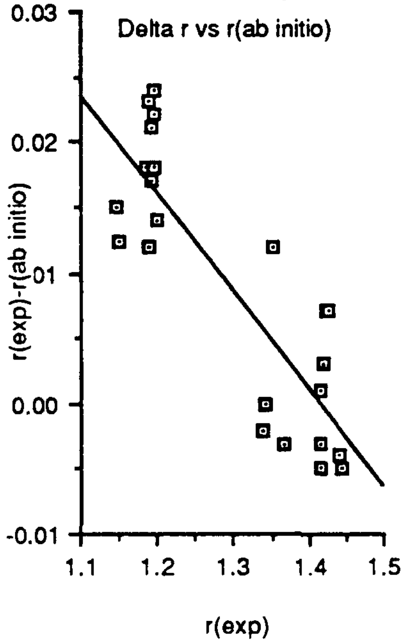

FIGURE 3-8

C-N Bond Lengths

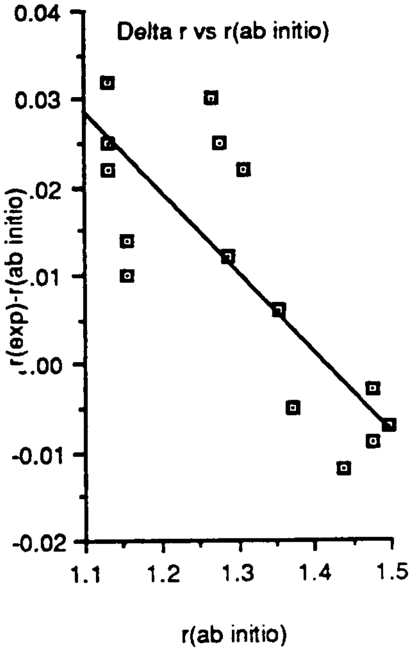

FIGURE 3-9

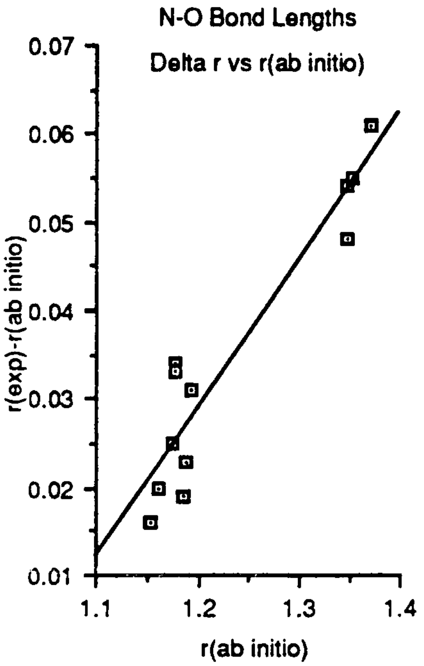

N-O Bond Lengths

Delta r vs r(ab initio)

FIGURE 3-10

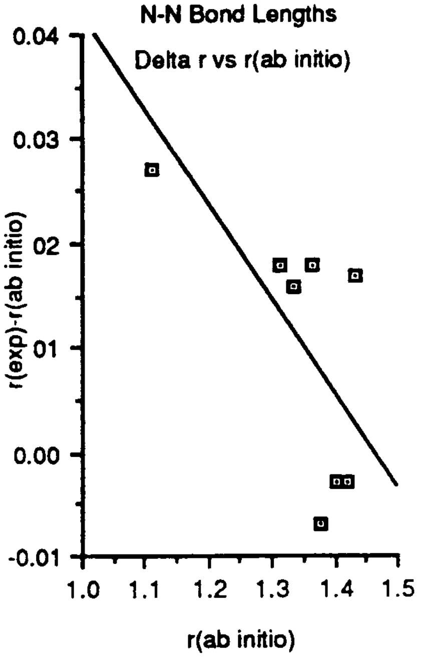

N-N Bond Lengths

Delta r vs r(ab initio)

CHAPTER FOUR

INTRODUCTION

The Scaled Quantum Mechanical Force Field (SQMFF) method [4,19,48] provides an efficient method for calculating molecular force fields that are often more accurate than experimentally derived force fields. In this chapter standard SQMFF scale factors for the 4-21NO* basis set will be developed from calculations on methanol, methylamine, nitromethane, nitric acid and pyrazole. Chapter Two and references [4] and [48] provide reviews of the SQMFF method.

Ab initio force constants are usually 20 to 30 per cent greater than corresponding experimental force constants and thus the ab initio fundamental vibration frequencies are 10 to 15 per cent higher than the observed fundamental vibration frequencies [4]. Fortunately the error in a particular type of force constant is almost constant from molecule to molecule. The SQMFF method corrects this deficiency by scaling the ab initio force field with a small set of scale factors, as shown in equation 2-40. Similar internal coordinates share the same scale factor, e.g. symmetric and asymmetric methyl deformation modes share the same scale factor. The scale factors are determined by performing a least squares fit to unambiguously assigned fundamental vibration frequencies. The resulting Scaled Quantum Mechanical Force Field is usually more accurate than an experimental force field because all of the force field elements are determined in an ab initio force field while an experimentally derived force field often assumes that many of the off-diagonal force field elements are zero. Fundamental vibration frequencies calculated from the SQMFF are usually within 10 to 15 cm^{-1} of observed fundamental vibration frequencies [4].

Although the above discussion suggests that we can not use the SQMFF method unless observed fundamental frequencies are available for the molecule under study, experience has shown that scale factors are transferable from molecule to molecule with properly defined internal coordinates [37,49,50,51]. Pulay's suggested internal coordinate definitions are designed to enhance transferability of the scale factors [4] and are used throughout this work. One can predict a priori fundamental frequencies by determining SQMFF scale factors from a molecule with assigned fundamental frequencies that is similar to the target molecule and then use these scale factors to scale the ab initio force field of the target molecule [4,48]. A priori fundamental vibration frequencies were calculated for naphthalene [50] and pyrazole [51] in this manner and the a priori fundamental frequencies were within 20 cm^{-1} of the experimental frequencies.

In this chapter, a set of standard scale factors is determined from the fundamental vibration frequencies of several small molecules. Gas phase or matrix isolated experimental fundamental vibration frequencies are used to derive the scale factors. Although no explicit corrections are made for anharmonic effects, such as Fermi resonance, the scale factors include some anharmonic corrections because observed frequencies rather than corrected harmonic frequencies are used in the least squares fitting procedure [4]. By averaging scale factors from several different molecules and isotopic species, we obtain an "effective" scale factor for an internal coordinate that should prevent biasing of the scale factor by the anharmonic effects of a single molecule.

METHANOL

Methanol belongs to the C_s symmetry point group with the staggered conformer being more stable than the eclipsed conformer, theoretically and experimentally. The symmetry plane contains the HCOH backbone and the molecule has 12 fundamental modes of vibration of which eight have A' symmetry and 4 have A" symmetry. Figure 4-1 shows the atom numbering scheme used in this work. Table 4-1 shows the experimental r_s [52], ab initio and estimated r_e geometries.

Günthard and coworkers have accurately assigned gas phase and argon matrix fundamental vibration frequencies for CH_3OH, CD_3OH, CD_3OD, CH_3OD, CH_2DOH, and CHD_2OH [53]. From their frequency data they derived a 33 term force field; the remaining 45 off-diagonal elements were assumed to be zero.

Schlegel and coworkers have calculated an ab initio force field for methanol using the 4-31G basis set [33]. They used the optimized 4-31G geometry as the reference geometry for their force field calculation. They did not scale the force field, but corrected the harmonic ab initio fundamental vibration frequencies for anharmonic effects using diagonal and semi-diagonal cubic force constants and diagonal quartic force constants. Their theoretical frequencies are within three per cent of the experimental frequencies.

In this work the estimated methanol r_e geometry, shown in Table 4-1, is used as the reference geometry for the force field calculation. Table 4-2 gives the definition of the internal coordinates. The ab initio force field was calculated as described in Chapter 2 and is shown in Table 4-3. The seven scale factors shown in Table 4-4 were used to scale the ab initio force field. Table 4-5 gives the ab initio, Scaled Quantum Mechanical and observed fundamental frequencies for CH_3OH; the SQM fundamental frequencies agree with the experimental frequencies to within eight cm^{-1} except for the CH stretching modes and the methyl deformation modes. The residual errors in the CH stretching modes are expected and are probably due to Fermi resonance. The residual errors in the methyl deformation modes, however, are unexpected. Obtaining a better fit to the deformation mode frequencies requires an individual scale factor for the symmetric and asymmetric modes. The residual errors are probably caused by anharmonic effects and to reduce the number of scale factors a single value is used for the methyl deformation modes.

In addition to methanol, the ab initio force field was scaled to fit the CD_3OH, CH_3OD and CD_3OD fundamental frequency assignments. Table 4-5 also shows ab initio, SQMFF and observed frequencies [53] for these molecules. The scale factors for each molecule are shown in Table 4-4 along with the average or effective scale factor for each mode. The average scale factors will be combined with corresponding scale factors from the other molecules discussed in this Chapter to obtain a standard set of scale factors.

METHYLAMINE

The staggered methylamine conformer is the ground state and belongs to the C_s symmetry point group. Nine of the 15 normal modes have A' symmetry while the six remaining normal modes have A" symmetry. The symmetry plane contains the HCO plane and bisects the HNH bond angle. The structure around nitrogen is non-planar. Figure 4-2 shows the atom numbering scheme used in this work and Table 4-6 shows the experimental r_s [54], ab initio and estimated r_e geometries. Table 4-7 shows the internal coordinate definitions used in this work.

The vibrational spectrum of methylamine has been studied by several groups [55-63] and experimental Urey-Bradley force fields [55-57] and a local symmetry force field [59] have been reported. Two of the fifteen fundamental frequencies, the NH_2 twisting, or asymmetric NH_2 deformation, and the asymmetric methyl rocking frequency, have not been assigned experimentally. The NH_2 twisting frequency has been assigned to lines at

1416 cm^{-1} [58], 1335 cm^{-1} [60], 1329 cm^{-1} [55], 1013 cm^{-1} [61], 977 cm^{-1} [56], and 831 cm^{-1} [62] by various authors, while the asymmetric methyl rocking frequency has been assigned to lines at 1335 cm^{-1} [63], 1224 cm^{-1} [61], 1178 cm^{-1} [56], and 1016 cm^{-1} [55] by various authors.

The uncertain assignment of the NH_2 twist and asymmetric methyl rock fundamental frequencies have made methylamine the focus of several theoretical studies and shows the value of combining theoretical and experimental data. Schlegel and coworkers calculated the methylamine force field with the 4-31G basis set using the optimized 4-31G geometry as the reference geometry [33]. They did not scale the ab initio force field, but treated anharmonicity using diagonal cubic and quartic and semi-diagonal cubic force constants. Their calculated fundamental frequencies were about three per cent higher than the experimental frequencies. They calculated the NH_2 twist frequency to be 1391 cm^{-1} and the asymmetric CH_3 rock frequency to be 992 cm^{-1}.

Pulay and Torok calculated the methylamine force field with the 7 3/3/1 basis set using the experimental geometry as the reference geometry [64]. They scaled the ab initio force field by reducing the stretching force constants by ten per cent and the bending force constants by twenty per cent. They calculated the NH_2 twist frequency to be 1332 cm^{-1} and the asymmetric CH_3 rock frequency to be 904 cm^{-1}.

Hamada and coworkers used a scheme similar to the SQMFF method to calculate the complete methylamine force field and assigned all of the fundamental frequencies [65]. They calculated the force field with the 4-31G basis set using the optimized 4-31G geometry as the reference geometry. They scaled the diagonal elements of the ab initio force field using a least squares fit to the unambiguously assigned experimental fundamental frequencies, but did not scale the off-diagonal force constants. Their theoretical frequencies confirmed the experimental assignments made by Gray and Lord [58] and based on their calculated frequency of 1341 cm^{-1} they assigned the weak band at 1335 cm^{-1} to the NH_2 twist.

Hamada and coworkers calculated the asymmetric methyl rock frequency to be 945 cm^{-1} and their theoretical intensity data suggest the band should be the weakest band in the methylamine vibrational spectrum [65]. The experimental gas phase spectrum does not show any bands within 70 cm^{-1} of the theoretical frequency, but the argon matrix spectrum shows a very weak band at 972 cm^{-1} which was assigned to the asymmetric

CH_3 rock. Note that unambiguous assignment of this fundamental frequency was possible only by combining theoretical and experimental data.

In this work the ab initio force field, shown in Table 4-7, was calculated with the 4-21NO*(P) and 4-21NO*(D6) basis sets, refer to Chapter Two for descriptions of the basis sets. Both basis sets lead to identical ab initio force fields, and, consequently, identical scale factors. The estimated r_e geometry, shown in Table 4-6 as r_{corr}, was used as the reference geometry. The eight scale factors shown in Table 4-9 were determined by least squares fitting to the fundamental frequency assignments of Hamada and coworkers. The NH_2 twist and asymmetric methyl rock frequencies were given zero weight in the least squares fitting procedure. The ab initio, scaled and experimental fundamental frequencies are listed in Table 4-10.

The calculated fundamental frequencies for the asymmetric methyl rocking mode, 944 cm^{-1}, and for the NH_2 twisting mode, 1327 cm^{-1}, confirm the assignments made by Hamada et al [65]. The 28 cm^{-1} difference between the calculated and experimental methyl rocking frequency is larger than expected. The reported experimental frequency assignment is taken from the argon matrix spectrum rather than from the gas phase spectrum [65]. The large discrepancy between the calculated and experimental frequencies may, therefore, be caused by matrix effects.

NITROMETHANE

Nitromethane exhibits an extremely low barrier to internal rotation of about six cal/mole [66] and, therefore, at room temperature the molecule freely rotates between the low energy staggered, or perpendicular, conformer and the eclipsed, or parallel, conformer. Both conformers belong to the C_s symmetry point group. Figure 4-3 shows the atom numbering scheme used in this work. In the staggered conformer the C1-H5 bond is approximately perpendicular to the NO_2 plane while in the eclipsed conformer one of the CH bonds eclipses one of the NO bonds. In the staggered conformer nine of the fifteen fundamental vibrations have A' symmetry and the remaining six fundamental vibrations have A" symmetry. In the eclipsed conformer ten fundamental vibrations have A' symmetry and five fundamental vibrations have A" symmetry. Table 4-11 shows the experimental r_s geometry [66], the eclipsed and staggered 4-21NO* ab initio geometries, and the estimated eclipsed and staggered r_e geometries.

McKean and Watt have assigned fundamental frequencies for fourteen fundamentals in the gas, argon matrix, liquid and crystal states for CH_3NO_2, CD_3NO_2, and CHD_2NO_2 [67]. The low energy torsion fundamental lies well below the frequency range they investigated. From their data, they were able determine the staggered conformer is more stable than the eclipsed conformer. They did not attempt to derive a force field from their data.

Rezchikova and Shlyapochnikov calculated force constants for the NO_2 group in a series of nitro compounds using the STO-3G and 4-31G basis sets [68]. They used the ab initio geometries as the reference geometry for their force constant calculations. They did not calculate fundamental frequencies or scale their force constants.

McKee calculated the nitromethane force field and fundamental frequencies using Multiconfiguration SCF (MCSCF) calculations [69]. He calculated the force field using the MCSCF geometry as the reference geometry. He did not scale his force field, but multiplied the fundamental frequencies by 0.9 to obtain reasonable agreement with the fundamental assignments of McKean and Watt [67]. Additionally these calculations indicate that single determinant SCF calculations are sufficiently accurate for the calculation of force constants and fundamental frequencies.

Bock and coworkers have calculated the nitromethane force field and fundamental frequencies using the SQMFF method with some minor variations [70]. They employed the 6-31G basis set and used the optimized ab initio geometry as the reference geometry for the force field calculation. They scaled the ab initio force field to reproduce the crystal fundamental frequency assignments of McKean and Watt with six scale factors. They selected the crystal frequency assignments because only the staggered conformer is present in the crystal spectrum.

The low barrier to internal rotation in nitromethane presents a few problems in this study. The 4-21NO* basis set incorrectly determines the eclipsed conformer to be more stable than the staggered conformer. Additionally by scaling the ab initio force field to the observed gas phase fundamental frequencies, we are scaling a fixed configuration force field to frequencies representative of a molecule with free internal rotation. In order to minimize the effects of these two problems, force field scale factors were calculated for staggered and eclipsed nitromethane. To minimize anharmonic effects for the methyl group, force field scale factors were also calculated for eclipsed CD_3NO_2. Effective nitromethane scale factors are then calculated by averaging these three sets of scale factors.

Table 4-12 shows the nitromethane internal coordinate definitions. Table 4-13 shows the ab initio force fields for staggered and eclipsed nitromethane. Comparing the two force fields we see that they are similar, i.e. internal rotation about the CN bond has little effect on the vibrational energy surface. The major change in the force field is a reordering of the relative strengths of the CH bonds during internal rotation. In the staggered conformer the diagonal Q4 force field element, the unique C1-H5 bond, is smaller than the diagonal force field elements for the two symmetric CH bonds while in the eclipsed conformer the Q4 diagonal force field is larger than the diagonal force field elements for the two symmetric CH bonds. The calculated change in the CH stretching diagonal force constant for the staggered conformer, 0.18 mdyne/Å, is in excellent agreement with the experimental change in the CH stretching diagonal force constant, 0.17 mdyne/Å, determined by McKean and Watt based on the crystal CHD_2NO_2 spectrum. The theoretical change in CH bond length during internal rotation, 0.006 Å, agrees exactly with McKean and Watt's analysis of the gas phase spectra of CHD_2NO_2 [67].

The optimized scale factors for staggered nitromethane are shown in the second column of Table 4-14. Table 4-15 shows the ab initio, SQMFF, and experimental fundamental vibration frequencies. The methyl torsional frequency was assigned a weight of zero in the least squares fitting process for the seven scale factors shown in Table 4-14. The calculated methyl torsional frequency is imaginary indicating the staggered conformation is a transition state at the 4-21NO* level of calculation. The agreement between the scaled and experimental frequencies is excellent except for the symmetric and asymmetric methyl deformation frequencies, numbers eight and nine in Table 4-15. As stated earlier in the methanol discussion, obtaining better agreement would require separate scale factors for the symmetric and asymmetric methyl deformation modes.

Table 4-16 shows the SQM and experimental fundamental frequencies for eclipsed nitromethane and eclipsed nitromethane (D3), respectively. The optimized scale factors are shown in the third and fourth columns of Table 4-14. The scale factors are very similar for the staggered and eclipsed conformers. The average scale factors shown in the fifth column of Table 4-14 will be combined the results for the other molecules studied in this Chapter to give final "effective" scale factors.

NITRIC ACID

Nitric acid is a planar molecule and belongs to the C_S symmetry group. Seven of the nine normal coordinates belong to the A' symmetry group while the remaining two belong to the A" symmetry group. Figure 4-4 shows the atom numbering scheme used in this study. Table 4-17 shows the experimental r_S [71], 4-21NO* ab initio, and estimated r_e geometries.

McGraw et al. [72] and Palm et al. [73] have independently assigned fundamental frequencies for nitric acid. McGraw derived a limited in-plane force field from his data that contained 14 force constants [72]. Palm and coworkers derived a complete quadratic in-plane force field except for the OH stretching interaction force constants [73]. Neither experimental work derived the out of plane force constants for the NO torsion or NO_2 wagging modes.

Ghosh, Blom, and Bauder have calculated the SQM force field for nitric acid using the 4-21 basis set [74]. Their reference geometry was derived by combining ab initio bond length and bond angle differences with observed rotational constants to give a modified r_S type structure. The ab initio force field was scaled with eight scale factors and the fundamental frequencies calculated with the scaled force field show good agreement with the observed fundamental frequencies.

As a further test of their scaled force field, Ghosh and coworkers calculated centrifugal distortion constants [74]. Their theoretical constants show excellent agreement with the observed centrifugal distortion constants while centrifugal distortion constants calculated from either of the experimentally derived force fields do not agree with the observed centrifugal distortion constants indicating the SQMFF is superior to either experimental force field.

Table 4-18 gives the definitions of the internal coordinates used in this study and Table 4-19 shows the ab initio force field in terms of these internal coordinates. The estimated r_e geometry was used as the reference geometry for determining the ab initio force field. The ab initio, SQM, and experimental fundamental frequencies are shown in

Table 4-20. The SQM fundamental frequencies were determined by scaling the ab initio force field with the seven scale factors shown in Table 4-21. Ghosh and coworkers scaled their ab initio force field with eight scale factors [74] and their SQM fundamental frequencies show better agreement with the observed fundamental frequencies, the average error is 0.8 per cent, than the scaled force field reported in this work which gives frequencies with an average error of 1.1 per cent. Table 4-22 compares the experimental centrifugal distortion constants with those calculated by Ghosh et al [74] and in this work. Again the force field of Ghosh and coworkers is seen to be a better description of the nitric acid molecule than the SQMFF reported in this work.

PYRAZOLE

Pyrazole is a planar five membered ring and belongs to the C_s symmetry group. Fifteen of the twenty-one normal coordinates are in-plane motions and have A' symmetry; the remaining six normal coordinates are out-of-plane motions and have A" symmetry. Figure 4-5 shows the atom numbering scheme used in the following discussion. Table 4-23 shows an estimate of the r_e geometry determined experimentally by Nygaard and coworkers [75], the ab initio geometry and the theoretical estimated r_e geometry. The experimental r_e geometry is derived from an extremely thorough microwave study in which the differences between the r_s and r_e geometries were estimated [86].

Zechina and coworkers studied the vapor, solution and solid infra-red spectra of pyrazole and assigned 19 fundamental frequencies [76]. They were unable to locate fundamental frequencies for one of the ring stretching modes and one of the CH stretching modes. King studied the infrared spectrum of argon matrix isolated pyrazole and assigned 17 fundamental frequencies [77]. He did not assign fundamental frequencies for the same ring stretching mode as Zechina et al. or for any of the CH stretching frequencies.

Fan and Boggs calculated the pyrazole force field and fundamental frequencies using the 4-21 basis set and the SQM force field method outlined in Chapter 2 [51]. They used the experimental estimate of the r_e geometry as the reference geometry for calculation of the force field. The ab initio force field was scaled with ten scale factors, identical scale factors were used for the CN and NN stretching coordinates, and the resulting fundamental frequencies had a mean deviation of 6.7 cm^{-1} from the experimental frequencies.

In this study the corrected ab initio geometry shown in column three of Table 4-23 was used as the reference geometry for calculation of the force field to maintain consistency with the calculations described above. Table 4-24 shows the definitions of the internal coordinates. They are identical to the ones used by Fan and Boggs [51] except for a renumbering of the atoms. Table 4-25 shows the in-plane ab initio force field and Table 4-26 shows the out-of-plane ab initio force field. Table 4-27 shows the ab initio, SQM and experimental fundamental frequencies for pyrazole. The SQM frequencies were obtained after scaling the ab initio force field with the eleven scale factors shown in Table 4-28 and they have a mean deviation of 9.7 cm^{-1} from the experimental frequencies.

The higher deviation of the scaled fundamental frequencies in this study compared to the scaled fundamental frequencies of Fan and Boggs is surprising because this study includes more scale factors in the least squares fitting procedure. The poorer agreement seen in this study is probably caused by the difference in reference geometries. The theoretical and experimental [75] estimates of the r_e geometry are similar except for the N1-C3 bond length which is 0.014 angstroms shorter in the theoretical r_e structure. This shorter bond length leads to an ab initio N1-C3 force constant that is significantly larger than the value determined by Fan and Boggs, 8.99 versus 8.04 mdyne/Å [51]. All of the other diagonal bond stretching force constants agree to within 0.25 mdyne/Å. In a strongly coupled ring system, the SQM scale factors cannot completely correct for this artificial shortening of the N1-C3 bond. The short N1-C3 bond length in the theoretical estimate of the r_e structure is presumably incorrect and may be caused by limitations of the 4-21NO* basis set.

The pyrazole scale factors calculated in this work are similar to those of Fan and Boggs [51] except for the NH wagging scale factor. The large difference in NH scale factors, 1.186 in this work compared to 0.497 in the earlier work, is caused by the differences in the two basis sets. The 4-21NO* basis set gives a different description of the electronic environment around nitrogen than does the 4-21 basis set and hence one should not expect similar bending or wagging scale factors for the 4-21 and 4-21NO* basis sets.

SUMMARY

In the preceding sections of this chapter, optimum SQM force field scale factors were calculated for five molecules. Effective scale factors are calculated by averaging the optimum scale factors, if possible, from different molecules. These effective scale factors, shown in Table 4-29, are not as accurate as the optimum scale factors for each molecule, but they eliminate bias caused by anharmonic effects in a single molecule. The mean deviation of fundamental frequencies calculated with the effective scale factors is about 15 cm^{-1} compared to a mean deviation of about 10 cm^{-1} for fundamental frequencies calculated with the optimum scale factors.

The effective scale factors shown in Table 4-29 cover all of the bond types that are examined in later Chapters. Unfortunately, scale factors were not calculated for all of the bending modes that will be examined. If scale factor has not been calculated for a bending mode, an assumed value of 0.8 will be used. Scale factors derived with the 4-21 basis set [19,49,51] will be used for C-C bonds. The correction factors determined in this chapter and in Chapter Three should provide us with a method for calculating the molecular internal partition function, equation 2-27, to an accuracy of about one or two per cent.

TABLE 4-1

METHANOL GEOMETRIES[a]

	exp[b]	r_{ab}[c]	r_{corr}[d]
C1-O2	1.421	1.421	1.421
O2-H3	0.963	0.960	0.956
C1-H4	1.094	1.081	1.086
C1-H5(6)	1.094	1.086	1.091
C1-O2-H3	108.0	106.8	106.8
H4-O2-C1	108.0	107.0	107.0
H4-C1-H5	108.5	108.3	108.3
H5-C1-H6		108.6	108.6

a. Bond lengths in angstroms. Bond angles in degrees.

b. Experimental r_s geometry from reference 52.

c. Ab initio geometry calculated with the 4-21NO* basis set.

d. Ab initio geometry corrected for basis set effects as described in Chapter Three.

TABLE 4-2

DEFINITION OF INTERNAL COORDINATES FOR METHANOL

No.	Internal coordinate	Description
1	R(1,2)	C-O stretch
2	R(2,3)	O-H stretch
3	R(1,4)	C-H stretch
4	R(1,5)	C-H stretch
5	R(1,6)	C-H stretch
6	<(1,2,3)	C-O-H bend
7	<(5,1,6)+<(5,1,4)+<(6,1,4)-<(4,1,2)-<(6,1,2)-<(5,1,2)	Methyl symmetric deformation
8	2*(<(5,1,6))-<(5,1,4)-<(6,1,4)	Methyl anti-symmetric Deformation
9	2*(<(4,1,2))-<(6,1,2)-<(5,1,2)	Methyl rock
10	<(5,1,4)-<(6,1,4)	Methyl anti-symmetric Deformation
11	<(6,1,2)-<(5,1,2)	Methyl rock
12	T(4,1,2,3)+T(5,1,2,3)+T(6,1,2,3)	Methyl torsion

TABLE 4-3

METHANOL AB INITIO FORCE FIELD[a]

Q1	6.36											
Q2	0.00	8.99										
Q3	0.17	-0.04	5.64									
Q4	0.25	0.00	0.06	5.40								
Q5	0.25	0.00	0.06	0.08	5.40							
Q6	0.46	0.15	0.03	0.00	0.00	0.99						
Q7	-0.60	0.01	0.08	0.09	0.09	-0.04	0.81					
Q8	0.00	-0.01	-0.17	0.09	0.09	0.01	-0.01	0.76				
Q9	0.01	0.06	0.09	-0.04	-0.04	0.14	0.01	-0.09	1.03			
Q10	0.00	0.00	0.00	0.15	-0.15	0.00	0.00	0.00	0.00	0.74		
Q11	0.00	0.00	0.00	-0.06	0.06	0.00	0.00	0.00	0.00	-0.04	0.96	
Q12	0.00	0.00	0.00	0.00	0.00	0.00	0.00	0.00	0.00	0.00	-0.01	0.02
	Q1	Q2	Q3	Q4	Q5	Q6	Q7	Q8	Q9	Q10	Q11	Q12

a. Energy in aJ, coordinates in Å and radian. Internal coordinates defined in Table 4-2.

TABLE 4-4

SCALED QUANTUM MECHANICAL FORCE FIELD SCALE FACTORS FOR METHANOL

Mode	CH_3OH	CD_3OH	CH_3OD	CD_3OD	Avg.
CO Stretch	0.855	0.844	0.809	0.867	0.844
OH Stretch	0.843	0.843	0.867	0.866	0.855
CH Stretch	0.870	0.887	0.869	0.889	0.879
COH Bend	0.724	0.756	0.790	0.781	0.763
CH_3 Deformation	0.772	0.767	0.773	0.751	0.766
CH_3 Rock	0.835	0.865	0.823	0.857	0.845
CH_3 Torsion	0.580	0.588			0.584

TABLE 4-5

METHANOL FUNDAMENTAL VIBRATION FREQUENCIES^a

No.	Sym.	Assignment	CH_3OH ab initio^b	CH_3OH Scaled^c	CH_3OH Expt.^{d}	CD_3OH ab initio^b	CD_3OH Scaled^c	CD_3OH Expt.^{d}	CH_3OD ab initio^b	CH_3OD Scaled^c	CH_3OD Expt.^{d}	CD_3OD ab initio^b	CD_3OD Scaled^c	CD_3OD Expt.^{d}
1	A"	C-O Torsion	357	272	272^e	337	259	259^e	283	222^f	N/A	259	197^g	N/A
2	A'	COH Bend/CH3 Rock	1148	1030	1034	923	852	853	966	863	864	846	765	775
3	A'	C-O Stretch	1170	1075	1075	966	899	898^e	1153	1038	1038^e	966	894	895^e
4	A"	CH3 Rock	1255	1145	1145	1077	973	985	1255	1137	1142	1068	967	980
5	A'	COH Bend/CH3 Rock	1536	1336	1334^e	1215	1064	1068^e	1364	1230	1225	1181	1053	1028
6	A'	CH3 Deformation	1635	1436	1454	1220	1069	1068^e	1635	1437	1455	1215	1055	1069
7	A"	CH3 Deformation	1676	1475	1465	1284	1143	1129	1676	1475	1463	1231	1079	1078
8	A'	CH3 Deformation	1688	1487	1478	1479	1296	1296	1687	1486	1479	1285	1145	1134
9	A'	C-H Stretch	3100	2891	2844	2225	2095	2074	2920	2718	2718	2225	2098	2074
10	A"	C-H Stretch	3143	2932	2970	2331	2195	2212	3100	2890	2841	2331	2198	2213
11	A'	C-H Stretch	3206	2990	2999	2376	2237	2242	3143	2931	2970	2375	2239	2250
12	A'	O-H Stretch	4011	3682	3682	4010	3683	3683	3207	2990	3001	2920	2717	2717

a. Frequencies given in cm^{-1}.

b. Fundamental vibrational frequencies calculated from the ab initio force field.

c. Fundamental vibrational frequencies calculated from the Scaled Quantum Mechanical Force Field.

d. Experimental gas phase fundamental vibrational frequencies from reference 53.

e. Experimental argon matrix fundamental vibrational frequency from reference 53.

f. Scale factor fixed at 0.616.

g. Scale factor fixed at 0.5801.

TABLE 4-6

METHYL AMINE GEOMETRIES[a]

	exp[b]	r_{ab}[c]	r_{corr}[d]
C1-N2	1.471	1.474	1.469
N2-H3(4)	1.010	1.010	1.010
C1-H5	1.099	1.089	1.094
C1-H6(7)	1.099	1.083	1.088
C1-N2-H3(4)	110.3	108.3	108.3
H3-N2-H4	107.1	105.2	105.2
H5-C1-N2	110.3	114.8	114.8
H5-C1-H6(7)	108.0	108.1	108.1
H6-C1-H7	108.0	107.7	107.7

a. Bond lengths in angstroms. Bond angles in degrees.

b. Experimental r_s geometry from reference 54.

c. Ab initio geometry calculated with the 4-21NO* basis set.

d. Ab initio geometry corrected for basis set effects as described in Chapter Three.

TABLE 4-7

DEFINITION OF INTERNAL COORDINATES FOR METHYLAMINE

No.	Internal coordinate	Description
1	R(1,2)	C-N stretch
2	R(2,3)	N-H stretch
3	R(2,4)	N-H stretch
4	R(1,5)	C-H stretch
5	R(1,6)	C-H stretch
6	R(1,7)	C-H stretch
7	2*<(4,2,3)-<(3,2,1)-<(4,2,1)	NH_2 deformation
8	<(3,2,1)-<(4,2,1)	NH_2 deformation
9	d(1,4,3,2)[a]	NH_2 wag
10	<(6,1,7)+<(5,1,6)+<(5,1,7)- <(5,1,2)-<(7,1,2)-<(6,1,2)	CH_3 deformation
11	2*<(6,1,7)-<(5,1,6)-<(5,1,7)	CH_3 deformation
12	<(5,1,6)-<(5,1,7)	CH_3 deformation
13	2*<(5,1,2)-<(7,1,2)-<(6,1,2)	CH_3 wag
14	<(7,1,2)-<(6,1,2)	CH_3 wag
15	T(5,1,2,3)[b]+T(6,1,2,3)+T(7,1,2,3) T(5,1,2,4)+T(6,1,2,4)+T(7,1,2,4)	CH_3 torsion

[a] d(a,b,c,d) is defined by motion of atom a out of the plane defined by atoms b, c and d. Atom d is the central atom in the group.

[b] T(a,b,c,d) is defined as the angle between the abc and bcd planes.

TABLE 4-8

METHYLAMINE AB INITIO FORCE FIELD[a]

Q1	5.88														
Q2	0.05	7.39													
Q3	0.05	0.01	7.39												
Q4	0.22	0.01	0.01	5.30											
Q5	0.14	0.01	-0.03	0.07	5.58										
Q6	0.14	-0.03	0.01	0.07	0.06	5.58									
Q7	-0.13	0.21	0.21	-0.01	-0.02	-0.02	0.93								
Q8	0.00	0.08	-0.08	0.00	-0.03	0.03	0.00	0.98							
Q9	-0.42	-0.22	-0.22	0.02	-0.01	-0.01	-0.20	0.00	0.54						
Q10	-0.52	-0.01	-0.01	0.11	0.09	0.09	0.03	0.00	0.02	0.77					
Q11	0.00	0.00	0.00	-0.17	0.08	0.08	0.00	0.00	0.00	0.01	0.73				
Q12	0.00	-0.01	0.01	0.00	0.14	-0.14	0.00	0.01	0.00	0.00	0.00	0.76			
Q13	-0.01	-0.04	-0.04	0.07	-0.05	-0.05	0.04	0.00	0.05	-0.01	-0.03	0.00	0.93		
Q14	0.00	0.04	-0.04	0.00	-0.09	0.09	0.00	0.18	0.00	0.00	0.00	-0.07	0.00	0.96	
Q15	0.00	0.00	0.00	0.00	0.00	0.00	0.00	-0.01	0.00	0.00	0.00	0.00	0.00	0.01	0.01
	Q1	Q2	Q3	Q4	Q5	Q6	Q7	Q8	Q9	Q10	Q11	Q12	Q13	Q14	Q15

a. Energy in aJ, coordinates in Å and radian. Internal coordinates defined in Table 4-7.

TABLE 4-9

SCALED QUANTUM MECHANICAL FORCE FIELD SCALE FACTORS FOR METHYLAMINE

Mode	Scale Factor
CN Stretch	0.849
NH Stretch	0.866
CH Stretch	0.859
NH_2 Deformation	0.768
NH_2 Wag	0.551
CH_3 Deformation	0.778
CH_3 Rock	0.793
CH_3 Torsion	0.564

TABLE 4-10

METHYLAMINE FUNDAMENTAL VIBRATION FREQUENCIES[a]

No.	Sym.	Assignment	ab initio[b]	Scaled[c]	Expt.[d]
1	A"	CH_3 torsion	351	264	264
2	A'	NH_2 wag	1015	780	780
3	A"	CH_3 rock	1067	944	972[e]
4	A'	CN stretch	1136	1044	1044
5	A'	CH_3 rock	1314	1129	1130
6	A"	NH_2 deformation	1507	1327	1335[e]
7	A'	CH_3 deformation	1615	1424	1430
8	A'	CH_3 deformation	1673	1476	1474
9	A"	CH_3 deformation	1688	1490	1485
10	A'	NH_2 deformation	1845	1623	1623
11	A'	CH stretch	3088	2863	2820
12	A'	CH stretch	3168	2936	2962
13	A"	CH stretch	3200	2966	2985
14	A'	NH stretch	3613	3361	3360
15	A"	NH stretch	3679	3423	3424

a. Frequencies given in cm^{-1}.

b. Fundamental vibrational frequencies calculated from the ab initio force field.

c. Fundamental vibrational frequencies calculated from the Scaled Quantum Mechanical Force Field.

d. Experimental gas phase fundamental vibrational frequencies from reference 65.

e. Experimental assignment uncertain. See text for discussion.

TABLE 4-11

NITROMETHANE GEOMETRIES[a]

	exp[b]	r_{ecl}[c]	r_{sta}[d]	r_{cecl}[e]	r_{csta}[f]
C1-N2	1.489	1.496	1.491	1.489	1.484
N2-O3	1.224	1.193	1.194	1.220	1.221
N2-O4	1.224	1.194	1.194	1.221	1.221
C1-H5	1.088	1.074	1.080	1.079	1.085
C1-H6	1.088	1.078	1.075	1.083	1.080
C1-H7	1.088	1.078	1.075	1.083	1.080
<C1-N2-O3	117.4	117.3	116.4	117.3	116.4
<C1-N2-O4	117.4	115.8	116.4	115.8	116.4
<H5-C1-N2	107.2	108.5	106.9	108.5	106.9
<H6-C1-N2	107.2	107.1	108.0	107.1	108.0
<H5-C1-H6	107.2	112.1	110.5	112.1	110.5
<H6-C1-H7	107.2	109.7	112.8	109.7	112.8

a. Bond lengths in Å. Bond angles in degrees.

b. Experimental r_s geometry from reference 66.

c. Eclipsed, N2-O3 parallel to C1-H5, nitromethane ab initio geometry calculated with the 4-21NO* basis set.

d. Staggered, N2-O3 perpendicular to C1-H5, nitromethane geometry calculated with the 4-21NO* basis set.

e. Eclipsed nitromethane ab initio geometry corrected for basis set effects as described in Chapter Three.

f. Staggered nitromethane ab initio geometry corrected for basis set effects as described in Chapter Three.

TABLE 4-12

DEFINITION OF INTERNAL COORDINATES FOR NITROMETHANE

No.	Internal coordinate	Description
1	R(1,2)	C-N stretch
2	R(2,3)	N-O stretch
3	R(2,4)	N-O stretch
4	R(1,5)	C-H stretch
5	R(1,6)	C-H stretch
6	R(1,7)	C-H stretch
7	2*<(4,2,3)-<(3,2,1)-<(4,2,1)	NO_2 deformation
8	<(3,2,1)-<(4,2,1)	NO_2 deformation
9	d(1,4,3,2)[a]	NO_2 wag
10	<(6,1,7)+<(5,1,6)+<(5,1,7)- <(5,1,2)-<(7,1,2)-<(6,1,2)	CH_3 deformation
11	2*<(6,1,7)-<(5,1,6)-<(5,1,7)	CH_3 deformation
12	<(5,1,6)-<(5,1,7)	CH_3 deformation
13	2*<(5,1,2)-<(7,1,2)-<(6,1,2)	CH_3 rock
14	<(7,1,2)-<(6,1,2)	CH_3 rock
15	T(5,1,2,3)[b]+T(6,1,2,3)+T(7,1,2,3) T(5,1,2,4)+T(6,1,2,4)+T(7,1,2,4)	CH_3 torsion

a. d(a,b,c,d) is defined by motion of atom a out of the plane defined by atoms b, c and d. Atom d is the central atom in the group.

b. T(a,b,c,d) is defined as the angle between the abc and bcd planes.

TABLE 4-13

STAGGERED NITROMETHANE AB INITIO FORCE FIELD[a]

	Q1	Q2	Q3	Q4	Q5	Q6	Q7	Q8	Q9	Q10	Q11	Q12	Q13	Q14	Q15
Q1	4.89														
Q2	0.47	10.7													
Q3	0.47	1.93	10.7												
Q4	0.07	-0.01	-0.01	5.75											
Q5	0.00	0.03	-0.01	0.04	5.93										
Q6	0.00	-0.01	0.03	0.04	0.02	5.93									
Q7	-0.32	0.23	0.23	0.00	0.01	0.01	1.62								
Q8	0.00	0.40	-0.40	0.00	-0.11	0.11	0.00	1.18							
Q9	0.03	-0.01	-0.01	0.03	-0.01	-0.01	-0.02	0.00	0.57						
Q10	-0.49	-0.06	-0.06	0.06	0.06	0.06	0.05	0.00	-0.01	0.79					
Q11	0.03	0.00	0.00	-0.15	0.06	0.06	-0.01	0.00	0.01	-0.01	0.64				
Q12	0.00	0.02	-0.02	0.00	0.11	-0.11	0.00	0.04	0.00	0.00	0.00	0.64			
Q13	-0.05	-0.03	-0.03	0.11	-0.05	-0.05	0.03	0.00	0.11	-0.01	0.00	0.00	0.86		
Q14	0.00	0.03	-0.03	0.00	-0.07	0.07	0.00	0.18	0.00	0.00	0.00	0.01	0.00	0.88	
Q15	0.00	0.00	0.00	0.00	-0.01	0.01	0.00	0.02	0.00	0.00	0.00	0.02	0.00	-0.01	0.001

ECLIPSED NITROMETHANE AB INITIO FORCE FIELD[a]

	Q1	Q2	Q3	Q4	Q5	Q6	Q7	Q8	Q9	Q10	Q11	Q12	Q13	Q14	Q15
Q1	4.89														
Q2	0.45	10.8													
Q3	0.49	1.94	10.6												
Q4	-0.01	0.04	-0.01	5.97											
Q5	0.05	-0.01	0.01	0.03	5.83										
Q6	0.05	-0.01	0.01	0.03	0.04	5.83									
Q7	-0.32	0.24	0.22	0.01	0.00	0.00	1.62								
Q8	0.01	0.42	-0.39	-0.12	0.07	0.07	-0.02	1.18							
Q9	0.00	0.00	0.00	0.00	-0.03	0.03	0.00	0.00	0.57						
Q10	-0.49	-0.06	-0.06	0.06	0.06	0.06	0.05	-0.01	0.00	0.79					
Q11	-0.04	-0.02	0.02	-0.11	0.07	0.07	0.01	-0.04	0.00	0.01	0.64				
Q12	0.00	0.00	0.00	0.00	0.12	-0.12	0.00	0.00	0.01	0.00	0.00	0.64			
Q13	0.04	0.00	0.06	0.08	-0.04	-0.04	-0.03	-0.18	0.00	0.01	0.01	0.00	0.88		
Q14	0.00	0.00	0.00	0.00	-0.09	0.09	0.00	0.00	0.11	0.00	0.00	0.00	0.00	0.86	
Q15	0.00	0.00	0.00	0.00	0.01	-0.01	0.00	0.00	-0.02	0.00	0.00	-0.02	0.00	0.01	0.002

a. Energy in aJ, coordinates in Å and radians. Internal coordinates defined in Table 5-15.

TABLE 4-14

SCALED QUANTUM MECHANICAL FORCE FIELD SCALE FACTORS FOR NITROMETHANE

Mode	s-CH_3NO_2	e-CH_3NO_2	e-CD_3NO_2	Avg.
CN Stretch	0.800	0.804	0.805	0.803
NO Stretch	0.919	0.917	0.892	0.909
CH Stretch	0.864	0.864	0.883	0.870
NO_2 Deformation	0.915	0.931	0.924	0.923
NO_2 Wag	0.831	0.804	0.811	0.815
CH_3 Deformation	0.763	0.762	0.788	0.771
CH_3 Rock	0.821	0.823	0.829	0.824

TABLE 4-15

STAGGERED NITROMETHANE FUNDAMENTAL VIBRATION FREQUENCIES[a]

No.	Sym.	Assignment	ab initio[b]	Scaled[c]	Expt.[d]
1	A"	CH_3 torsion	-31[e]	-31[f]	N/A[g]
2	A"	NO_2 deformation	502	478	476
3	A'	NO_2 wag	659	602	603
4	A'	CN stretch/NO_2 def.	704	654	657
5	A'	CN stretch/NO_2 def.	992	922	918
6	A"	CH_3 rock	1192	1090	1099
7	A'	CH_3 rock	1247	1128	1119
8	A'	CH_3 deformation	1506	1364	1378
9	A"	CH_3 deformation	1562	1414	1397
10	A'	NO stretch/CH_3 def.	1602	1423	1428
11	A'	NO stretch/CH_3 def.	1634	1438	1438[h]
12	A"	NO stretch	1678	1586	1584
13	A'	CH stretch	3190	2965	2974
14	A'	CH stretch	3279	3049	3044
15	A"	CH stretch	3318	3084	3080

a. Frequencies given in cm^{-1}.

b. Fundamental vibrational frequencies calculated from the ab initio force field.

c. Fundamental vibrational frequencies calculated from the Scaled Quantum Mechanical Force Field.

d. Unless noted otherwise experimental gas phase fundamental vibration frequencies from reference 67.

e. Imaginary frequency. See text for discussion.

f. Scale factor fixed at 1.0.

g. Fundamental not observed in the experimental spectra.

h. Experimental argon matrix isolated fundamental frequency from reference 67.

TABLE 4-16

ECLIPSED NITROMETHANE FUNDAMENTAL VIBRATION FREQUENCIES[a]

No.	Sym.	Assignment	CH_3NO_2 Scaled[b]	CH_3NO_2 Expt.[c]	CD_3NO_2 Scaled[b]	CD_3NO_2 Expt.[c]
1	A"	CH_3 torsion	28[d]	N/A[e]	20[d]	N/A[e]
2	A'	NO_2 deformation	478	476	426	426
3	A"	NO_2 wag	602	603	538	542
4	A'	CN stretch/NO2 def.	653	657	617	625
5	A'	CN stretch/NO2 def.	924	918	880	883
6	A'	CH_3 rock	1091	1099	896	894
7	A"	CH_3 rock	1126	1119	948	941
8	A'	CH_3 deformation	1363	1378	1041	1038[f]
9	A'	CH_3 deformation	1413	1397	1047	1046[f]
10	A"	CH_3 deformation	1430	1428	1077	1081
11	A'	NO stretch	1432	1438[f]	1415	1388
12	A'	NO stretch	1586	1584	1550	1572
13	A'	CH stretch	2968	2974	2149	2152[g]
14	A"	CH stretch	3047	3044	2284	2283
15	A'	CH stretch	3084	3080	2317	2315

a. Frequencies given in cm^{-1}.

b. Fundamental vibrational frequencies calculated from the Scaled Quantum Mechanical Force Field.

c. Unless noted otherwise experimental gas phase fundamental vibration frequencies from reference 78.

d. Scale factor fixed at 1.0.

e. Fundamental not observed in the experimental spectra.

f Experimental argon matrix isolated fundamental frequency from reference 67.

g. Suggested assignment of McKean and Watt from reference 67.

TABLE 4-17

NITRIC ACID GEOMETRIES[a]

	exp[b]	r_{ab}[c]	r_{corr}[d]
N1-O2	1.406	1.351	1.405
O2-H3	0.964	0.968	0.964
N1-O4	1.199	1.174	1.198
N1-O5	1.211	1.188	1.215
<N1-O2-H3	102.1	102.9	102.9
<O4-N1-O2	113.9	114.4	114.4
<O5-N1-O2	115.9	115.5	115.5

a. Bond lengths in angstroms. Bond angles in degrees.

b. Experimental r_s geometry from reference 71.

c. Ab initio geometry calculated with the 4-21NO* basis set.

d. Ab initio geometry corrected for basis set effects as described in Chapter Three.

TABLE 4-18

DEFINITION OF INTERNAL COORDINATES FOR NITRIC ACID

No.	Internal coordinate	Description
1	R(1,2)	NO stretch
2	R(2,3)	OH stretch
3	R(1,4)	NO stretch
4	R(1,5)	NO stretch
5	<(3,2,1)	NOH bend
6	2*<(5,1,4)-<(4,1,2)-<(5,1,2)	NO_2 deformation
7	<(4,1,2)-<(5,1,2)	NO_2 deformation
8	d(2,5,4,1)[a]	NO_2 wag
9	T(3,2,1,4)[b]+T(3,2,1,5)	NO torsion

a. (a,b,c,d) is defined by motion of atom a out of the plane defined by atoms b, c and d. Atom d is the central atom in the group.

b. (a,b,c,d) is defined as the angle between the abc and bcd planes.

TABLE 4-19

NITRIC ACID AB INITIO FORCE FIELD[a]

Q1	4.50								
Q2	0.03	8.76							
Q3	0.96	-0.09	11.4						
Q4	1.00	-0.09	2.03	10.0					
Q5	0.42	0.14	0.09	0.13	1.11				
Q6	-0.54	0.06	0.32	0.22	-0.05	1.57			
Q7	0.09	0.11	0.45	-0.52	0.29	0.05	1.53		
Q8	0.00	0.00	0.00	0.00	0.00	0.00	0.00	0.62	
Q9	0.00	0.00	0.00	0.00	0.00	0.00	0.00	0.01	0.065
	Q1	Q2	Q3	Q4	Q5	Q6	Q7	Q8	Q9

a. Energy in aJ, coordinates in Å and radians. Internal coordinates defined in Table 4-18.

TABLE 4-20

NITRIC ACID FUNDAMENTAL VIBRATION FREQUENCIES[a]

No.	Sym.	Assignment	ab initio[b]	Scaled[c]	Expt.[d]
1	A"	NO torsion	521	456	456
2	A'	NO2 deformation	591	574	579
3	A'	NO stretch/NO2 def.	686	634	647
4	A"	NO2 wag	839	762	762
5	A'	NO2 def./NO stretch	965	901	879
6	A'	NO stretch/NOH bend	1361	1307	1324
7	A'	NO stretch/NOH bend	1415	1358	1330
8	A'	NO stretch/NOH bend	1768	1698	1708
9	A'	OH stretch	3956	3550	3550

a. Frequencies given in cm^{-1}.

b. Fundamental vibrational frequencies calculated from the ab initio force field.

c. Fundamental vibrational frequencies calculated from the Scaled Quantum Mechanical Force Field.

d. Experimental gas phase fundamental vibrational frequencies from references 72 and 73.

TABLE 4-21

SCALED QUANTUM MECHANICAL FORCE FIELD SCALE FACTORS FOR NITRIC ACID

Mode	Scale Factor
N-O stretch	0.785
OH stretch	0.805
N=O stretch	0.940
NOH bend	0.887
NO_2 deformation	0.943
NO_2 wag	0.825
NO torsion	0.766

TABLE 4-22

NITRIC ACID CENTRIFUGAL DISTORTION CONSTANTS

	Exp.[a]	Blom[a]	This work
Δ_J	14.00	14.50	14.82
Δ_{JK}	-20.17	-21.13	-21.82
Δ_K	7.44	7.98	8.41
δ_J	-1.18	-1.02	-1.25
δ_K	20.57	18.01	12.57

a. Reference 74.

TABLE 4-23

PYRAZOLE GEOMETRIES[a]

	exp[b]	r_{ab}[c]	r_{corr}[d]
N1-N2	1.351	1.335	1.347
N1-C3	1.333	1.309	1.319
N2-C4	1.359	1.353	1.359
C3-C5	1.415	1.416	1.421
C4-C5	1.380	1.363	1.377
N2-H6	0.997	0.998	0.998
C3-H7	1.077	1.067	1.072
C4-H8	1.076	1.066	1.071
C5-H9	1.075	1.064	1.069
<N1-N2-C4	113.1	113.0	112.9
<N1-C3-C5	111.9	111.8	111.8
<N2-N1-C3	104.2	104.5	104.7
<N2-C4-C5	106.3	106.2	106.2
<C3-C5-C4	104.5	104.3	104.4
<N1-C3-H7	119.7	120.5	120.4
<N1-N2-H6	118.7	119.3	119.4
<N2-C4-H8	121.4	122.3	122.3
<C3-C5-H9	127.9	127.9	127.9

a. Bond lengths in Å. Bond angles in degrees.

b. Experimental estimated r_e geometry from reference 75.

c. Ab initio geometry calculated with the 4-21NO* basis set.

d. Ab initio geometry corrected for basis set effects as described in Chapter Three.

TABLE 4-24

DEFINITION OF INTERNAL COORDINATES FOR PYRAZOLE

No.	Internal coordinate	Description
1	R(2,6)	NH Stretch
2	R(4,8)	CH Stretch
3	R(5,9)	CH Stretch
4	R(3,7)	CH Stretch
5	R(4,2)	CN Stretch
6	R(4,5)	CC Stretch
7	R(3,5)	CC Stretch
8	R(3,1)	CN Stretch
9	R(1,2)	NN Stretch
10	<(1,2,6)-<(4,2,6)	NH Deformation
11	<(2,4,8)-<(5,4,8)	CH Deformation
12	<(4,5,9)-<(3,5,9)	CH Deformation
13	<(5,3,7)-<(1,3,7)	CH Deformation
14	<(1,2,4)-a*<(2,4,5)-a*<(2,1,3) +b*<(4,5,3)+b*<(5,3,1)	Ring Deformation[a]
15	(a-b)*(<(2,1,3)-<(2,4,5)) +(1-a)*(<(4,5,3)-<(5,3,1))	Ring Deformation
16	d(6,4,1,2)[b]	NH Wag
17	d(8,5,2,4)	CH Wag
18	d(9,4,3,5)	CH Wag
19	d(7,5,1,3)	CH Wag
20	b*T(1,2,4,5)[c]+b*T(3,1,2,4) -a*T(2,4,5,3)-a*T(5,3,1,2)+T(4,5,3,1)	Ring Torsion[a]
21	(a-b)*(T(2,4,5,3)-T(5,3,1,2)) +(1-a)*(T(3,1,2,4)-T(1,2,4,5))	Ring Torsion

a. a=cos(144°); b=cos(72°).

b. d(a,b,c,d) is defined by motion of atom a out of the plane defined by atoms b, c and d. Atom d is the central atom in the group.

c. T(a,b,c,d) is defined as the angle between the abc and bcd planes.

TABLE 4-25

IN-PLANE PYRAZOLE AB INITIO FORCE FIELD[a]

Q1	8.25														
Q2	0.01	6.25													
Q3	0.00	0.01	6.32												
Q4	0.00	0.00	0.01	6.19											
Q5	0.05	0.08	-0.01	-0.05	7.56										
Q6	-0.05	0.03	0.04	0.00	0.88	7.96									
Q7	0.01	0.00	0.04	0.05	-0.45	0.75	6.35								
Q8	-0.07	-0.05	-0.01	0.15	0.50	-0.34	0.97	8.99							
Q9	0.11	-0.04	-0.06	-0.04	0.51	0.34	-0.16	0.72	6.73						
Q10	-0.01	-0.01	0.00	0.01	-0.07	0.02	-0.02	-0.02	0.18	0.59					
Q11	0.00	0.02	0.00	-0.01	0.21	-0.07	0.02	-0.02	-0.06	0.01	0.54				
Q12	0.00	0.00	0.01	0.00	-0.02	0.15	-0.11	0.01	0.00	-0.01	0.01	0.52			
Q13	0.00	0.00	0.00	-0.01	0.04	-0.01	0.11	-0.24	-0.01	-0.02	-0.01	0.01	0.58		
Q14	-0.10	0.11	-0.04	-0.05	0.05	-0.61	0.63	-0.67	-0.02	-0.05	0.09	-0.08	0.09	2.32	
Q15	0.00	0.08	-0.15	0.14	-0.67	0.39	0.10	-0.27	0.87	0.10	-0.04	0.03	-0.03	-0.05	2.17
	Q1	Q2	Q3	Q4	Q5	Q6	Q7	Q8	Q9	Q10	Q11	Q12	Q13	Q14	Q15

a. Energy in aJ, coordinates in Å and radian. Internal coordinates defined in Table 4-24.

TABLE 4-26

OUT-OF-PLANE PYRAZOLE AB INITIO FORCE FIELD[a]

Q16	0.19					
Q17	-0.03	0.51				
Q18	-0.04	0.07	0.51			
Q19	-0.04	-0.01	-0.04	0.57		
Q20	0.00	-0.16	-0.24	0.26	0.66	
Q21	-0.23	0.19	0.11	0.11	-0.04	0.61
	Q16	Q17	Q18	Q19	Q20	Q21

a. Energy in aJ, coordinates in Å and radian. Internal coordinates defined in Table 4-24.

TABLE 4-27

PYRAZOLE FUNDAMENTAL VIBRATION FREQUENCIES[a]

No.	Sym.	Assignment	ab initio[b]	Scaled[c]	Expt.[d]
1	A"	NH wag	499	505	515
2	A"	Ring torsion	699	614	612
3	A"	Ring torsion	745	676	668
4	A"	CH wag	874	736	744
5	A"	CH wag	997	840	833
6	A"	CH wag	1048	878	879
7	A'	Ring deformation	1007	917	910
8	A'	Ring deformation	1012	923	931
9	A'	CH deformation	1101	1023	1021
10	A'	CH deformation	1115	1044	1057
11	A'	NH deformation	1184	1101	1121
12	A'	Ring stretching[e]	1235	1156	1164[f]
13	A'	CH deformation	1365	1257	1253
14	A'	Ring stretching	1469	1363	1359
15	A'	Ring stretching	1507	1386	1394
16	A'	Ring stretching	1573	1449	1446
17	A'	Ring stretching	1681	1558	1530
18	A'	CH stretch	3361	3084	3074
19	A'	CH stretch	3379	3100	3090[f]
20	A'	CH stretch	3410	3130	3140
21	A'	NH stretch	3863	3500	3500[g]

a. Frequencies given in cm^{-1}.

b. Fundamental vibrational frequencies calculated from the ab initio force field.

c. Fundamental vibrational frequencies calculated from the Scaled Quantum Mechanical Force Field.

d. Unless noted otherwise experimental gas phase fundamental vibrational frequencies from reference 76.

e. Combination of the ring CC, CN and NN stretching modes.

f. Frequency predicted in reference 51. Frequency omitted from the least squares fit.

g. Fundamental frequency assignment from reference 51.

TABLE 4-28

SCALED QUANTUM MECHANICAL FORCE FIELD SCALE FACTORS FOR PYRAZOLE

Mode	Scale Factor
CH stretch	0.842
CH deformation	0.816
CH wag	0.706
CC stretch	0.927
CN stretch	0.884
NN stretch	0.888
Ring deformation	0.828
Ring torsion	0.745
NH stretch	0.821
NH deformation	0.803
NH wag	1.186

TABLE 4-29

EFFECTIVE SCALED QUANTUM MECHANICAL FORCE FIELD SCALE FACTORS FOR THE 4-21NO* BASIS SET

Mode	Scale Factor
CH stretch	0.864
OH stretch	0.845
NH stretch	0.844
CC stretch	0.920[a]
CN stretch (non NO_2)	0.866
CN stretch (NO_2)	0.803
CO stretch	0.844
NN stretch	0.888
N-O stretch	0.785
N=O stretch	0.927
COH bend	0.763
Methyl deformation	0.769
Methyl rock	0.831
Methyl torsion	0.577
NOH bend	0.887
NO2 deformation	0.933
NO2 wag	0.820
NO torsion	0.766
NH2 deformation	0.768
NH2 wag	0.551
CH deformation	0.816
CH wag	0.706
NH deformation	0.803
NH wag	1.186
Ring deformation[b]	0.828
Ring torsion[b]	0.745

[a] Value for the 4-21 basis set taken from reference 19.

[b] Five membered ring.

FIGURE 4-1
Numbering Scheme for Methanol

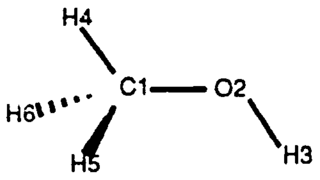
H4
C1
O2
H6
H5
H3

FIGURE 4-2
Numbering Scheme for Methylamine

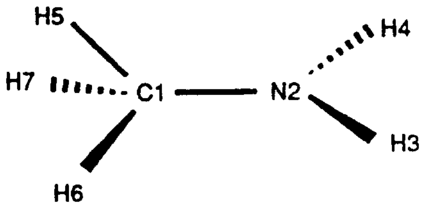
H5
H4
H7
C1
N2
H3
H6

FIGURE 4-3
Numbering Scheme for Nitromethane

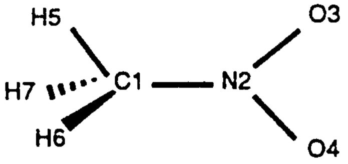
H5
O3
H7
C1
N2
H6
O4

FIGURE 4-4
Numbering Scheme for Nitric Acid

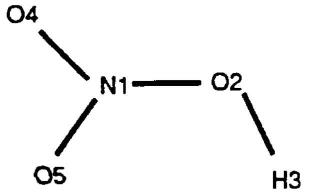
O4
N1
O2
O5
H3

FIGURE 4-5
Numbering Scheme for Pyrazole

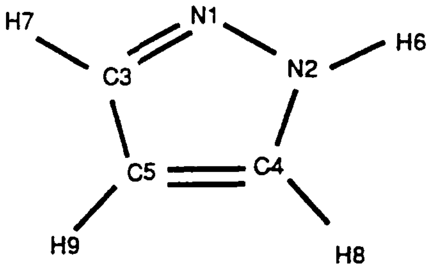
H7
N1
H6
C3
N2
C5
C4
H9
H8

CHAPTER FIVE

Chapters Three and Four derived correction factors that permit estimation of the equilibrium geometry and calculation of fundamental vibration frequencies from the results of ab initio calculations using the 4-21NO* basis set. From these data we can calculate internal molecular partition functions or, equivalently, thermodynamic quantities with the appropriate equations from Chapter 2, but we have not developed a method for calculating E_0, the energy of a molecule relative to some arbitrary definition of zero energy. By convention E_0 is usually defined as the molecular heat of formation at 0 K [3]. By definition the elements have zero energy (E_0 equal to zero) at 0 K if they are in the standard state that exists at 298 K. For polyatomic molecules E_0 includes the zero point vibration energy.

In theoretical calculations zero energy is defined as the energy at infinite separation of the electrons and nuclei and does not include zero point vibration energy. Calculating heats of formation at 0 K and 298 K from the results of single determinant closed shell ab initio calculations has been the subject of several studies [39-41,78]. This Chapter examines three possible methods for calculating E_0 a priori.

Direct Calculation of E_0

Conceptually, direct calculation of E_0 using theoretical methods is simple. To calculate the heat of formation for methylnitrate, we would calculate molecular energies for the atoms and molecules shown in equation 5-1 and then use standard thermodynamic relationships to determine the ab initio heat of formation at 0 K for non-vibrating molecules. Fundamental vibration frequencies for each of the molecules may be calculated using the Scaled Quantum Mechanical Force Field method outlined in Chapter 4. With these frequencies the zero point vibration energy may be calculated and adding this energy to the ab initio heat of formation gives an a priori value for E_0.

$$2C(graphite)+3H_2(g)+3O_2(g)+N_2(g) \rightarrow 2CH_3ONO_2(g) \tag{5-1}$$

Several subtle difficulties stemming from the use of single determinant closed shell calculations preclude application of this method. First, the single determinant SCF method cannot determine accurate energies for open shell ground state species, e.g. the oxygen triplet ground state. Next the electron correlation energy may be different for the reactants and products and this difference should be included to determine an accurate heat of reaction. Finally, solid state ab initio calculations are still in their infancy and accurate calculation of the energy associated with a solid state molecule is difficult. The size of the molecules studied in Chapters 7, 8, and 9 preclude the use of sophisticated methods that have the capability to address the first two problems. As a result, we must adopt a more pragmatic approach to the calculation of E_0 energies. Several studies have examined this problem [39-41,78] and two of the more promising approaches [39-41] are discussed in the remainder of this Chapter.

Isodesmic Reactions

Pople and coworkers have used isodesmic reactions to calculate theoretical heats of reaction [36] in an effort to overcome the problems identified in the previous section. An isodesmic reaction is one in which the number and type of formal bonds are maintained in both the reactants and products, only the relationships between the bonds change. Equation 5-2 is the isodesmic bond separation reaction for methylnitrate. Isodesmic reactions should minimize changes in electron correlation energy and, therefore, closed shell SCF calculations should produce reaction energies that agree with experimental reaction energies. Using the 4-31G basis set, Pople calculated a series of theoretical bond separation energies for reactions similar to the one shown in equation 5-2 [39]. The mean deviation between the theoretical and experimental reaction energies was 3.5 kcal/mol after correcting the experimental reaction energies for zero point vibration energies. Based on Pople's work, theoretical isodesmic reaction energies should provide reasonably accurate a priori E_0 energies.

$$CH_3ONO_2(g)+2NH_3(g)+H_2O(g)+H_2(g) \rightarrow CH_3OH(g)+3NH_2OH(g) \qquad (5\text{-}2)$$

Calculating E_0 once we know the bond separation energy for a chemical process analogous to equation 5-2 is a simple task using the method given Chapter 2. Although this procedure is not overly demanding, it does require a large amount of data (fundamental frequencies, several E_0 energies, and several ab initio molecular energies) that may not be available, and in some situations this is a serious deficiency. For example, the complete set of fundamental frequencies is not available for methylamine which may increase the error in heats of reaction calculated for molecules containing C-N bonds. In view of the above, we need to develop another procedure for estimating E_0 for any molecule, not just those for which sufficient data exist.

Atom Equivalents

Wiberg noted that Pople's isodesmic reaction method was essentially a group equivalent method and proposed using atom equivalents to calculate heats of formation at 298 K from ab initio molecular energies [40]. By combining experimental and theoretical data for a series of hydrocarbons, Wiberg calculated group equivalents for CH_3, CH_2, CH, $=CH_2$ and =CH groups for the 6-31G* basis set and with these five constants calculated theoretical heats of formation that had an average error of less than two kcal/mol compared to experimental heats of formation.

Ibrahim and Schleyer extended Wiberg's work to include molecules containing C, N, O, F, and H [41]. Instead of group equivalents, they used atom equivalents based on the molecular environment; for example a methyl carbon has an atom equivalent energy that is different from a methylene carbon. Although this method leads to a relatively large number of constants, Ibrahim and Schleyer calculated theoretical heats of formation at 298 K, ΔH_f^{298}, from 6-31G* and 3-21G basis set energies that had an average error of only 1.3 kcal/mol for "classical" molecules [41]. For highly strained molecules or for molecules with delocalized bonding the average error was higher, 3.4 kcal/mol for ΔH_f^{298} energies calculated with the 6-31G* basis set and 11.6 kcal/mol for ΔH_f^{298} energies calculated with the 3-21G basis set.

$$E_0^{PROD} = \Delta H_f^{298} + E_0^{REACT} - (\Delta H_{298} - \Delta H_0)^{PROD} + (\Delta H_{298} - \Delta H_0)^{REACT} \qquad (5\text{-}3)$$

E_0 - Heat of formation at 0 K.

ΔH_f^{298} - Heat of formation at 298 K.

$\Delta H_{298} - \Delta H_0$ - Enthalpy change on heating from 0 K to 298 K.

Calculation of molecular E_0 energies from ΔH_f^{298} energies is accomplished via equation 5-3 and the chemical equation for formation of the molecule, a reaction analogous to equation 5-1. The thermodynamic values for the reactants, all elements in this case, are readily available from the JANAF tables [3]. The atom equivalent method is an easy and accurate method for a priori calculation of ΔH_f^{298} and E_0 energies. The remainder of this Chapter describes the derivation of atom equivalents for the 4-21NO* basis set.

Derivation of Atom Equivalents

Atomic equivalent energies were calculated for the 4-21NO* basis set closely following the method of Ibrahim and Schleyer [41] except for the way in which carbon-hetero atom bonds and the nitro, NO_2, group are handled. Ibrahim and Schleyer assumed that any carbon atom group bonded to a hetero atom was equivalent to the CH_3 group. This seems rather arbitrary and forces the hetero atom group to absorb all of the energy differences caused by the presence of a carbon multiple bond. In this work carbon atoms maintain their hybridization and bonding designation in all bonds. Ibrahim and Schleyer did not calculate a separate group energy for the nitro group [41]. During the course of this work, the theoretical and experimental heats of formation showed better agreement when the nitro group was treated as a single entity.

In this study calculations were completed with two versions of the 4-21NO* basis set: the 4-21NO*(P) and the 4-21NO*(D6), see Chapter 2 for descriptions of these basis sets. Calculations with the two basis sets lead to almost identical geometries and force fields, but molecular energies calculated with the 4-21NO*(D6) basis set were consistently lower by a minimum of five kcal/mol than molecular energies calculated with the 4-21NO*(P) basis set. Independent sets of atomic equivalents are, therefore, required for the 4-21NO*(P) basis set and the 4-21NO*(D6) basis set.

A least squares fit between the ab *initio energies and experimental* heats of formation was made for the 55 molecules shown in Table 5-1 using the 19 parameters shown in Table 5-2. The theoretical ΔH_f^{298} values calculated with the 4-21NO*(P) basis set atomic equivalents shown in Table 5-2 and the ab initio energies shown in Table 5-1 have an average error of 1.6 kcal/mol, a root mean square error of 1.9 kcal/mol and a maximum error of 4.0 kcal/mol when compared to the corresponding experimental ΔH_f^{298}

values. Theoretical ΔH_f^{298} values calculated with the 4-21NO*(D6) basis set atomic equivalents shown in Table 5-2 and the ab initio energies shown in Table 5-1 have an average error of 1.5 kcal/mol, a root mean square error of 1.8 kcal/mol and a maximum error of 3.6 kcal/mol when compared to the corresponding experimental ΔH_f^{298} values. A priori theoretical ΔH_f^{298} energies derived from molecular energies calculated with either basis set and the corresponding atomic equivalents should be accurate to about 3 kcal/mol for classical molecules, an accuracy comparable to ΔH_f^{298} energies derived from the 6-31G* basis set. For strongly delocalized systems ΔH_f^{298} energies calculated from the 4-21NO* basis sets will have a higher uncertainty because d functions are not placed on the carbon atoms in the ring.

The notation used to define the group energies in Table 5-2 follows the notation developed in reference 41. The atomic equivalent energy applies to the first atom listed. The subscript following the atom designation describes the bond type with no subscript indicating a single bond, a "d" indicating a double bond and a "t" indicating a triple bond. The group of symbols following the hyphen shows the number of hydrogen atoms bonded to the first atom. The following example for methyl nitrate, CH_3ONO_2, shows how to calculate a theoretical heat of formation at 298 K from the 4-21NO*(D6) atomic equivalents given in Table 5-2:

> The ab initio energy is -317.856630 Hartree, see Table 5-1. The appropriate energy equivalents are H-(C) (-0.57053 Hartree), C-(H_3)X (-37.80480 Hartree), O-XY (-74.64805 Hartree) and NO_2-(X) (-203.64263 Hartree). The heat of formation is calculated by subtracting the sum of the atomic equivalents from the ab initio energy, in this example -317.85663-(-317.82138)=-0.04956 Hartree or -30.9 kcal/mol.

The atomic equivalents given in Table 5-2 are designed for use with specific basis sets. Using the values derived for the 4-21NO*(P) basis set to correct a molecular energy calculated with the 4-21NO*(D6) basis set will result in an erroneous heat of formation. Two other possible definitions of the 4-21NO* basis set exist. One defines the d orbitals with five displaced p functions and one s function, while the other version defines the d orbitals with only five d functions. Heats of formation calculated from the ab initio molecular energies associated with either of these basis sets and the atomic equivalents given Table 5-2 will be in error by about five to ten kcal/mol.

TABLE 5-1

Data for the Determination of Atomic Equivalents[a]

		4-21NO*P	4-21NO*P	4-21NO*P	4-21NO*D6	4-21NO*D6	4-21NO*D6
Molecule	ΔH_f(exp)[c]	E[d]	ΔH_f	Error[e]	E[d]	ΔH_f	Error[e]
Methane	-17.89	-40.11331[f]	-16.41	1.48	-40.11331[f]	-16.56	1.33
Ethane	-20.24	-79.06773[f]	-21.88	-1.64	-79.06773[f]	-21.93	-1.69
Propane	-24.83	-118.02375[f]	-26.89	-2.06	-118.02375[f]	-26.94	-2.11
Butane	-30.36	-156.97976[f]	-31.89	-1.53	-156.97976[f]	-31.95	-1.59
Pentane	-35.10	-195.93562[f]	-36.80	-1.70	-195.93562[f]	-36.87	-1.77
Cyclobutane	6.78	-155.77881[f]	8.38	1.60	-155.77881[f]	8.35	1.57
Ethylene	12.45	-77.87203[f]	11.25	-1.20	-77.87203[f]	11.18	-1.27
Propene	4.88	-116.83267[f]	2.13	-2.75	-116.83267[f]	2.10	-2.78
Isobutene	-4.26	-155.79081[g]	-4.87	-0.61	-155.79081[g]	-4.94	-0.68
Isobutane	-32.41	-156.98056[f]	-32.41	0.00	-156.98056[f]	-32.41	0.00
Cyclopentane	-18.44	-194.76879	-17.94	0.50	-194.76879	-17.99	0.45
Cyclopentene	8.23	-193.58196	7.16	-1.07	-193.58196	7.17	-1.06
Cyclopentadiene	31.94	-192.39634	31.49	-0.45	-192.39634	32.32	0.38
1 Butene	-0.20	-155.78605	-1.22	-1.02	-155.78605	-1.26	-1.06
1,3 Butadiene	26.11	-154.60068[h]	24.22	-1.89	-154.60068[h]	24.20	-1.92
Allene	45.63	-115.62527	49.10	3.47	-115.62527	49.04	3.41
Acetylene	54.34	-76.66486[i]	55.19	0.85	-76.66486[i]	55.18	0.84
Propyne	44.39	-115.63163	45.04	0.65	-115.63163	45.02	0.63
Dibutyne	113.0	-152.19574	111.83	-1.18	-152.19574	111.84	-1.16
2 Butyne	34.71	-154.59732	35.56	0.85	-154.59732	35.55	0.84
1,4 Pentadiene	25.25	-193.54350	26.24	0.99	-193.54350	26.24	0.99
Formamide	-44.50	-168.58320	-43.48	1.03	-168.58740	-43.60	0.90
Diazomethane	55.0	-147.56626	56.55	1.55	-147.57649	56.88	1.88
Acetamide	-57.0	-207.54860	-55.03	1.97	-207.55294	-55.28	1.72
Nitroethane	-24.38	-282.13881	-23.85	0.53	-282.14453	-23.52	0.86
Hydroxylamine	-9.0	-130.71965	-11.64	-2.64	-130.72460	-11.51	-2.51
Methylisocyanide	35.60	-131.62888	35.59	-0.01	-131.63463	35.35	-0.25
Acetonitrile	20.90	-131.67868	17.95	-2.95	-131.68046	17.87	-3.03

Molecule	ΔH_f(exp)[c]	E[d]	ΔH_f	Error[e]	E[d]	ΔH_f	Error[e]
Formic Acid	-90.57	-188.37104	-90.71	-0.14	-188.37079	-90.42	0.15
Ethylmethylether	-51.72[j]	-192.70652	-49.11	2.62	-192.70706	-49.07	2.65
Acetic Acid	-103.26	-227.33987	-104.42	-1.16	-227.33959	-104.15	-0.89
Ketene	-11.40	-151.41890	-14.85	-3.45	-151.41767	-14.44	-3.04
Acetaldehyde	-39.73	-152.59670	-38.04	1.69	-152.59637	-38.16	1.57
Propenal	-18.0	-190.36509	-16.20	1.80	-190.36472	-16.28	1.72
Acetone	-51.70	-191.56426	-50.95	0.75	-191.56383	-51.05	0.65
Ethanol	-56.24	-153.75611	-53.21	3.03	-153.75662	-53.14	3.11
Water	-57.80	-75.84741	-57.80	0.00	-75.84819	-57.80	0.00
Dimethylether	-43.99	-153.74638	-41.51	2.48	-153.74682	-41.41	2.58
Ammonia	-11.0	-56.07284	-11	0.00	-56.07717	-11.00	0.00
Methylamine	-5.50	-95.02018	-5.94	-0.44	-95.02415	-5.65	-0.15
Carbon Dioxide	-94.05	-187.25894	-97.52	-3.47	-187.25741	-97.20	-3.15
Methanol	-48.07	-114.79524	-45.16	2.91	-114.79579	-45.10	2.97
Formaldehyde	-25.92	-113.62702	-23.20	2.72	-113.62679	-23.41	2.51
Glyoxal	-50.66	-226.11818	-49.50	1.16	-226.11724	-49.52	1.14
Methylnitrate	-29.80[k]	-317.84895	-30.63	-0.83	-317.85630	-30.89	-1.09
Urea	-58.70	-223.52595	-54.72	3.98	-223.53506	-55.13	3.57
Propanitrile	12.10	-170.63421	13.25	1.15	-170.63595	13.17	1.07
Methyl Formate	-83.70	-227.32047	-85.18	-1.48	-227.32019	-85.04	-1.34
Ethylamine	-11.35	-133.97891	-12.66	-1.31	-133.98283	-12.33	-0.98
Cyanogen	73.84	-184.26259	74.74	0.90	-184.26579	74.82	0.98
Hydrazine	22.80	-110.95743	19.52	-3.28	-110.96604	19.74	-3.06
Methylnitrite	-15.60	-243.19381	-18.39	-2.79	-243.19938	-18.41	-2.81
Nitric Acid	-32.10[l]	-278.89703	-33.80	-1.70	-278.90470	-34.22	-2.12
Nitromethane	-17.90	-243.17810	-15.90	2.00	-243.18380	-15.55	2.35
trans Nitrous acid	-18.84	-204.23804	-19.14	-0.30	-204.24426	-19.54	-0.70

a. 4-21NO* basis set defines the d orbitals with 6 displaced p functions. See Chapter Two for a complete definition of the basis set.

c. Unless otherwise noted data taken from reference 41. Values given in kcal/mole.

d. Molecular energy in Hartrees. Unless noted otherwise calculated in this work.

e. H_f(calc)-H_f(exp).

f. Energy from reference 45.

g. Energy from V. O. Williams, C. Van Alsenoy, J. N. Scarsdale and L. Schafer, J. Mol. Struct. 103 (86) 1981.

h. Energy from reference 19.

i. Energy from reference 24.

j. Enthalpy from E. S. Domalski, J. Phys. Chem. Ref. Data, 1 (2) 1972.

k. Enthalpy from R. C. Weast, M. J. Astle, and W. H. Beyer (Eds), CRC HANDBOOK OF CHEMISTRY and PHYSICS 68th Ed., CRC Press Inc., Boca Raton, FL 1987.

l. Enthalpy from reference 3.

TABLE 5-2

Atom Equivalents for the 4-21NO* Basis Sets

Atomic Group	4-21NO*P Energy Equivalent	4-21NO*D6 Energy Equivalent
H-(C)	-0.57072	-0.57053
C-(H_3)X	-37.80426	-37.80480
C-(H_2)XY	-37.80659	-37.80697
C-(H)XYZ	-37.80890	-37.80920
C_d-(H_2)X	-37.80357	-37.80391
C_d-(H)XY	-37.80390	-37.80412
C_d-(X_d)YZ	-37.80517	-37.80518
C_d-(X_d)$_2$	-37.81349	-37.81348
C_t-(H)	-37.80569	-37.80587
C_t-(X)	-37.81057	-37.81059
H-(O)	-0.54847	-0.54856
O-(H)X	-74.65836	-74.65896
O-(XY)	-74.64737	-74.64805
O_d-(X)	-74.64502	-74.64452
H-(N)	-0.56104	-0.56089
N-(H_2)X	-54.37219	-54.37697
N_d-(XY)	-54.35568	-54.36109
N_t-(X)	-54.38029	-54.38192
NO_2-(X)	-203.63633	-203.64263

CHAPTER SIX

INTRODUCTION

In this chapter we test the method of calculating a priori thermodynamic data outlined in Chapter Two using the data developed in Chapters Three, Four, and Five. Water, benzene and naphthalene were selected as test molecules because they have been previously studied with the 4-21 basis set [44,50] and accurate thermodynamic functions have been calculated from experimental data [3,79,80,81]. The water and benzene calculations will serve to validate the method, but are not strict tests because water and benzene experimental fundamental frequencies were used during scaling of the ab initio force fields [44]. The naphthalene calculation is completely a priori (the ab initio force field was scaled with benzene scale factors [50]) and is, thus, a comprehensive end to end test of the method.

Water

Water has been extensively studied theoretically and experimentally. Exceptionally accurate thermodynamic functions, which are not bound by the limits of the rigid rotor harmonic oscillator approximation, have been calculated from experimental data [3]. Additionally, exceptionally accurate theoretical wavefunctions have been calculated for water [82]. Before calculating theoretical thermodynamic data for water from the results of calculations employing the 4-21NO* basis set, we will critically examine the assertion made in Chapter Two that even very advanced theoretical techniques are not always able to accurately calculate thermodynamic data without some type of scaling. Yamaguchi and Schaefer systematically calculated the optimized structure of water and fundamental vibration frequencies using computational techniques ranging from single determinant SCF with a double zeta quality basis set to all single and double excitations configuration interaction with a triple zeta plus polarization functions basis set [82]. The geometries, rotational constants and fundamental vibration frequencies determined by Yamaguchi and Schaefer are summarized in Table 6-1 with the corresponding experimental data [83,84].

Yamaguchi and Schaefer did not correct the theoretical geometries for basis set effects and calculated theoretical harmonic fundamental vibration frequencies, ignoring all anharmonic effects [82]. The differences between the experimental geometry and the various theoretical geometries are similar to those observed in other molecules. The SCF calculations give an OH bond length that is too short, while the CI calculations give an OH bond length that is in excellent agreement with the experimental value provided d functions are included in the basis set. The double zeta basis set calculations give an HOH angle that is larger than the experimental value in agreement with earlier SCF studies. Including CI with the double zeta basis set does not correct the error in the HOH bond angle. All of the calculations including polarization functions in the basis set give a reasonably accurate value for the HOH angle.

The errors in the theoretical rotational constants, shown in Table 6-1, follow the errors in the theoretical geometries. The superior CI geometries provide rotational constants that show good agreement with the experimental rotational constants while the SCF geometries provide rotational constants that have significant errors. The error in any one rotational constant is not significant, because the rotational partition function is proportional to the product $I_aI_bI_c$. If one theoretical rotational constant is larger than its corresponding experimental value while another theoretical rotational constant is smaller than its corresponding experimental value, the two errors will tend to cancel one another. The resulting theoretical rotational partition function will accidentally show good agreement with the experimental rotational partition function. For example, individually the DZ CI theoretical rotational constants show large errors when compared to the experimental rotational constants (I_a is 11.3 per cent greater, I_b is 10.9 per cent less and I_c is 4.3 per cent less than the experimental values), but the product of the theoretical rotational constants is only 5.2 per cent less than the product of the experimental rotational constants.

The theoretical vibration frequencies shown in Table 6-1 exhibit the expected agreement with the experimental frequencies. All of the fundamental frequencies shown in Table 6-1 are harmonic oscillator fundamental frequencies. The SCF based calculations lead to fundamental frequencies that are about 10 per cent higher than the experimental frequencies while the CI based calculations lead to fundamental frequencies that are within three per cent of the experimental frequencies. The residual errors in the CI fundamental frequencies are presumably caused by neglect of third and fourth order substitutions and truncation of the basis set.

Using the data compiled in Table 6-1 to calculate the thermodynamic quantities $(G_0-E_0)/T$ and entropy leads to the values shown in Tables 6-2 and 6-3, respectively. Table 6-2 shows that the maximum error in the theoretical $(G_0-E_0)/T$ values is only 0.7 per cent for the free energies derived from the double zeta basis set SCF calculations. The theoretical energies derived from the configuration interaction calculations show outstanding agreement with the experimental energies. Table 6-3 shows that the same trend for the theoretical entropy values with a maximum error of 1.1 per cent for entropy values derived from the double zeta basis set SCF calculations.

The relatively small errors associated with the theoretical thermodynamic values calculated for water are not representative of the situation encountered in larger molecules. If we assume equipartition of energy, the total energy of water is 6 kT with translational modes contributing 3/2 kT, rotational modes contributing 3/2 kT and the three normal modes of vibration contributing 3 kT. In larger molecules the contribution of the normal modes of vibration to the total energy is significantly greater. The total energy of benzene, again assuming equipartition, is 33 kT with translational and rotational modes contributing 3 kT and the normal modes of vibration contributing 30 kT. This example shows the vibrational modes make a larger contribution to the total energy in larger molecules and we can infer that thermodynamic functions for larger molecules will be more sensitive to errors in the vibrational partition function.

The energy associated with each of the fundamental vibrations in water is also different from larger molecules. All of the water fundamental vibrations are high energy motions, the frequencies are greater than 1500 cm^{-1}. In larger molecules out of plane deformation, torsional, and heavy atom bending modes are usually low energy motions with a frequency less than 1500 cm^{-1}. Low energy fundamentals make a significantly larger contribution to the partition function than high energy fundamentals. For example, at 298 K a fundamental frequency of 200 cm^{-1} contributes 0.996 to the vibrational partition function, a fundamental frequency of 1600 cm^{-1} contributes 0.021 to the vibrational partition function, while a fundamental frequency of 3000 cm^{-1} contributes only 7.16×10^{-4}. A ten per cent error in the fundamental frequency will produce about a ten per cent error in its contribution to the vibrational partition function. For low frequency fundamentals an error of this magnitude is significant while for the higher frequency fundamentals an error of this magnitude is hardly noticeable. The point of the last two paragraphs is simply that water thermodynamic functions may be less sensitive to errors in the vibrational partition function than the thermodynamic functions of larger molecules.

If the thermodynamic functions for water are calculated via the method outlined in Chapter Two, they would exhibit almost perfect agreement with the experimentally derived values. The ab initio force field would be scaled with two scale factors, one for the OH bond and the other for the HOH bending motion, and this would provide near perfect agreement with the experimental frequencies. Additionally, the OH bond length correction factor was derived from a comparison of the ab initio and experimental OH bond lengths and, again, perfect agreement with the experimental data would be obtained. For these reasons, water is not a sufficient test of the method.

BENZENE

Benzene is a logical step forward in testing the method. Thermodynamic functions for benzene have been determined experimentally [84]. Pulay, Fogarasi, and Boggs calculated the benzene Scaled Quantum Mechanical force field and fundamental frequencies with the 4-21 basis set using the method presented in Chapter Two [44]. Table 6-4 summarizes theoretical and experimental rotational constants and fundamental frequencies. The data in Table 6-4 lead to the theoretical and experimental thermodynamic quantities given in Table 6-5. The excellent agreement between the experimental and theoretical thermodynamic functions is encouraging. The maximum error is only 1.3 per cent for the specific heat at constant pressure at 300 K. All of the remaining theoretical values are within one per cent of the corresponding experimental values.

The benzene E_0 energy may be determined using either the atomic equivalent method or the isodesmic reaction method. For the atomic equivalent method subtracting the 4-21NO*(P) basis set atomic equivalents for C_d-(H)XY and C-H given in Table 5-2 from the 4-21 basis set ab initio energy, -230.23378 H [24], leads to a ΔH_f^{298} equal to 8.7 kcal/mol. Using the 4-21NO*(D6) basis set atomic equivalents given Table 5-2 leads to a ΔH_f^{298} equal to 8.9 kcal/mol. The theoretical ΔH_f^{298} energies do not agree with the experimental ΔH_f^{298} energy, 19.8 kcal/mol [85]. The error is caused by the C_d-(H)XY atomic equivalents which were calculated from molecules with a true C-C double bond vice the aromatic C-C bond in benzene. Obtaining better agreement between the theoretical and experimental values requires determination of a new atomic equivalent for the aromatic C-C bond. Correcting the average theoretical ΔH_f^{298}, 8.8 kcal/mol, to 0 K gives an E_0 value of 11.7 kcal/mol which is, as expected, quite different from the experimental value of 24.0 kcal/mol [79]. In the next section an estimate of the aromatic carbon atomic equivalent will be derived from a combination of benzene and naphthalene data.

$$C_6H_6 + 6\ CH_4 \rightarrow 3\ C_2H_4 + 3\ C_2H_6 \qquad (6\text{-}1)$$

Table 6-6 summarizes the data we need to calculate the benzene E_0 value employing the isodesmic reaction shown in equation 6-1. The ab initio reaction energy is 0.0977 H or 61.3 kcal/mol. The change in zero point energy for reaction 6-1 is 4.7 kcal/mol which leads to a theoretical heat of reaction at 0 K of 66.0 kcal/mol. From the theoretical heat of reaction and the known E_0 values for ethane, ethylene, and methane we may calculate a theoretical benzene E_0 of 22.6 kcal/mol which is in satisfactory agreement with the experimental value of 24.0 kcal/mol [79].

The agreement between the theoretical and experimental thermodynamic functions for benzene is excellent, but benzene is still not the ultimate test for the method outlined in Chapter Two. The fundamental frequencies used to calculate the vibrational partition function were calculated by scaling the ab initio force field to the known experimental fundamental frequencies of benzene. To fully test this method of calculating a priori thermodynamic functions, we must use fundamental frequencies that are calculated a priori. As stated in Chapter Two, we use "a priori fundamental frequencies" to mean ones that are calculated by transferring force field scale factors from different, although closely related molecules.

NAPHTHALENE

Naphthalene was selected as the final test molecule for examining how accurately a priori calculation of thermodynamic functions compares with experimental calculation of thermodynamic functions. Unfortunately, naphthalene is not the ideal molecule for this comparison. It does, however, illustrate problems that commonly arise in the use of only experimentally derived vibrational data in the statistical mechanic calculation of thermodynamic properties of larger molecules. Complete unambiguous assignment of the gas phase fundamental frequencies has not been completed for naphthalene despite several extensive experimental studies [86-103]. Group theory considerations show that the four A_u fundamental frequencies are not active by symmetry in either the IR or Raman gas phase spectra. Additionally, a recent theoretical study suggests that several of the weaker fundamental frequencies have not been observed experimentally [50]. These problems are not unique to naphthalene and are representative of the difficulties encountered in assigning the vibrational spectra of any large molecule. The ambiguous assignment of naphthalene fundamental frequencies has led to the reporting of several different experimental thermodynamic functions [5,80,81,93,103-106]. We will compare the a priori results calculated in this work to the recent experimental results of Lielmezs, Bennett and McFee [81] and to those of Chen, Kudchadker, and Wilhoit [80].

Sellers, Pulay and Boggs calculated the fundamental frequencies of naphthalene a priori by scaling the naphthalene ab initio force field with benzene scale factors [50]. The theoretical frequencies were within 15 cm^{-1} of the unambiguously assigned experimental frequencies except for the B_{2u} fundamental at 1361 cm^{-1}. The a priori frequency for this fundamental is 1341 cm^{-1} and its value is very sensitive to the value of the off diagonal CC-CC interaction force constants. These interaction force constants do not have a counterpart in benzene and we should not expect outstanding agreement for this specific case. Sellers, Pulay, and Boggs were able to correct this error by fitting their ab initio force field to the unambiguously assigned experimental fundamental frequencies and including a separate scale factor for the CC-CC interaction force constants. The a priori fundamental assignments also clarified most of the ambiguously assigned experimental frequencies and provided reasonably accurate assignments for the four inactive A_u fundamental frequencies [50].

A priori thermodynamic functions were calculated for naphthalene using rotational constants calculated from the corrected ab initio geometry determined by Sellers and Boggs [107], shown in Table 6-7, and the a priori fundamental frequencies calculated by Sellers, Pulay and Boggs [50], shown in Table 6-8. Table 6-8 also shows the fundamental assignments selected in the experimental studies of Chen et al [80] and of Lielmezs et al [81]. The symmetry assignments of the fundamental frequencies shown in Table 6-8 correspond to the symmetry axes selected by Sellers and coworkers [50]. The different fundamental frequency assignments made in the experimental studies of naphthalene thermodynamic functions clearly illustrate the difficulties encountered in assigning the infrared and Raman spectra of larger molecules.

Tables 6-9 through 6-11 show the a priori and experimental $(G_0\text{-}E_0)/T$, $(H_0\text{-}E_0)/T$, and entropy values for naphthalene as a function of temperature. The a priori thermodynamic data agree almost exactly with the thermodynamic data calculated by Chen and coworkers. Lielmezs and coworkers Set A thermodynamic data closely agree with the a priori data, the maximum error is less than 0.4 per cent, while their Set B thermodynamic data are uniformly about 0.3 per cent less than the a priori data. The agreement between the a priori and Chen and coworkers thermodynamic functions strongly suggests that they are the best available thermodynamic functions for naphthalene.

The close agreement between the experimental and a priori thermodynamic data for naphthalene shows that a priori calculation of thermodynamic data for medium sized molecules should be as accurate as experimental calculation within the rigid rotor harmonic oscillator approximation. A priori calculation of thermodynamic data does not suffer from possible inaccuracies caused by gross misassignment of fundamental vibration frequencies and, in most cases, is easier and faster than calculation of thermodynamic data through experimental methods.

Tables 6-9 and 6-10 give values derived from the naphthalene internal partition function and we require an a priori value for E_0 to complete the a priori thermodynamic tables. The ab initio energy calculated with the 4-21 basis set at the optimized geometry determined by Sellers and Boggs [107] is -382.575218 H. Subtracting atomic group energies for the C_d-(H)XY and C-H groups given in Table 5-2 leads to ΔH_f^{298} energies of 18.5 kcal/mol for the 4-21NO*(P) basis set and 19.0 kcal/mol for the 4-21NO*(D6) basis set. These values do not agree with the experimental ΔH_f^{298} value of 36.0 kcal/mol [80]. The source of the error in the a priori ΔH_f^{298} values is the C_d-(H)XY group equivalent energy which was calculated from localized C-C double bonds. The C-C bonding in benzene and naphthalene is delocalized and we should not expect a group energy calculated from localized bonds to give reasonable ΔH_f^{298} values for an aromatic system. An aromatic carbon group equivalent energy of -37.80676 H, C_a-(H)XY in the nomenclature of Table 6-2, was calculated from the benzene and naphthalene ab initio energies with the C-H group energy fixed at 0.57072 H. This new group equivalent energy leads to ΔH_f^{298} energies of 19.5 kcal/mol for benzene and 36.5 kcal/mol for naphthalene, which agree well with the experimental ΔH_f^{298} energies of 19.8 kcal/mol and 36.0 kcal/mol. The improved ΔH_f^{298} energies lead to a priori E_0 energies of 23.7 kcal/mol for benzene and 42.2 kcal/mol for naphthalene which are in better agreement with the experimentally derived energies of 24.0 and 41.6 kcal/mol [80].

$$C_{10}H_8 + 12\ CH_4 \rightarrow 5\ C_2H_4 + 6\ C_2H_6 \qquad (6\text{-}2)$$

The final step in this study of naphthalene is calculating E_0 based on the isodesmic reaction shown in Equation 6-2 and the data given in Table 6-6. The ab initio reaction energy for equation 6-2 is 109.1 kcal/mol and the change in zero point energy is 11.2 kcal/mol. The theoretical heat of reaction is thus 120.3 kcal/mol which leads to an E_0 energy of 45.2 kcal/mol, 3.6 kcal/mol higher than the experimental value.

The benzene and naphthalene a priori thermodynamic functions show excellent agreement with the available experimental data. A priori thermodynamic values calculated from the internal partition function, e.g. C_v or entropy, appear to be as accurate as experimentally derived values. A priori E_0 values appear to be less accurate with a maximum error of about 5 kcal/mol. One will usually be able to calculate the a priori thermodynamic function of medium sized molecule easier and faster than the experimental thermodynamic function.

TABLE 6-1

SUMMARY OF WATER STRUCTURAL DATA, ROTATIONAL CONSTANTS AND VIBRATION FREQUENCIES

	DZ SCF[a]	DZ CI[a]	DZ+P SCF[a]	DZ+P CI[a]	NHF SCF[a]	NHF CI[a]	Exp.
r(O-H)	0.951	0.976	0.944	0.959	0.941	0.955	0.957[b]
<HOH	112.5	110.6	106.6	104.9	106.5	105.4	104.5[b]
I_a[c]	1018.0	921.3	893.2	832.2	895.2	848.0	828.1
I_b[c]	403.7	393.0	440.9	437.8	444.5	438.2	441.3
I_c[c]	289.1	275.5	295.2	286.9	297.0	288.9	287.9
Prod.[d]	11.88	9.973	11.63	10.45	11.82	10.74	10.52
v_1	4028	3710	4164	3967	4128	3937	3834[e]
v_2	1710	1649	1751	1693	1757	1688	1647[e]
v_3	4204	3880	4287	4088	4234	4043	3943[e]

a. Data from reference 82. DZ basis set is 9s/5p contracted to 4s/2p. NHF basis set is 10s/6p contracted to 6s/4p.

b. Data from reference 83.

c. Rotational constants calculated from the given structure in Mhz.

d. The product $I_a{*}I_b{*}I_c$. The number shown should be multiplied by 1×10^{16} Mhz.

e. Harmonic oscillator frequencies from reference 84.

TABLE 6-2[a]

WATER $(G-E_0)/T$ (cal/mole/K) VALUES FOR DIFFERENT BASIS SETS

	DZ	DZ	DZ+P	DZ+P	NHF	NHF	EXP.	EXP.	EXP.
T	SCF	CI	SCF	CI	SCF	CI	H.O.[b]	I.G.[c]	OBS.[d]
200	-33.79	-33.96	-33.81	-33.91	-33.79	-33.88	-33.91	-33.91	-34.00
300	-37.01	-37.18	-37.02	-37.14	-37.01	-37.11	-37.13	-37.13	-37.22
500	-41.08	-41.26	-41.10	-41.21	-41.09	-41.19	-41.21	-41.21	-41.29
1000	-46.77	-46.96	-46.78	-46.90	-46.76	-46.88	-46.91	-46.93	-47.02
1500	-50.31	-50.54	-50.30	-50.45	-50.29	-50.43	-50.48	-50.52	-50.62
2000	-52.99	-53.26	-52.97	-53.14	-52.96	-53.12	-53.19	-53.25	-53.36

a. Basis sets defined in Table 6-1.

b. Data derived from harmonic oscillator vibration frequencies.

c. Data derived from observed vibration frequencies.

d. Observed thermodynamic functions from reference 3.

TABLE 6-3

WATER ENTROPY VALUES FOR DIFFERENT BASIS SETS

	DZ	DZ	DZ+P	DZ+P	NHF	NHF	EXP.[a]	EXP.[b]	EXP.[c]
T	SCF	CI	SCF	CI	SCF	CI	H.O.	I.G.	OBS.
200	41.73	41.91	41.76	41.86	41.74	41.84	41.86	41.86	41.92
300	44.96	45.14	44.98	45.09	44.97	45.06	45.08	45.09	45.16
500	49.10	49.29	49.12	49.24	49.10	49.21	49.24	49.25	49.33
1000	55.24	55.49	55.22	55.38	55.20	55.37	55.43	55.49	55.59
1500	59.35	59.69	59.30	59.52	59.29	59.51	59.61	59.73	59.86
2000	62.59	63.00	62.52	62.78	62.51	62.78	62.89	63.06	63.23

a. Data based on Harmonic Oscillator fundamental frequencies.

b. Data based on observed fundamental frequencies.

c. Data from reference 3.

TABLE 6-4

BENZENE ROTATIONAL CONSTANTS AND FUNDAMENTAL FREQUENCIES

PARAMETER	4-21[a]	EXP[b]
A	5682.6	5688.7[c]
B	5682.6	5688.7[c]
C	2841.3	
ν_1	983	993
ν_2	3095	3073
ν_3	1365	1350
ν_4	701	707
ν_5	996	990
ν_6	607	606
ν_7	3061	3056
ν_8	1607	1599
ν_9	1183	1178
ν_{10}	843	846
ν_{11}	667	673
ν_{12}	997	1010
ν_{13}	3051	3057
ν_{14}	1297	1309
ν_{15}	1162	1146
ν_{16}	402	398
ν_{17}	969	967
ν_{18}	1036	1037
ν_{19}	1482	1482
ν_{20}	3080	3064

a. Rotational constants calculated from the corrected theoretical structure and 4-21 SQM fundamental frequencies reported in reference 44.

b. Experimental vibrational frequencies taken from reference 44.

c. J. Kauppinen, P. Jensen and S. Brodersen, J. Mol. Spectrosc., 83 (1980) 161.

TABLE 6-5

THERMODYNAMIC FUNCTIONS FOR BENZENE

	ENTROPY		$(H_0-E_0)/T$		C_P	
TEMP	EXP[a]	A PRIORI[b]	EXP[a]	A PRIORI[b]	EXP[a]	A PRIORI[b]
300	64.5	64.5	11.46	11.47	19.65	19.80
500	77.7	77.9	17.50	17.61	32.80	33.14
1000	106.7	107.1	30.16	30.37	50.16	50.38
1500	128.7	129.1	38.24	38.43	57.67	57.77

a. Data from reference 79.

b. This work.

TABLE 6-6

DATA FOR CALCULATING BENZENE E_0

Parameter	C_6H_6	C_2H_6	C_2H_4	CH_4
$E_{ab\ initio}$[a]	-230.23378[b]	-79.06651[b]	-77.87080[b]	-40.11264[b]
Zero Point Energy[c]	61.3[d]	45.3[e]	30.9[e]	27.1[e]
E_0		-16.5[f]	14.5[f]	-16.0[f]

a. Energy in Hartrees.

b. Reference 24.

c. Energy in kcal/mole.

d. Calculated from fundamental frequencies given in Table 6-4.

e. Reference 39.

f. Reference 79.

TABLE 6-7

NAPHTHALENE GEOMETRY

Parameter	Ab Initio[a]	Corrected[b]	Exp.[c]
C1-C2	1.356	1.371	1.381
C2-C3	1.415	1.420	1.417
C10-C9	1.409	1.415	1.412
C9-C1	1.420	1.425	1.422
C1-H1	1.073	1.078	1.092
C2-H2	1.072	1.077	1.092
<C9C1C2	120.8	120.8	
<C1C2C3	120.4	120.4	
<C10C9C1	118.9	118.9	119.5
<C9C1H1	118.8	118.8	
<C1C2H2	120.1	120.1	

a. Bond lengths in Å. Bond angles in degrees.

b. Reference 106.

c. Reference 108.

TABLE 6-8[a]

NAPHTHALENE FUNDAMENTAL FREQUENCIES (in cm^{-1})

Sym	A Priori[b]	Chen[c]	McFee (A)[d]	McFee (B)[d]	Sym.	A Priori[b]	Chen[c]	McFee (A)[d]	McFee (B)[d]
A_g	505	512	512	512	B_{2g}	471	466	469	469
	757	761	762	762		773	778	783	783
	1023	1025	1019	1019		878	876	875	875
	1170	1145	1145	1145		987	980	979	979
	1385	1380	1379	1379	B_{2u}	626	617	619	619
	1458	1463	1462	1462		1003	1008	870	1008
	1590	1577	1574	1574		1158	1144	1139	1139
	3056	3030	3031	3031		1204	1209	1212	1212
	3085	3060	3060	3060		1341	1361	1362	1362
A_u	188	191	213	213		1515	1509	1513	1513
	622	581	575	575		3052	3027	2987	2987
	825	841	843	843		3083	3090	3076	3076
	981	970	935	935	B_{3g}	512	506	508	508
B_{1g}	387	386	388	388		940	936	935	935
	705	725	724	724		1156	1168	1167	1167
	952	950	945	945		1255	1242	1242	1242
B_{1u}	354	359	361	361		1458	1443	1442	1442
	792	877	747	810		1644	1628	1624	1624
	1137	1125	1132	1132		3047	3060	2978	2978
	1272	1265	1270	1270		3067	3092	3076	3076
	1391	1389	1391	1391	B_{3u}	172	176	176	176
	1595	1595	1599	1599		480	472	476	476
	3049	3058	3027	3027		777	782	785	785
	3070	3065	3060	3060		969	958	958	958

a. Symmetry assignments taken from reference 50.

b. Reference 50.

c. Reference 80.

d. Reference 81.

TABLE 6-9

Naphthalene $-(G_0-E_0)/T$ Values (cal/mole/K)

T	A Priori[a]	Chen[b]	McFee (A)[c]	McFee (B)[c]
300	63.2	63.1	63.0	63.0
600	79.5	79.5	79.5	79.3
900	94.9	94.9	94.9	94.7
1200	108.9	108.9	109.0	108.7

a. This work.

b. Reference 80.

c. Reference 81.

TABLE 6-10

Naphthalene $-(H_0-E_0)/T$ Values (cal/mole/K)

T	A Priori[a]	Chen[b]	McFee (A)[c]	McFee (B)[c]
300	16.7	16.7	16.8	16.7
600	32.0	32.0	32.2	32.0
900	44.1	44.1	44.4	44.2
1200	53.1	53.1	53.3	53.1

a. This work.

b. Reference 80.

c. Reference 81.

TABLE 6-11

Naphthalene Entropy Values (cal/mole/K)

T	A Priori[a]	Chen[b]	McFee (A)[c]	McFee (B)[c]
300	79.9	79.8	79.8	79.6
600	111.5	111.5	111.7	111.4
900	139.1	139.0	139.3	138.9
1200	162.0	162.0	162.3	161.9

a. This work.

b. Reference 80.

c. Reference 81.

CHAPTER SEVEN

INTRODUCTION

The detonation of nitromethane has been extensively studied experimentally and theoretically as a prototypical system for detonation processes involving the nitro group, NO_2 [109-117]. Bardo recently proposed that the first step in the detonation of nitromethane is the formation of (hydroxy-methyl-amino)-nitro-methanol, shown in Figure 7-1, from a nitromethane dimer [118]. Bardo's hypothesis, developed from the results of a series of MNDO and MINDO/3 calculations, leads to the observed detonation products in only ten steps instead of the sixty steps required by an earlier detonation path [110]. The reactions in this new detonation process are accelerated at high temperature and pressure.

The interaction energy of two nitromethane molecules is the subject of two studies by Bartlett and coworkers [118,119]. They calculated the interaction energy for a variety of dimer configurations assuming the geometry of the individual molecules was fixed at the optimum 4-31G geometry. A single point ab initio calculation employing the 4-31G basis set and Bardo's MINDO/3 optimized geometry showed (hydroxy-methyl-amino)-nitro-methanol is about 20 kcal/mol more stable than the most stable nitromethane dimer configuration.

Dr. Bardo requested we calculate the fundamental vibration frequencies for (hydroxy-methyl-amino)-nitro-methanol to aid future studies of the detonation of nitromethane. All of the results reported in this Chapter are derived from ab initio SCF calculations employing the 4-21NO*(P) basis set and the methods outlined in Chapter Two. The Chapter opens with a comparison of the optimized 4-21NO* ab initio geometry to the MINDO/3 geometry, then describes the rotational potential surfaces for the major bonds, followed by a description of Scaled Quantum Mechanical force field and fundamental frequencies and closes with the calculation of thermodynamic functions.

OPTIMUM GEOMETRY

Table 7-1 summarizes several different (hydroxy-methyl-amino)-nitro-methanol geometries, see Figure 7-1 for the atomic numbering scheme. The second column shows the optimized 4-21NO*(P) geometry, optimization criteria are given in Chapter Two. The third column shows the estimated r_e geometry calculated from the optimized ab initio geometry and the appropriate bond length corrections given in Chapter Three. The fourth column shows the optimized MINDO/3 geometry determined by Bardo [117].

Later in this Chapter we will examine the torsional potential energy surfaces for each of the "backbone" bonds in (hydroxy-methyl-amino)-nitro-methanol. None of the minima identified in this study correspond to the configuration determined in the MINDO/3 study. In order to ensure that the MINDO/3 geometry was not the true ab initio ground state, a second geometry optimization was performed employing the 4-21NO*(D6) basis set with the MINDO/3 geometry as the starting structure. Column five of Table 7-1 shows the geometry that was derived from this series of calculations. The torsional angle differences between the MINDO/3 optimized geometry and this new structure clearly indicate that important basic differences exist between the ab initio and MINDO/3 wave functions. Additionally, the results of these calculations suggest that Bartlett and coworkers estimation of the stabilization of (hydroxy-methyl-amino)-nitro-methanol relative to the nitromethane dimer [119] is too small by about 30 kcal/mol.

Comparing the 4-21NO*(P) optimum C-N bond lengths to those of nitromethane, shown in Table 4-11, provides a basis for examining C-N bonding changes during formation of (hydroxy-methyl-amino)-nitro-methanol from nitromethane. At the beginning of the reaction, the C-N bond lengths are approximately 1.49 Å long. As (hydroxy-methyl-amino)-nitro-methanol forms, the C1-N2 bond becomes stronger, the C8-N9 bond becomes much weaker (it lengthens by about 0.075 Å), and a new bond forms between C8 and N2 that is stronger than either of the original C-N bonds.

CALCULATION OF ROTATIONAL POTENTIAL ENERGY SURFACES

Ab initio potential energy surfaces were calculated for the five major bonds (C1-N2, N2-C8, N2-O4, C8-O3 and C8-N9) of (hydroxy-methyl-amino)-nitro-methanol. The primary focus of this investigation was to ensure that the true optimum ab initio structure at this computational level had been located. The calculation of the rotational potential surfaces was a trivial matter after these calculations had been completed.

TORSION OF THE C1-N2 BOND

Torsion around the C1-N2 bond corresponds to internal rotation of the methyl group. Table 7-2 summarizes the important geometry and energy changes as a function of the change in T(O4-N2-C1-H5) from the equilibrium value of -61.4°. Figure 7-3 is the view of (hydroxy-methyl-amino)-nitro-methanol along the C1-N2 bond. The C-H bonds are arranged around C1 in a nearly tetrahedral pattern and the bonding around N2 is approximately sp^3 in nature. From these observations, we should expect the rotational potential surface to be a perturbed threefold rotor similar to the methyl amine rotational potential surface, and not a perturbed six-fold rotor similar to the nitromethane rotational potential surface.

Figure 7-4 is a plot of the relative energy data versus the change in T(O4-N2-C1-H5). The solid line is a Stineman interpolation of the energy data points. The dotted line is a plot of equation 7-1, which was derived via a least squares fit to the data. The barrier to internal rotation calculated from equation 7-1 is 3.6 kcal/mol, similar in magnitude to the ethane barrier to internal rotation. The potential surface is slightly asymmetric; for a pure three-fold rotor potential function V(30°) equals V(90°), but in this case V(30°) is 0.2 kcal/mol lower in energy than V(90°).

$$V(x)=1.812(1-\cos(3x))-0.092\sin(3x)+0.156\cos(1-\cos(6x))+0.092\sin(6x) \qquad (7\text{-}1)$$

x = the change in T(O4-N2-C1-H5) from the equilibrium value of -61.4°.
V = the relative energy in kcal/mol.

Examination of the geometry changes shown in Table 7-2 shows that only the C1-N2 bond length, N2-O4 bond length, and C1-N2-O4 bond angle change significantly during rotation of the methyl group. Figures 7-5 and 7-6 show these changes as a function of change in T(O4-N2-C1-H5). All three parameters change in a similar fashion possessing minima at 0° and maxima at 60° reflecting the three-fold nature of the potential surface.

TORSION AROUND THE N2-C8 BOND

Torsion around the N2-C8 bond does not correspond to any simple classical internal rotation potential function, although the potential surface may be considered a strongly perturbed three-fold rotor. Figure 7-7 shows (hydroxy-methyl-amino)-nitro-methanol viewed along the N2-C8 bond. This view clearly shows the intramolecular O4 to H12 and O11 to H13 hydrogen bonds. Table 7-3 summarizes the important structural changes and energy differences as a function of change in T(N9-C8-N2-C1).

Figure 7-8 is a plot of the relative energy data versus the change in T(N9-C8-N2-C1) from the equilibrium value of 53.1°. The solid line is a cubic spline interpolation of the data. Equation 7-2, shown as the dashed line in Figure 7-8, is an interpolating function of the relative energy data given in Table 7-3

$$V(x)=0.490(1-\cos(x))-1.39\sin(x)+2.17(1-\cos(2x))-2.34\sin(2x)+3.49(1-\cos(3x))+0.319\sin(3x) \qquad (7\text{-}2)$$

V = the relative energy in kcal/mol.

x = the change in T(N9-C8-N2-C1) from the equilibrium value of 53.1°

The rotational potential surface is complex with three distinct minima and maxima. The ground state is stabilized by two strong hydrogen bonds between H12 and O4, 2.024 Å long, and H13 and O11, 1.951 Å long. The minimum at 120°, ΔE = 4.8 kcal/mol, is stabilized by a weaker hydrogen bond between H12 and O11, 2.180 Å long. The minimum at 230°, ΔE = 2.5 kcal/mol, is stabilized by a weak hydrogen bond between H13 and O3, 2.334 Å long, and a strong hydrogen bond between H12 and O11, 1.977 Å long. The maximum at 70°, ΔE = 7.7 kcal/mol, occurs when the C8-N9 bond eclipses the N2-O4 bond. The maximum near 170°, ΔE = 8.1 kcal/mol, occurs when the C8-O3 bond eclipses the C1-N2 bond. The maximum near 300°, ΔE = 13.7 kcal/mol, occurs when the C8-N9 bond eclipses the C1-N2 bond and the N2-O4 bond eclipses the C8-O3 bond.

Changes in T(C1-N2-C8-N9) cause profound changes in other structural parameters throughout the molecule. This situation is different from the usual study of torsional motion because the C1-N2-C8-N9 torsion angle is the central torsional motion in (hydroxy-methyl-amino)-nitro-methanol instead of a peripheral methyl or hydroxyl group.

Figures 7-9 and 7-10 are plots of the C1-N2, N2-C8, and N2-O4 bond lengths as a function of change in T(N9-C8-N2-C1). The C1-N2 and N2-O4 bond lengths decrease when these bonds eclipse another bond and increase when these bonds bisect two bonds. The C1-N2 bond length is a minimum when it eclipses the C8-H14 bond, while the N2-O4 bond length is a minimum when it eclipses the C8-O3 bond. The maximum C1-N2 and N2-O4 bond lengths occur when these bonds bisect the O3-C8 and C8-N9 bonds. The maximum N2-C8 bond length occurs at -60° when the C8-N9 eclipses the C1-N2 bond and the N2-O4 bond eclipses the O3-C8 bond and the minimum bond length occurs at 0° when all of the major bonds are staggered.

The O3-C8 bond length changes in a manner that differs for the other bonds considered in this section. Figure 7-10 shows the O3-C8 potential function exhibits only a single maximum, which occurs when the O3-C8 bond eclipses the N2-O4 bond, and a single minimum, which occurs when the O3-C8 bond eclipses the N2 electron lone pair.

The C8-N9, N9-O10, and N9-O11 bond length changes correlate with changes in hydrogen bonding. Figures 7-11 and 7-12 show that all three bond lengths change rapidly from 0° to 120°. In this region a hydrogen bond forms between O10 and H13, while the hydrogen bond between H12 and O11 breaks. After 120° of rotation the O10-H13 hydrogen bond breaks and a hydrogen bond forms between O11 and H13.

Figures 7-13 through 7-16 are plots of the angles around N2, C8, and N9 as a function of change in T(N9-C8-N2-C1). The C1-N2-O4, O4-N2-C8, C1-N2-C8, and N2-C8-O3 angles change a "normal" manner; they increase when the major bonds are eclipsed and decrease when the major bonds are staggered. The N2-C8-N9 angle changes in a simple periodic fashion with a single minimum, which occurs when the C1-N2 bond eclipses the O3-C8 bond, and a single maximum, which occurs when the C1-N2 bond eclipses the C8-N9 bond. The N9-C8-O3 angle changes in a complex non-traditional manner. The minimum value occurs when the O3-C8 and N9-C8 bonds eclipse the N2-O4 and N2-C1 bonds, while the location of the maximum does not correlate with any significant structural feature. The C8-N9-O10 and C8-N9-O11 angles change in response to the formation of a hydrogen bond between O10 and H13. The NO_2 group remains planar during torsion around the N2-C8 bond.

Figures 7-17 and 7-18 are plots of T(N2-C8-O3-H12), T(H13-O4-N2-C1), T(O10-N9-C8-N2), and T(O11-N9-C8-N2) as a function of change in T(N9-C8-N2-C1). All of these torsion angles change in a way that tends to maximize the effectiveness of intramolecular hydrogen bonding. The increase in T(N2-C8-O3-H12) occurs in response to the formation of a hydrogen bond between O4 and H12. The decrease in T(H13-O4-N2-C1) occurs in response to the formation of a hydrogen bond between O11 and H13. The changes in T(O10-N9-C8-N2) and T(O11-N9-C8-N2) are in response to the formation of a hydrogen bond between O10 and H13 and the breaking of the hydrogen bond between O11 and H12.

TORSION AROUND THE N2-O4 BOND

Torsion around the N2-O4 bond corresponds to internal rotation of the NOH group. Figure 7-19 shows the optimum (hydroxy-methyl-amino)-nitro-methanol amine geometry viewed along the N2 to O4 axis. Table 7-4 shows the geometry and energy changes as a function of change in T(H13-O4-N2-C1) from the equilibrium value of -64.4°. A positive change of T(H13-O4-N2-C1) results in a counter-clockwise rotation of H13 as viewed in Figure 7-19.

Figure 7-20 is a plot of the relative energy data shown in Table 7-4. The solid line is a cubic spline interpolation of the data, while the dashed line is a plot of equation 7-3, a six term sine/cosine interpolating function. The large overshoots exhibited by equation 7-3 at -150° and -90° indicate additional data points are required to provide an adequate basis for deriving a quantitative description of the rotational potential surface.

$$V(x)=-1.215(1-\cos(x))+0.234\sin(x)+3.659(1-\cos(2x))-1.159\sin(2x)$$
$$+1.323(1-\cos(3x))+0.699\sin(3x) \qquad (7\text{-}3)$$

V = the relative energy in kcal/mol.

x = the change in T(H13-O4-N2-C1) from the equilibrium value of -64.4°

The minimum shown at 181.8°, $\Delta E = 0.074$ kcal/mol, was determined with a complete geometry optimization. In this new conformer H12 forms hydrogen bonds with O4, 2.390 Å long, and O11, 2.151 Å long. H13 is not involved in hydrogen bonding, but the repulsion between the O4-H13 bond and the C1-N2 and N2-C8 bonds is minimized.

Although the equilibrium structure is more crowded than the T(H13-O4-N2-C1) = 181.8° structure, the stability provided by the two strong hydrogen bonds, O4-H12 and O11-H13, offsets the increased repulsion between the O4-H13 bond and the C1-N2 and N2-C8 bonds.

The N2-O4 rotational potential surface is an asymmetric two-fold rotor. In the positive direction, the barrier height is approximately 7.8 kcal/mol and located near 75°. In the negative direction the barrier height is approximately 8.5 kcal/mol and located near -75°. Conceptually the potential surface may be considered a perturbed two-fold rotor, but the location of the second minimum at a point other than 180° with a non-zero relative energy and the asymmetric barrier heights produce the complicated form of equation 7-3.

Figures 7-21 through 7-24 are plots of the C1-N2, N2-C8, N2-O4, O3-C8, C8-N9, N9-O10, and N9-O11 bond lengths as a function of change in T(H13-O4-N2-C1). The C1-N2 bond length exhibits only minor changes, a maximum of 0.006 Å, caused by steric interactions between the methyl group and the O4-H13 bond during rotation of the NOH group. The N2-C8 and N2-O4 bond lengths exhibit maxima when the O4-H13 bond eclipses either the C1-N2 or N2-C8 bonds. The N2-O4 bond length exhibits minima when the O4-H13 bond is bisecting or is anti to the C1-N2 or N2-C8 bonds. The maximum O3-C8 bond length occurs when the H13 to O3 distance is a minimum and the minimum O3-C8 bond length occurs when the O4-H13 bond eclipses the C1-N2 bond. The C8-N9 bond length is a minimum when the O4-H13 bond eclipses either the C1-N2 or N2-C8 bonds and is a maximum when the O11 to H12 or H13 distance is a minimum. The N9-O10 and N9-O11 bond lengths change in a coupled manner. The N9-O11 bond length is inversely proportional to the O11 to H12 or H13 distance. The N9-O10 bond length appears to change in response to perturbations of the electronic structure of the NO_2 group.

Figures 7-25 through 7-27 are plots of the C1-N2-O4, O4-N2-C8, C8-N2-C1, O3-C8-N2, and N9-C8-N2 angles as a function of change in T(H13-O4-N2-C1). The changes in the O4-N2-C1, O4-N2-C8, and C8-N2-C1 angles are related to steric interactions between the O4-H13 bond and the C1-N2 and N2-C8 bonds. When the O4-H13 bond eclipses either the C1-N2 or N2-C8 bonds the "included" angle is a maximum while the "opposite" angle is a minimum; e.g. at -70° O4-H13 eclipses N2-C8 and the O4-N2-C8 angle is a maximum, while the O4-N2-C1 angle is a minimum. The changes in the C1-N2-C8 angle are minor, less than 2°, and appear to be in response to the changes in the O4-N2-C1 and O4-N2-C8 angles. The minimum in the N2-C8-O3 potential surface correlates with the minimum distance between O3 and H13. The maxima in the N9-C8-N2 potential surface occur when either the O11 to H12 distance or the O11 to H13 distance is a minimum. The N9-C8-N2 angle is a minimum when the O4-H13 bond ecllipses the N2-C8 bond. The NO_2 group angles do not change significantly during rotation of the NOH group.

TORSION AROUND THE C8-N9 BOND

Torsion around the C8-N9 bond is equivalent to rotation of the NO_2 group. Figure 7-28 shows (hydroxy-methyl-amino)-nitro-methanol viewed along the C8-N9 bond. For convenience the coordinate Q(NO2) is defined as [T(O10-N9-C8-N2)+T(O11-N9-C8-N2)]/2 and the labelling of O10 and O11 are assumed to interchange after 180° of rotation. This assumption is equivalent to assuming the C8, N9, O10 and O11 atoms lie in the same plane in the equilibrium geometry, reduces the number of calculations required to determine the rotational potential surface by a factor of two, and should be accurate because C8 is only 1.4° out of the plane defined by N9, O10 and O11 in the equilibrium geometry.

$$V(x)=2.199(1-\cos(2x))-0.469(1-\cos(4x)) \tag{7-4}$$

$$V(x)=1.726(1-\cos(2x))-0.751\sin(2x) \tag{7-5}$$

V = relative energy in kcal/mol.
x = change in Q(NO2) from the equilibrium value of -49.0°.

Table 7-5 summarizes the geometry and energy changes as a function of change in Q(NO2). The solid line in Figure 7-29 is a cubic spline interpolation of the relative energy data given and indicates the barrier to internal rotation is 4.2 kcal/mol at 95°. Equations 7-4 and 7-5 were derived by performing a least squares fit of the relative energy data in Table 7-5 to two different two term expansions. The barrier to internal rotation derived from equation 7-4, is 4.26 kcal/mol at 90° while that derived from equation 7-5 is

3.61 kcal/mol at 102°. Neither equation 7-4 nor equation 7-5 provides a satisfactory description of the rotational potential surface. Although equation 7-4 provides an accurate barrier height, it does not provide an accurate description of the asymmetry of the potential surface. Equation 7-5 does not give an accurate barrier height and incorrectly locates the energy minimum near 10°, but it does provide a more accurate description of the asymmetry of the potential surface.

$$V(x)=2.054*(1-\cos(2x))-0.643*\sin(2x)-0.352*(1-\cos(4x)) \qquad (7\text{-}6)$$

V = relative energy in kcal/mol.
x = change in Q(NO2) from the equilibrium value of -49.0°.

Equation 7-6 is a three-term interpolating function of the relative energy data given in Table 7-6. This equation provides an accurate barrier height , 4.17 kcal/mol, and a reasonable description of the asymmetry of the potential function, but the energy minimum is incorrectly located near 18° instead of 0°. Deriving a more accurate description of the potential surface would require calculation of additional data points and is beyond the intended scope of this work.

Figures 7-30 through 7-32 are plots of the N2-C8, O3-C8, C8-N9, and N9-O10 bond lengths as a function of change in Q(NO_2). The N2-C8, O3-C8, and C8-N9 bond lengths change in response to steric interactions between the N9-O11, or N9-O10, bond and the C8-O3 and N2-C8 bonds. These three bond lengths achieve their maximum or minimum length when the N9-O11 bond eclipses either the C8-O3 bond, near 45°, or the N2-C8 bond, near 125°. A plot of the N9-O11 bond length is identical to Figure 7-32, except for a 180° phase shift. The NO_2 group NO bond length is about 1.205 Å if the oxygen atom is involved in hydrogen bonding, otherwise it is about 1.182 Å.

Figures 7-33 through 7-36 are plots of the C1-N2-O4, O3-C8-N2, N9-C8-N2, N9-C8-O3, C8-N2-C1, and O10-N9-C8 angles as a function of change in Q(NO_2). The changes in the C1-N2-O4, O3-C8-N2, N9-C8-N2, and N9-C8-O3 angles are caused by steric interactions between the N9-O11, or N9-O10, bond and the N2-C8 and O3-C8 bonds. Their maximum or minimum values occur when the N9-O11 bond eclipses either the C8-O3 or N2-C8 bond. The C8-N2-C1 angle is inversely proportional to the C1 to O10 or O11 distance, the angle is a maximum when the C1-O11 distance is a minimum. The

O10-N9-C8 angle exhibits maxima when the N9-O10 bond eclipses another bond and minima when the N9-O10 bond bisects two bonds. The O10-N9-O11 bond angle is almost constant during rotation of the NO_2 group, the maximum change is only 0.7°, indicating the NO_2 group reacts to changes in the molecular environment as a rigid body.

TORSION AROUND THE O3-C8 BOND

Torsion around the O3-C8 bond corresponds to internal rotation of the COH group. Table 7-6 shows the geometry and energy changes as a function of change in T(N2-C8-O3-H12) from the equilibrium value of -27.1°. Figure 7-37 shows (hydroxy-methyl-amino)-nitro-methanol viewed along the O3-C8 bond. In the equilibrium geometry the O3-H12 bond does not bisect the N2-C8-N9 angle, but instead it is rotated toward O4 to help form the hydrogen bond between O4 and H12.

Figure 7-38 is a plot of the relative energy data given in Table 7-6. The solid line is a cubic spline interpolation of the data. The barrier to internal rotation is approximately 7.8 kcal/mol at 130° and occurs when the O3-H12 bond eclipses the C8-H14 bond and the O3 electron lone pairs eclipse the N2-C8 and C8-N9 bonds, assuming sp^3 hybridization for O3. The dashed line is a plot of equation 7-7 which was derived via a least squares fit to the relative energy data. This potential function overestimates barrier height by about 0.5 kcal/mol and is too "flat" in the region from -180° to -100°. Equation 7-8 is a six term interpolating function of the data and provides a satisfactory representation of the potential surface.

$$V(x)=3.238(1-\cos(x))+0.816\sin(x)+1.392(1-\cos(2x))-0.491\sin(2x) \tag{7-7}$$

$$\begin{aligned} V(x)=&3.140(1-\cos(x))+0.816\sin(x)+1.291(1-\cos(2x))-0.486\sin(2x)\\ &+0.248(1-\cos(3x))+0.014\sin(3x) \end{aligned} \tag{7-8}$$

V = the relative energy in kcal/mol

x = the change T(N2-C8-O3-H12) from the equilibrium value of -27.1°

Geometry changes occurring during torsion of the O3-C8 bond are caused by interactions between the O3 electron lone pairs and the N2-C8 and C8-N9 bonds and by changes in hydrogen bonding. Figures 7-39 through 7-42 are plots of the N2-O4, C8-N2, O3-C8, C8-N9, N9-O10, and N9-O11 bond lengths as a function of change in T(N2-C8-O3-H12). The maximum N2-O4 bond length occurs when the O4-H12 distance is a minimum. The minimum C8-N2 and C8-N9 bond lengths occur when these bonds bisect the O3 lone pairs. The N9-O10 and N9-O11 bond lengths change in response the formation of hydrogen bond between O10 and H12 in the vicinity of -130°.

Figures 7-43 through 7-46 are plots of the C8-N2-C1, N9-C8-N2, O3-C8-N2, N9-C8-O3, C8-N2-O4, O10-N9-C8, and O11-N9-C8 angles as a function of change in T(N2-C8-O3-H12). The maximum C8-N2-C1 angle occurs in the region of maximum crowding between the O3 lone pairs and the methyl group. The N9-C8-N2, O3-C8-N2, and N9-C8-O3 angles change in a complex manner and the maximum and minimum values do not correspond to significant structural features. The minimum C8-N2-O4 angle occurs when the O3 lone pairs are "pointed" away from O4, decreasing steric crowding. The O10-N9-O11 angle, which is not plotted, is an almost constant 126.8° indicating the NO_2 group is responding to changes in the environment as a nearly rigid body. The changes in the C8-N9-O10 and C8-N9-O11 are caused by the NO_2 group tilting toward H12 to form either the O10 to H12 or O11 to H12 hydrogen bond.

CALCULATION OF FORCE CONSTANTS AND VIBRATIONAL FREQUENCIES

In this section, we determine the ab initio and scaled quantum mechanical force fields and the fundamental vibration frequencies of (hydroxy-methyl-amino)-nitro-methanol employing the formalism outlined in Chapter Two. The reference geometry for the ab initio force field calculation is shown in the third column of Table 7-1 and was derived from the optimized ab initio geometry and the appropriate bond length correction factors derived in Chapter Three. The internal coordinates, shown in Table 7-7, are defined as suggested by Pulay [4]. The ab initio force field, shown in Table 7-8, was calculated by the finite difference method.

The Scaled Quantum Mechanical force field (SQMFF) shown in Table 7-8 was derived from the ab initio force field and the scale factors shown in Table 7-9. Scale factors for the bending motions defined by coordinates 19, 20, 22, 23, 24, 25, 26, and 27 were not derived in Chapter Four and are assumed to be 0.8. Similarly, scale factors for the torsions defined by coordinates 34, 35, and 36 were not derived and are assumed to be 0.7.

The formation of the O11-H13 hydrogen bond, which weakens the N9-O11 bond, causes the diagonal force field elements for the two NO_2 N-O bonds to be quite different, 10.75 for N9-O10 and 8.643 for N9-O11 in the SQMFF. The diagonal force field element for deformation of the N2-C8-N9 angle, 3.190, is larger than usual for a bending coordinate. The diagonal force field elements for the methyl, C8-O3 and C8-N9 torsions are extremely small which is typical of low energy internal rotations.

The interaction force field elements show that the interactions are, for the most part, limited to "adjacent" internal coordinates. The interaction between the NO_2 deformation and the O4-H13 stretch, presumably related to the H13-O11 hydrogen bond, violates this general observation. Additionally, the torsional motions defined by internal coordinates 33 (torsion of the N2-O4 bond), 34 (torsion of the C2-N8 bond) and 36 (torsion of the C8-N9 bond) exhibit complex interactions with other internal coordinates.

Theoretical intensities associated with each of the fundamental vibration frequencies were calculated from the dipole moment derivatives. Table 7-10 gives the ab initio and SQM fundamental vibration frequencies, their associated theoretical intensities, and proposed assignments. The proposed assignments are based on the major M matrix contributions, this method usually shows good correlation with experimental assignments and there is not a one-to-one correspondence between the definitions of the internal coordinates and the frequency assignments.

Figure 7-47 is the scaled quantum mechanical vibrational spectrum for (hydroxy-methyl-amino)-nitro-methanol showing only the fundamental transitions and ignoring any possible Fermi resonances. The two strongest transitions are caused by torsion of the N2-O4 bond, at 661 cm^{-1}, and by a NO_2 bond stretching mode, at 1598 cm^{-1}. Four other moderately strong transitions are located at 1406 cm^{-1} (the other NO_2 stretching mode), 1431 cm^{-1} (the CH rocking mode), 3581 cm^{-1} and 3616 cm^{-1} (the two OH stretching modes). The theoretical spectrum suggests the transitions at 42 cm^{-1}, the NO_2 torsional mode, and 200 cm^{-1}, the methyl torsional mode, will be too weak to observe experimentally. Additionally six other transitions at 284 cm^{-1}, 355 cm^{-1}, 385 cm^{-1}, 1130

cm^{-1}, 1316 cm^{-1}, and 3037 cm^{-1} are likely to be characterized as very weak transitions and may be obscured in the experimental spectrum by stronger transitions. The observed vibrational spectrum will be more complicated than the SQM spectrum because of a variety of effects including Fermi resonance and the presence of overtone and combination bands.

THERMODYNAMIC DATA FOR (HYDROXY-METHYL-AMINO)-NITRO-METHANOL

The SQM vibrational frequencies calculated in the previous section (see Table 7-10), the molecular weight (122.03 gm/mole) and the rotational constants calculated from the a priori r_e geometry (I_A =2905.76 MHz, I_B =1866.25 MHZ and I_C =1621.22 MHz) provide the basis for calculating a table of thermodynamic values for (hydroxy-methyl-amino)-nitro-methanol employing the methods outlined in Chapter Two. Table 7-11 shows the specific heat at constant volume, entropy, free energy, and enthalpy from 200 K to 1500 K.

At higher temperatures the data in Table 7-11 will be too high because the internal rotations have not been treated properly. In the limit of equipartition of energy, the calculated thermodynamic quantities will be too high by 0.5 RT per torsional mode because the torsional motions are treated as vibrational modes and not internal rotors in this work. For an ethane-like molecule with a 3 kcal/mol barrier to internal rotation, the error at 800 K is approximately 0.25 RT. One of the original aims of this study was to develop a method to use the eigenvalues calculated from ab initio rotational potential functions to eliminate this error, but a concurrent study by Macdonald and coworkers [120] suggests theoretical eigenvalues derived from SCF ab initio rotational potential functions are not accurate enough for calculating thermodynamic data.

We now turn to the calculation of E_0 to complete the thermodynamic functions presented in Table 7-11. We cannot use the isodesmic reaction method outlined in Chapter Two because accurate vibrational frequencies are not available for H_2NOH. Employing the atomic equivalent method for calculating E_0, we start by subtracting the sum of the appropriate atomic equivalents given in Table 5-2, equal to -486.318220 H, from the ab initio energy, -486.411409 H, to yield the heat of formation at 298 K, -58.5 kcal/mol, which is in excellent agreement with the MINDO/3 heat of formation [117], -58.7

kcal/mol. E_0 is calculated from equation 5-2 and the following inputs; the heat of formation at 298 K, the values of H_0-E_0 for (hydroxy-methyl-amino)-nitro-methanol (5.83 kcal/mol), the standard reference states shown in Table 7-12 and the chemical reaction shown in equation 7-8. These data yield a (hydroxy-methyl-amino)-nitro-methanol E_0 energy of -51.6 kcal/mol.

$$2C(gr)+N_2(g)+O_2(g)+3H_2 \rightarrow CH_3NOHCHOHNO_2 \qquad (7\text{-}8)$$

SUMMARY

This Chapter has presented data for (hydroxy-methyl-amino)-nitro-methanol derived from the results of ab initio calculations with the 4-21NO* basis set. The disagreement between the ab initio and MINDO/3 optimized geometries is striking and disconcerting. For large flexible molecules, one may need to conduct a survey of a large number of possible geometries employing a semi-empirical method or an ab initio method with a minimal basis set and then perform more sophisticated calculations on a small number of the more stable conformers to find the optimum geometry. The results of this study suggest the differences between semi-empirical calculations at the MINDO/3 level and ab initio calculations employing a split valence shell basis set may be so great that the true optimum geometry may not be contained in the selected conformer subset .

Combining the results of this study with the earlier results of Bartlett and coworkers indicates (hydroxy-methyl-amino)-nitro-methanol is at least 50 kcal/mol more stable than the nitromethane dimer instead of the 25 kcal/mol reported previously [118].

The (hydroxy-methyl-amino)-nitro-methanol ground state conformer is stabilized by two intramolecular hydrogen bonds, one between O4 and H12 and one between O11 and H13. A conformation with hydrogen bonds between O4 and H12 and O11 and H12 is only 0.074 kcal/mol less stable than the equilibrium conformation. The relative order of these two conformations may change if more sophisticated calculations are completed.

The internal rotation barriers for (hydroxy-methyl-amino)-nitro-methanol are relatively high when compared to other molecules. The rotational potential surfaces calculated in this study should be considered as semi-quantitative because of limitations inherent in the level of ab initio calculations employed in their derivation. The geometry changes that occur during internal rotation are largely caused by changes in hydrogen bonding and bond crowding effects.

The vibrational frequency spectrum of (hydroxy-methyl-amino)-nitro-methanol should be dominated by lines attributed to the two O-H stretching modes, the N-O stretching modes and the N2-O4 torsional mode. The theoretical spectrum indicates that at least two and, possibly, up to eight of the transitions will not be observed experimentally.

The thermodynamic results show that formation of (hydroxy-methyl-amino)-nitro-methanol from standard reference state elements is exothermic. The thermodynamic values calculated in this study should be accurate to 5 kcal/mol at low temperatures. At higher temperatures the a priori thermodynamic functions will be biased by up to +2.5 RT because the effects of internal rotation were neglected.

TABLE 7-1[a]

Theoretical (Hydroxy-Methyl-Amino)-Nitro-Methanol Geometries

Parameter	4-21NO*(P)	r_e[b]	MINDO/3[c]	4-21D6/MNDO
C1-N2	1.467	1.462	1.425	1.469
O4-N2	1.407	1.471	1.366	1.405
C1-H5	1.078	1.083	1.123	1.085
C1-H6	1.084	1.088	1.118	1.078
C1-H7	1.082	1.087	1.118	1.081
C8-N2	1.432	1.431	1.444	1.443
C8-O3	1.371	1.374	1.357	1.384
C8-N9	1.554	1.542	1.507	1.530
N9-O10	1.183	1.209	1.229	1.184
N9-O11	1.207	1.237	1.231	1.201
O3-H12	.968	.964	.964	0.968
O4-H13	.970	.966	.953	0.970
C8-H14	1.075	1.080	1.150	1.074
<O4-N2-C1	110.5	110.5	113.2	109.0
<H5-C1-N2	107.4	107.4	118.2	112.2
<H6-C1-N2	112.7	112.7	111.7	107.4
<H7-C1-N2	108.6	108.6	111.3	109.3
<H7-C1-H6	109.6	109.6	105.0	109.1
<C8-N2-C1	115.6	115.6	125.6	114.1
<C8-N2-O4	108.7	108.7	111.3	105.8
<O3-C8-N2	111.8	111.8	119.9	115.9
<N9-C8-N2	111.7	111.7	104.3	106.4
<N9-C8-O3	106.7	106.7	112.1	108.8
<O10-N9-C8	116.4	116.4	113.2	116.6
<O11-N9-C8	117.1	117.1	115.5	115.7
<O11-N9-O10	126.5	126.5	131.3	127.7
<H12-O3-C8	104.7	104.7	118.8	106.2
<H13-O4-N2	104.6	104.6	115.4	105.4
<H14-C8-N2	111.3	111.3	111.9	108.0

Parameter	4-21NO*(P)	r_e[b]	MNDO/3[c]	4-21D6/MNDO[d]
<H14-C8-O3	111.8	111.8	99.5	110.9
T(O4-N2-C1-H5)	-61.4	-61.4	-75.2	-56.7
T(C8-N2-C1-H5)	174.6	174.6	67.1	61.3
T(H13-O4-N2-C1)	-64.4	-64.4	64.5	60.5
T(O3-C8-N2-C1)	172.6	172.6	-8.9	-47.8
T(N9-C8-N2-C1)	53.1	53.1	117.6	73.2
T(N2-C8-O3-H12)	-27.1	-27.1	23.5	96.3
T(O10-N9-C8-N2)	-139.5	-139.5	-60.1	75.0
T(O11-N9-C8-N2)	41.5	41.5	118.7	-103.9
E(H)(+486H)[e]	-.411409	-.406057	-.358342	-.411796
Delta E[f]	-.000	3.4	33.3	4.6[g]

a. Bond lengths in angstroms. Bond and torsion angles in degrees. Unless noted otherwise all values determined with the 4-21NO*(P) basis set.

b. Estimated r_e geometry derived from the optimized geometry and correction factors given in Chapter Three.

c. MINDO/3 optimized geometry determined by Bardo. See reference 117.

d. 4-21NO*D6 optimized geometry derived by starting at the MNDO/3 geometry.

e. Total energy in Hartrees.

f. Relative energy in Kcal/mole.

g. Reference energy is -486.419044 H with the 4-21NO*(D6) basis set.

TABLE 7-2[a]

Data for Calculating the C1-N2 Potential Surface

Parameter	Q+0[b]	Q+120.6[b]	Q+98.2[b]	Q+66.7[b]	Q+28.4[b]
DELTA E[c]	.000	.004	1.330	3.641	1.894
C1-N2	1.467	1.467	1.471	1.480	1.473
O4-N2	1.407	1.407	1.406	1.408	1.410
C1-H5	1.078	1.084	1.083	1.079	1.077
C1-H6	1.084	1.082	1.083	1.084	1.084
C1-H7	1.082	1.078	1.078	1.080	1.082
C8-N2	1.432	1.433	1.433	1.431	1.431
O3-C8	1.371	1.371	1.370	1.370	1.371
C8-N9	1.554	1.553	1.554	1.555	1.554
O10-N9	1.183	1.183	1.184	1.184	1.183
O11-N9	1.207	1.207	1.207	1.207	1.207
<O4N2C1	110.5	110.5	110.9	111.8	111.1
<H5C1N2	107.4	112.7	111.1	109.0	107.1
<H6C1N2	112.7	108.6	109.4	112.0	113.9
<H7C1N2	108.6	107.4	109.1	103.2	108.3
<H7C1H6	109.6	108.9	110.1	109.2	108.4
<C8N2C1	115.6	115.6	115.3	115.3	116.0
<C8N2O4	108.7	108.7	108.7	108.4	108.3
<O3C8N2	111.8	111.8	111.9	112.1	111.9
T(O4N2C1H5)[d]	-61.4	59.2	36.9	4.6	-32.9
T(C8N2C1H5)[d]	174.6	-64.8	-87.2	-119.9	-157.1

a. Bond lengths in angstroms. Bond and torsion angles in degrees.

b. Q+x denotes the change from the optimum geometry shown in Table 7-1. X is the change in T(4215) from the equilibrium value of -61.4°.

c. The change in energy relative to the optimum energy in kcal/mole.

d. T(abcd) is the torsion angle defined as the angle between planes abc and bcd.

TABLE 7-3^a

Data for Calculating the N2-C8 Torsional Potential Surface

PARAMETER	Q+0^b	Q-120.3^b	Q-60.5^b	Q+59.2^b	Q+120.7^b	Q+180.9^b
DELTA E^c	0.0	3.125	13.728	7.167	4.822	7.880
C1-N2	1.467	1.471	1.468	1.465	1.467	1.466
O4-N2	1.407	1.405	1.395	1.396	1.400	1.400
C1-H5	1.078	1.078	1.078	1.079	1.078	1.079
C1-H6	1.084	1.086	1.087	1.087	1.090	1.086
C1-H7	1.082	1.079	1.078	1.081	1.078	1.078
C8-N2	1.432	1.448	1.474	1.457	1.450	1.456
O3-C8	1.371	1.383	1.380	1.368	1.373	1.375
C8-N9	1.554	1.524	1.538	1.528	1.520	1.535
O10-N9	1.183	1.181	1.184	1.204	1.187	1.181
O11-N9	1.207	1.201	1.200	1.179	1.193	1.201
H12-O3	.968	.968	.970	.965	.968	.970
H13-O4	.970	.969	.964	.968	.969	.969
H14-C8	1.075	1.073	1.075	1.077	1.081	1.076
<O4N2C1	110.5	108.4	110.7	110.5	109.5	109.8
<H5C1N2	107.4	106.9	106.3	107.5	107.6	106.7
<H6C1N2	112.7	112.3	113.7	112.4	112.0	112.8
<H7C1N2	108.6	109.7	109.0	108.9	108.8	109.5
<H7C1H6	109.6	109.4	109.6	109.5	109.3	108.8
<C8N2C1	115.6	114.4	118.5	114.5	111.2	115.1
<C8N2O4	108.7	104.2	109.8	112.7	108.3	108.8
<O3C8N2	111.8	115.4	114.3	114.0	111.2	115.7
<N9C8N2	111.7	107.1	109.1	108.3	106.0	104.9
<N9C8O3	106.7	108.6	106.3	109.8	109.2	107.6
<O10N9C8	116.4	116.6	116.8	113.7	116.6	116.6
<O11N9C8	117.1	115.6	115.7	118.4	115.0	115.4
<O11N9O10	126.5	127.8	127.5	127.9	128.4	127.9
<H12O3C8	104.7	106.0	105.2	107.1	105.1	105.1
<H13O4N2	104.6	105.2	106.4	106.0	107.2	106.3

PARAMETER	Q+0[b]	Q-120.3[b]	Q-60.5[b]	Q+59.2[b]	Q+120.7[b]	Q+180.9[b]
<H14C8N2	111.3	108.0	110.6	111.9	114.6	110.4
<H14C8O3	111.8	111.0	112.0	109.0	109.9	112.0
T(O4N2C1H5)[d]	-61.4	-61.4	-52.4	-57.4	-61.8	-57.4
T(C8N2C1H5)[d]	174.6	-177.2	179.5	174.1	178.7	179.5
T(H13O4N2C1)[d]	-64.4	-62.9	-85.9	-61.8	-60.5	-53.6
T(O3C8N2C1)[d]	172.6	53.8	111.4	-125.1	-67.6	-9.3
T(N9C8N2C1)[d]	53.1	-67.2	-7.4	112.3	173.8	-127.8
T(N2C8O3H12)[d]	-27.1	-93.1	-98.4	-43.4	-66.9	-94.1
T(O10N9C8N2)[d]	-139.5	-78.9	-83.0	-65.4	-99.5	-78.0
T(O11N9C8N2)[d]	41.5	99.9	96.1	114.2	80.8	100.3

a. Bond lengths in angstroms. Bond and torsion angles in degrees.

b. Q+x denotes the change from the optimum geometry shown in Table 7-1. X is the change in T(9-8-2-1) from the equilibrium value of 53.1°.

c. The change in energy relative to the optimum energy in kcal/mole.

d. T(abcd) is the torsion angle defined as the angle between planes abc and bcd.

TABLE 7-4[a]

Data for Calculating the N2-O4 Potential Surface

PARAMETER	Q+0[b]	Q-118.3[b]	Q-58.5[b]	Q+61.4[b]	Q+122.6[b]	Q+181.8[b]
DELTA E[c]	-.000	2.778	8.162	6.832	4.681	.074
C1-N2	1.467	1.468	1.471	1.469	1.473	1.471
O4-N2	1.407	1.417	1.425	1.423	1.426	1.414
C1-H5	1.078	1.079	1.078	1.081	1.082	1.079
C1-H6	1.084	1.079	1.082	1.083	1.079	1.079
C1-H7	1.082	1.081	1.081	1.080	1.081	1.081
C8-N2	1.432	1.435	1.435	1.446	1.442	1.441
O3-C8	1.371	1.382	1.378	1.364	1.366	1.368
C8-N9	1.554	1.548	1.534	1.538	1.539	1.539
O10-N9	1.183	1.187	1.189	1.197	1.196	1.193
O11-N9	1.207	1.197	1.197	1.188	1.187	1.191
H12-O3	.968	.970	.964	.966	.966	.966
H13-O4	.970	.964	.966	.962	.962	.962
H14-C8	1.075	1.078	1.076	1.075	1.075	1.075
<O4N2C1	110.5	105.7	106.2	111.1	108.7	107.6
<H5C1N2	107.4	106.9	107.0	107.6	107.5	107.3
<H6C1N2	112.7	112.4	112.6	113.2	112.7	112.6
<H7C1N2	108.6	108.9	108.7	108.6	108.7	108.8
<H7C1H6	109.6	109.7	109.9	108.6	109.6	109.5
<C8N2C1	115.6	116.2	114.5	115.4	115.0	115.7
<C8N2O4	108.7	107.1	110.7	104.6	103.5	106.0
<O3C8N2	111.8	109.5	111.2	112.4	112.5	112.4
<N9C8N2	111.7	112.8	110.4	110.0	110.3	110.6
<N9C8O3	106.7	107.0	106.9	108.6	108.5	107.9
<O10N9C8	116.4	115.9	115.6	115.2	115.1	115.6
<O11N9C8	117.1	116.8	116.8	117.2	117.2	116.7
<O11N9O10	126.5	127.3	127.5	127.5	127.7	127.7
<H12O3C8	104.7	105.3	106.3	106.0	106.1	105.4
<H13O4N2	104.6	101.6	107.0	106.7	103.6	102.5

PARAMETER	Q+0[b]	Q-118.3[b]	Q-58.5[b]	Q+61.4[b]	Q+122.6[b]	Q+181.8[b]
<H14C8N2	111.3	109.8	110.0	109.8	109.6	109.7
<H14C8O3	111.8	113.6	113.7	110.9	110.8	111.2
T(O4N2C1H5)[d]	-61.4	-69.2	-59.1	-68.4	-71.7	-68.7
T(C8N2C1H5)[d]	174.6	172.1	178.3	172.7	172.9	173.1
T(H13-O4N2C1)[d]	-64.4	177.3	-122.9	-3.0	58.2	117.4
T(O3C8N2C1)[d]	172.6	175.9	-175.9	178.2	-179.7	177.6
T(N9C8N2C1)[d]	53.1	56.9	65.6	57.1	59.0	57.0
T(N2C8O3-H12)[d]	-27.1	-120.1	8.6	-55.2	-56.0	-73.0
T(O10-N9C8N2)[d]	-139.5	-71.1	-95.4	-82.1	-80.3	-81.4
T(O11-N9C8N2)[d]	41.5	109.6	81.0	95.2	98.5	96.9

a. Bond lengths in angstroms. Bond angles and torsion angles in degrees.

b. Change from the equilibrium value of T(H13-O4N2C1), -64.4 degrees.

c. Relative energy in kcal/mole.

d. T(abcd) is the angle between the plane defined by (abc) and the plane defined by (bcd).

TABLE 7-5[a]

Data for Calculating the C8-N9 Rotational Potential Surface

PARAMETER	Q+0[b]	Q+45.1[b]	Q+90.7[b]	Q+125.3[b]
DELTA E[c]	.000	.715	4.123	2.717
C1-N2	1.467	1.467	1.467	1.467
O4-N2	1.407	1.406	1.403	1.403
C1-H5	1.078	1.078	1.079	1.079
C1-H6	1.084	1.084	1.080	1.080
C1-H7	1.082	1.081	1.082	1.082
C8-N2	1.432	1.444	1.434	1.424
O3-C8	1.371	1.362	1.368	1.373
C8-N9	1.554	1.542	1.551	1.561
O10-N9	1.183	1.191	1.204	1.206
O11-N9	1.207	1.198	1.180	1.180
H12-O3	.968	.967	.966	.967
H13-O4	.970	.970	.969	.969
H14-C8	1.075	1.074	1.077	1.078
<O4N2C1	110.5	110.2	111.0	111.8
<H5C1N2	107.4	107.1	107.0	107.1
<H6C1N2	112.7	113.2	113.0	113.1
<H7C1N2	108.6	108.7	108.5	108.3
<H7C1H6	109.6	108.9	109.4	109.6
<C8N2C1	115.6	116.3	118.3	118.4
<C8N2O4	108.7	107.8	108.3	108.4
<O3C8N2	111.8	111.9	113.3	112.6
<N9C8N2	111.7	108.0	110.0	112.6
<N9C8O3	106.7	109.1	108.0	106.6
<O10N9C8	116.4	116.0	114.9	117.6
<O11N9C8	117.1	116.5	117.9	115.7
<O11N9O10	126.5	127.2	127.1	126.7
<H12O3C8	104.7	105.5	106.5	105.3
<H13O4N2	104.6	106.8	105.4	104.4

PARAMETER	Q+0[b]	Q+45.1[b]	Q+90.7[b]	Q+125.3[b]
<H14C8N2	111.3	111.2	110.5	110.7
<H14C8O3	111.8	111.8	109.8	110.4
T(O4N2C1H5)[d]	-69.2	-62.2	-63.4	-62.7
T(C8N2C1H5)[d]	172.1	174.8	170.5	170.2
T(H13-O4N2C1)[d]	-77.3	-64.6	-54.1	-60.9
T(O3C8N2C1)[d]	175.9	174.9	-158.7	-167.9
T(N9C8N2C1)[d]	56.9	54.8	80.2	71.6
T(N2C8O3-H12)[d]	-120.1	-34.1	-43.7	-33.2
T(O10-N9C8N2)[d]	-71.1	-91.1	-48.1	-14.4
T(O11-N9C8N2)[d]	49.6	83.3	131.5	167.0

a. Bond lengths in angstroms. Bond angles and torsion angles in degrees.

b. Change from the equilibrium value of [T(N2-C8-N9-O10)+T(N2-C8-N9-O11)]/2, -49.0 degrees.

c. Relative energy in kcal/mole.

d. T(abcd) is the angle between the plane defined by (abc) and the plane defined by (bcd).

TABLE 7-6[a]

Data for Calculating O3-C8 Rotational Potential Surfaces

PARAMETER	Q+0[b]	Q-120.8[b]	Q-59.5[b]	Q+59.9[b]	Q+119.9[b]	Q+179.4[b]
DELTA E[c]	-.000	5.525	3.681	4.277	7.774	6.795
C1-N2	1.467	1.467	1.467	1.468	1.468	1.469
O4-N2	1.407	1.397	1.400	1.402	1.399	1.399
C1-H5	1.078	1.079	1.078	1.078	1.078	1.078
C1-H6	1.084	1.081	1.086	1.084	1.084	1.082
C1-H7	1.082	1.082	1.081	1.083	1.083	1.083
C8-N2	1.432	1.418	1.437	1.428	1.424	1.418
O3-C8	1.371	1.375	1.368	1.383	1.384	1.380
C8-N9	1.554	1.563	1.544	1.538	1.541	1.554
O10-N9	1.183	1.192	1.186	1.184	1.185	1.189
O11-N9	1.207	1.194	1.204	1.203	1.201	1.199
H12-O3	.968	.966	.966	.964	.961	.962
H13-O4	.970	.967	.968	.968	.967	.967
H14-C8	1.075	1.083	1.075	1.078	1.078	1.078
<O4N2C1	110.5	111.2	110.1	110.3	110.1	110.6
<H5C1N2	107.4	106.9	107.1	107.3	107.3	107.0
<H6C1N2	112.7	113.1	113.1	112.3	112.6	112.9
<H7C1N2	108.6	108.8	109.0	109.1	109.3	109.1
<H7C1H6	109.6	109.5	108.9	109.7	109.5	109.7
<C8N2C1	115.6	117.5	115.7	115.0	114.6	115.0
<C8N2O4	108.7	110.7	109.6	110.8	111.4	111.1
<O3C8N2	111.8	111.9	113.1	112.0	112.9	111.2
<N9C8N2	111.7	112.5	108.9	113.4	113.7	114.2
<N9C8O3	106.7	106.7	108.0	103.5	103.1	104.7
<O10N9C8	116.4	115.7	117.1	116.2	115.7	113.9
<O11N9C8	117.1	117.6	115.5	116.9	117.4	119.2
<O11N9O10	126.5	126.7	127.1	126.9	126.9	126.8
<H12O3C8	104.7	106.3	106.2	105.7	107.8	107.6
<H13O4N2	104.6	105.0	106.9	104.7	104.8	104.8

PARAMETER	Q+0[b]	Q-120.8[b]	Q-59.5[b]	Q+59.9[b]	Q+119.9[b]	Q+179.4[b]
<H14C8N2	111.3	109.2	110.2	109.6	109.3	109.8
<H14C8O3	111.8	113.4	112.0	114.4	114.4	114.3
T(O4N2C1H5)d	-61.4	-59.9	-60.8	-60.0	-59.7	-59.0
T(C8N2C1H5)	174.6	171.2	174.2	173.9	173.8	174.2
T(H13-O4N2C1)	-64.4	-58.8	-63.8	-72.4	-70.5	-66.5
T(O3C8N2C1)	172.6	-161.1	178.6	172.0	173.7	179.9
T(N9C8N2C1)	53.1	78.8	58.6	55.3	56.7	61.6
T(N2C8O3-H12)	-27.1	-147.9	-86.6	32.8	92.8	152.3
T(O10-N9C8N2)	-139.5	153.2	-90.5	-141.7	-147.2	-164.3
T(O11-N9C8N2)	41.5	-29.2	84.8	38.2	33.4	17.3

a. Bond lengths in angstroms. Bond angles and torsion angles in degrees.

b. Change of T(N2-C8-O3-H12) from its equilibrium value of 23.5 degrees.

c. Relative energy in kcal/mole.

d. T(abcd) is the angle between the plane defined by (abc) and the plane defined by (bcd).

TABLE 7-7

DEFINITION OF INTERNAL COORDINATES FOR (HYDROXY-METHYL-AMINO)-NITRO-METHANOL

Q	Name	Definition[a]	Q	Name	Definition[a]
1	C N Stretch	R(1,2)	20	NO Rock	<(4,2,1)-<(4,2,8)
2	C-N Stretch	R(2,8)	21	N2O4 Wag	O4 out of <(8,2,1)
3	N2O4 Stretch	R(2,4)	22	NOH Bend	<(13,4,2)
4	C-N Stretch	R(8,9)	23	CH Rock	2<(14,8,2)-<(14,8,9)-<(14,8,3)
5	C-O Stretch	R(8,3)	24	CH Rock	<(14,8,9)-<(14,8,3)
6	N O Stretch (NO_2)	R(9,10)	25	NCN Deformation	4<(9,8,2)+<(9,8,3)+<(2,8,3)
7	N-O Stretch (NO_2)	R(9,11)	26	NCO Deformation	<(9,8,2)+4<(9,8,3)+<(2,8,3)
8	C-H Stretch	R(1,5)	27	NCO Deformation	<(9,8,2)+<(9,8,3)+4<(2,8,3)
9	C-H Stretch	R(1,6)	28	COH Bend	<(12,3,8)
10	C-H Stretch	R(1,7)	29	NO_2 Deformation	2<(10,9,11)-<(10,9,8)-<(11,9,8)
11	C-H Stretch	R(8,14)	30	NO_2 Rock	<(10,9,8)-<(11,9,8)
12	O-H Stretch	R(4,13)	31	NO_2 Wag	C8 out of (10,9,11)
13	O-H Stretch	R(3,12)	32	Methy Torsion	T(5,1,2,4)+T(6,1,2,4)+T(7,1,2,4)+T(5,1,2,8)+T(6,1,2,8)+T(7,1,2,8)
14	Methyl Symm. Def.	<(6,1,7)+<(6,1,5)+<(7,1,5)-<(5,1,2)-<(7,1,2)-<(6,1,2)	33	N2O4 Torsion	T(13,4,2,1)+T(13,4,2,8)
15	Methyl Asymm. Def.	2<(6,1,7)-<(6,1,5)-<(7,1,5)	34	N2C8 Torsion	T(4,2,8,3)+T(4,2,8,9)+T(4,2,8,14)+T(1,2,8,3)+T(1,2,8,9)+T(1,2,8,14)
16	Methyl Asymm. Def.	<(6,1,5)-<(7,1,5)	35	CO Torsion	T(12,3,8,14)+T(12,3,8,9)+T(12,3,8,2)
17	Methyl Rock	2<(5,1,2)-<(7,1,2)-<(6,1,2)	36	NO_2 Torsion	T(10,9,8,3)+T(10,9,8,2)+T(10,9,8,14)+T(11,9,8,3)+T(11,9,8,2)+T(11,9,8,14)
18	Methyl Rock	<(7,1,2)-<(6,1,2)			
19	CNC Deformation	2<(8,2,1)-<(4,2,1)-<(4,2,8)			

[a] *Internal coordinates defined as suggested by Pulay.* T(a,b,c,d) defines the angle between the abc and bcd planes.

TABLE 7-8[a]

Ab Initio Force Field for (Hydroxy-Methyl-Amino)-Nitro-Methanol

Element	Ab Initio	SQM	Element	Ab Initio	SQM	Element	Ab Initio	SQM
1,1	5.717	4.951	2,11	0.087	0.075	3,22	0.503	0.420
1,2	0.179	0.155	2,12	0.011	0.010	3,23	0.080	0.063
1,3	0.101	0.083	2,13	-0.107	-0.091	3,24	-0.001	-0.001
1,4	0.004	0.004	2,14	-0.012	-0.010	3,25	-0.068	-0.054
1,5	-0.027	-0.023	2,15	0.009	0.007	3,26	-0.024	-0.019
1,6	-0.036	-0.032	2,16	0.004	0.003	3,27	0.013	0.010
1,7	0.002	0.002	2,17	0.050	0.041	3,28	0.028	0.022
1,8	0.102	0.088	2,18	0.034	0.029	3,29	-0.024	-0.021
1,9	0.156	0.135	2,19	0.329	0.273	3,30	0.044	0.037
1,10	0.095	0.082	2,20	-0.481	-0.400	3,31	-0.019	-0.015
1,11	0.006	0.005	2,21	-0.707	-0.588	3,32	-0.011	-0.007
1,12	0.038	0.033	2,22	-0.050	-0.044	3,33	0.030	0.023
1,13	0.001	0.001	2,23	0.264	0.219	3,34	0.017	0.013
1,14	-0.533	-0.435	2,24	-0.059	-0.049	3,35	0.012	0.009
1,15	0.007	0.006	2,25	0.844	0.702	3,36	-0.003	-0.002
1,16	0.008	0.007	2,26	-0.387	-0.322	4,4	3.697	3.201
1,17	0.053	0.043	2,27	0.820	0.683	4,5	0.617	0.527
1,18	-0.092	-0.078	2,28	-0.043	-0.035	4,6	0.164	0.147
1,19	0.394	0.328	2,29	-0.189	-0.170	4,7	0.113	0.101
1,20	0.119	0.099	2,30	-0.101	-0.091	4,8	-0.002	-0.002
1,21	-0.324	-0.270	2,31	-0.013	-0.011	4,9	0.005	0.004
1,22	-0.008	-0.007	2,32	-0.003	-0.002	4,10	0.009	0.008
1,23	-0.004	-0.003	2,33	0.004	0.003	4,11	0.053	0.045
1,24	0.007	0.006	2,34	0.029	0.023	4,12	-0.130	-0.111
1,25	0.036	0.030	2,35	0.001	0.001	4,13	-0.008	-0.007
1,26	-0.033	-0.027	2,36	0.010	0.008	4,14	-0.023	-0.019
1,27	0.039	0.033	3,3	4.681	3.675	4,15	0.009	0.008
1,28	0.000	0.000	3,4	0.020	0.017	4,16	-0.004	-0.004
1,29	0.013	0.011	3,5	0.009	0.008	4,17	-0.025	-0.020
1,30	-0.007	-0.006	3,6	-0.062	-0.053	4,18	-0.028	-0.024
1,31	0.029	0.025	3,7	0.161	0.138	4,19	-0.016	-0.013
1,32	0.000	0.000	3,8	0.007	0.006	4,20	-0.164	-0.136
1,33	0.004	0.003	3,9	0.041	0.034	4,21	-0.280	-0.233
1,34	0.017	0.014	3,10	-0.009	-0.007	4,22	0.004	0.003
1,35	0.000	0.000	3,11	-0.025	-0.020	4,23	-0.271	-0.226
1,36	0.015	0.011	3,12	0.096	0.078	4,24	0.286	0.238
2,2	6.445	5.582	3,13	-0.037	-0.030	4,25	1.072	0.892
2,3	0.315	0.260	3,14	-0.017	-0.014	4,26	0.257	0.214
2,4	0.723	0.626	3,15	0.011	0.009	4,27	-0.336	-0.280
2,5	0.365	0.312	3,16	-0.019	-0.015	4,28	-0.017	-0.014
2,6	-0.026	-0.023	3,17	-0.055	-0.043	4,29	-0.335	-0.301
2,7	0.237	0.212	3,18	0.108	0.087	4,30	-0.243	-0.218
2,8	-0.018	-0.015	3,19	-0.268	-0.212	4,31	0.038	0.032
2,9	-0.066	-0.057	3,20	-0.224	-0.178	4,32	-0.002	-0.002
2,10	0.002	0.002	3,21	-0.458	-0.363	4,33	0.007	0.005

Element	Ab Initio	SQM	Element	Ab Initio	SQM	Element	Ab Initio	SQM
4,34	-0.098	-0.077	6,19	-0.034	-0.029	8,8	5.789	5.001
4,35	0.014	0.011	6,20	0.085	0.073	8,9	0.054	0.047
4,36	0.045	0.035	6,21	0.152	0.131	8,10	0.043	0.037
5,5	7.249	6.118	6,22	-0.082	-0.075	8,11	-0.001	-0.001
5,6	0.074	0.065	6,23	-0.003	-0.003	8,12	0.003	0.003
5,7	0.159	0.140	6,24	0.051	0.044	8,13	-0.003	-0.003
5,8	0.008	0.007	6,25	-0.051	-0.044	8,14	0.072	0.058
5,9	-0.001	-0.001	6,26	0.005	0.005	8,15	-0.145	-0.118
5,10	-0.007	-0.006	6,27	-0.045	-0.039	8,16	0.005	0.004
5,11	0.156	0.133	6,28	-0.020	-0.017	8,17	0.100	0.082
5,12	0.050	0.042	6,29	0.256	0.238	8,18	-0.002	-0.001
5,13	0.223	0.188	6,30	0.449	0.417	8,19	0.041	0.034
5,14	-0.004	-0.003	6,31	0.001	0.001	8,20	-0.030	-0.025
5,15	-0.005	-0.004	6,32	0.004	0.003	8,21	0.006	0.005
5,16	0.001	0.001	6,33	-0.042	-0.035	8,22	-0.001	-0.001
5,17	0.036	0.029	6,34	0.015	0.012	8,23	-0.004	-0.003
5,18	-0.012	-0.010	6,35	-0.004	-0.003	8,24	0.000	0.000
5,19	0.132	0.109	6,36	-0.028	-0.022	8,25	-0.005	-0.004
5,20	0.135	0.111	7,7	9.323	8.643	8,26	-0.005	-0.004
5,21	0.041	0.034	7,8	0.000	0.000	8,27	0.016	0.013
5,22	-0.001	-0.001	7,9	0.021	0.019	8,28	0.000	0.000
5,23	-0.207	-0.170	7,10	-0.016	-0.014	8,29	-0.002	-0.002
5,24	-0.385	-0.316	7,11	-0.006	-0.005	8,30	0.000	0.000
5,25	-0.510	-0.419	7,12	-0.187	-0.166	8,31	0.002	0.002
5,26	0.489	0.401	7,13	-0.039	-0.035	8,32	0.007	0.005
5,27	0.365	0.300	7,14	-0.028	-0.024	8,33	-0.005	-0.004
5,28	0.564	0.453	7,15	-0.010	-0.008	8,34	0.003	0.002
5,29	-0.049	-0.043	7,16	-0.010	-0.009	8,35	0.000	0.000
5,30	0.056	0.050	7,17	-0.009	-0.008	8,36	0.002	0.002
5,31	0.112	0.093	7,18	-0.042	-0.037	9,9	5.550	4.795
5,32	-0.002	-0.002	7,19	0.021	0.018	9,10	0.048	0.042
5,33	0.018	0.015	7,20	-0.128	-0.110	9,11	0.000	0.000
5,34	-0.018	-0.014	7,21	-0.168	-0.145	9,12	-0.011	-0.010
5,35	-0.024	-0.019	7,22	0.139	0.126	9,13	-0.001	-0.001
5,36	0.015	0.011	7,23	-0.051	-0.045	9,14	0.091	0.074
6,6	11.597	10.750	7,24	0.039	0.034	9,15	0.067	0.055
6,7	2.001	1.855	7,25	0.211	0.182	9,16	0.132	0.112
6,8	0.002	0.001	7,26	0.046	0.040	9,17	-0.026	-0.021
6,9	0.008	0.007	7,27	-0.072	-0.062	9,18	-0.050	-0.042
6,10	0.014	0.012	7,28	0.034	0.028	9,19	-0.078	-0.065
6,11	0.058	0.052	7,29	0.319	0.297	9,20	-0.021	-0.018
6,12	0.090	0.079	7,30	-0.317	-0.294	9,21	0.097	0.081
6,13	-0.002	-0.002	7,31	0.032	0.028	9,22	0.027	0.023
6,14	0.006	0.005	7,32	0.000	0.000	9,23	0.019	0.016
6,15	0.009	0.007	7,33	0.055	0.046	9,24	-0.023	-0.019
6,16	0.004	0.004	7,34	-0.007	0.006	9,25	-0.108	-0.090
6,17	0.009	0.007	7,35	0.019	0.015	9,26	0.049	0.041
6,18	0.015	0.013	7,36	0.022	0.018	9,27	0.024	0.020

Element	Ab Initio	SQM	Element	Ab Initio	SQM	Element	Ab Initio	SQM
9,28	-0.004	-0.003	11,22	-0.002	-0.002	13,20	0.025	0.021
9,29	0.003	0.003	11,23	-0.005	-0.009	13,21	-0.015	-0.012
9,30	0.022	0.020	11,24	0.036	0.030	13,22	0.007	0.006
9,31	-0.031	-0.026	11,25	-0.084	-0.070	13,23	0.009	0.008
9,32	-0.006	-0.004	11,26	-0.056	-0.047	13,24	-0.006	-0.005
9,33	-0.010	-0.008	11,27	-0.078	-0.065	13,25	0.074	0.061
9,34	-0.042	-0.033	11,28	0.019	0.015	13,26	-0.014	-0.012
9,35	0.002	0.001	11,29	0.011	0.009	13,27	-0.080	-0.066
9,36	-0.030	-0.023	11,30	-0.102	-0.091	13,28	0.330	0.265
10,10	5.645	4.878	11,31	-0.005	-0.004	13,29	0.010	0.009
10,11	0.015	0.013	11,32	-0.002	-0.002	13,30	-0.009	-0.008
10,12	-0.009	-0.007	11,33	-0.002	-0.001	13,31	-0.006	-0.005
10,13	0.003	0.003	11,34	0.004	0.003	13,32	0.001	0.000
10,14	0.068	0.055	11,35	-0.011	-0.009	13,33	-0.004	-0.003
10,15	0.082	0.067	11,36	0.003	0.003	13,34	-0.006	-0.004
10,16	-0.128	-0.108	12,12	8.492	7.176	13,35	0.000	0.000
10,17	-0.067	-0.054	12,13	-0.028	-0.023	13,36	0.003	0.002
10,18	0.108	0.091	12,14	0.007	0.006	14,14	0.790	0.608
10,19	-0.027	-0.022	12,15	-0.002	-0.002	14,15	-0.014	-0.011
10,20	0.048	0.040	12,16	0.007	0.006	14,16	0.000	0.000
10,21	-0.025	-0.021	12,17	0.011	0.009	14,17	0.014	0.011
10,22	-0.005	-0.004	12,18	-0.017	-0.015	14,18	0.014	0.011
10,23	0.002	0.002	12,19	0.034	0.028	14,19	-0.062	-0.049
10,24	0.001	0.001	12,20	-0.027	-0.022	14,20	-0.015	-0.012
10,25	0.025	0.021	12,21	0.047	0.038	14,21	0.033	0.026
10,26	-0.003	-0.002	12,22	0.127	0.110	14,22	-0.016	-0.013
10,27	0.001	0.000	12,23	-0.018	-0.015	14,23	-0.007	-0.006
10,28	-0.008	-0.006	12,24	0.044	0.037	14,24	0.004	0.003
10,29	-0.002	-0.002	12,25	-0.130	-0.107	14,25	-0.032	-0.025
10,30	-0.007	-0.006	12,26	0.004	0.003	14,26	0.013	0.010
10,31	0.001	0.001	12,27	0.041	0.033	14,27	-0.016	-0.013
10,32	0.002	0.002	12,28	0.044	0.035	14,28	0.007	0.005
10,33	0.004	0.003	12,29	0.116	0.103	14,29	0.010	0.009
10,34	0.006	0.005	12,30	0.095	0.085	14,30	0.002	0.001
10,35	0.001	0.000	12,31	0.002	0.002	14,31	0.004	0.003
10,36	0.005	0.004	12,32	0.001	0.000	14,32	-0.002	-0.001
11,11	5.866	5.068	12,33	0.050	0.040	14,33	0.003	0.003
11,12	-0.001	-0.001	12,34	0.046	0.035	14,34	0.005	0.004
11,13	-0.028	-0.024	12,35	0.001	0.000	14,35	-0.002	-0.001
11,14	-0.004	-0.003	12,36	-0.005	-0.004	14,36	0.001	0.001
11,15	0.000	0.000	13,13	8.659	7.137	15,15	0.710	0.546
11,16	0.003	0.003	13,14	0.000	0.000	15,16	-0.016	-0.013
11,17	0.002	0.001	13,15	0.002	0.002	15,17	-0.053	-0.041
11,18	0.001	0.001	13,16	-0.002	-0.001	15,18	0.008	0.006
11,19	-0.023	-0.019	13,17	-0.014	-0.012	15,19	0.045	0.035
11,20	-0.025	-0.020	13,18	0.012	0.010	15,20	-0.019	-0.015
11,21	-0.007	-0.006	13,19	-0.016	-0.013	15,21	-0.026	-0.021

Element	Ab Initio	SQM	Element	Ab Initio	SQM	Element	Ab Initio	SQM
15,22	-0.002	-0.002	17,29	0.007	0.297	20,23	-0.098	-0.079
15,23	0.000	0.000	17,30	0.011	-0.294	20,24	0.030	0.024
15,24	0.002	0.002	17,31	-0.005	0.028	20,25	-0.151	-0.121
15,25	0.032	0.041	17,32	0.026	0.017	20,26	-0.062	-0.049
15,26	-0.011	-0.014	17,33	-0.003	-0.002	20,27	-0.222	-0.178
15,27	-0.007	-0.009	17,34	0.005	0.004	20,28	0.082	0.064
15,28	-0.001	-0.001	17,35	-0.001	0.000	20,29	0.123	0.106
15,29	-0.003	-0.002	17,36	-0.002	-0.002	20,30	0.137	0.118
15,30	-0.008	-0.006	18,18	0.936	0.778	20,31	-0.002	-0.002
15,31	0.003	0.002	18,19	-0.079	-0.064	20,32	0.000	0.000
15,32	-0.012	-0.008	18,20	0.141	0.115	20,33	-0.091	-0.071
15,33	0.007	0.006	18,21	-0.023	-0.019	20,34	0.016	0.012
15,34	0.000	0.000	18,22	-0.011	-0.010	20,35	-0.013	-0.010
15,35	0.000	0.000	18,23	0.008	0.006	20,36	0.000	0.000
15,36	0.002	0.002	18,24	-0.002	-0.001	21,21	1.017	0.814
16,16	0.700	0.582	18,25	-0.043	-0.035	21,22	-0.037	-0.032
16,17	0.007	0.005	18,26	0.040	0.033	21,23	-0.012	-0.009
16,18	-0.006	-0.005	18,27	-0.030	-0.024	21,24	0.074	0.059
16,19	-0.003	-0.002	18,28	-0.003	-0.002	21,25	-0.811	-0.649
16,20	0.000	0.000	18,29	0.011	0.010	21,26	0.049	0.039
16,21	0.004	0.003	18,30	0.001	0.000	21,27	0.020	0.016
16,22	-0.006	-0.005	18,31	-0.006	-0.005	21,28	0.028	0.022
16,23	-0.003	-0.002	18,32	0.017	0.012	21,29	0.222	0.192
16.24	0.007	0.006	18,33	-0.004	-0.003	21,30	0.303	0.262
16,25	-0.002	-0.001	18,34	-0.012	-0.009	21,31	-0.057	-0.046
16,26	-0.002	-0.001	18,35	-0.003	-0.003	21,32	0.008	0.005
16.27	0.003	0.003	18,36	-0.007	-0.005	21,33	-0.006	-0.005
16,28	0.002	0.002	19,19	1.436	1.149	21,34	0.096	0.072
16,29	0.002	0.002	19,20	0.140	0.112	21,35	0.018	0.014
16,30	0.000	0.000	19,21	-0.226	-0.180	21,36	-0.043	-0.032
16,31	0.005	0.004	19,22	0.018	0.015	22,22	1.163	1.031
16,32	0.004	0.003	19,23	-0.052	-0.042	22,23	0.022	0.019
16,33	-0.003	-0.003	19,24	0.070	0.056	22,24	-0.013	-0.011
16,34	0.011	0.008	19,25	0.184	0.147	22,25	-0.119	-0.100
16,35	0.000	0.000	19,26	-0.223	-0.178	22,26	-0.007	-0.006
16,36	0.007	0.006	19,27	0.043	0.034	22,27	0.029	0.025
17,17	0.953	0.733	19,28	0.039	0.031	22,28	0.012	0.010
17,18	0.016	0.013	19,29	0.022	0.019	22,29	0.001	0.001
17,19	0.080	0.063	19,30	0.023	0.020	22,30	0.062	0.056
17,20	-0.055	-0.043	19,31	0.064	0.052	22,31	-0.023	-0.019
17,21	0.035	0.028	19,32	-0.014	-0.010	22,32	-0.004	-0.003
17,22	-0.007	-0.005	19,33	0.038	0.030	22,33	-0.027	-0.023
17.23	-0.010	-0.007	19,34	0.100	0.075	22,34	-0.010	-0.008
17,24	0.002	0.002	19,35	0.010	0.008	22,35	-0.002	-0.001
17,25	-0.080	-0.063	19,36	0.037	0.028	22,36	-0.021	-0.016
17,26	0.020	0.016	20,20	1.576	1,261	23,23	0.826	0.661
17,27	0.071	0.056	20,21	0.184	0.148	23,24	-0.047	-0.037
17,28	0.004	0.003	20,22	-0.010	-0.009	23,25	0.002	0.001

Element	Ab Initio	SQM	Element	Ab Initio	SQM	Element	Ab Initio	SQM
23,26	-0.012	-0.010	26,36	0.021	-0.031	33,33	0.130	0.100
23,27	0.052	0.042	27,27	2.916	2.333	33,34	0.051	0.037
23,28	-0.057	-0.045	27,28	-0.130	-0.101	33,35	0.024	0.017
23,29	0.032	0.028	27,29	0.061	0.053	33,36	0.018	0.013
23,30	0.075	0.064	27,30	-0.009	-0.007	34,34	0.165	0.115
23,31	-0.005	-0.004	27,31	-0.014	-0.012	34,35	0.024	0.017
23,32	0.001	0.001	27,32	0.002	0.002	34,36	0.021	0.015
23,33	0.005	0.004	27,33	-0.011	-0.008	35,35	0.052	0.037
23,34	-0.011	-0.008	27,34	0.018	0.013	35,36	0.006	0.004
23,35	0.027	0.020	27,35	0.013	0.010	36,36	0.021	0.015
23,36	-0.005	-0.004	27,36	-0.009	-0.007			
24,24	0.991	0.793	28,28	1.125	0.858			
24,25	-0.117	-0.093	28,29	0.007	0.006			
24,26	-0.014	-0.011	28,30	0.028	0.023			
24,27	-0.096	-0.077	28,31	0.008	0.007			
24,28	-0.073	-0.057	28,32	0.000	0.000			
24,29	0.033	0.029	28,33	0.011	0.008			
24,30	-0.003	-0.003	28,34	-0.002	-0.002			
24,31	-0.012	-0.010	28,35	0.002	0.001			
24,32	-0.001	-0.001	28,36	-0.004	-0.003			
24,33	0.020	0.016	29,29	1.687	1.574			
24,34	0.093	0.070	29,30	0.157	0.146			
24,35	0.029	0.022	29,31	-0.055	-0.048			
24,36	0.014	0.010	29,32	0.001	0.001			
25,25	3.988	3.190	29,33	-0.005	-0.004			
25,26	-0.322	-0.258	29,34	0.081	0.066			
25,27	-0.610	-0.488	29,35	-0.002	-0.001			
25,28	-0.069	-0.054	29,36	-0.021	-0.017			
25,29	-0.548	-0.474	30,30	1.260	1.176			
25,30	-0.507	-0.438	30,31	-0.028	-0.025			
25,31	0.013	0.011	30,32	0.003	0.002			
25,32	-0.019	-0.013	30,33	0.016	0.014			
25,33	0.031	0.025	30,34	0.118	0.095			
25,34	-0.166	-0.124	30,35	0.009	0.007			
25,35	-0.011	-0.008	30,36	-0.046	-0.037			
25,36	0.126	0.094	31,31	0.519	0.425			
26,26	2.186	1.749	31,32	-0.003	-0.002			
26,27	-0.380	-0.304	31,33	0.018	0.014			
26,28	0.009	0.007	31,34	0.023	0.018			
26,29	-0.028	-0.024	31,35	0.011	0.008			
26,30	0.038	0.033	31,36	0.028	0.022			
26,31	0.140	0.114	32,32	0.022	0.012			
26,32	0.008	0.006	32,33	0.000	0.000			
26,33	-0.029	-0.023	32,34	-0.003	-0.002			
26,34	-0.072	-0.054	32,35	0.000	0.000			
26,35	0.031	0.023	32,36	0.000	0.000			

a. Energy in aJ, coordinates in Å and radians.

TABLE 7-9[a]

SCALE FACTORS

Q	Factor	Q	Factor
1	0.866	19	0.8[b]
2	0.866	20	0.8[b]
3	0.785	21	0.887
4	0.866	22	0.8[b]
5	0.844	23	0.8[b]
6	0.927	24	0.8[b]
7	0.927	25	0.8[b]
8	0.864	26	0.8[b]
9	0.864	27	0.8[b]
10	0.864	28	0.763
11	0.864	29	0.933
12	0.845	30	0.933
13	0.845	31	0.820
14	0.769	32	0.577
15	0.769	33	0.766
16	0.831	34	0.7[b]
17	0.769	35	0.7[b]
18	0.831	36	0.7[b]

a. Internal coordinates defined in Table 8-7. Scale factors derived in Chapter 5.

b. Assumed value.

TABLE 7-10[a]

Fundamental Vibration Frequencies

Number	Ab Initio	SQM	Intensity	Assignment
1	50	42	51	NO_2 Torsion
2	169	141	327	N2C8 Torsion
3	242	200	49	Methyl Torsion
4	261	215	1819	NCN Deformation NCO Deformation
5	317	284	464	CNC Deformation NCO Deformation
6	328	300	2052	NCO Deformation
7	384	355	751	NO Rock NO_2 Rock
8	426	385	720	CNC Deformation N2O4 Wag
9	487	432	6130	CO Torsion
10	513	447	1209	C8N9 Stretch N2O4 Wag
11	624	571	3070	C8N9 Stretch NCO Deformation
12	755	661	20326	N2O4 Torsion
13	803	726	5474	NO_2 Wag
14	840	760	4876	N2O4 Stretch
15	865	796	7837	NO_2 Deformation
16	946	889	2104	C8N9 Stretch NO_2 Deformation
17	1088	987	4521	C8N2 Stretch Methyl Rock
18	1213	1110	3789	C1N2 Stretch
19	1239	1130	694	Methyl Rock
20	1268	1132	9488	CO Stretch

Number	Ab Initio	SQM	Intensity	Assignment
21	1372	1244	1314	C2N8 Stretch Methyl Rock CH Rock
22	1405	1278	8906	CH Rock
23	1467	1316	395	CO Stretch COH Bend
24	1491	1398	2929	Methyl Deformation
25	1524	1406	14290	N9O11 Stretch
26	1595	1431	13598	COH Bend
27	1620	1443	8068	Methyl Deformation NOH Bend
28	1642	1458	3216	Methyl Deformation
29	1675	1526	4037	Methyl Deformation
30	1691	1598	20775	N9O10 Stretch
31	3141	2920	1801	CH Stretch
32	3210	2984	1653	CH Stretch
33	3253	3024	1046	CH Stretch
34	3268	3037	733	C8H14 Stretch
35	3895	3581	9385	O4H13 Stretch
36	3934	3616	12203	O3H12 Stretch

a. Frequencies given in cm^{-1}. Assignments reflect the major contributions to the M matrix.

TABLE 7-11

THERMODYNAMIC DATA FOR (HYDROXY-METHYL-AMINO)-NITRO-METHANOL

T(K)	C_V[a]	Entropy[b]	$-(G_0-E_0)/T$[c]	$-(H_0-E_0)/T$[d]
100	13.29	64.86	53.82	11.05
200	22.12	78.27	62.82	15.45
300	29.79	89.51	69.88	19.63
400	36.76	99.63	76.08	23.56
500	42.69	108.9	81.73	27.21
600	47.54	117.5	86.99	30.54
700	51.50	125.5	91.93	33.54
800	54.76	132.8	96.58	36.24
900	57.48	139.7	101.0	38.68
1000	59.79	146.1	105.2	40.87
1100	61.75	152.0	109.2	42.87
1200	63.44	157.7	113.0	44.68
1300	64.90	163.0	116.6	46.33
1400	66.16	168.0	120.1	47.85
1500	67.26	172.7	123.5	49.24

a. Specific heat at constant volume in cal/mol/K.

b. Entropy in cal/mol/K.

c. Free energy in cal/mol/K.

d. Enthalpy in cal/mol/K.

TABLE 7-12

$H^{298}-E_0$ for Some Reference Atoms and Molecules

Atom/Molecule	$H^{298}-E_0$[a]
$H_2(g)$	2.024
C(graphite)	0.252
$O_2(g)$	2.072
$N_2(g)$	2.074

a. *Enthalpy in kcal/mol.*

FIGURE 7-1
LABELING OF ATOMS FOR (HYDROXY-METHYL-AMINO)-NITRO-METHANOL

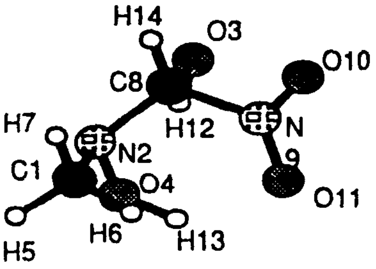
H14
O3
O10
C8
H7
H12
N
9
N2
C1
O4
O11
H5
H6
H13

FIGURE 7-2
MNDO/3 OPTIMUM GEOMETRY

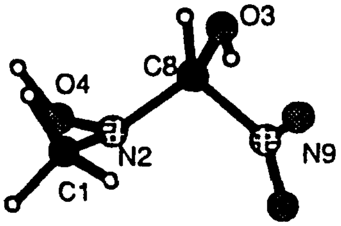
O3
C8
O4
N2
N9
C1

FIGURE 7-3
(HYDROXY-METHYL-AMINO)-NITRO-METHANOL LOOKING DOWN THE C1-N2 BOND

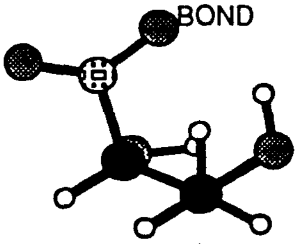

FIGURE 7-4
C1-N2 TORSION POTENTIAL SURFACE

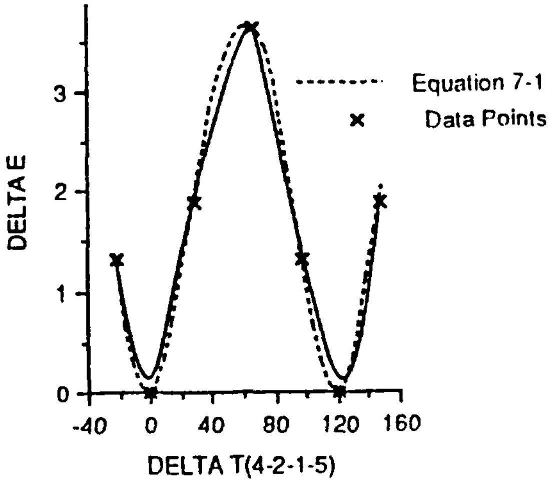

FIGURE 7-5
C1-N2 AND N2-O4 BONDS LENGTHS

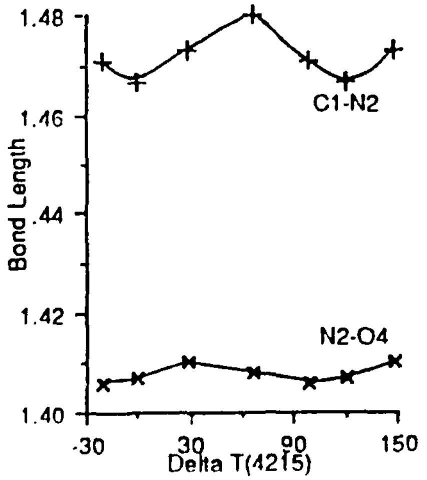

FIGURE 7-6
C1-N2-O4 ANGLE

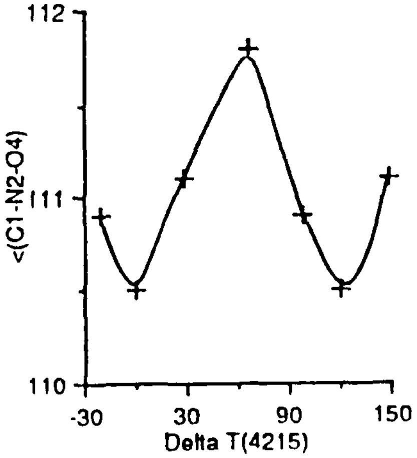

FIGURE 7-7

(Hydroxy-Methyl-Amino)-Nitro-Methanol
Looking Along the N2-C8 Bond

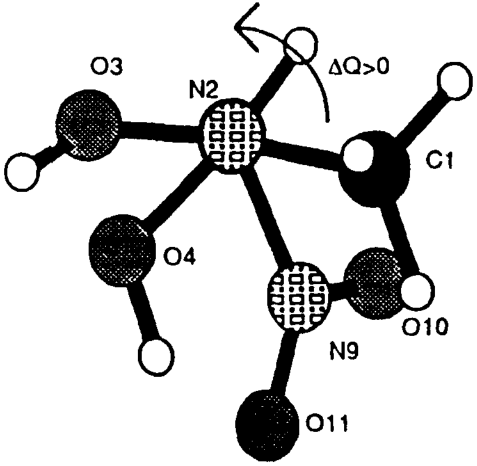
O3
N2
ΔQ>0
C1
O4
O10
N9
O11

FIGURE 7-8

C8-N2 TORSION POTENTIAL SURFACE

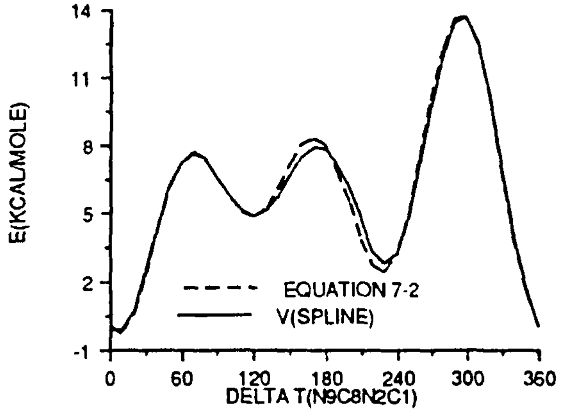

FIGURE 7-9

C1-N2 AND N2-C8 BOND LENGTHS

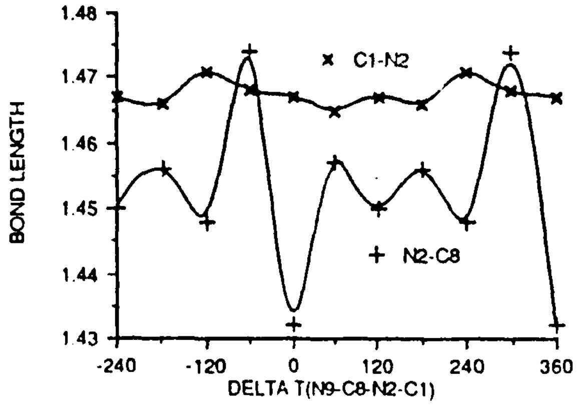

FIGURE 7-10

N2-O4 AND O3-C8 BOND LENGTHS

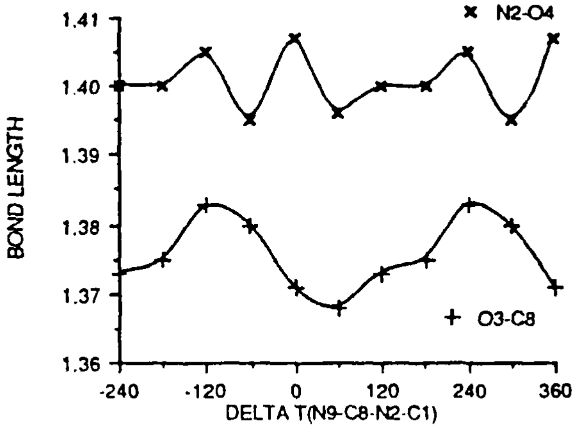

FIGURE 7-11
C8-N9 BOND LENGTH

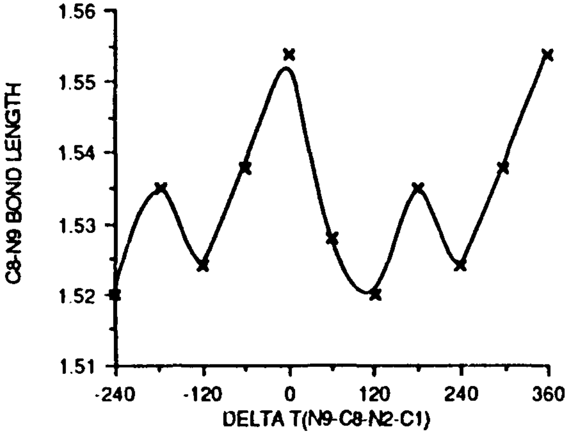

FIGURE 7-12
N9-O10 AND N9-O11 BOND LENGTHS

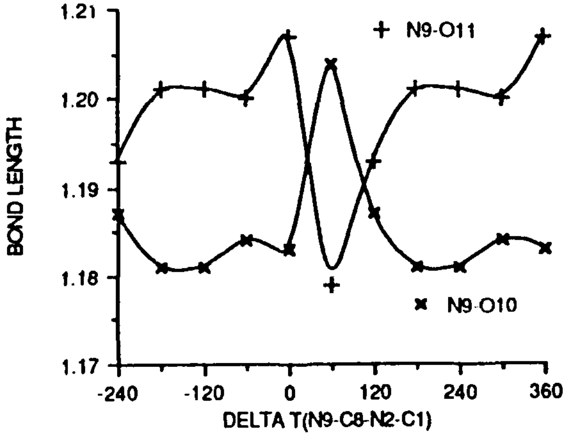

FIGURE 7-13
C1-N2-O4 AND C1-N2-C8 ANGLES

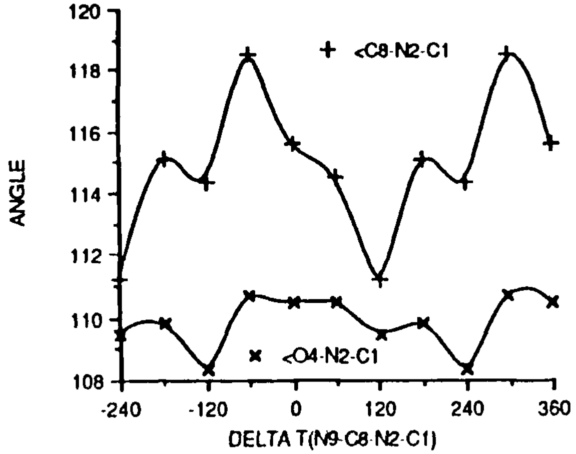

FIGURE 7-14
C8-N2-O4 AND N9-C8-N2 ANGLES

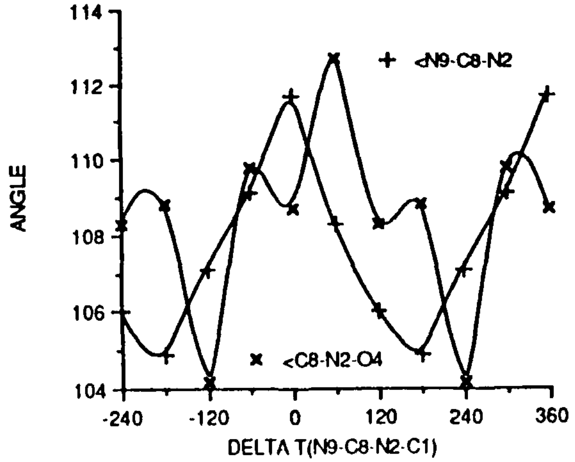

FIGURE 7-15
O3-C8-N2 AND N9-C8-O3 ANGLES

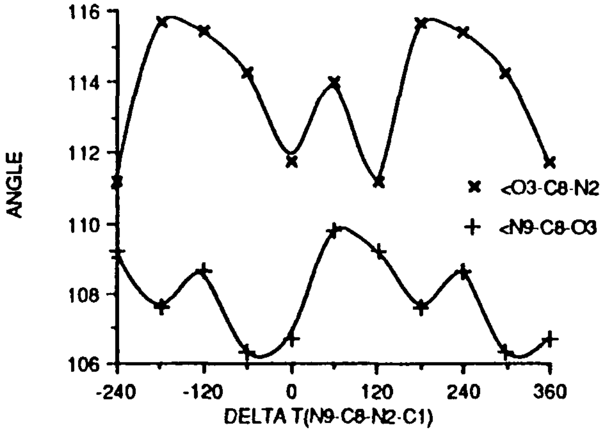

FIGURE 7-16
O10-N9-C8 AND O11-N9-C8 ANGLES

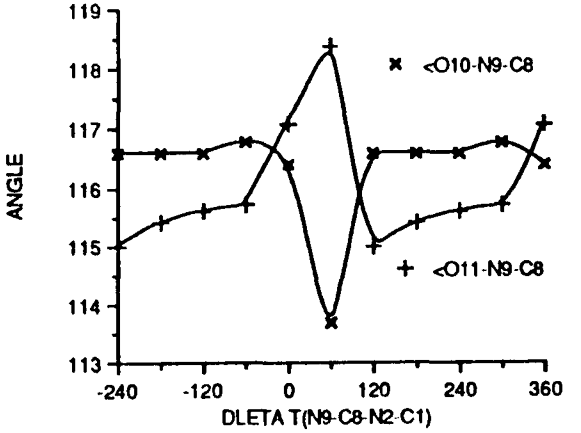

FIGURE 7-17
T(N2-C8-O3-H12) AND T(H13-O4-N2-C1)

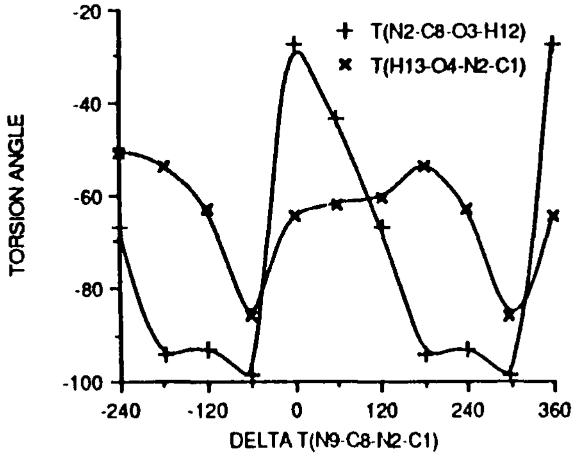

FIGURE 7-18
T(O10-N9-C8-N2) AND T(O11-N9-C8-N2)

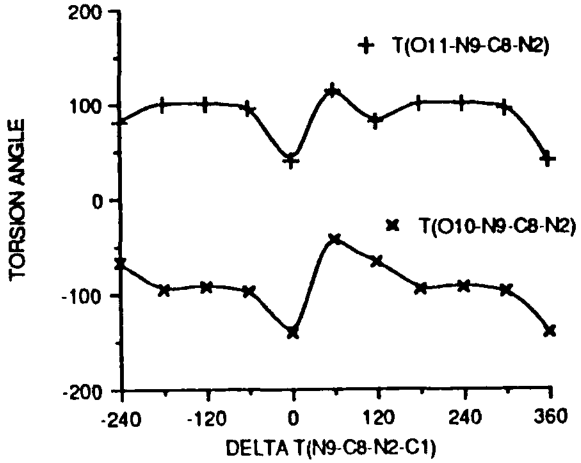

FIGURE 7-19
(Hydroxy-Methyl-Amino)-Nitro-Methanol
Viewed Along The N2-O4 Bond

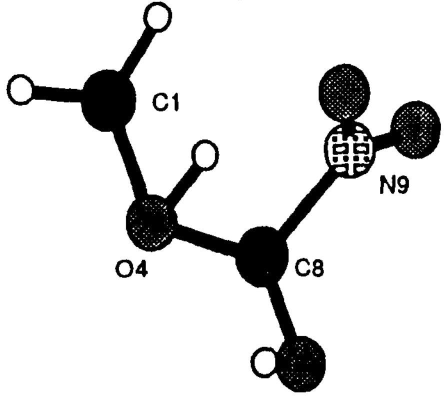

FIGURE 7-20
N2-O4 POTENTIAL SURFACE

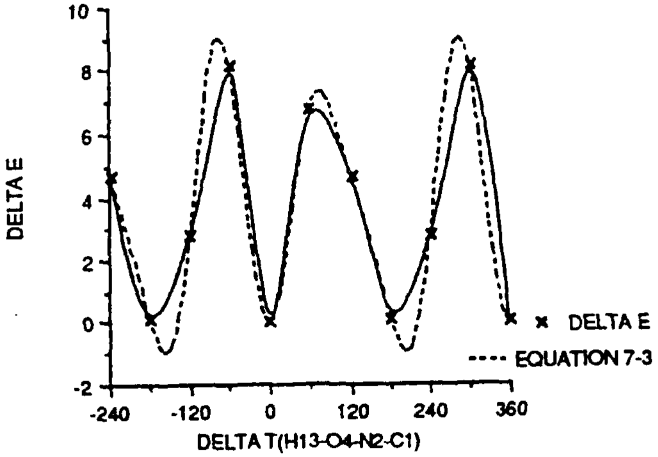

FIGURE 7-21
C1-N2 AND N2-C8 BOND LENGTHS

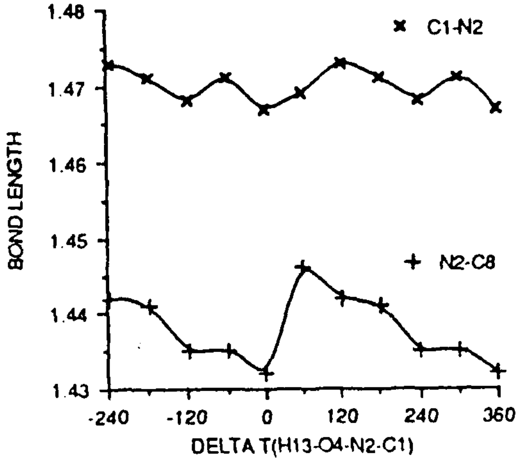

FIGURE 7-22
N2-O4 AND O3-C8 BOND LENGTHS

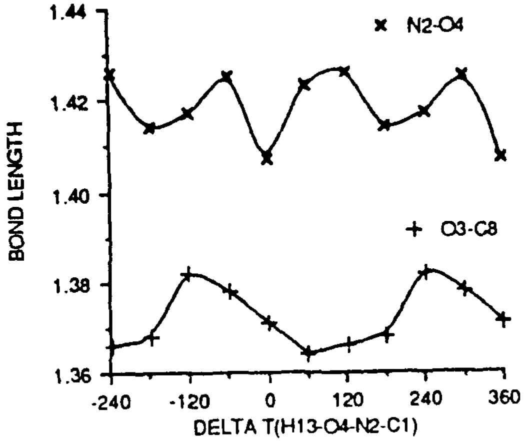

FIGURE 7-23

C8-N9 BOND LENGTH

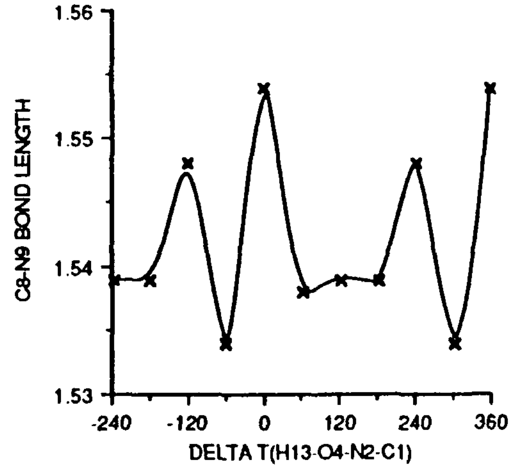

FIGURE 7-24

N9-O10 AND N9-O11 BOND LENGTHS

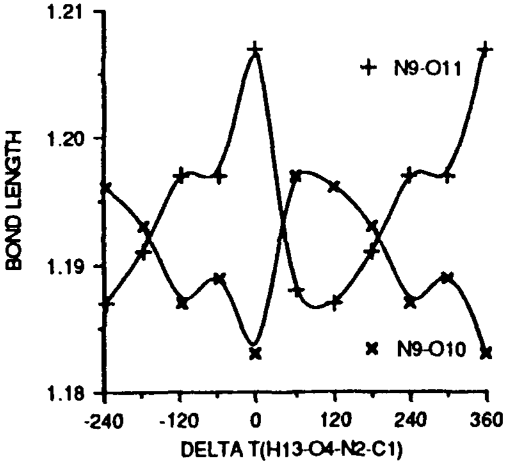

FIGURE 7-25

C1-N2-O4 AND O4-N2-C8 ANGLES

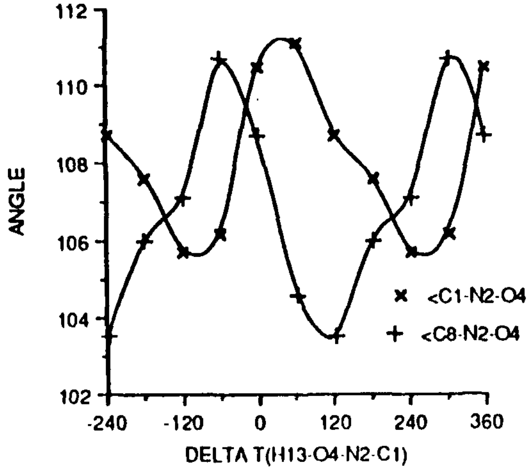

FIGURE 7-26

C8-N2-C1 AND O3-C8-N2 ANGLES

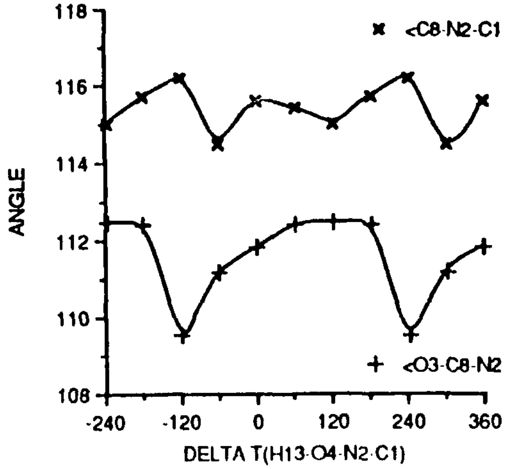

FIGURE 7-27
N9-C8-N2 ANGLE

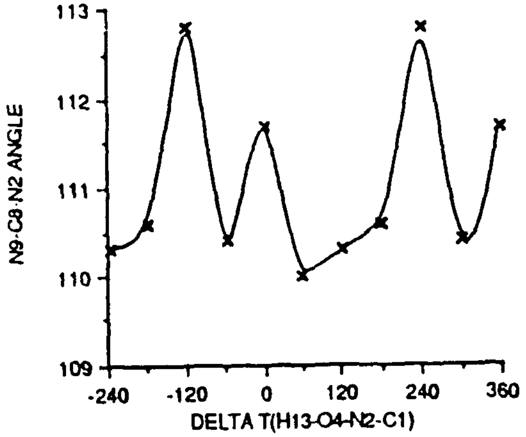

FIGURE 7-28
(Hydroxy-Methyl-Amino)-Nitro-Methanol
Viewed Along the C8-N9 Bond

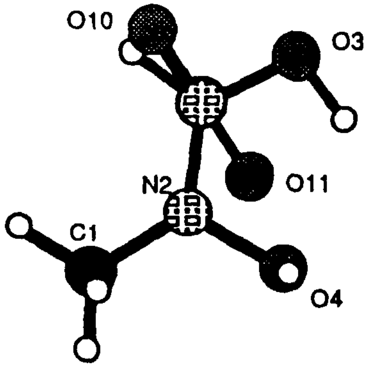

FIGURE 7-29
N9-C8 POTENTIAL SURFACE

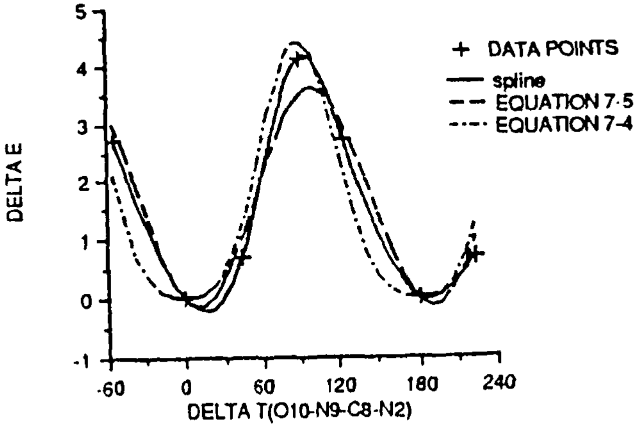

FIGURE 7-30
N2-O4 AND O3-C8 BOND LENGTHS

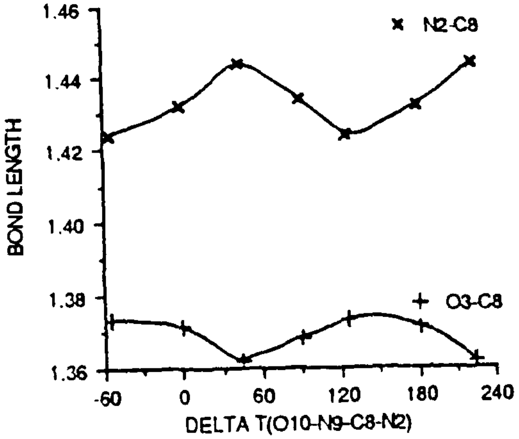

FIGURE 7-31
C8-N9 BOND LENGTH

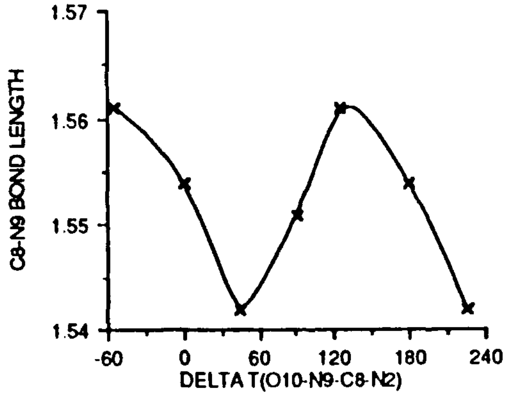

FIGURE 7-32
N9-O10 BOND LENGTH

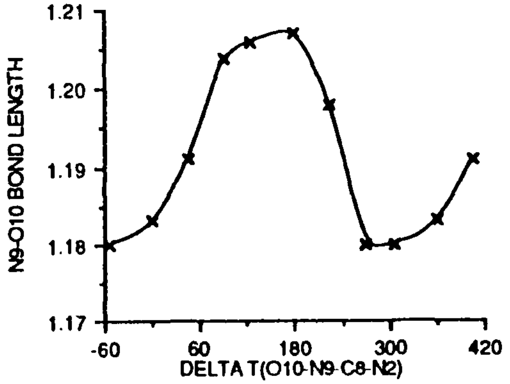

FIGURE 7-33
<C1-N2-O4 AND <O3-C8-N2 ANGLES

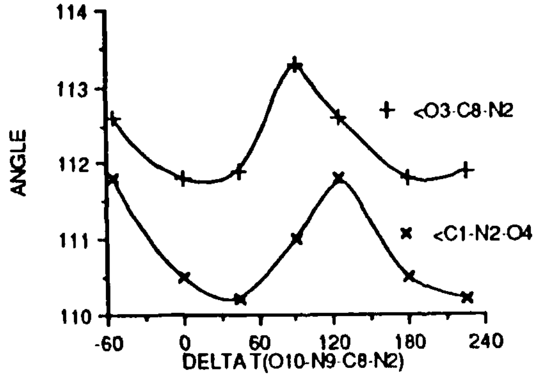

FIGURE 7-34
C8-N2-C1 AND N9-C8-N2 ANGLES

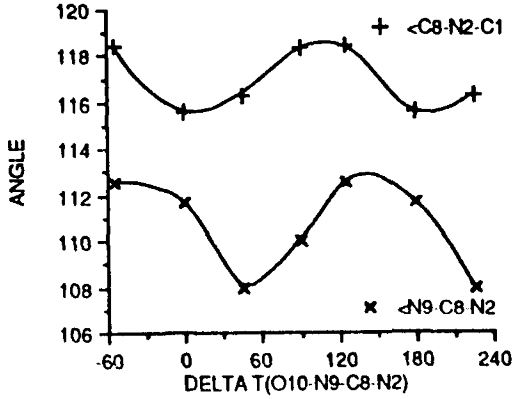

FIGURE 7-35
N9-C8-O3 ANGLE

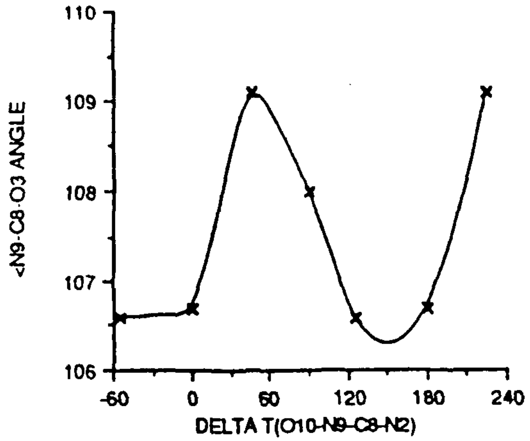

FIGURE 7-36
O10-N9-C8 ANGLE

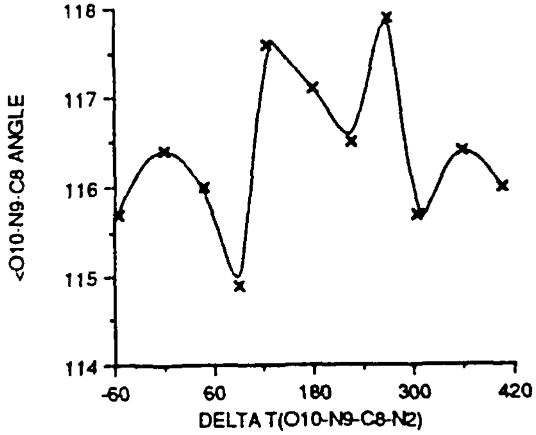

FIGURE 7-37
(Hydroxy-Methyl-Amino)-Nitro-Methanol
Viewed Along the O3-C8 Bond

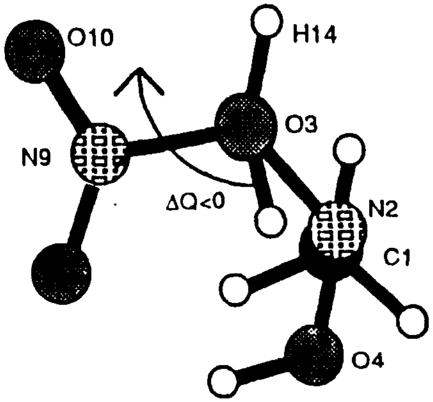
O10
H14
O3
N9
ΔQ<0
N2
C1
O4

FIGURE 7-38
C8-O3 POTENTIAL SURFACE

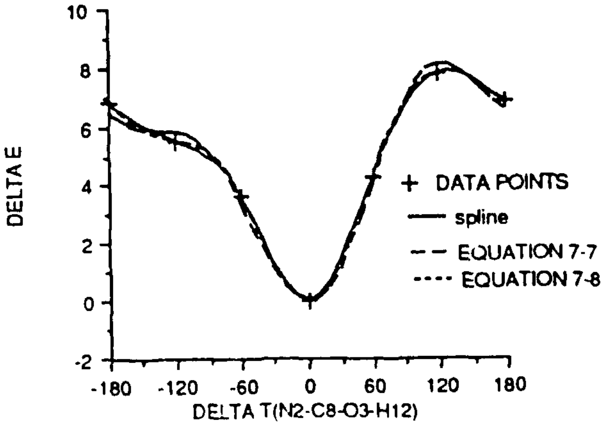

FIGURE 7-39
N2-O4 AND C8-N2 BOND LENGTHS

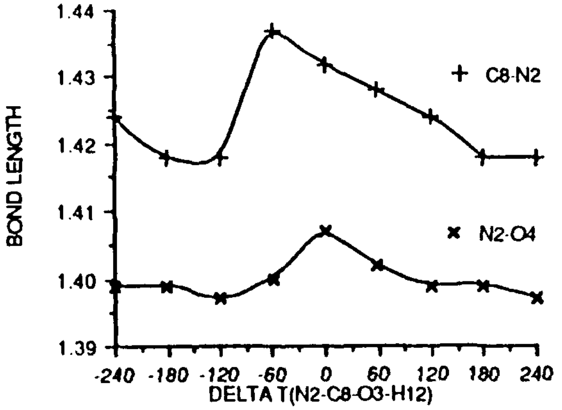

FIGURE 7-40
O3-C8 BOND LENGTH

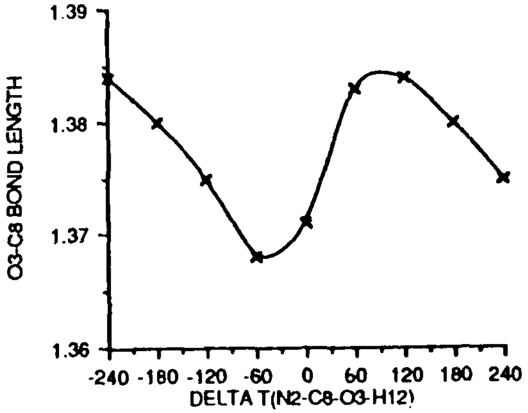

FIGURE 7-41
C8-N9 BOND LENGTH

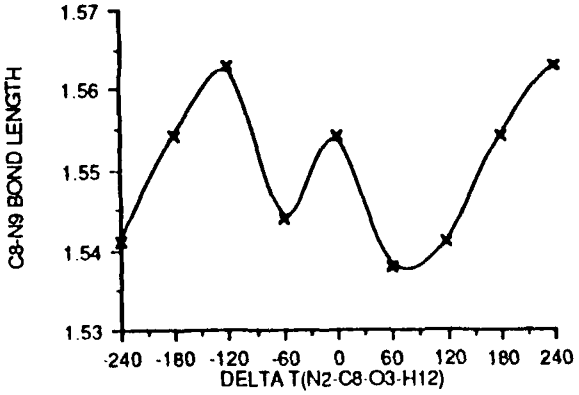

FIGURE 7-42
N9-O10 AND N9-O11 BOND LENGTHS

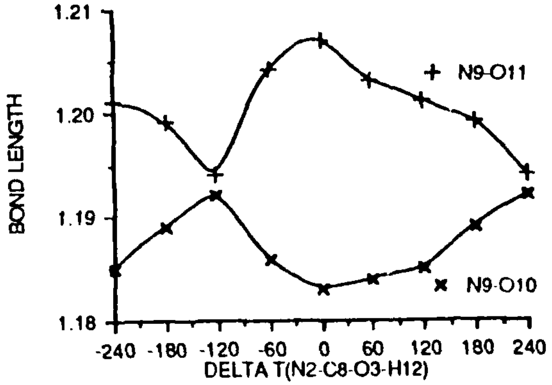

FIGURE 7-43

C8-N2-C1 AND N9-C8-N2 ANGLES

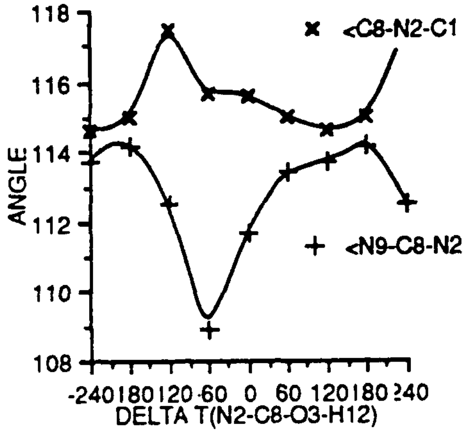

FIGURE 7-44

O3-C8-N2 AND N9-C8-O3 ANGLES

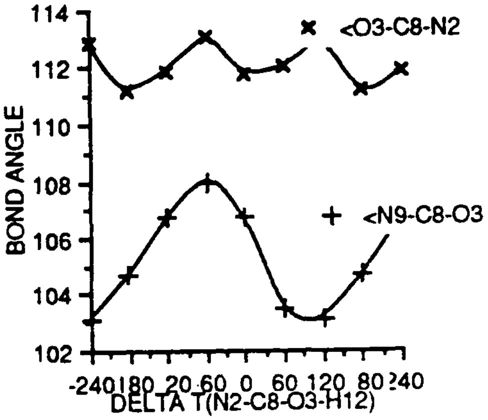

FIGURE 7-45

C8-N2-O4 ANGLE

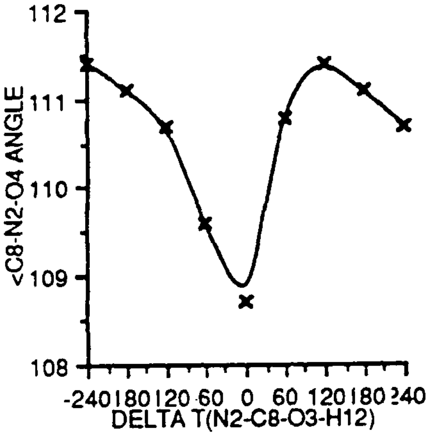

FIGURE 7-46

O10-N9-C8 AND O11-N9-C8 ANGLES

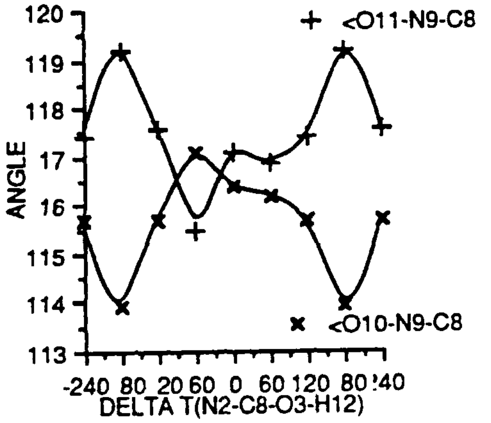

FIGURE 7-47

Scaled Quantum Mechanical IR Spectrum

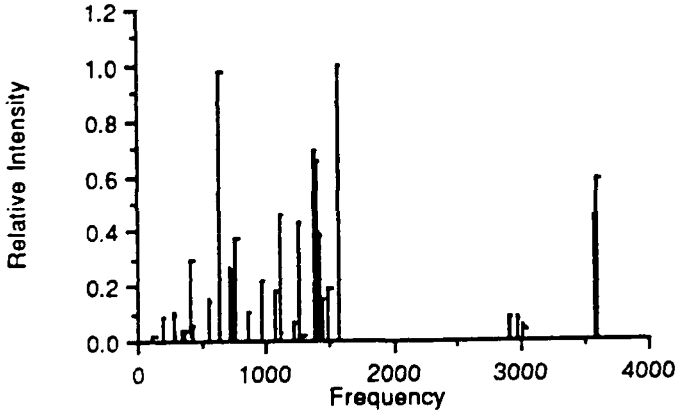

CHAPTER EIGHT

INTRODUCTION

One of the primary target molecules of the Navy's Energetic Materials program is 2,4,6,8-tetranitro-2,4,6,8-tetraazabicyclo[3.3.0]octane [121], shown in Figure 8-1, which is commonly called bicyclo HMX. As the common name suggests, this molecule is derived from the explosive HMX, 1,3,5,7-tetranitro-1,3,5,7-tetraazacyclooctane, also shown in Figure 8-1. Bicyclo HMX has the same structure as HMX, except for the bridging C-C bond which increases the ring strain and should increase the energy released during detonation. Additionally, analysis suggests that bicyclo HMX will have a density greater than HMX which should improve the explosive efficiency of bicyclo HMX even further.

Bicyclo HMX has not been synthesized, but several promising precursors have been synthesized [122,123,124]. The molecule 1,1,7,7 tetrakis(trifluoromethyl)-2,4,6,8-tetranitro-2,4,6,8-tetraazabicyclo[3.3.0]octane is a particularly promising high density, 2.18 g/cm^3, energetic molecule that is potentially useful as either a propellant or an explosive [122]. The high molecular density is attributed to intramolecular crowding, not efficient packing of molecules in the crystal structure. Attempts to remove the four CF_3 groups have been unsuccessful, all syntheses having resulted in ring decomposition products.

As a result of the difficulties encountered during the attempts to synthesize bicyclo HMX from 1,1,7,7-tetrakis(trifluoromethyl)-2,4,6,8-tetranitro-2,4,6,8-tetraazabicyclo[3.3.0]octane, experimentalists have started investigating other synthetic paths and have attempted synthesis of additional bicyclo HMX precursors. One of the new target molecules is the backbone of bicyclo HMX, 2,4,6,8-tetraazabicyclo[3.3.0]octane [121,122]. Unfortunately, synthesis of this molecule has proven to be another difficult problem. The experimental results indicate 2,4,6,8-tetraazabicyclo[3.3.0]octane is unstable and susceptible to electrophilic substitution at the ring nitrogens which leads to ring opening.

An initial goal of this study was the calculation of thermodynamic functions for bicyclo HMX, but the computer resources required to complete a calculation of this size with the 4-21NO*(P) basis set were considered to be excessive. Bicyclo HMX contains four carbon, eight nitrogen, eight oxygen, and four hydrogen atoms, which equates to 288 contracted basis functions with the 4-21NO* basis set. For a calculation of this size the CDC 175/750 would require about 713,000 CPU seconds, 8.2 days of dedicated CPU time, and the CRAY XMP would require about 83,600 CPU seconds, 23 CPU hours, to complete a single bicyclo HMX ab initio gradient calculation. The CDC CPU time requirements for a calculation of this size are clearly excessive, but one can consider undertaking a calculation of this size on the CRAY XMP.

The CPU time requirements described in the preceding paragraph are exacerbated by the number of possible bicyclo HMX conformations and by the number of calculations required to complete the force field calculation, 96 if the molecule is asymmetric and 52 if the molecule has one symmetry plane or C_2 axis. Selecting only two or three conformers for study based solely on chemical intuition does not appear to be feasible. The study of (hydroxy-methyl-amino)-nitro-methanol, discussed in Chapter Seven, indicates a series of semi-empirical calculations or minimal basis set ab initio calculations cannot conclusively identify only two or three conformers for study with the full 4-21NO* basis set. Based on these concerns, I elected to conduct a study of the backbone of bicyclo HMX, 2,4,6,8-tetraazabicyclo[3.3.0]octane.

Figure 8-2 shows the 2,4,6,8-tetraazabicyclo[3.3.0]octane numbering scheme used in this work. The geometries of three symmetrical configurations (cis, trans and twist) were optimized with the 4-21 basis set to examine the relative energies of these basic configurations. These initial calculations indicated the cis and trans backbone configurations have similar energies and an extensive series of geometry optimizations, examining 18 different conformers, were completed with the 4-21NO*(P) basis set. To examine the effect of substitution at the terminal carbons, C3 and C7, the geometry of 2,4.6,8-tetraazabicyclo[3.3.0]octane-3,7-dione was optimized from two different initial structures, one derived from the cis conformer and the other from the trans conformer. Geometry optimization criteria are given in Chapter Two. Next the potential surface describing the transformation from the cis conformer to the trans conformer and the ab initio and Scaled Quantum Mechanical force fields were derived with the methods given in Chapter 2. Finally, thermodynamic functions were calculated from the scaled quantum mechanical fundamental vibration frequencies, rotational constants calculated from the reference geometry, and the molecular weight.

Geometry Optimization Studies

Preliminary geometry optimization calculations were completed for three different backbone configurations using the 4-21 basis set to examine the relative stabilities of these conformations. To complete this series of calculations as quickly as possible, only the three symmetric conformers shown in Figure 8-3 were considered. Conformer A, a cis conformation with C3 bent toward the C1-C5 bond, belongs to the C_s symmetry group with the symmetry plane defined by C3, C7, and the midpoint of the C1-C5 bond. Conformer B, a trans conformation with C3 bent away from the C1-C5 bond, belongs to the C_{2v} symmetry group, one symmetry plane is defined by C3, C7, and the midpoint of the C1-C5 bond, the other symmetry plane is defined by C1, C5, H8, and H14, and the C_2 axis is defined by the intersection of the two symmetry planes. Conformer C, a "twist" conformation, belongs to the C_2 symmetry group with the symmetry axis passing through C3, C7, and the midpoint of the C1-C5 bond.

Table 8-1 shows the relative energies and optimized geometries for each of the three conformations. Conformer A is the most stable with conformer B 9.8 kcal/mol higher in energy and conformer C 30.0 kcal/mol higher in energy. The N-H bonds eclipse one another in conformer B resulting in increased intramolecular crowding and this may artificially increase the relative energy of conformer B. Based on these results, conformers A and B were selected for further study with the larger 4-21NO*(P) basis set.

Geometry optimizations for ten different variations of conformer A, shown in Figure 8-4, and seven different variations of conformer B, shown in Figure 8-5, were completed with the 4-21NO*(P) basis set. The position of the N-H bonds is different in each conformation with the hydrogen "above" the CNC plane, towards the top of the paper in Figures 8-4 and 8-5, or "below" the CNC plane, towards the bottom of the paper. The optimized geometries and relative energies for the cis conformations derived from conformer A are shown in Table 8-2. The optimized geometries and relative energies for the trans conformations derived from conformer B are shown in Table 8-3. To provide a consistent point of reference for comparing the data given in Tables 8-2 and 8-3 with the data given in Table 8-1, the relative energy of conformer 2, which has the same basic structure as conformer A, is assigned a relative energy of zero kcal/mol.

The most stable conformer, conformer 1 in Figure 8-4, is a cis configuration with the N-H bonds staggered, or alternating above and below the CNC plane. The most stable trans conformer, conformer 11 in Figure 8-5, is 1.4 kcal/mol higher in energy than conformer 1 and the N-H bonds are staggered in a manner similar to conformer 1. Conformer 15 and conformer B share the same basic structure, but conformer 15 has a relative energy of only 7.3 kcal/mol calculated with the 4-21NO* basis set instead of the 9.8 kcal/mol calculated with the 4-21 basis set. The least stable cis conformer, conformer 10, is 5.3 kcal/mol higher in energy than conformer 1 and all of the N-H bonds are above the CNC plane. The least stable trans conformer, conformer 17, is 15.7 kcal/mol higher in energy than conformer 1 and all of the N-H bonds are below the CNC plane.

Conformer 18, see Table 8-4 for the relative energy and optimum geometry, has the same basic C_2 structure as conformer C and has a relative energy of 25.4 kcal/mol which is significantly lower than the relative energy calculated with the 4-21 basis set, 30.0 kcal/mol. This result combined with a comparison of the relative energies for conformer 15 and conformer B reflects the increased flexibility inherent in the 4-21NO* basis set and indicates the crowded high energy conformers may be stabilized in relation to the lower energy conformers. Employing a larger basis set or including electron correlation effects may provide additional stabilization for the higher energy conformers and, as a result, the relative energies reported in this work may be an upper bound to the true relative energies.

The geometry differences between the various conformers shown in Tables 8-2 and 8-3 can be related to the position of the N-H bonds. In this discussion the normal ring configuration has one N-H bond above and one N-H bond below the CNC plane. The changes that occur in a cis ring, the right ring in the conformers shown in Figure 8-5, are opposite in sense to the changes that occur in a trans ring. This should be expected because the cis ring is essentially a mirror image of the trans ring and the relative direction of "above" and "below" the CNC plane in a cis ring is opposite to a trans ring. The N-H bond length does not correlate with the N-H bond position.

The ring "width", the distance between the nitrogen atoms across the ring, is strongly affected by the position of the N-H bonds. When both N-H bonds are above the CNC plane, the trans ring becomes wider and the cis ring becomes narrower. Conversely, when the both N-H bonds are below the CNC plane, the trans ring becomes narrower and the cis ring becomes wider.

The C1-C5 bond length exhibits a strong correlation with ring width, becoming longer as the ring becomes wider. The C1-C5 bond length reaches its maximum length when both rings in the molecule are wide, conformers 2 and 15. The C1-C5 bond length reaches its minimum length in the cis conformer when both rings are narrow, conformer 9, and in the trans conformer when only one of the rings is narrow, conformer 14. In the cis conformers, the width of the cis ring has a stronger influence on the length of the C1-C5 bond than does the width of the trans ring. For example, in conformer 8 all of the NH bonds are below the CNC plane. In this conformer the cis ring is driving the C1-C5 bond towards a longer length while the trans ring is driving the C1-C5 bond towards a shorter length. The C1-C5 bond length is 1.584 Å, longer than the normal C1-C5 bond length of 1.575 Å.

The changes in the terminal CN bond lengths (C3-N2, C3-N4, C7-N6, and C7-N8) correlate with the position of the attached N-H bond, but the changes in the interior CN bond lengths (C1-N2, C1-N8, C5-N4, and C5-N6) do not correlate with the position of the attached N-H bond. In a trans ring, the terminal CN bond length is less than 1.471 Å with the N-H bond below the CNC plane and greater than 1.471 Å with the N-H bond above the CNC plane. In a cis ring, the terminal CN bond length is greater than 1.474 Å with the N-H bond below the CNC plane and is less than 1.471 Å with the N-H bond above the CNC plane.

Changes in the NCN angle correlate with the ring width, but the changes in the CCN angles do not correlate with the ring width. In the normal configuration, the NCN angle is between 103° and 106°. With the ring in the narrow configuration, the NCN angle is less than 103° and with the ring in the wide configuration the NCN angle is greater than 106°.

The greater stability of the cis conformer of 2,4,6,8-tetraazabicyclo[3.3.0]octane relative to the trans conformer differs from the situation observed in the crystal structures of the bicyclo HMX precursors which exhibit the trans configuration. The optimum ab initio geometry of 2,4,6,8-tetraazabicyclo[3.3.0]octane-3,7-dione was calculated to investigate the effects of electronegative ring substituents. Two series of calculations were undertaken, one starting with a cis backbone and the other starting with a trans backbone. Both series of calculations converged to the trans configuration geometry shown in Table

8-5, suggesting the trans conformation is stabilized by bulky or electron withdrawing substituents.

Calculation of the Potential Surface Describing the Transition from Conformer 1 to Conformer 11

The symmetrical ring torsion, internal coordinate 23 from the definitions given in the next section, potential surface is an asymmetric double well with conformer 1 defining one minima and conformer 11 defining the other minima. The harmonic oscillator approximation, quite obviously, breaks down in this situation and cannot adequately describe the energy levels or the potential surface associated with this internal coordinate. Constrained geometry optimization calculations were completed for seven conformations to define individual points on the potential surface using the procedure presented in Chapter Two. The relative energies and geometries resulting from this series of calculations are shown in Table 8-6 along with the results for conformers 1 and 11. The conformer 11 geometry reported in Table 8-6 is the mirror image of the conformer 11 geometry reported in Table 8-3.

For convenience in the following discussion two dummy coordinates were defined to simplify analyzing and visualizing the potential surface. The first coordinate is the change in the C3-D2-D1 angle from 180° with D1 defined as the midpoint of the C1-C5 bond and D2 defined as the midpoint of the line segment joining N2 and N4. The second dummy coordinate is the C7-D3-D1 angle with D1 again defined as the midpoint of the C1-C5 bond and D3 defined as the midpoint of the line segment joining N6 and N8. The C3-D2-D1 coordinate tracks bending changes in the right ring, as the molecule is shown in Figures 8-4 and 8-5, while the C7-D3-D1 angle tracks bending changes in the left ring.

The potential energy surface is an asymmetric double well surface. Conformer 1 defines one minimum at 41.4° with $\Delta E = 0$ kcal/mol and conformer 11 defines the other minimum at -36.9° with $\Delta E = 1.44$ kcal/mol. The transition barrier, the hump in the potential surface, is located near 0° with $\Delta E \sim 3.9$ kcal/mol.

Equation 8-1, shown graphically in Figure 8-6, is the result of a least squares fit of a fourth order polynomial to the relative energy data given in Table 8-6. This function provides a poor description of the potential surface. The conformer 11 minimum is properly located near -37°, but the well is too deep with ΔE = 1.32 kcal/mol. The transition barrier is located at -4° and the barrier height is too high with ΔE = 3.97 kcal/mol. The conformer 1 minimum is located at 40° and is too shallow with ΔE = 0.23 kcal/mol.

$$V(x)=3.968-7.217E\text{-}3*x-4.316E\text{-}3*x^{2}-4.742E\text{-}6*x^{3}+1.467E\text{-}6*x^{4} \tag{8-1}$$

$$\begin{aligned} V(x)=\;&3.899+2.374E\text{-}2*x-4.046E\text{-}3*x^{2}-4.493E\text{-}5*x^{3}+1.348E\text{-}6*x^{4}\\ &+1.073E\text{-}8*x^{5} \end{aligned} \tag{8-2}$$

V = The potential energy in kcal/mol.
x = The change in the C3-D2-D1 angle defined in the text.

Equation 8-2, plotted in Figure 8-7, is the result of a least squares fit of a fifth order polynomial to the relative energy data of Table 8-6. This function provides a better description of the potential surface. The conformer 1 minimum is too broad with the minimum located at -34° and the depth of the well is too shallow with ΔE = 1.49 kcal/mol. The transition barrier is located at -2° and the barrier is too high with ΔE = 3.93 kcal/mol. The conformer 1 minimum is located at 41° and the depth of the well is described correctly with a relative energy of 0.03 kcal/mol.

The geometry changes associated with the transition of conformer 1 to conformer 11 are given in Table 8-6. Figure 8-8 is a plot of the C7-D3-D1 angle, which is defines the degree of bending in the conformer 1 trans ring, the left ring in Figure 8-4, as a function of change in the C3-D2-D1 angle. The maximum value of the C7-D3-D1 angle occurs in the vicinity of 0°, i.e. when the right ring is planar, or equivalently when the molecule is at the "top" of the transition barrier. When the right ring is perturbed to C3-D2-D1 angles greater than +40° or less than -40°, the trans ring flattens.

Figures 8-9 and 8-10 show the cis, or right, ring CN bond lengths as a function of change in the C3-D2-D1 angle. The C1-N2 and N4-C5 bond lengths, shown in Figure 8-9, change along different paths in response to changes in the degree of right ring "twisting" during the transition from conformer 1 to conformer 11. Figure 8-10 shows the N2-C3 and C3-N4 bond lengths as a function of change in the C3-D2-D1 angle. The maximum bond length for both of these bonds occurs in the vicinity of 0°. Figure 8-11 shows the C1-C5 bond length as a function of change in the C3-D2-D1 angle. This bond length changes in a simple manner during the transition from conformer 1 to conformer 11 achieving its minimum length when the cis ring is planar. The changes in the C1-C5, C1-N2, N2-C3, C3-N4, and N4-C5 bond lengths are consistent with the ring becoming wider, increasing distance between N2 and N4 , during the transition from conformer 1 to conformer 11. The C1-C5 bond length changes indicate the ring reaches its maximum width when the right ring is planar.

The left ring, the trans ring in conformer 1, CN bond lengths exhibit less significant changes, as one would expect, than the right ring CN bond lengths as a result of changing the C3-D2-D1 angle. Figures 8-12 and 8-13 show the C1-N8, C5-N6, N6-C7, and C7-N8 bond lengths as a function of change in the C3-D2-D1 angle. The C5-N6 and N6-C7 bond lengths exhibit only minor changes while the C7-N8 bond length exhibits a very sharp transition at 0°. The C1-N8 bond length smoothly decreases during the transition from the cis to the trans conformer.

Figures 8-14, 8-15, 8-16, and 8-17 show the values of the right ring angles (N2-C1-N6, N6-C5-N4, C1-N2-C3, C3-N4-C5, N4-C3-N2, C5-C1-N2, and N4-C5-C1) as a function of change in the C3-D2-D1 angle. All of these angles change in a similar manner, becoming larger as the ring becomes planar, i.e. as C3-D2-D1 approaches 0°, and becoming smaller as the ring bending increases.

Figures 8-18, 8-19, and 8-20 show the values of the left ring angles (C7-N6-C5, C7-N8-C1, N8-C7-N6, C5-C1-N8, and C1-C5-N6) as a function of change in the C3-D2-D1 angle. These angles change by less than one degree, reflecting the relatively minor left ring flattening of 6°, during the transition from conformer 1 to conformer 11. The angles exhibit transition points, maxima or minima, near C3-D2-D1 equal to 0°.

The geometry changes associated with the transition of conformer 1 to conformer 11, in general, follow simple paths when compared to the geometry changes examined in Chapter Seven associated with hindered internal rotation. The bond length and angle changes in the right ring, as shown in Figures 8-4 and 8-5, are caused by ring closure requirements as the ring becomes planar at the transition point. The bond length and angle changes in the left ring of the molecule are relatively minor and are a result of the left ring flattening by 6° at the top of the transition barrier.

Calculation of the Ab Initio and Scaled Quantum Mechanical Force Fields

The formalism outlined in Chapter 2 for calculating the ab initio and Scaled Quantum Mechanical Force Fields states the first step in the process is determining a reference geometry, usually by correcting the most stable ab initio geometry for the basis set offset. For 2,4,6,8-tetraazabicyclo[3.3.0]octane, I decided to deviate from this procedure. The goal of this study is the examination of the bicyclo HMX backbone which should have a trans structure instead of the cis structure exhibited in the most stable 2,4,6,8-tetraazabicyclo[3.3.0]octane conformer. As a result, the higher energy conformer 11 geometry, given in Table 8-6, instead of the conformer 1 geometry was used as the basis for determining the reference geometry. This selection, as a side benefit, reduces the computational effort required to calculate the ab initio force field by about 40 per cent because we can take advantage of the C_2 symmetry present in the trans conformer. The reference geometry was calculated with the bond length correction formulae developed in Chapter Three and is given in Table 8-7. The ring bond angles given in Table 8-7 are slightly different from the conformer 11 bond angles given Table 8-6, another minor deviation from the procedure outlined in Chapter Two, because of ring closure constraints. The internal coordinates were defined as suggested by Pulay [4,24] and are shown in Table 8-8.

The ab initio force field was calculated with the finite difference method outlined in Chapter 2 and is shown in Table 8-9. The Scaled Quantum Mechanical (SQM) Force Field, given in Table 8-11, was derived from the ab initio force field using the appropriate scale factors, shown in Table 8-10, derived in Chapter Four. Scale factors for the CH_2 rocking coordinates (internal coordinates 41, 42, 47, and 48) were not derived in Chapter Four and they are assumed equal to 0.8.

Theoretical fundamental vibration frequencies were calculated using Wilson's GF method [34] from the ab initio and SQM force fields. Table 8-12 shows the ab initio and SQM fundamental frequencies and the theoretical intensities. Figure 8-21 is a stick plot of the SQM infrared vibrational frequency spectrum using relative intensities assuming the intensity of the NH rock transition at 1392 cm^{-1}, the strongest theoretical line, equals one. The theoretical intensities are not accurately proportional to the observed experimental intensities, but are related in a semi-quantitative fashion. The theoretical intensity data suggest 15 of the 48 transition lines in the 2,4,6,8-tetraazabicyclo[3.3.0]octane infrared vibrational spectrum will be difficult to observe experimentally. The N-H stretch transitions (at ~3600 cm^{-1}) are much weaker than the C-H stretch transitions (at ~2950 cm^{-1}). The region from 900 cm^{-1} to 1500 cm^{-1} is crowded and dominated by the NH wag transition at 1101 cm^{-1}, the CH_2 wag transition at 1237 cm^{-1}, the CH rock transition at 1353 cm^{-1}, and the NH rock transition at 1392 cm^{-1}. Experimentally identifying all of the vibration lines in this region will be a difficult task.

Thermodynamic Functions for 2,4,6,8-Tetraazabicyclo[3.3.0]octane

A priori thermodynamic functions for 2,4,6,8-tetraazabicyclo[3.3.0]octane were calculated with the SQM fundamental frequencies determined in the preceding section, the rotational constants given in Table 8-13 (determined from the reference geometry given in Table 8-7), the rotational symmetry number (2), and the molecular weight, 154.15 gm/mole. The table of thermodynamic values is shown as Table 8-14 and was calculated using the rigid rotor harmonic oscillator formalism outlined in Chapter Two.

The 2,4,6,8-tetraazabicyclo[3.3.0]octane E_0 energy, which is required to complete the table of thermodynamic values, may be calculated via Pople's isodesmic reaction method [11,36] or via the atomic equivalents determined in Chapter Five. In the isodesmic reaction method, we start by calculating the ab initio heat of reaction for the isodesmic reaction given as equation 8-3, 0.059578 Hartree or 37.364 kcal/mol, using the reference data provided in Table 8-15. Next the ab initio heat of reaction is corrected for the change in zero point vibrational energy, 10.006 kcal/mol, to yield the 0 K theoretical heat of reaction, 47.37 kcal/mol. Finally, the value of E_0 for 2,4,6,8-tetraazabicyclo[3.3.0]octane, 54.256 kcal/mol, is calculated from the reaction 8-3 theoretical heat of reaction and the E_0 values of the other molecules involved in the chemical reaction.

$$C_4N_4H_{10} + 4NH_3 + 6CH_4 \rightarrow 8CH_3NH_2 + C_2H_6 \tag{8-3}$$

$$5H_2 + 4C(graphite) + 2N_2 \rightarrow C_4N_4H_{10} \tag{8-4}$$

To calculate the E_0 energy with the atomic equivalent method, we subtract the sum of the appropriate atomic equivalents from Table 5-2, -374.388212 Hartree, from the optimum ab initio energy, -374.320308 Hartree, to obtain the 2,4,6,8-tetraazabicyclo[3.3.0]octane heat of formation at 298.15 K, 42.61 kcal/mol. The E_0 energy, 53.23 kcal/mol, is calculated from this heat of formation and the $H^{298.15}$-E_0 values of the atoms and molecules shown in the formation reaction defined by equation 8-4. The value of E_0 obtained from the isodesmic reaction method is averaged with the value of E_0 obtained from the atomic equivalent method to give the final E_0 value of 53.7 kcal/mol.

The equilibrium constant at constant pressure, K_p, can be calculated from the thermodynamic data given in Table 8-15, the value of E_0 for 2,4,6,8-tetraazabicyclo[3.3.0]octane and standard thermodynamic data for other atoms and molecules. For the combustion reaction defined by equation 8-5, $\ln(K_p)$ is on the order of 1175 at 298 K and on the order of 374 at 1000 K indicating 2,4,6,8-tetraazabicyclo[3.3.0]octane is very unstable thermodynamically, in accord with the experimental observation.

$$C_4N_4H_{10} + 10.5\ O_2 \rightarrow 4CO_2 + 4NO_2 + 5H_2O \qquad (8\text{-}5)$$

In this section, we have determined the thermodynamic functions for a specific conformer of 2,4,6,8-tetraazabicyclo[3.3.0]octane assuming the rigid-rotor harmonic-oscillator approximation and ignoring the complications of the double well potential surface that describes the transition of conformer 1 to conformer 11. The specific heat and entropy should be accurate to about ±2% and the free energy and enthalpy should be accurate to about ±5 kcal/mol for conformer 11 as suggested in Chapter 2, but for the molecular system as a whole the thermodynamic functions given in Table 8-14 will be less accurate. In particular the calculated entropy is probably too low, because the contributions of other low energy conformers have been ignored.

Summary

In this chapter optimized geometries, the potential surface describing the conversion of conformer 1 to conformer 11, ab initio and Scaled Quantum Mechanical force fields, fundamental vibration frequencies and theoretical intensities, and thermodynamic functions have been calculated for 2,4,6,8-tetraazabicyclo[3.3.0]octane, the backbone of bicyclo HMX. The most stable conformer is a cis conformer with the N-H bonds alternating above and below the CNC plane. The most stable trans conformer is 1.4 kcal/mol higher in energy than this cis conformer. The position of the NH bonds strongly influences the molecular geometry. The "normal" ring configuration is one NH bond above the CNC plane and the other NH bond below the CNC plane. When the two NH bonds are above the CNC plane, a trans ring widens and a cis ring narrows. When the two NH bonds are below the CNC plane, a trans ring narrows and a cis ring widens. Adding electronegative substituents to C3 and C7 stabilizes the trans ring relative to the cis ring and this suggests that most stable conformer of bicyclo HMX will be a trans conformation.

The theoretical infrared vibration spectrum indicates 15 of the 48 fundamental transitions will be difficult to observe experimentally. The region from 900 cm^{-1} to 1500 cm^{-1} will be quite complex and dominated by four intense transitions. The a priori thermodynamic data show 2,4,6,8-tetraazabicyclo[3.3.0]octane is thermodynamically unstable with respect to the standard state elements below 1500 K, the highest temperature considered in this work.

The thermodynamic data calculated in this Chapter were derived from a single conformer. The actual system may consist of a number of low energy conformations and this will increase the entropy, i.e. the a priori entropy reported here is too low. Additionally the system will probably be in the solid state and this will create additional perturbations to the energy levels of the system. The "isolated molecule" thermodynamic functions reported here provide a starting point for further investigations of the bicyclo HMX solid state.

The results of this work may be extended to a study of bicyclo HMX. The optimized geometry of conformer 11 provides a good starting point for the geometry of the ring and the ab initio force field should help reduce the number of iterations required for calculating the optimum geometry of bicyclo HMX. Unfortunately, this study does not provide any information concerning the orientation of the four nitro groups in bicyclo HMX. Presumably, the nitro groups will be in an alternating configuration similar to the NH bonds in this study, but the more critical question is "What are the torsion angles for each of nitro groups?" This question may be answered with a series of calculations employing the 4-21 or 3-21 basis sets or possibly with a series of semi-empirical calculations, prior to undertaking more expensive calculations employing the 4-21NO* basis set. The discrepancies between the MNDO and ab initio geometries discussed in Chapter 8 indicate this type of approach must be well planned and may not conclusively identify the bicyclo HMX equilibrium configuration.

Table 8-1

2,4,6,8 Tetraazabicyclo[3.3.0] octane Geometries Calculated with the 4-21 Basis Set

Parameter^{a}	Conf A	Conf B	Conf C	Parameter	Conf A	Conf B	Conf C	Parameter	Conf A	Conf B	Conf C
Energy^{b}	-4.213713	-4.198073	-4.165850	N8-C1-N2	111.3	114.0	126.3	T(N4-C3-N2-C1)^{d}	31.3	-31.8	-14.3
Delta E^{c}	0.0	9.8	30.0	N8-C1-C5	105.4	105.4	103.0	T(C5-N4-C3-N2)^{d}	-31.3	31.8	-14.3
C1-N2	1.471	1.481	1.473	N8-C7-N6	107.2	107.2	108.9	T(N4-C5-C1-N2)^{d}	0.0	0.0	-47.5
N2-C3	1.480	1.481	1.520	C7-N8-C1	107.5	106.0	102.2	T(N6-C5-C1-N2)^{d}	117.8	120.9	180.0
C3-N4	1.480	1.481	1.520	H9-C1-N2	110.8	110.1	107.4	T(N4-C5-C1-N8)^{d}	-117.8	-120.9	180.0
C1-C5	1.596	1.598	1.520	H9-C1-C5	112.7	111.4	108.2	T(N6-C5-C1-N8)^{d}	0.0	0.0	47.4
N4-C5	1.471	1.481	1.473	H9-C1-N8	111.0	110.3	107.8	T(N6-C5-N4-C3)^{d}	-95.0	-134.0	153.7
C5-N6	1.474	1.481	1.473	H10-N2-C1	113.0	112.3	112.5	T(C7-N6-C5-N4)^{d}	129.3	133.7	-153.6
N6-C7	1.479	1.481	1.520	H10-N2-C3	113.4	112.5	111.3	T(N8-C7-N6-C5)^{d}	-25.9	-31.3	14.3
C1-N8	1.474	1.481	1.473	H11-C3-N2	111.7	111.5	109.5	T(C7-N8-C1-C5)^{d}	-15.6	-18.7	-36.6
C7-N8	1.479	1.481	1.520	H11-C3-N4	111.7	111.5	109.8	D(H9,N8-C1-N2)^{e}	-50.7	-50.6	-48.0
C1-H9	1.078	1.076	1.082	H12-C3-N2	108.9	108.7	109.8	D(H10,C3-N2-C1)^{e}	-48.9	50.8	53.6
N2-H10	1.002	1.003	1.005	H12-C3-N4	108.9	108.7	109.5	D(H11,N4-C3-N2)^{e}	-51.9	51.9	54.8
C3-H11	1.078	1.079	1.078	H12-C3-H11	109.1	109.2	109.6	D(H12,N4-C3-N2)^{e}	57.3	-57.3	-54.8
C3-H12	1.078	1.078	1.078	H13-N4-C3	113.4	112.5	111.3	D(H13,C5-N4-C3)^{e}	-48.9	50.8	-53.6
N4-H13	1.002	1.003	1.005	H13-N4-C5	113.0	112.3	112.5	D(H14,N6-C5-N4)^{e}	50.7	50.6	-48.0
C5-H14	1.078	1.076	1.082	H14-C5-C1	112.7	111.4	108.2	D(H15,C7-N6-C5)^{e}	49.7	50.6	-53.5
N6-H15	1.002	1.003	1.005	H14-C5-N4	110.8	110.1	107.4	D(H16,N8-C7-N6)^{e}	52.3	51.9	54.8
C7-H16	1.079	1.079	1.078	H14-C5-N6	111.0	110.3	107.8	D(H17,N8-C7-N6)^{e}	-56.6	-57.3	-54.8
C7-H17	1.079	1.078	1.078	H15-N6-C5	110.1	112.3	112.5	D(H18,C7-N8-C1)^{e}	-49.7	-50.6	-53.5
N8-H18	1.002	1.003	1.005	H15-N6-C7	114.8	112.6	111.4				
C3-N2-C1	106.4	105.9	102.1	H16-C7-N6	111.3	111.5	109.8				
N4-C3-N2	106.5	107.1	108.6	H16-C7-N8	111.3	111.5	109.5				
C5-C1-N2	105.3	105.4	103.0	H17-C7-N6	109.1	108.7	109.5				
C5-N4-C3	106.4	105.9	102.1	H17-C7-N8	109.1	108.7	109.8				
N4-C5-C1	105.3	105.4	103.0	H17-C7-H16	108.9	109.2	109.6				
N6-C5-C1	105.4	105.4	103.0	H18-N8-C1	110.1	112.3	112.5				
N6-C5-N4	111.3	114.0	126.3	H18-N8-C7	114.8	112.6	111.4				
C7-N6-C5	107.5	106.0	102.2	T(C3-N2-C1-C5)^{d}	-18.8	18.9	36.6				

a. Bond lengths in Å. Bond angles, torsion angles, and deformation angles in degrees.

b. Total energy in Hartrees plus 370 H.

c. Relative energy in kcal/mole assuming conformer A equals 0.

d. T(a-b-c-d) is the angle between the plane defined by a-b-c and the plane defined by b-c-d.

e. D(a,b-c-d) is the angle between the a-c bond and the plane defined by b-c-d.

Table 8-2[a]

2,4,6,8 Tetraazabicyclo[3.3.0] octane Geometries Calculated with the 4-21NO*(P) Basis Set

Parameter	Conf 1	Conf 2	Conf 3	Conf 4	Conf 5	Conf 6	Conf 7	Conf 8	Conf 9	Conf 10
Energy[b]	-4.320308	-4.320084	-4.319615	-4.818744	-4.316692	-4.315078	-4.314182	-4.312737	-4.311846	-4.311819
Delta E[c]	-0.1	0.0	0.3	0.8	2.1	3.1	3.7	4.6	5.2	5.2
C1-N2	1.465	1.469	1.465	1.476	1.469	1.464	1.473	1.466	1.467	1.464
N2-C3	1.475	1.474	1.472	1.470	1.467	1.469	1.472	1.477	1.473	1.469
C3-N4	1.472	1.474	1.482	1.474	1.480	1.482	1.472	1.477	1.473	1.469
C1-C5	1.575	1.593	1.582	1.579	1.579	1.568	1.567	1.584	1.563	1.579
N4-C5	1.471	1.469	1.471	1.460	1.463	1.472	1.457	1.466	1.467	1.464
C5-N6	1.477	1.472	1.477	1.481	1.486	1.475	1.485	1.464	1.475	1.483
N6-C7	1.463	1.472	1.467	1.475	1.468	1.475	1.463	1.466	1.468	1.474
C1-N8	1.472	1.472	1.462	1.475	1.465	1.464	1.475	1.464	1.475	1.483
C7-N8	1.477	1.472	1.471	1.473	1.471	1.462	1.479	1.466	1.468	1.474
C1-H9	1.083	1.080	1.085	1.079	1.084	1.084	1.082	1.084	1.082	1.079
N2-H10	1.011	1.010	1.013	1.009	1.013	1.013	1.010	1.013	1.011	1.009
C3-H11	1.081	1.080	1.080	1.081	1.081	1.081	1.081	1.080	1.082	1.081
C3-H12	1.084	1.082	1.078	1.088	1.084	1.082	1.092	1.078	1.088	1.095
N4-H13	1.010	1.010	1.010	1.010	1.010	1.011	1.009	1.013	1.011	1.009
C5-H14	1.079	1.080	1.080	1.080	1.080	1.082	1.079	1.084	1.082	1.079
N6-H15	1.010	1.010	1.010	1.013	1.013	1.008	1.013	1.007	1.009	1.013
C7-H16	1.081	1.081	1.081	1.081	1.081	1.082	1.081	1.082	1.082	1.080
C7-H17	1.088	1.083	1.089	1.083	1.088	1.094	1.087	1.095	1.093	1.082
N8-H18	1.010	1.011	1.009	1.011	1.009	1.008	1.009	1.007	1.009	1.013
C3-N2-C1	103.3	104.2	102.1	105.2	103.0	102.2	105.7	102.6	104.2	105.8
N4-C3-N2	104.2	108.7	108.0	104.6	103.8	104.4	101.7	107.5	101.4	101.1
C5-C1-N2	103.1	105.8	106.2	105.9	106.5	106.6	104.4	105.8	104.2	103.7
C5-N4-C3	104.4	104.2	104.7	104.5	105.0	104.9	105.2	102.6	104.2	105.8
N4-C5-C1	105.9	105.8	105.1	103.0	102.8	103.4	103.7	105.8	104.2	103.7
N6-C5-C1	106.3	105.9	106.3	105.6	106.1	105.1	105.8	103.5	104.2	105.8
N6-C5-N4	111.3	111.8	112.1	115.7	115.7	114.4	115.1	111.2	113.6	115.4
C7-N6-C5	105.5	104.5	105.1	102.7	103.4	106.5	103.4	106.1	106.6	103.3
N8-C1-N2	114.3	111.8	110.7	112.0	111.1	110.0	114.1	111.2	113.6	115.4
N8-C1-C5	103.2	105.9	102.1	105.9	102.8	102.5	104.0	103.5	104.2	105.8

Table 8-2[a]

2,4,6,8 Tetraazabicyclo[3.3.0] octane Geometries Calculated with the 4-21NO*(P) Basis Set

Parameter	Conf 1	Conf 2	Conf 3	Conf 4	Conf 5	Conf 6	Conf 7	Conf 8	Conf 9	Conf 10
N8-C7-N6	105.4	109.3	104.9	108.7	104.0	102.1	104.8	101.2	102.4	108.0
C7-N8-C1	105.0	104.5	104.9	104.8	105.1	106.2	105.6	106.1	106.6	103.3
H9-C1-N2	110.0	110.5	110.5	110.2	110.0	110.5	109.3	110.2	109.7	110.3
H9-C1-C5	112.9	112.5	113.0	112.5	112.7	112.9	112.6	112.5	112.4	112.6
H9-C1-N8	112.8	110.2	113.9	110.3	113.4	113.8	112.1	113.2	112.3	109.0
H10-N2-C1	108.7	107.9	107.0	107.3	106.4	106.7	107.6	107.1	107.8	110.8
H10-N2-C3	109.9	108.1	107.5	106.9	105.9	106.3	109.3	107.1	109.2	112.0
H11-C3-N2	111.3	111.4	111.8	110.8	111.2	110.8	110.7	111.6	110.5	110.6
H11-C3-N4	110.7	111.4	111.1	111.0	110.7	110.8	110.2	111.6	110.5	110.6
H12-C3-N2	112.4	108.5	107.7	108.8	108.1	108.0	112.5	108.0	112.2	113.1
H12-C3-N4	108.8	108.5	108.7	113.3	113.6	112.9	113.1	108.0	112.2	113.1
H12-C3-H11	109.3	108.2	109.4	108.2	109.3	109.8	108.6	110.0	109.7	108.3
H13-N4-C3	106.8	108.1	108.0	112.1	112.5	109.8	111.9	107.1	109.2	112.0
H13-N4-C5	107.3	107.9	108.1	110.5	110.6	107.4	110.5	107.1	107.8	110.8
H14-C5-C1	112.4	112.5	112.5	112.8	112.9	112.6	112.8	112.5	112.4	112.6
H14-C5-N4	110.5	110.5	110.6	110.8	110.5	109.5	111.0	110.2	109.7	110.3
H14-C5-N6	110.3	110.2	110.1	108.9	108.8	111.6	108.5	113.2	112.3	109.0
H15-N6-C5	105.5	106.3	105.2	106.7	106.0	110.0	106.2	111.1	110.1	106.6
H15-N6-C7	108.5	109.2	108.2	106.6	105.3	109.7	105.7	111.6	109.8	106.5
H16-C7-N6	110.8	111.3	110.8	111.4	110.9	110.6	111.0	110.6	110.6	111.5
H16-C7-N8	111.0	111.3	111.0	111.4	111.1	110.5	111.0	110.6	110.6	111.5
H17-C7-N6	108.9	108.3	108.8	108.2	108.6	112.1	108.6	113.0	112.5	108.6
H17-C7-N8	112.3	108.3	112.8	108.7	113.4	113.0	112.7	113.0	112.5	108.6
H17-C7-H16	108.4	108.3	108.5	108.5	108.7	108.4	108.6	108.5	108.4	108.7
H18-N8-C1	110.1	106.3	110.8	105.9	110.8	111.1	110.0	111.1	110.1	106.6
H18-N8-C7	110.1	109.2	111.9	109.2	112.1	111.8	110.3	111.6	109.8	106.5
T(C3-N2-C1-C5)[d]	-33.2	-19.4	-29.0	-13.2	-24.7	-29.0	-20.8	-22.8	-27.5	-26.5
T(N4-C3-N2-C1)[d]	44.9	33.2	38.3	33.8	41.4	42.7	39.7	39.1	44.9	43.0
T(C5-N4-C3-N2)[d]	-37.4	-33.2	-31.9	-42.4	-43.1	-40.3	-44.1	-39.1	-44.9	-43.0
T(N4-C5-C1-N2)[d]	10.8	0.0	10.7	-12.1	-0.8	5.1	-6.1	0.0	0.0	0.0
T(N6-C5-C1-N2)[d]	129.3	118.8	129.7	109.7	121.0	125.4	115.4	117.1	119.3	121.9

Table 8-2[a]

2,4,6,8 Tetraazabicyclo[3.3.0] octane Geometries Calculated with the 4-21NO*(P) Basis Set

Parameter	Conf 1	Conf 2	Conf 3	Conf 4	Conf 5	Conf 6	Conf 7	Conf 8	Conf 9	Conf 10
T(N4-C5-C1-N8)[d]	-108.4	-118.8	-105.3	-131.2	-117.7	-110.5	-126.0	-117.1	-119.3	-121.9
T(N6-C5-C1-N8)[d]	10.1	0.0	13.7	-9.4	4.1	9.7	-4.5	0.0	0.0	0.0
T(N6-C5-N4-C3)[d]	-99.2	-95.5	-102.8	-82.0	-89.0	-92.9	-84.3	-88.9	-85.3	-88.6
T(C7-N6-C5-N4)[d]	128.5	133.0	125.7	140.0	134.8	128.7	141.0	139.5	136.6	135.5
T(N8-C7-N6-C5)[d]	-32.6	-31.2	-32.6	-36.3	-39.9	-35.8	-40.3	-42.8	-38.8	-37.0
T(C7-N8-C1-C5)[d]	-29.7	-18.2	-33.5	-12.2	-28.5	-32.5	-19.9	-26.3	-23.9	-21.6
D(H9,N8-C1-N2)[e]	-47.6	52.5	-48.4	-51.8	-49.1	-48.8	-49.5	-49.0	-49.0	-51.0
D(H10,C3-N2-C1)[e]	57.8	-59.7	-61.8	-61.0	-63.4	63.2	58.3	-62.0	58.9	52.8
D(H11,N4-C3-N2)[e]	-54.3	-51.2	-51.5	-54.3	-54.6	-54.6	-56.4	-51.5	-56.4	-56.4
D(H12,N4-C3-N2)[e]	55.0	57.1	57.9	53.9	54.6	55.1	52.2	58.4	53.3	-52.9
D(H13,C5-N4-C3)[e]	-61.5	-59.7	-59.6	53.6	52.8	58.4	53.5	-62.0	58.9	52.8
D(H14,N6-C5-N4)[e]	-52.6	51.7	51.5	50.4	50.8	49.6	51.0	49.0	49.0	51.0
D(H15,C7-N6-C5)[e]	61.1	60.0	61.8	62.7	64.2	-55.5	63.7	-52.7	-55.2	62.7
D(H16,N8-C7-N6)[e]	53.9	51.2	54.2	51.4	54.4	56.0	54.0	56.4	55.9	51.5
D(H17,N8-C7-N6)[e]	-54.5	-57.1	-54.3	-57.1	-54.2	-52.4	-54.5	-52.1	-52.4	-57.2
D(H18,C7-N8-C1)[e]	55.6	-60.0	53.4	-60.3	53.0	52.5	55.2	52.7	55.2	-62.7

a. Bond lengths in Å. Bond angles, torsion angles, and deformation angles in degrees.

b. Total energy in Hartrees plus 370 H.

c. Relative energy in kcal/mole assuming conformer 2 equals 0 kcal/mole.

d. T(a-b-c-d) is the angle between the plane defined by a-b-c and the plane defined by b-c-d.

e. D(a,b-c-d) is the angle between the a-c bond and the plane defined by b-c-d.

Table 6-3^{a}

2,4,6,8 Tetraazabicyclo[3.3.0]octane Geometries Calculated with the 4-21NO*(P) Basis Set

Parameter	Conf 11	Conf 12	Conf 13	Conf 14	Conf 15	Conf 16	Conf 17
Energy^{b}	-4.318014	-4.315164	-4.313677	-4.310876	-4.308399	-4.307819	-4.295198
Delta E^{c}	1.3	3.1	4.0	5.8	7.3	7.7	15.6
C1-N2	1.464	1.468	1.467	1.467	1.476	1.468	1.466
N2-C3	1.482	1.471	1.479	1.484	1.476	1.477	1.470
C3-N4	1.463	1.471	1.467	1.465	1.476	1.469	1.470
C1-C5	1.572	1.575	1.583	1.550	1.593	1.577	1.562
N4-C5	1.477	1.468	1.479	1.467	1.476	1.475	1.466
C5-N6	1.464	1.473	1.475	1.456	1.476	1.475	1.466
N6-C7	1.482	1.476	1.480	1.496	1.476	1.469	1.470
C1-N8	1.477	1.473	1.474	1.473	1.476	1.468	1.466
C7-N8	1.463	1.476	1.473	1.469	1.476	1.477	1.470
C1-H9	1.083	1.083	1.084	1.082	1.080	1.088	1.088
N2-H10	1.008	1.008	1.009	1.006	1.012	1.009	1.008
C3-H11	1.081	1.082	1.081	1.082	1.080	1.081	1.082
C3-H12	1.087	1.093	1.087	1.093	1.082	1.088	1.095
N4-H13	1.012	1.008	1.012	1.008	1.012	1.012	1.008
C5-H14	1.083	1.083	1.080	1.087	1.080	1.080	1.088
N6-H15	1.008	1.012	1.012	1.008	1.012	1.012	1.008
C7-H16	1.081	1.081	1.081	1.081	1.080	1.081	1.082
C7-H17	1.087	1.083	1.082	1.085	1.082	1.088	1.095
N8-H18	1.012	1.012	1.012	1.010	1.012	1.009	1.008
C3-N2-C1	105.8	106.1	104.9	106.4	103.1	104.7	106.1
N4-C3-N2	105.6	102.6	105.1	102.8	108.9	104.9	102.7
C5-C1-N2	104.4	104.2	103.6	106.1	105.9	103.5	104.5
C5-N4-C3	103.9	106.1	103.5	104.4	103.1	103.2	106.1
N4-C5-C1	106.1	104.2	106.1	99.5	105.9	106.4	104.5
N6-C5-C1	104.4	106.2	106.1	106.8	105.9	106.4	104.5
N6-C5-N4	111.9	112.0	114.6	112.3	115.2	114.4	113.5
C7-N6-C5	105.7	103.5	103.4	106.1	103.1	103.2	106.1
N8-C1-N2	111.9	112.0	112.7	111.3	115.2	114.3	113.5
N8-C1-C5	106.1	106.2	106.1	103.5	105.9	103.5	104.5
N8-C7-N6	105.6	108.7	108.9	108.8	108.9	104.9	102.7
C7-N8-C1	104.0	103.5	103.2	105.7	103.1	104.7	106.1
H9-C1-N2	113.4	113.1	113.2	112.6	109.3	112.1	111.8
H9-C1-C5	111.5	111.2	111.2	113.0	111.0	110.7	110.2
H9-C1-N8	109.3	109.7	109.7	110.0	109.4	112.1	111.8
H10-N2-C1	110.7	110.7	110.6	110.5	107.6	110.7	110.6
H10-N2-C3	110.8	110.3	110.8	110.2	107.1	110.6	110.0
H11-C3-N2	110.7	110.4	111.0	110.7	111.3	111.0	110.3
H11-C3-N4	110.8	110.4	110.7	110.5	111.3	110.6	110.3
H12-C3-N2	112.3	112.4	112.7	111.4	108.3	113.1	112.6
H12-C3-N4	108.9	112.4	108.6	113.1	108.3	108.5	112.6
H12-C3-H11	108.5	108.5	108.7	108.4	108.6	108.6	108.3
H13-N4-C3	107.5	110.3	105.9	111.5	107.1	105.5	110.0
H13-N4-C5	104.4	110.7	106.9	111.5	107.6	106.6	110.6
H14-C5-C1	111.5	111.2	111.2	113.4	111.0	110.9	110.2

Parameter	Conf 11	Conf 12	Conf 13	Conf 14	Conf 15	Conf 16	Conf 17
H14-C5-N4	109.3	113.1	109.2	113.1	109.3	109.3	111.8
H14-C5-N6	113.4	109.7	109.6	111.1	109.4	109.3	111.8
H15-N6-C5	110.7	104.1	107.3	108.3	107.6	106.6	110.6
H15-N6-C7	110.9	107.5	106.9	108.6	107.1	105.5	110.0
H16-C7-N6	110.7	111.2	111.0	110.7	111.3	110.6	110.3
H16-C7-N8	110.8	111.2	111.5	109.6	111.3	111.0	110.3
H17-C7-N6	112.3	108.6	108.2	109.8	108.3	108.5	112.6
H17-C7-N8	108.9	108.6	108.6	109.8	108.3	113.1	112.6
H17-C7-H16	108.5	108.5	108.5	108.2	108.6	108.6	108.3
H18-N8-C1	104.4	104.1	104.6	104.1	107.6	110.7	110.6
H18-N8-C7	107.5	107.5	108.0	107.9	107.1	110.6	110.0
T(C3-N2-C1-C5)[d]	19.7	24.3	25.2	-2.2	20.8	25.4	23.9
T(N4-C3-N2-C1)[d]	-36.2	-39.7	-41.0	-24.7	-36.0	-41.5	-38.9
T(C5-N4-C3-N2)[d]	37.4	39.7	39.1	44.0	36.0	39.7	38.9
T(N4-C5-C1-N2)[d]	2.9	0.0	-1.7	27.9	0.0	-1.5	0.0
T(N6-C5-C1-N2)[d]	121.2	118.5	120.7	144.7	122.9	120.9	119.5
T(N4-C5-C1-N8)[d]	-115.5	-118.5	-120.5	-89.4	-122.9	-120.9	-119.5
T(N6-C5-C1-N8)[d]	2.9	0.0	1.9	27.5	0.0	1.5	0.0
T(N6-C5-N4-C3)[d]	-137.7	-138.3	-139.4	-156.6	-137.5	-140.2	-137.1
T(C7-N6-C5-N4)[d]	134.0	133.2	135.5	94.3	137.5	140.2	137.1
T(N8-C7-N6-C5)[d]	-36.2	-34.2	-34.2	-5.1	-35.9	-39.7	-38.9
T(C7-N8-C1-C5)[d]	-24.4	-20.0	-21.7	-30.1	-20.8	-25.4	-23.9
D(H9,N8-C1-N2)[e]	-49.4	-49.2	-48.7	-49.9	-51.8	-46.2	-47.4
D(H10,C3-N2-C1)[e]	-54.0	-54.4	-54.6	-54.5	61.3	-54.7	-54.8
D(H11,N4-C3-N2)[e]	54.1	56.1	54.2	55.7	51.3	54.3	56.2
D(H12,N4-C3-N2)[e]	-54.4	-52.4	-54.5	-52.7	-57.3	-54.2	-52.1
D(H13,C5-N4-C3)[e]	63.4	-54.4	62.9	-53.3	61.3	63.6	-54.8
D(H14,N6-C5-N4)[e]	49.4	49.2	52.1	47.5	51.8	52.4	47.4
D(H15,C7-N6-C5)[e]	-54.0	63.8	61.7	-58.2	61.3	63.6	-54.8
D(H16,N8-C7-N6)[e]	54.1	51.6	51.4	53.7	51.3	54.3	56.2
D(H17,N8-C7-N6)[e]	-54.4	-56.8	-57.1	-54.4	-57.4	-54.2	-52.1
D(H18,C7-N8-C1)[e]	-63.4	-63.8	-63.1	-62.8	-61.3	54.7	54.8

a. Bond lengths in Å. Bond angles, torsion angles, and deformation angles in degrees.

b. Total energy in Hartrees plus 370 H.

c. Relative energy in kcal/mole assuming conformer 2 equals 0 kcal/mole.

d. T(a-b-c-d) is the angle between the plane defined by a-b-c and the plane defined by b-c-d.

e. D(a,b-c-d) is the angle between the a-c bond and the plane defined by b-c-d.

Table 8-4

2,4,6,8 Tetraazabicyclo[3.3.0] octane C_2 Geometry Calculated with the 4-21NO*(P) Basis Set

Parameter[a]	Conf 18
Energy[b]	-4.279559
Delta E[c]	25.4
C1-N2	1.464
N2-C3	1.512
C3-N4	1.512
C1-C5	1.515
N4-C5	1.464
C5-N6	1.464
N6-C7	1.512
C1-N8	1.464
C7-N8	1.512
C1-H9	1.087
N2-H10	1.013
C3-H11	1.080
C3-H12	1.080
N4-H13	1.013
C5-H14	1.087
N6-H15	1.013
C7-H16	1.080
C7-H17	1.080
N8-H18	1.013
C3-N2-C1	100.6
N4-C3-N2	110.7
C5-C1-N2	103.7
C5-N4-C3	100.6
N4-C5-C1	103.7
N6-C5-C1	103.7
N6-C5-N4	125.5
C7-N6-C5	100.6
N8-C1-N2	125.5
N8-C1-C5	103.7
N8-C7-N6	110.7
C7-N8-C1	100.6
H9-C1-N2	107.5
H9-C1-C5	108.0
H9-C1-N8	107.5
H10-N2-C1	107.5
H10-N2-C3	107.0
H11-C3-N2	109.2
H11-C3-N4	109.5
H12-C3-N2	109.5
H12-C3-N4	109.2
H12-C3-H11	108.6
H13-N4-C3	107.0
H13-N4-C5	107.5
H14-C5-C1	108.0
H14-C5-N4	107.5
H14-C5-N6	107.5
H15-N6-C5	107.5
H15-N6-C7	107.0
H16-C7-N6	109.5
H16-C7-N8	109.2
H17-C7-N6	109.2
H17-C7-N8	109.5
H17-C7-H16	108.6
H18-N8-C1	107.5
H18-N8-C7	107.0
T(C3-N2-C1-C5)[d]	35.9
T(N4-C3-N2-C1)[d]	-14.1
T(C5-N4-C3-N2)[d]	-14.1
T(N4-C5-C1-N2)[d]	-47.6
T(N6-C5-C1-N2)[d]	-180.0
T(N4-C5-C1-N8)[d]	180.0
T(N6-C5-C1-N8)[d]	47.6
T(N6-C5-N4-C3)[d]	154.1
T(C7-N6-C5-N4)[d]	-154.1
T(N8-C7-N6-C5)[d]	14.1
T(C7-N8-C1-C5)[d]	-35.9
D(H9,N8-C1-N2)[e]	-49.0
D(H10,C3-N2-C1)[e]	62.3
D(H11,N4-C3-N2)[e]	54.3
D(H12,N4-C3-N2)[e]	-54.3
D(H13,C5-N4-C3)[e]	-62.3
D(H14,N6-C5-N4)[e]	-49.0
D(H15,C7-N6-C5)[e]	-62.3
D(H16,N8-C7-N6)[e]	54.3
D(H17,N8-C7-N6)[e]	-54.3
D(H18,C7-N8-C1)[e]	-62.3

a. Bond lengths in Å. Bond angles, torsion angles, and deformation angles in degrees.

b. Total energy in Hartrees plus 370 H.

c. Relative energy in kcal/mole assuming conformer 2 equals 0 kcal/mole.

d. T(a-b-c-d) is the angle between the plane defined by a-b-c and the plane defined by b-c-d.

e. D(a,b-c-d) is the angle between the a-c bond and the plane defined by b-c-d.

Table 8-5

2,4,6,8 Tetraazabicyclo[3.3.0]octane-3,7-dione Geometry Calculated with the 4-21NO*(P) Basis Set

Parameter[a]	Conf 19
Energy[b]	-1.506056
C1-N2	1.447
N2-C3	1.395
C3-N4	1.391
C1-C5	1.562
N4-C5	1.456
C5-N6	1.447
N6-C7	1.396
C1-N8	1.456
C7-N8	1.390
C1-H9	1.079
N2-H10	1.005
C3-O11	1.193
N4-H12	1.004
C5-H13	1.079
N6-H14	1.005
C7-H15	1.193
N8-H16	1.004
C3-N2-C1	110.2
N4-C3-N2	107.1
C5-C1-N2	102.1
C5-N4-C3	111.6
N4-C5-C1	100.8
N6-C5-C1	102.1
N6-C5-N4	115.4
C7-N6-C5	110.2
N8-C1-N2	115.4
N8-C1-C5	100.8
N8-C7-N6	107.1
C7-N8-C1	111.6
H9-C1-N2	111.1
H9-C1-C5	113.6
H9-C1-N8	112.9
H10-N2-C1	118.1
H10-N2-C3	114.4
O11-C3-N2	126.3
O11-C3-N4	126.6
H12-N4-C3	115.6
H12-N4-C5	120.2
H13-C5-C1	113.6
H13-C5-N4	112.9
H13-C5-N6	111.1
H14-N6-C5	118.1
H14-N6-C7	114.4
H15-C7-N6	126.3
H15-C7-N8	126.6
H16-N8-C1	120.2
H16-N8-C7	115.6
T(C3-N2-C1-C5)[c]	-25.7
T(N4-C3-N2-C1)[c]	13.3
T(C5-N4-C3-N2)[c]	6.5
T(N4-C5-C1-N2)[c]	27.2
T(N6-C5-C1-N2)[c]	146.4
T(N4-C5-C1-N8)[c]	-92.0
T(N6-C5-C1-N8)[c]	27.2
T(N6-C5-N4-C3)[c]	-130.5
T(C7-N6-C5-N4)[c]	82.7
T(N8-C7-N6-C5)[c]	13.3
T(C7-N8-C1-C5)[c]	-21.4
D(H9,N8-C1-N2)[d]	-45.4
D(H10,C3-N2-C1)[d]	39.3
D(O11,N4-C3-N2)[d]	-1.2
D(H12,C5-N4-C3)[d]	-33.7
D(H13,N6-C5-N4)[d]	45.4
D(H14,C7-N6-C5)[d]	39.3
D(O15,N8-C7-N6)[d]	-1.2
D(H16,N8-C7-N6)[d]	33.7

a. Bond lengths in Å. *Bond angles, torsion angles,* and deformation angles in degrees.

b. Total energy in Hartrees plus 520 H.

c. T(a-b-c-d) is the angle between the plane defined by a-b-c and the plane defined by b-c-d.

d. D(a,b-c-d) is the angle between the a-c bond and the plane defined by b-c-d.

Table 8-6[a]

Data for Calculating the Conformer 1 to Conformer 11 Potential Surface

Parameter	Conf 1	Conf 1A	Conf 1B	Conf 1C	Conf 1D	Conf 1E	Conf 11[b]	Conf 11A	Conf 11B
Energy[c]	-4.320308	-4.315066	-4.319641	-4.314903	-4.314294	-4.315060	-4.318014	-4.317677	-4.314758
Delta E[d]	0.0	3.29	0.42	3.39	3.77	3.29	1.44	1.65	3.48
C3-D2-D1	41.4	55.1	35.1	14.9	2.2	-10.9	-36.9	-30.8	-50.7
C7-D3-D1	143.8	144.9	143.7	146.1	148.0	146.3	143.1	143.6	142.5
C1-N2	1.465	1.475	1.464	1.475	1.476	1.476	1.477	1.476	1.479
N2-C3	1.475	1.476	1.476	1.482	1.478	1.471	1.463	1.464	1.465
C3-N4	1.472	1.474	1.473	1.477	1.484	1.487	1.482	1.484	1.482
C1-C5	1.575	1.591	1.571	1.565	1.561	1.563	1.572	1.569	1.585
N4-C5	1.471	1.477	1.471	1.457	1.455	1.455	1.464	1.462	1.471
C5-N6	1.477	1.472	1.478	1.476	1.476	1.477	1.477	1.477	1.475
N6-C7	1.463	1.464	1.463	1.460	1.460	1.460	1.463	1.462	1.465
C1-N8	1.472	1.469	1.472	1.471	1.468	1.467	1.464	1.465	1.462
C7-N8	1.477	1.480	1.477	1.484	1.488	1.486	1.482	1.483	1.482
C1-H9	1.083	1.083	1.084	1.083	1.082	1.083	1.083	1.083	1.083
N2-H10	1.011	1.014	1.011	1.008	1.008	1.009	1.012	1.011	1.012
C3-H11	1.081	1.081	1.081	1.082	1.084	1.085	1.081	1.081	1.081
C3-H12	1.084	1.080	1.085	1.085	1.083	1.082	1.087	1.087	1.087
N4-H13	1.010	1.011	1.010	1.008	1.006	1.005	1.008	1.007	1.011
C5-H14	1.079	1.079	1.079	1.081	1.081	1.082	1.083	1.083	1.083
N6-H15	1.010	1.009	1.010	1.011	1.011	1.011	1.012	1.012	1.012
C7-H16	1.081	1.081	1.081	1.081	1.081	1.081	1.081	1.081	1.081
C7-H17	1.088	1.087	1.088	1.087	1.087	1.087	1.087	1.087	1.088
N8-H18	1.010	1.009	1.010	1.008	1.008	1.008	1.008	1.008	1.008
C3-N2-C1	103.3	99.9	104.5	108.3	108.2	107.5	103.9	105.1	100.6
N4-C3-N2	104.2	100.2	105.6	108.6	109.1	108.7	105.6	106.7	102.2
C5-C1-N2	103.1	101.2	103.9	105.5	105.3	105.6	106.1	106.1	105.2
C5-N4-C3	104.4	100.7	105.5	107.2	107.6	108.3	105.7	106.9	102.3
N4-C5-C1	105.9	104.8	106.3	107.1	107.0	106.7	104.4	105.1	102.6
N6-C5-C1	106.3	106.3	106.4	105.6	105.1	105.3	106.1	106.0	106.1
N6-C5-N4	111.3	111.9	111.3	112.0	112.5	112.6	111.9	112.2	112.3
C7-N6-C5	105.5	105.6	105.5	104.2	103.9	103.8	103.9	103.9	104.0

Parameter	Conf 1	Conf 1A	Conf 1B	Conf 1C	Conf 1D	Conf 1E	Conf 11[b]	Conf 11A	Conf 11B
N8-C1-N2	114.3	114.9	114.1	112.2	111.2	111.0	111.9	111.6	112.8
N8-C1-C5	103.2	103.4	103.2	105.0	105.4	105.2	104.4	104.6	104.0
N8-C7-N6	105.4	106.0	105.3	106.1	106.5	106.2	105.6	105.7	105.6
C7-N8-C1	105.0	105.4	104.9	106.3	106.5	106.3	105.7	105.9	105.7
H9-C1-N2	110.0	110.3	110.0	109.7	110.0	109.8	109.3	109.4	108.8
H9-C1-C5	112.9	113.2	112.7	112.3	112.4	112.1	111.5	111.5	111.8
H9-C1-N8	112.8	113.1	112.7	112.0	112.3	112.8	113.4	113.3	113.8
H10-N2-C1	108.7	108.1	108.6	105.7	105.0	104.5	104.3	104.3	105.0
H10-N2-C3	109.9	110.3	109.6	109.2	109.3	109.0	107.5	107.9	106.6
H11-C3-N2	111.3	111.4	111.1	110.9	110.7	110.0	110.8	110.5	111.6
H11-C3-N4	110.7	111.1	110.6	109.4	109.2	109.9	110.7	110.7	110.9
H12-C3-N2	112.4	113.6	112.0	110.9	110.1	109.8	108.9	109.0	109.2
H12-C3-N4	108.8	110.1	108.6	109.5	110.3	110.7	112.3	111.7	113.6
H12-C3-H11	109.3	110.1	108.9	107.6	107.5	107.7	108.5	108.3	109.2
H13-N4-C3	106.8	105.6	107.1	108.5	109.1	109.9	110.9	110.7	111.2
H13-N4-C5	107.3	106.9	107.3	108.3	108.9	110.0	110.7	110.8	110.0
H14-C5-C1	112.4	112.6	112.3	112.3	112.3	111.9	111.5	111.4	111.9
H14-C5-N4	110.5	110.6	110.4	110.8	111.1	111.7	113.4	113.1	113.7
H14-C5-N6	110.3	110.6	110.1	108.9	108.6	108.4	109.3	108.9	109.9
H15-N6-C5	105.5	106.7	105.3	106.2	106.3	105.7	104.3	104.6	104.3
H15-N6-C7	108.5	109.1	108.4	108.3	108.5	108.4	107.5	107.8	107.2
H16-C7-N6	110.8	110.7	110.8	110.8	110.7	110.8	110.8	110.8	110.7
H16-C7-N8	111.0	110.9	111.0	110.8	110.8	110.7	110.7	110.7	110.7
H17-C7-N6	108.9	108.8	108.9	108.7	108.7	108.8	108.9	108.9	108.8
H17-C7-N8	112.3	112.1	112.3	111.9	111.7	111.8	112.3	112.2	112.4
H17-C7-H16	108.4	108.4	108.5	108.4	108.4	108.5	108.5	108.5	108.6
H18-N8-C1	110.1	110.3	110.0	110.3	110.5	110.7	110.7	110.7	110.9
H18-N8-C7	110.1	110.1	110.1	110.2	110.4	110.6	110.9	110.8	111.0
T(C3-N2-C1-C5)[e]	-33.2	-38.8	-29.8	-0.9	12.0	18.2	24.3	22.7	30.0
T(N4-C3-N2-C1)[e]	44.9	57.4	38.8	11.7	-3.2	-15.6	-37.5	-32.3	-49.6
T(C5-N4-C3-N2)[e]	-37.4	-51.1	-31.3	-18.3	-7.7	6.2	36.4	29.4	50.5
T(N4-C5-C1-N2)[e]	10.8	8.2	11.0	-10.3	-16.8	-14.4	-2.6	-5.1	-0.2
T(N6-C5-C1-N2)[e]	129.3	126.8	129.6	109.3	103.1	105.5	115.7	113.6	117.8

Parameter	Conf 1	Conf 1A	Conf 1B	Conf 1C	Conf 1D	Conf 1E	Conf 11[b]	Conf 11A	Conf 11B
T(N4-C5-C1-N8)[e]	-108.4	-111.0	-108.3	-129.0	-134.5	-131.9	-121.0	-123.3	-119.0
T(N6-C5-C1-N8)[e]	10.1	7.6	10.3	-9.4	-14.6	-12.0	-2.6	-4.5	-1.0
T(N6-C5-N4-C3)[e]	-99.2	-89.1	-103.1	-97.9	-100.0	-110.0	-134.3	-129.0	-143.0
T(C7-N6-C5-N4)[e]	128.5	128.8	128.8	144.3	147.1	145.8	137.6	139.6	134.5
T(N8-C7-N6-C5)[e]	-32.6	-32.5	-32.6	-36.7	-36.4	-37.2	-37.5	-37.4	-37.4
T(C7-N8-C1-C5)[e]	-29.7	-27.0	-30.0	-12.6	-7.3	-10.4	-19.9	-18.0	-21.5
D(H9,N8-C1-N2)[f]	-47.6	-46.6	-48.1	-50.4	-50.3	-50.0	-49.4	-49.6	-48.8
D(H10,C3-N2-C1)[f]	57.8	59.2	57.6	59.2	59.7	60.8	63.5	62.8	64.7
D(H11,N4-C3-N2)[f]	-54.3	-55.5	-54.0	-53.8	-53.9	-54.2	54.1	53.9	54.7
D(H12,N4-C3-N2)[f]	55.0	54.5	54.9	53.8	53.6	53.5	-54.4	-54.3	-54.4
D(H13,C5-N4-C3)[f]	-61.5	-64.0	-60.7	-57.9	-56.6	-54.3	-54.0	-53.4	-55.6
D(H14,N6-C5-N4)[f]	-52.6	51.1	52.1	52.6	52.3	51.7	49.4	50.0	48.2
D(H15,C7-N6-C5)[f]	61.1	59.4	61.4	61.1	61.0	61.6	63.5	63.1	63.8
D(H16,N8-C7-N6)[f]	53.9	53.9	54.0	53.8	53.7	53.8	54.1	54.1	54.2
D(H17,N8-C7-N6)[f]	-54.5	-54.5	-54.4	-54.6	-54.7	-54.6	-54.4	-54.4	-54.3
D(H18,C7-N8-C1)[f]	55.6	55.3	55.7	54.8	54.3	53.9	54.0	54.0	53.7

a. Bond lengths in Å. Bond angles, torsion angles, and deformation angles in degrees.

b. This geometry is the "mirror image" of the Conformer 11 geometry reported in Table 8-3.

c. Total energy in Hartrees plus 370 H.

d. Relative energy in kcal/mole assuming conformer 1 equals 0 kcal/mole.

e. T(a-b-c-d) is the angle between the plane defined by a-b-c and the plane defined by b-c-d.

f. D(a,b-c-d) is the angle between the a-c bond and the plane defined by b-c-d.

TABLE 8-7[a]

REFERENCE GEOMETRY FOR CALCULATION OF THE 2,4,6,8 TETRAAZABICYCLO[3.3.0]OCTANE AB INITIO FORCE FIELD

Parameter	Value	Parameter	Value	Parameter	Value
N2-C1	1.472	C3-N2-C1	103.9	H12-C3-N2	108.9
C3-N2	1.459	N4-C3-N2	105.4	H12-C3-N4	112.3
N4-C3	1.476	C5-C1-N2	106.3	H12-C3-H11	108.6
C5-C1	1.552	C5-N4-C3	105.6	H13-N4-C3	110.9
C5-N4	1.460	N4-C5-C1	104.5	H13-N4-C5	110.7
N6-C5	1.472	N6-C5-C1	106.3	H14-C5-C1	111.4
C7-N6	1.459	N6-C5-N4	111.8	H14-C5-N4	113.3
N8-C1	1.460	C7-N6-C5	103.9	H14-C5-N6	109.2
N8-C7	1.476	N8-C1-N2	111.8	H15-N6-C5	104.4
H9-C1	1.088	N8-C1-C5	104.5	H15-N6-C7	107.5
H10-N2	1.012	N8-C7-N6	105.4	H16-C7-N6	110.8
H11-C3	1.086	C7-N8-C1	105.6	H16-C7-N8	110.7
H12-C3	1.092	H9-C1-N2	109.2	H17-C7-N6	108.9
H13-N4	1.008	H9-C1-C5	111.4	H17-C7-N8	112.3
H14-C5	1.088	H9-C1-N8	113.3	H17-C7-H16	108.6
H15-N6	1.012	H10-N2-C1	104.4	H18-N8-C1	110.7
H16-C7	1.086	H10-N2-C3	107.5	H18-N8-C7	110.9
H17-C7	1.092	H11-C3-N2	110.8		
H18-N8	1.008	H11-C3-N4	110.7		

a. Bond lengths in angstroms. Angles in degrees. Torsion and out-of-plane angles given in Table 9-6 for conformer 11.

TABLE 8-8

DEFINITION OF INTERNAL COORDINATES

Q	Name	Definition
1	CN Stretch	R(1,2)
2	CN Stretch	R(2,3)
3	CN Stretch	R(3,4)
4	CN Stretch	R(4,5)
5	CC Stretch	R(5,1)
6	CN Stretch	R(5,6)
7	CN Stretch	R(6,7)
8	CN Stretch	R(7,8)
9	CN Stretch	R(8,1)
10	CH Stretch	R(1,9)
11	NH Stretch	R(2,10)
12	CH Stretch	R(3,11)
13	CH Stretch	R(3,12)
14	NH Stretch	R(4,13)
15	CH Stretch	R(5,14)
16	NH Stretch	R(6,15)
17	CH Stretch	R(7,16)
18	CH Stretch	R(7,17)
19	NH Stretch	R(8,18)
20	Symm. Ring Def.[a]	(4,3,2)+a[(5,4,3)+(3,2,1)]+b[(4,5,1)+(5,1,2)]
21	Asymm. Ring Def.[b]	c[(5,4,3)-(3,2,1)]+d[(4,5,1)-(5,1,2)]
22	Symm. Ring Tors[a]	T(4,5,1,2)+a[T(5,1,2,3)+T(3,4,5,1)]+b[T(1,2,3,4)+T(2,3,4,5)]
23	Asymm Ring Tors[b]	c[T(5,1,2,3)-T(3,4,5,1)]+d[T(1,2,3,4)-T(2,3,4,5)]
24	Symm. Ring Def.[a]	(6,7,8)+a[(7,8,1)+(7,6,5)]+b[(8,1,5)+(6,5,1)]
25	Asymm. Ring Def.[b]	c[(7,8,1)-(7,6,5)]+d[(8,1,5)-(6,5,1)]
26	Symm. Ring Tors[a]	T(8,1,5,6)+a[T(1,5,6,7)+T(7,8,1,5)]+b[T(5,6,7,8)+T(6,7,8,1)]
27	Asymm. Ring Tors[b]	c[T(1,5,6,7)-T(7,8,1,5)]+d[T(5,6,7,8)-T(6,7,8,1)]

28	Ring-Ring Def.	T(6,5,1,2)-T(4,5,1,8)
29	CH Rock	2(5,1,9)-(2,1,9)-(8,1,9)
30	CH Rock	(8,1,9)-(2,1,9)
31	CH Rock	2(1,5,14)-(6,5,14)-(4,5,14)
32	CH Rock	(4,5,14)-(6,5,14)
33	NH Rock	(10,2,1)-(10,2,3)
34	NH Wag	D(10,1,2,3)
35	NH Rock	(13,4,5)-(13,4,3)
36	NH Wag	D(13,3,4,5)
37	NH Rock	(15,6,5)-(15,6,7)
38	NH Wag	D(15,7,6,5)
39	NH Rock	(18,8,1)-(18,8,7)
40	NH Wag	D(18,7,8,1)
41	CH_2 Scissor	5(11,3,12)+(2,3,4)
42	CH_2 Rock	(11,3,4)-(12,3,4)+(11,3,2)-(12,3,2)
43	CH_2 Wag	(11,3,4)+(12,3,4)-(11,3,2)-(12,3,2)
44	CH_2 Rock	(11,3,4)-(12,3,4)-(11,3,2)+(12,3,2)
45	CH_2 Rock	(16,7,6)-(17,7,6)+(16,7,8)-(17,7,8)
46	CH_2 Wag	(16,7,6)+(17,7,6)-(16,7,8)-(17,7,8)
47	CH_2 Rock	(16,7,6)-(17,7,6)-(16,7,8)+(17,7,8)
48	CH_2 Scissor	5(16,7,17)+(8,7,6)

a. a=cos(144°). b=cos(72°).

b. c=cos(144°)-cos(72°). d=1-cos(144°).

TABLE 8-9

2,4,6,8-TETRAAZABICYCLO[3.3.0]OCTANE AB INITIO FORCE FIELD

Q	1	2	3	4	5	6	7	8	9	10	11	12	13	14	15	16	17	18
1	5.625																	
2	0.078	5.779																
3	0.068	0.344	5.397															
4	0.013	-0.001	0.121	5.891														
5	0.293	0.002	-0.106	0.327	4.464													
6	0.019	0.055	-0.041	0.428	0.293	5.625												
7	-0.055	0.030	0.022	-0.079	-0.002	0.078	5.779											
8	-0.041	0.022	0.038	-0.054	-0.106	0.068	0.344	5.397										
9	0.428	-0.079	0.054	-0.014	0.327	0.013	-0.001	0.121	5.891									
10	0.221	0.011	-0.036	-0.013	0.070	0.001	-0.043	0.009	0.165	5.425								
11	0.037	0.059	0.007	-0.006	-0.020	-0.001	-0.006	0.001	-0.016	-0.008	7.427							
12	-0.028	0.083	0.162	-0.010	-0.029	0.006	0.000	-0.002	0.009	0.003	0.016	5.600						
13	0.003	0.191	0.228	-0.008	-0.015	-0.001	-0.003	-0.003	0.004	0.010	-0.024	0.082	5.300					
14	-0.027	-0.005	0.015	-0.008	0.014	0.015	-0.002	-0.002	0.006	0.002	-0.004	0.006	0.020	7.530				
15	0.001	-0.043	0.009	0.165	0.070	0.221	0.011	-0.036	-0.013	0.033	-0.002	0.004	0.008	0.026	5.425			
16	0.001	-0.006	0.001	-0.016	-0.020	0.037	0.059	0.007	-0.006	-0.002	0.003	-0.001	-0.001	-0.007	-0.008	7.427		
17	0.006	0.000	-0.002	0.009	-0.029	-0.028	0.083	0.162	-0.010	0.004	-0.001	0.001	0.001	0.001	0.003	0.016	5.600	
18	-0.001	0.003	-0.003	0.004	-0.015	0.003	0.192	0.228	-0.008	0.008	-0.001	0.001	0.002	0.001	0.010	-0.024	0.082	5.300
19	0.015	-0.002	-0.002	0.006	0.014	-0.027	-0.005	0.015	-0.008	0.026	-0.007	0.001	0.001	0.000	0.002	-0.004	0.006	0.020
20	-0.360	0.091	0.027	-0.330	0.225	-0.059	0.045	0.037	-0.141	-0.013	-0.025	-0.094	-0.037	0.074	-0.014	0.004	-0.002	-0.004
21	-0.136	0.346	-0.303	0.055	-0.010	-0.229	0.053	-0.037	0.323	0.065	-0.015	0.010	-0.002	0.028	-0.083	0.014	0.000	0.005
22	0.001	-0.069	0.091	-0.086	0.000	-0.056	0.042	-0.016	0.092	-0.038	-0.028	0.002	-0.007	-0.029	0.025	0.038	-0.003	-0.002
23	0.002	-0.072	-0.010	0.046	0.010	-0.018	0.013	0.003	-0.022	-0.006	0.004	-0.010	-0.005	0.034	0.013	0.003	0.000	0.000
24	-0.059	0.045	0.037	-0.141	0.255	-0.360	0.091	0.027	-0.330	-0.014	0.004	-0.002	-0.004	-0.010	-0.013	-0.025	-0.095	-0.037
25	0.229	-0.053	0.037	-0.324	0.010	0.136	-0.346	0.303	-0.055	0.083	-0.014	0.000	-0.005	-0.012	-0.065	0.015	-0.011	0.002
26	-0.056	0.042	-0.017	0.092	0.000	0.001	-0.069	0.091	-0.086	0.025	0.038	-0.003	-0.002	0.011	-0.038	-0.028	0.002	-0.007
27	0.018	-0.013	-0.003	0.022	-0.010	-0.002	0.072	0.010	-0.046	-0.013	-0.003	0.000	0.000	0.003	0.006	-0.004	0.010	0.005
28	0.185	-0.086	-0.056	0.369	0.125	0.185	-0.086	-0.056	0.369	-0.073	-0.096	0.010	0.008	0.037	-0.073	-0.096	0.010	0.008
29	-0.260	0.016	0.031	0.013	0.182	0.022	0.017	0.051	-0.186	0.034	-0.025	-0.001	0.000	0.001	-0.006	-0.002	-0.002	0.000
30	-0.326	0.000	-0.017	0.009	0.018	0.008	0.001	-0.025	0.289	-0.015	-0.028	0.000	-0.010	-0.001	-0.002	0.000	0.004	0.011
31	0.022	0.017	0.051	-0.186	0.182	-0.260	0.016	0.031	0.013	-0.006	-0.002	-0.002	0.000	0.023	0.034	-0.025	-0.001	0.000

TABLE 8-9

2,4,6,8-TETRAAZABICYCLO[3.3.0]OCTANE AB INITIO FORCE FIELD

Q	1	2	3	4	5	6 7	8	9	10	11	12	13	14	15	16	17	18	
32	-0.008	-0.001	0.025	-0.289	-0.018	0.326	0.001	0.017	-0.009	0.002	0.000	-0.004	-0.011	0.025	0.015	0.028	0.000	0.010
33	0.308	-0.284	0.000	0.003	0.006	0.007	-0.006	0.013	-0.030	0.030	0.039	0.004	-0.034	0.003	-0.002	0.002	0.000	-0.007
34	0.295	0.285	0.000	-0.053	-0.025	0.004	0.005	0.007	-0.039	0.003	0.211	-0.014	0.007	-0.007	-0.003	0.001	-0.002	-0.003
35	0.004	-0.006	-0.152	0.228	-0.047	0.020	0.003	-0.001	0.011	0.003	0.004	-0.018	-0.007	-0.007	0.004	-0.005	0.002	0.001
36	-0.090	0.059	0.259	0.311	0.037	-0.020	0.008	0.000	0.008	0.007	0.004	-0.008	-0.016	0.142	-0.024	0.002	0.000	0.000
37	0.007	-0.006	0.013	-0.030	0.006	0.308	-0.284	0.000	0.003	-0.002	0.002	0.000	-0.007	0.001	0.030	0.039	0.004	-0.034
38	0.004	0.005	0.007	-0.039	-0.025	0.295	0.285	0.000	-0.053	-0.003	0.009	-0.002	-0.003	-0.006	0.003	0.211	-0.014	0.007
39	0.020	0.003	-0.001	0.011	-0.047	0.004	-0.006	-0.152	0.228	0.004	-0.005	0.002	0.001	0.001	0.003	0.004	-0.018	-0.007
40	-0.020	0.008	0.000	0.008	0.037	-0.090	0.059	0.259	0.311	-0.024	0.002	0.000	0.000	0.000	0.007	0.004	-0.008	-0.016
41	-0.021	-0.191	-0.212	-0.013	-0.014	-0.005	0.002	0.002	-0.011	-0.008	-0.002	0.128	0.126	-0.002	-0.007	0.003	-0.001	-0.001
42	0.038	0.004	-0.001	0.103	-0.017	0.001	-0.002	-0.004	0.010	0.006	-0.047	0.120	-0.144	0.017	0.004	0.004	0.001	0.000
43	0.028	-0.417	0.438	-0.040	0.000	0.007	-0.005	0.006	-0.027	-0.008	-0.011	0.001	-0.007	-0.007	0.009	-0.002	0.000	-0.001
44	0.042	0.109	-0.053	-0.002	-0.010	-0.003	0.000	0.002	-0.008	-0.001	0.018	-0.009	0.020	0.031	0.002	0.003	0.000	0.000
45	0.001	-0.002	-0.004	0.010	-0.017	0.038	0.004	-0.001	0.103	0.004	0.004	0.001	0.000	0.000	0.006	-0.047	0.120	-0.144
46	-0.007	0.005	-0.006	0.027	0.000	-0.028	0.417	-0.438	0.040	-0.009	0.002	0.000	0.001	0.001	0.008	0.011	-0.001	0.007
47	0.003	0.000	-0.002	0.008	0.010	-0.042	-0.109	0.053	0.002	-0.002	-0.003	0.000	0.000	0.000	0.001	-0.018	0.009	-0.020
48	-0.005	0.002	0.002	-0.011	-0.014	-0.021	-0.191	-0.212	-0.013	-0.007	0.003	-0.001	-0.001	-0.001	-0.008	-0.002	0.128	0.126

TABLE 8-9

2,4,6,8 TETRAAZABICYCLO[3.3.0]OCTANE AB INITIO FORCE FIELD

Q	19	20	21	22	23	24	25	26	27	28	29	30	31	32	33	34	35	36
19	7.530																	
20	0.010	1.891																
21	0.012	0.038	1.922															
22	0.011	0.013	0.154	0.302														
23	-0.003	0.060	-0.047	0.034	0.166													
24	0.075	0.075	0.027	0.027	0.010	1.891												
25	-0.028	0.027	0.300	0.139	0.008	0.038	1.922											
26	-0.029	0.027	-0.139	-0.246	-0.002	0.013	-0.154	0.302										
27	-0.034	0.010	0.008	0.002	0.002	-0.060	-0.047	-0.034	0.166									
28	0.037	-0.227	0.051	-0.005	-0.017	-0.227	-0.051	-0.005	0.017	1.335								
29	0.023	0.033	-0.025	0.004	0.011	0.057	0.022	0.025	0.003	0.001	0.867							
30	-0.025	0.016	0.028	0.020	0.020	-0.009	0.000	0.004	-0.004	-0.022	0.028	0.845						
31	0.001	0.057	-0.022	0.025	-0.003	0.033	0.025	0.004	-0.011	0.001	-0.022	0.003	0.867					
32	0.001	0.009	0.000	-0.004	-0.004	0.016	0.028	-0.0220	0.020	0.022	-0.003	0.007	-0.028	0.845				
33	0.001	0.028	-0.020	-0.026	0.042	0.005	-0.008	0.034	-0.006	-0.084	-0.046	-0.078	0.003	0.000	1.000			
34	-0.006	0.113	-0.134	-0.002	-0.023	0.006	0.005	0.40	0.007	-0.037	-0.006	-0.011	0.005	0.002	0.059	0.623		
35	0.001	-0.079	0.056	-0.020	-0.025	-0.009	-0.023	0.018	0.002	0.034	0.010	0.001	0.003	0.012	-0.003	0.002	0.861	
36	0.000	0.230	0.179	0.030	-0.023	0.009	0.000	0.011	-0.006	-0.009	0.008	-0.001	0.017	0.026	-0.002	0.017	0.020	0.513
37	0.003	0.005	0.008	0.034	0.006	0.028	0.020	-0.026	-0.042	-0.084	0.003	0.000	-0.046	0.078	0.000	0.006	-0.002	0.003
38	-0.007	0.006	-0.005	0.040	-0.007	0.113	0.134	-0.002	0.023	-0.037	0.005	-0.002	-0.006	0.011	0.006	0.015	-0.006	0.022
39	-0.007	-0.009	0.023	0.018	-0.002	-0.079	-0.056	-0.020	0.025	0.034	0.003	-0.012	0.010	-0.001	-0.002	-0.006	0.002	0.002
40	0.142	0.009	0.000	0.011	0.006	0.230	-0.179	0.030	0.023	-0.009	0.017	-0.026	0.008	0.001	0.003	0.022	0.002	0.005
41	-0.001	0.024	-0.001	0.003	0.008	0.003	0.003	0.000	0.000	-0.018	0.000	0.003	0.003	0.005	0.024	-0.002	-0.006	0.010
42	0.000	-0.139	0.019	0.004	-0.009	-0.003	0.003	-0.003	0.002	-0.014	-0.008	-0.011	-0.004	-0.016	0.041	-0.043	-0.024	0.015
43	-0.001	-0.011	-0.071	-0.009	0.018	0.000	-0.028	0.015	-0.003	-0.015	0.008	0.005	-0.010	-0.011	0.052	0.007	0.006	-0.019
44	0.000	0.019	0.072	-0.004	-0.045	0.003	-0.003	-0.004	0.001	-0.004	0.001	-0.001	-0.005	-0.005	-0.072	0.024	-0.011	0.011
45	0.017	-0.003	-0.003	-0.003	-0.002	-0.139	-0.019	0.004	0.009	-0.014	-0.004	0.016	-0.008	0.011	0.004	-0.002	0.002	0.001
46	0.007	0.000	0.028	-0.015	-0.003	0.011	-0.071	0.009	0.018	0.015	0.010	-0.011	-0.008	0.005	0.007	0.001	0.002	-0.002
47	-0.031	0.003	-0.003	0.004	0.001	-0.019	0.072	0.004	-0.045	0.004	0.005	-0.005	-0.001	-0.001	-0.004	0.001	0.001	0.000
48	0.002	0.003	0.003	0.000	0.000	0.024	0.001	0.003	-0.008	-0.016	0.0003	-0.005	0.000	-0.003	0.002	0.001	-0.001	0.000

TABLE 8-9

2,4,6,8 TETRAAZABICYCLO[3.3.0]OCTANE AB INITIO FORCE FIELD

Q	37	38	39	40	41	42	43	44	45	46	47	48
37	1.000											
38	0.059	0.623										
39	-0.003	0.002	0.861									
40	-0.002	0.017	0.020	0.513								
41	0.002	0.001	-0.001	0.000	0.990							
42	0.004	-0.002	0.002	0.001	0.001	1.038						
43	-0.007	-0.001	-0.002	0.002	0.018	-0.009	0.920					
44	0.004	-0.001	-0.001	0.000	0.012	0.031	-0.059	0.850				
45	0.041	-0.043	-0.024	0.015	0.000	0.002	0.001	0.000	1.038			
46	-0.052	-0.007	-0.006	0.019	0.000	-0.001	0.005	0.000	0.009	0.920		
47	0.072	-0.024	0.011	-0.011	0.000	0.000	0.000	0.002	-0.031	-0.059	0.850	
48	0.024	-0.002	-0.006	0.010	0.000	0.000	0.000	0.000	0.001	-0.018	-0.012	0.990

TABLE 8-10[a]

SCALE FACTORS FOR 2,4,6,8 TETRAAZABICYCLO[3.3.0]OCTANE

Q	TYPE	FACTOR	Q	TYPE	FACTOR
1	CN Stretch	0.866	25	Ring Def.	0.828
2	CN Stretch	0.866	26	Ring Tors.	0.745
3	CN Stretch	0.866	27	Ring Tors.	0.745
4	CN Stretch	0.866	28	Ring-Ring Def.	0.745
5	CC Stretch	0.920	29	CH Rock	0.831
6	CN Stretch	0.866	30	CH Rock	0.831
7	CN Stretch	0.866	31	CH Rock	0.831
8	CN Stretch	0.866	32	CH Rock	0.831
9	CN Stretch	0.866	33	NH Rock	0.803
10	CH Stretch	0.864	34	NH Wag	1.186
11	NH Stretch	0.844	35	NH Rock	0.803
12	CH Stretch	0.864	36	NH Wag	1.186
13	CH Stretch	0.864	37	NH Rock	0.803
14	NH Stretch	0.844	38	NH Wag	1.186
15	CH Stretch	0.864	39	NH Rock	0.803
16	NH Stretch	0.844	40	NH Wag	1.186
17	CH Stretch	0.864	41	CH_2 Scissor	0.8[b]
18	CH Stretch	0.864	42	CH_2 Rock	0.8[b]
19	NH Stretch	0.844	43	CH_2 Wag	0.71
20	Ring Def.	0.828	44	CH_2 Rock	0.8[b]
21	Ring Def.	0.828	45	CH_2 Rock	0.8[b]
22	Ring Tors.	0.745	46	CH_2 Wag	0.71
23	Ring Tors.	0.745	47	CH_2 Rock	0.8[b]
24	Ring Def.	0.828	48	CH_2 Scissor	0.8[b]

a. Scale factors from Chapter Four.

b. Assumed value.

TABLE 8-11

2,4,6,8-TETRAAZABICYCLO[3.3.0]OCTANE SCALED QUANTUM MECHANICAL FORCE FIELD

Q	1	2	3	4	5	6	7	8	9	10	11	12	13	14	15	16	17	18
1	4.872																	
2	0.067	5.005																
3	0.059	0.298	4.674															
4	0.011	-0.001	0.105	5.101														
5	0.262	-0.002	-0.095	0.292	4.107													
6	0.017	-0.048	-0.036	0.371	0.262	4.872												
7	-0.048	0.026	0.019	-0.068	-0.002	0.067	5.005											
8	-0.036	0.019	0.033	-0.047	-0.095	0.059	0.298	4.674										
9	0.371	-0.068	-0.047	-0.012	0.292	0.011	-0.001	0.105	5.101									
10	0.191	0.010	-0.031	-0.011	0.062	0.001	-0.037	0.008	0.142	4.678								
11	0.032	0.051	0.006	-0,005	-0.018	-0.001	-0.005	0.001	-0.014	-0.007	6.268							
12	-0.024	0.072	0.140	-0.009	-0.025	0.005	0.000	-0.002	0.008	0.003	0.014	4.838						
13	0.003	0.166	0.197	-0.007	-0.014	-0.001	-0.002	-0.003	0.004	0.009	-0.021	0.071	4.580					
14	-0.023	-0.004	0.012	-0.007	0.013	0.013	-0.002	-0.002	0.005	0.002	-0.003	0.005	0.017	6.356				
15	0.001	-0.037	0.008	0.142	0.062	0.191	0.010	-0.031	-0.011	0.028	-0.002	0.004	0.007	0.022	4.687			
16	-0.001	-0.005	0.001	-0.014	-0.018	0.032	0.051	0.006	-0.005	-0.002	0.002	-0.001	-0.001	-0.006	-0.007	6.268		
17	0.005	0.000	-0.002	0.007	-0.025	-0.024	0.072	0.140	-0.009	0.004	-0.001	0.001	0.001	0.001	0.003	0.014	4.838	
18	-0.001	-0.002	-0.003	0.004	-0.014	0.003	0.166	0.197	-0.007	0.007	-0.001	0.001	0.002	0.001	0.009	-0.021	0.071	4.580
19	0.013	-0.002	-0.002	0.005	0.013	-0.023	-0.004	0.012	-0.007	0.022	-0.006	0.001	0.001	0.000	0.002	-0.003	0.005	0.017
20	-0.305	0.077	0.023	-0.280	0.196	-0.050	0.038	0.031	-0.120	-0.011	-0.021	-0.080	-0.032	0.062	-0.012	0.004	-0.002	-0.003
21	-0.115	0.293	-0.257	0.047	-0.009	-0.194	0.045	-0.032	0.274	0.055	-0.012	0.009	-0.002	0.023	-0.070	0.012	0.000	0.004
22	0.001	-0.056	0.073	-0.069	0.000	-0.045	0.034	-0.014	0.074	-0.030	-0.022	0.001	-0.006	-0.023	0.020	0.030	-0.002	-0.002
23	0.002	-0.057	-0.008	0.037	0.083	-0.014	0.010	0.003	-0.017	-0.005	0.003	-0.008	-0.004	0.027	0.011	0.002	0.000	0.000
24	-0.050	0.038	0.031	-0.120	0.196	-0.305	0.077	0.023	-0.280	-0.012	0.004	-0.002	-0.003	-0.008	-0.011	-0.021	-0.080	-0.032
25	0.194	-0.045	0.032	-0.274	0.009	0.115	-0.293	0.257	-0.047	0.070	-0.012	0.000	-0.004	-0.010	-0.055	0.012	-0.009	0.002
26	-0.045	0.034	-0.014	0.074	0.000	0.001	-0.056	0.073	-0.069	0.020	0.030	-0.002	-0.002	0.009	-0.030	-0.022	0.001	-0.006
27	0.014	-0.010	-0.003	0.017	-0.083	-0.002	0.057	0.008	-0.037	-0.011	-0.002	0.000	0.000	0.003	0.005	-0.003	0.008	0.004
28	0.148	-0.069	-0.045	0.296	0.104	0.148	-0.069	-0.045	0.296	-0.059	-0.076	0.008	0.006	0.029	-0.059	-0.076	0.008	0.006
29	-0.220	0.014	0.027	0.011	0.159	0.019	0.014	0.043	-0.158	0.029	-0.021	-0.001	0.000	0.001	-0.005	0.002	-0.002	0.000
30	-0.277	0.000	-0.014	0.008	0.016	0.006	0.001	0.021	0.245	-0.013	-0.023	0.000	-0.008	-0.001	0.002	0.000	0.004	0.010
31	0.019	0.014	0.043	-0.158	0.159	-0.220	0.014	0.027	0.011	-0.005	-0.002	-0.002	0.000	0.019	0.029	-0.021	-0.001	0.000

TABLE 8-11

2,4,6,8-TETRAAZABICYCLO[3.3.0]OCTANE SCALED QUANTUM MECHANICAL FORCE FIELD

Q	1	2	3	4	5	6	7	8	9	10	11	12	13	14	15	16	17	18
32	-0.006	-0.001	0.021	-0.245	-0.016	0.277	0.000	0.014	-0.008	0.002	0.000	-0.004	-0.010	0.021	0.013	0.023	0.000	0.008
33	0.257	-0.237	0.000	0.002	0.005	0.006	-0.005	0.011	-0.025	0.025	0.032	0.003	-0.029	0.003	-0.001	0.002	0.000	-0.006
34	0.299	0.289	0.000	-0.054	-0.026	0.004	0.005	0.007	-0.039	0.003	0.211	-0.014	0.007	-0.007	-0.003	0.001	-0.002	-0.003
35	0.003	-0.005	-0.0127	0.190	-0.040	0.017	0.002	-0.001	0.010	0.003	0.004	-0.015	-0.006	-0.006	0.004	-0.004	0.002	0.001
36	-0.091	0.059	0.262	0.315	0.038	-0.020	0.008	0.000	0.008	0.007	0.004	-0.008	-0.017	0.142	-0.024	0.002	0.000	0.000
37	0.006	-0.005	0.011	-0.025	0.005	0.257	-0.237	0.000	0.002	-0.001	0.002	0.000	-0.006	0.001	0.025	0.032	0.003	-0.029
38	0.004	0.005	0.007	-0.039	-0.026	0.299	0.289	0.000	-0.054	-0.003	0.001	-0.002	-0.003	-0.006	0.003	0.211	-0.014	0.007
39	0.017	0.002	-0.001	0.010	-0.040	0.003	-0.005	-0.127	0.190	0.004	-0.004	0.002	0.0001	0.001	0.003	0.004	-0.015	-0.006
40	-0.020	0.008	0.000	0.008	0.038	-0.091	0.059	0.262	0.315	-0.024	0.002	0.000	0.000	0.000	0.007	0.004	-0.008	-0.017
41	-0.018	-0.159	-0.176	-0.011	-0.012	-0.004	0.002	0.001	-0.009	-0.006	-0.002	0.107	0.104	-0.001	-0.006	0.002	-0.001	-0.001
42	0.032	0.003	-0.001	0.086	-0.014	0.001	-0.001	-0.003	0.009	0.005	-0.039	0.100	-0.120	0.014	0.003	0.004	0.001	0.000
43	0.022	-0.327	0.344	-0.031	0.000	0.006	-0.004	0.004	-0.021	-0.006	-0.008	0.001	-0.006	-0.006	0.007	-0.002	0.000	-0.001
44	0.035	0.091	-0.044	0.001	-0.009	-0.002	0.000	0.002	-0.007	-0.001	0.015	-0.007	0.017	0.025	0.001	0.003	0.000	0.000
45	0.001	-0.001	-0.003	0.009	-0.014	0.032	0.003	-0.001	0.086	0.003	0.004	0.001	0.000	0.000	0.005	-0.039	0.100	-0.120
46	-0.006	0.004	-0.004	0.021	0.000	-0.022	0.327	-0.344	0.031	-0.007	0.002	0.000	0.001	0.001	0.006	0.008	-0.001	0.006
47	0.002	0.000	-0.002	0.007	0.009	-0.035	-0.091	0.044	0.001	-0.001	-0.003	0.000	0.000	0.000	0.001	-0.015	0.007	-0.017
48	-0.004	0.002	0.001	-0.009	-0.012	-0.018	-0.159	-0.176	-0.011	-0.006	0.002	-0.001	-0.001	-0.001	-0.007	-0.002	0.107	0.104

TABLE 8-11

2,4,6,8 TETRAAZABICYCLO[3.3.0]OCTANE SCALED QUANTUM MECHANICAL FORCE FIELD

Q	19	20	21	22	23	24	25	26	27	28	29	30	31	32	33	34	35	36
19	6.356																	
20	-0.008	1.566																
21	0.010	-0.032	1.591															
22	0.009	0.010	0.121	0.225														
23	-0.003	0.047	-0.037	0.025	0.124													
24	0.062	0.062	0.022	0.021	0.008	1.566												
25	-0.023	-0.022	0.248	0.109	0.006	0.032	1.591											
26	-0.023	0.021	-0.109	-0.181	-0.002	0.010	-0.121	0.255										
27	-0.027	-0.008	0.006	0.002	0.002	-0.047	-0.037	-0.025	0.124									
28	0.029	-0.178	0.040	-0.004	-0.012	-0.178	-0.040	-0.004	0.012	0.995								
29	0.019	0.028	-0.021	0.003	0.009	0.047	0.018	0.020	0.002	0.001	0.721							
30	-0.021	-0.013	0.023	0.016	0.016	-0.008	0.000	0.003	-0.003	-0.017	0.023	0.703						
31	0.001	0.047	-0.018	0.020	-0.002	0.028	0.021	0.003	-0.009	0.001	-0.019	0.002	0.721					
32	0.001	0.008	0.000	-0.003	-0.003	0.013	0.023	-0.016	0.013	0.017	-0.002	0.006	-0.023	0.703				
33	0.001	0.022	-0.016	-0.020	0.032	0.004	-0.007	0.026	-0.004	-0.065	-0.038	-0.064	0.002	0.000	0.803			
34	-0.006	0.112	-0.133	-0.001	-0.022	0.006	0.005	0.038	0.007	-0.035	-0.006	-0.011	0.005	0.002	0.057	0.738		
35	0.001	-0.064	0.046	-0.015	-0.019	-0.007	-0.019	0.014	0.002	0.026	0.008	0.001	0.003	0.009	-0.003	0.002	0.691	
36	0.000	0.227	0.177	0.028	-0.022	0.009	0.000	0.010	-0.006	-0.008	0.008	-0.001	0.017	0.026	-0.002	0.020	0.019	0.608
37	0.003	0.004	0.007	0.026	0.004	0.022	0.016	-0.020	-0.032	-0.065	0.002	0.000	-0.038	0.064	0.000	0.005	-0.002	0.003
38	-0.007	0.006	-0.005	0.038	-0.007	0.112	0.133	-0.001	0.022	-0.035	0.005	-0.002	-0.006	0.011	0.005	0.018	-0.006	0.026
39	-0.006	-0.007	0.019	0.014	-0.002	-0.064	-0.046	-0.015	0.019	0.026	0.003	-0.009	0.008	-0.001	-0.002	-0.006	0.001	0.002
40	0.142	0.009	0.000	0.010	0.006	0.227	-0.177	0.028	0.022	-0.008	0.017	-0.026	0.008	0.001	0.003	0.026	0.002	0.006
41	-0.001	0.019	-0.001	0.002	0.007	0.002	0.002	0.000	0.000	-0.012	0.000	0.003	0.002	0.004	0.019	-0.002	-0.004	0.010
42	0.000	-0.113	0.016	0.003	-0.007	-0.002	0.002	-0.002	0.001	-0.011	-0.007	-0.009	-0.003	-0.013	0.033	-0.042	-0.019	0.014
43	-0.001	-0.009	-0.055	-0.007	0.013	0.000	-0.021	0.011	-0.002	-0.011	0.006	0.004	-0.008	-0.008	0.039	0.006	0.005	-0.018
44	0.000	0.016	-0.059	-0.003	-0.034	0.002	-0.003	-0.003	0.001	-0.003	0.001	-0.001	-0.004	-0.004	-0.058	0.023	-0.009	0.011
45	0.014	-0.002	-0.002	-0.002	-0.001	-0.113	-0.016	0.003	0.007	-0.011	-0.003	0.013	-0.007	0.009	0.003	-0.002	0.001	0.001
46	0.006	0.000	-0.021	-0.011	-0.002	0.009	-0.055	0.007	0.013	0.011	0.008	-0.008	-0.006	0.004	0.005	0.001	0.002	-0.002
47	-0.025	0.002	-0.003	0.003	0.001	-0.016	-0.059	0.003	-0.034	0.003	0.004	-0.004	-0.001	-0.001	-0.004	0.001	0.001	0.000
48	-0.001	0.002	-0.002	0.000	0.000	0.019	0.001	0.002	-0.007	-0.012	0.002	-0.004	0.000	-0.003	0.002	0.001	-0.001	0.000

TABLE 8-11

2,4,6,8 TETRAAZABICYCLO[3.3.0]OCTANE SCALED QUANTUM MECHANICAL FORCE FIELD

Q	37	38	39	40	41	42	43	44	45	46	47	48
37	0.803											
38	0.057	0.738										
39	-0.003	0.002	0.691									
40	-0.002	0.020	0.019	0.608								
41	0.002	0.001	-0.001	0.000	0.792							
42	0.003	-0.002	0.001	0.001	0.001	0.830						
43	-0.005	-0.001	-0.002	0.002	0.013	-0.007	0.653					
44	0.004	-0.001	-0.001	0.000	0.010	0.025	-0.045	0.680				
45	0.033	-0.042	-0.019	0.014	0.000	0.002	0.001	0.000	0.830			
46	-0.039	-0.006	-0.005	0.018	0.000	-0.001	0.004	0.000	0.007	0.653		
47	0.058	-0.023	0.009	-0.011	0.000	0.000	0.000	0.001	-0.025	-0.045	0.680	
48	0.019	-0.002	-0.004	0.010	0.000	0.000	0.000	0.000	0.001	-0.013	-0.010	0.792

TABLE 8-12[a]

FUNDAMENTAL VIBRATIONAL FREQUENCIES FOR 2,4,6,8-TETRAAZABICYCLO[3.3.0]OCTANE

N	AB INITIO FREQUENCY	SQM FREQUENCY	ASSIGNMENT	INTENSITY	SYMMETRY
1	99	85	Ring Tors.	693	A
2	205	177	Ring Tors.	45	A
3	272	236	Ring Tors.	1866	B
4	438	389	Ring Tors.	13	B
5	485	425	Ring-Ring Tors.	21	A
6	625	579	Ring Def.	1145	A
7	662	609	Ring Def.	554	A
8	703	659	Ring Def.	812	B
9	807	745	Ring Def.	953	B
10	877	825	CC Stretch	3330	A
11	981	940	CN Stretch	386	B
12	989	955	CH_2 Rock	5507	A
13	1031	969	CN Stretch	185	B
14	1044	976	CN Stretch	3552	A
15	1056	998	CN Stretch	6941	A
16	1072	1022	CH_2 Rock	353	B
17	1091	1055	CN Stretch	1440	B
18	1111	1101	NH Wag	16977	A
19	1194	1113	CN Stretch	231	B
20	1202	1126	CN Stretch	4151	A
21	1229	1168	CN Stretch	2493	B
22	1250	1171	CN Stretch	2852	A
23	1270	1197	CH_2 Rock, NH Wag	1332	B
24	1313	1199	CH_2 Rock	3790	A
25	1364	1237	CH_2 Wag	16851	A
26	1369	1245	CH_2 Wag	4660	B

N	AB INITIO FREQUENCY	SQM FREQUENCY	ASSIGNMENT	INTENSITY	SYMMETRY
27	1405	1280	CH Rock, NH Rock	2388	A
28	1453	1307	CH_2 Wag	22	B
29	1458	1353	CH Rock	13034	B
30	1477	1356	CH Rock, NH Wag	8938	A
31	1531	1392	NH Rock, CH_2 Wag	23339	A
32	1548	1400	CH Rock, NH Wag	8117	B
33	1590	1431	NH Rock	256	B
34	1596	1436	NH Rock	751	A
35	1629	1462	NH Rock	6450	B
36	1631	1466	CH Rock, NH Rock	3185	A
37	1702	1524	CH_2 Scissor	937	A
38	1704	1525	CH_2 Scissor	423	B
39	3105	2887	CH Stretch	104	B
40	3106	2887	CH Stretch	15648	A
41	3138	2917	CH Stretch	54	B
42	3164	2941	CH Stretch	13579	A
43	3203	2977	CH Stretch	331	B
44	3203	2978	CH Stretch	7391	A
45	3669	3370	NH Stretch	97	B
46	3670	3371	NH Stretch	575	A
47	3697	3396	NH Stretch	65	B
48	3697	3396	NH Stretch	324	A

a. Frequencies in cm^{-1}. Intensities in cm/mmole.

TABLE 8-13

MOLECULAR CONSTANTS FOR 2,4,6,8-TETRAAZABICYCLO[3.3.0]OCTANE

Parameter	Value
Molecular Weight	114.0 gm/mole
I_A	4086.68 Mhz
I_B	2071.03 Mhz
I_C	1540.95 Mhz
Rotational Symmetry Number	2

TABLE 8-14

THERMODYNAMIC DATA FOR 2,4,6,8-TETRAAZABICYCLO[3.3.0]OCTANE

T[a]	C_v[b]	Entropy[c]	$-(G_0-E_0)/T$[d]	$(H_0-E_0)/T$[e]
100	10.21	60.33	50.63	9.701
200	16.11	70.46	58.14	12.32
300	25.07	79.40	63.74	15.66
400	35.37	88.59	68.79	19.80
500	44.76	97.97	73.69	24.28
600	52.61	107.2	78.51	28.70
700	59.07	116.1	83.25	32.87
800	64.41	124.6	87.90	36.74
900	68.89	132.7	92.43	40.29
1000	72.67	140.4	96.85	43.54
1100	75.90	147.7	101.1	46.52
1200	78.67	154.6	105.3	49.26
1300	81.05	161.1	109.4	51.77
1400	83.11	167.3	113.3	54.07
1500	84.90	173.3	117.1	56.20

a. Temperature in degrees Kelvin.

b. Specific heat at constant volume in cal/(mole K).

c. Entropy in cal/(mole K).

d. Free energy in cal/(mole K).

e. Enthalpy in cal/(mole K).

Table 8-15

Reference Data for Calculating 2,4,6,8-Tetraazabicyclo[3.3.0]octane Thermodynamic Functions

Molecule	E_0[a]	Zero Point Energy[b]	E(4-21NO*)[c]
NH_3	-9.37[d]	20.54[e]	-56.072837[f]
CH_4	-15.99[d]	27.08[e]	-40.112649[g]
CH_3NH_2	-1.91[d]	38.72[h]	-95.020176[f]
C_2H_6	-16.52[d]	45.32[i]	-79.066519[g]

a. E_0 in kcal/mole.

b. Zero point energy in kcal/mole.

c. Ab initio energy in Hartree calculated with 4-21NO* basis set.

d. D. A. McQuarrie, Statistical Mechanics, pg 155, Harper & Row, New York, New York, 1976.

e. G. Herzberg, Infrared and Raman Spectra, D. Van Nostrand, N.Y. 1945.

f. This work.

g. P. Pulay, G. Fogarasi, F. Pang and J. E. Boggs, J. Amer. Chem. Soc., 2550 (101) 1979.

h. Calculated from fundamental assignments given in reference 65.

i. I. Nakagawa and T. Shimanouchi, J. Mol. Spectros., 255 (39) 1971.

FIGURE 8-1

2,4,6,8 TETRANITRO 2,4,6,8 TETRAAZABICYCLO[3.3.0] OCTANE (BICYCLO HMX)

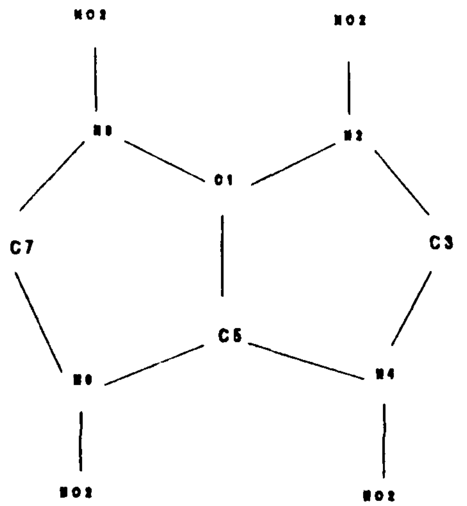
NO2
NO2
N8
N2
C1
C7
C3
C5
N6
N4
NO2
NO2

1,3,5,7 TETRANITRO 1,3,5,7 TETRAAZA CYCLOOCTANE (HMX)

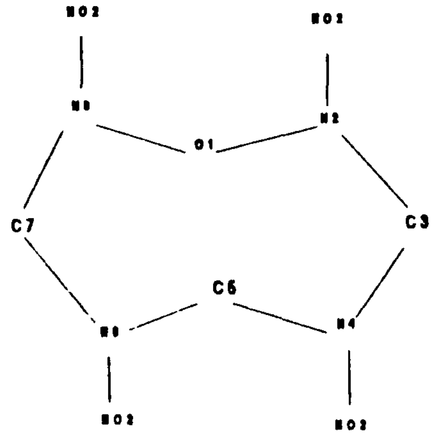
NO2
NO2
N8
N2
C1
C7
C3
C5
N6
N4
NO2
NO2

FIGURE 8-2

ATOM NUMBERING SCHEME FOR 2,4,6,8 TETRAAZABICYCLO[3.3.0]OCTANE

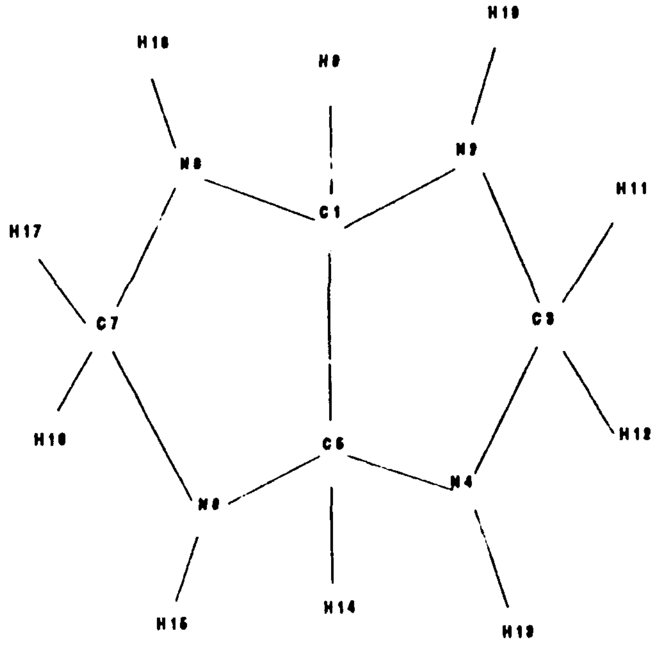
H10
H16
H9
N8
N2
C1
H11
H17
C7
C3
H18
C5
H12
N6
N4
H15
H14
H13

Figure 8-3
2,4,6,8 Tetraazabicyclo[3.3.0]octane Structures Calculated with the 4-21 Basis Set

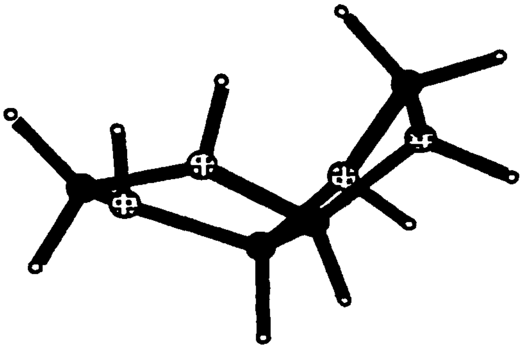

Conformation A
Delta E = 0.0
kcal/mole

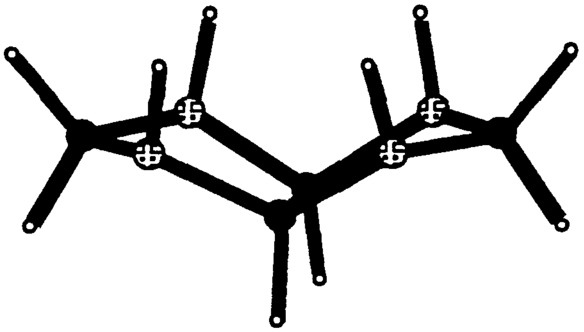

Conformation B
Delta E = 9.8 kcal/mole

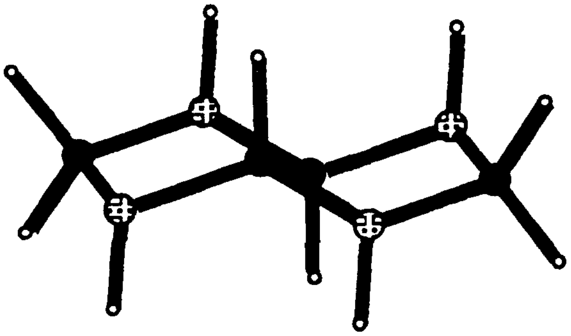

Conformation C
Delta E = 30.0 kcal/mole

Figure 8-4
2,4,6,8-Tetraazabicyclo[3.3.0]octane

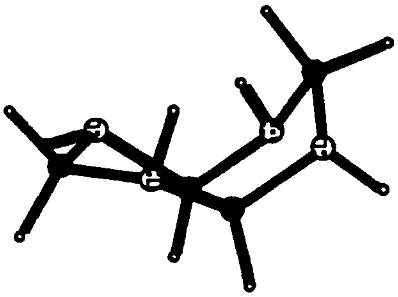

Conformation 1
Delta E = -0.1 kcal/mole

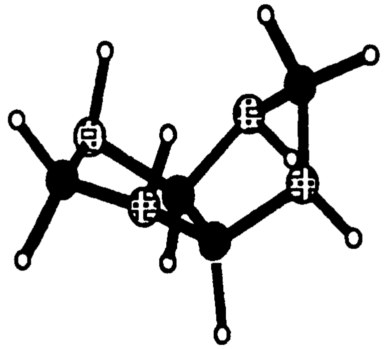

Conformation 2
Delta E = 0.0 kcal/mole

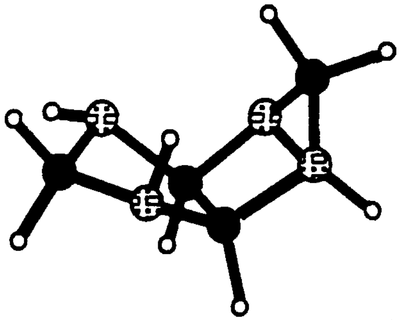

Conformation 3
Delta E = 0.3 Kcal/mole

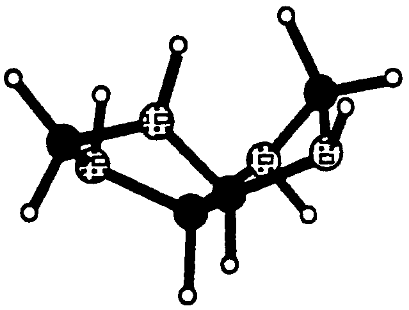

Conformation 4
Delta E = 0.8 Kcal/mole

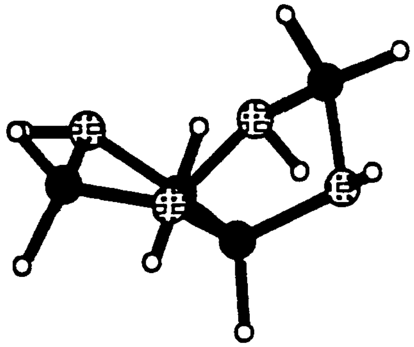

Conformation 5
Delta E = 2.1 Kcal/mole

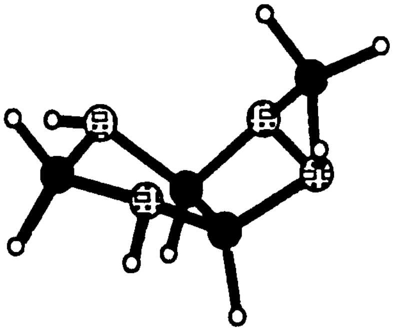

Conformation 6
Delta E = 3.1 kcal/mole

Figure 8-4
2,4,6,8-Tetraazabicyclo[3.3.0]octane

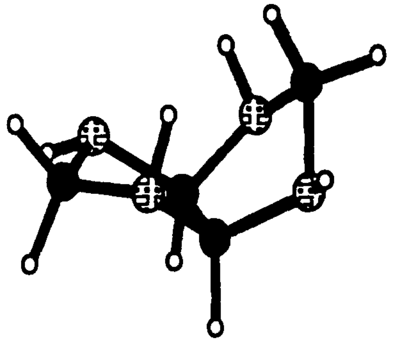

Conformation 7
Delta E = 3.7 Kcal/mole

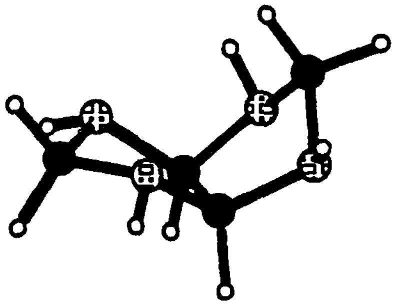

Conformation 9
Delta E = 5.2 Kcal/mole

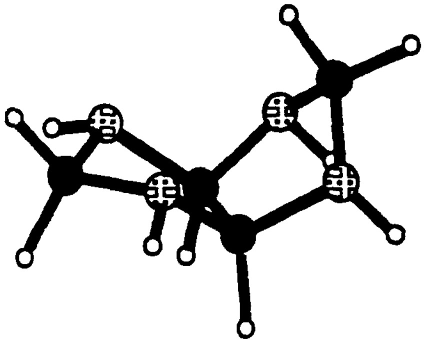

Conformation 8
Delta E = 4.6 Kcal/mole

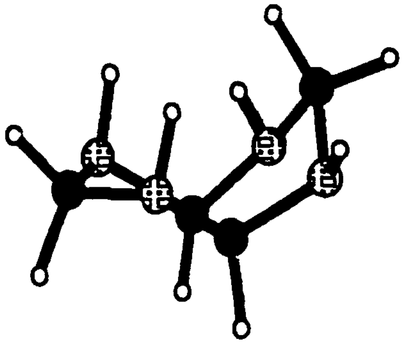

Conformation 10
Delta E = 5.2 Kcal/mole

Figure 8-5
2,4,6,8 Tetraazabicyclo[3.3.0]octane

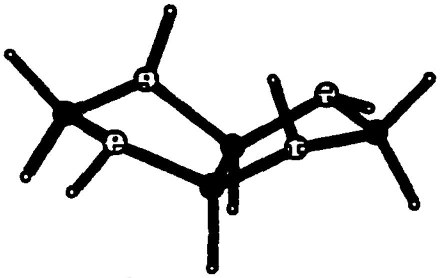

Conformation 11
Delta E = 1.3 kcal/mole

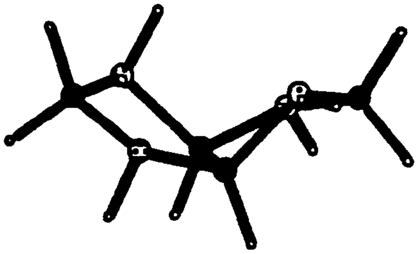

Conformation 14
Delta E = 5.8 kcal/mole

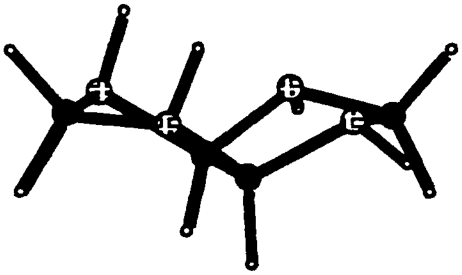

Conformation 12
Delta E = 3.1 kcal/mole

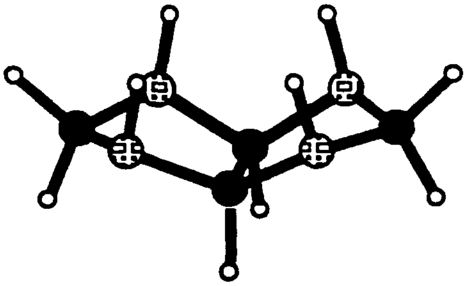

Conformation 15
Delta E = 7.3 kcal/mole

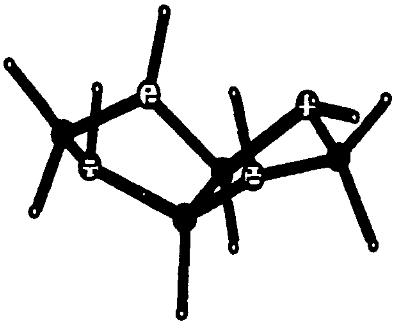

Conformation 13
Delta E = 4.0 kcal/mole

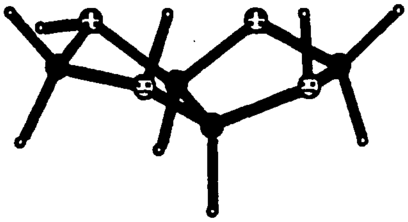

Conformation 16
Delta E = 7.7 kcal/mole

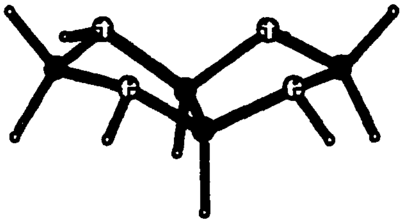

Conformation 17
Delta E = 15.6 kcal/mole

Figure 8-6
Fourth Order Polynomial Fit

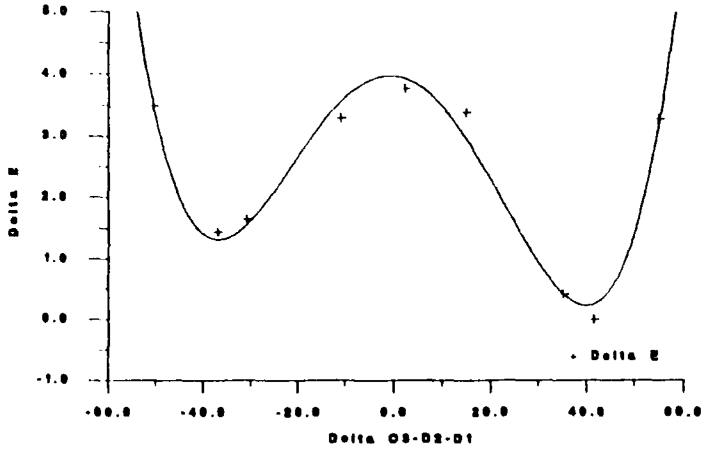

Figure 8-7
Fifth Order Polynomial Fit

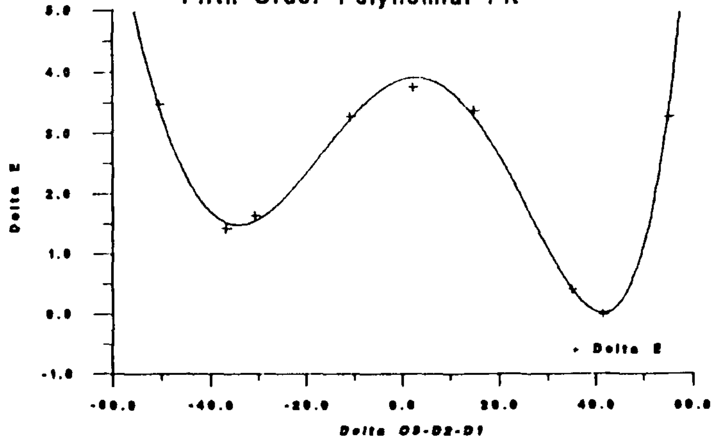

Figure 8-8
C7-D3-D1 Angle

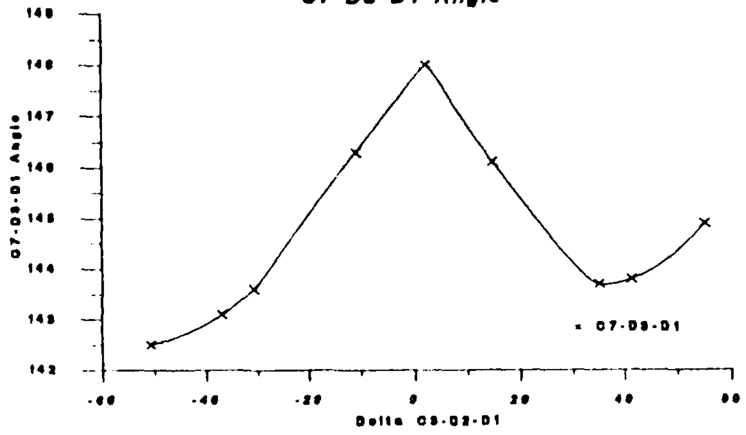

Figure 8-9
C1-N2 and N4-C5 Bond Lengths

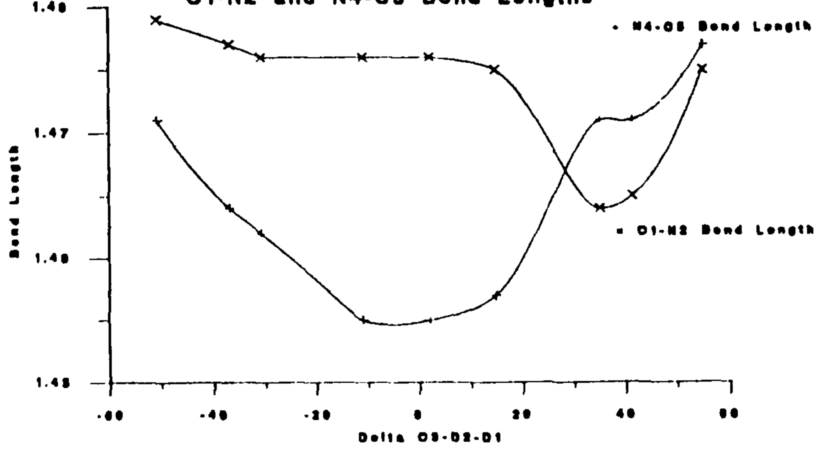

Figure 8-10
N2-C3 and C3-N4 Bond Lengths

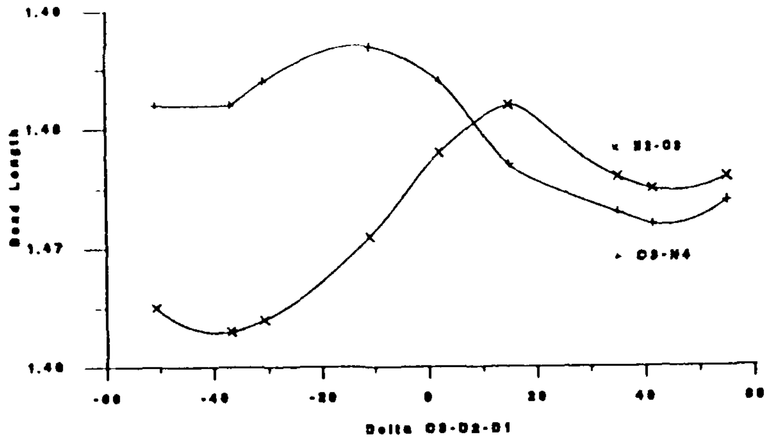

Figure 8-11
C1-C5 Bond Length

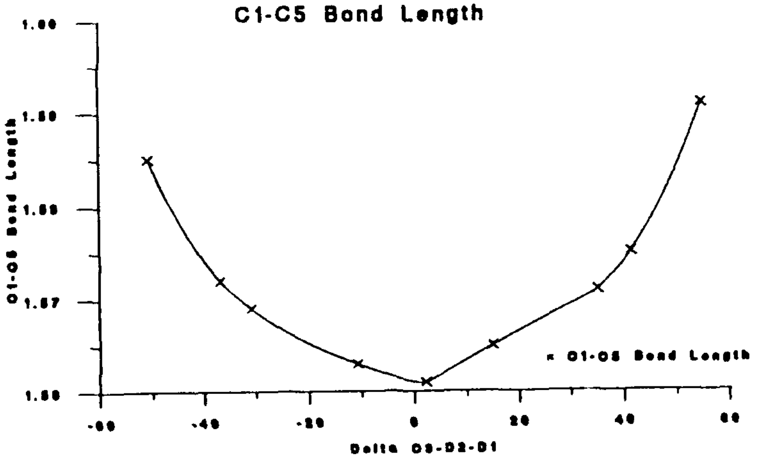

Figure 8-12
C5-N6 and C1-N8 Bond Lengths

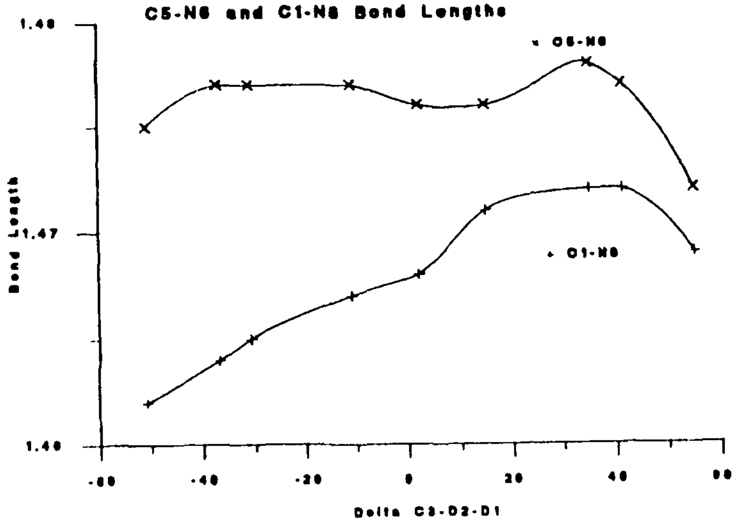

Figure 8-13
N6-C7 and C7-N8 Bond Lengths

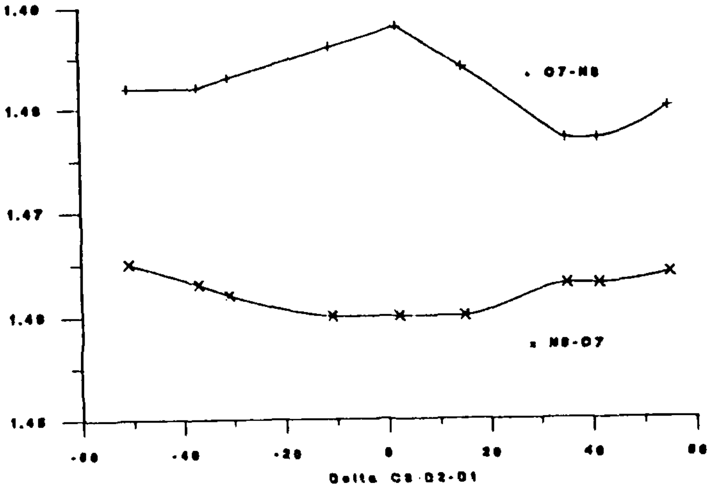

Figure 8-14
N2-C1-N8 and N6-C5-N4 Angles

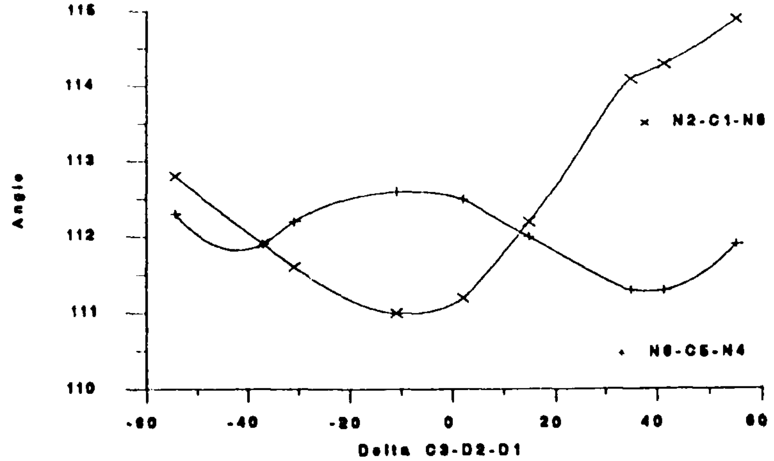

Figure 8-15
C1-N2-C3 and C3-N4-C5 Angles

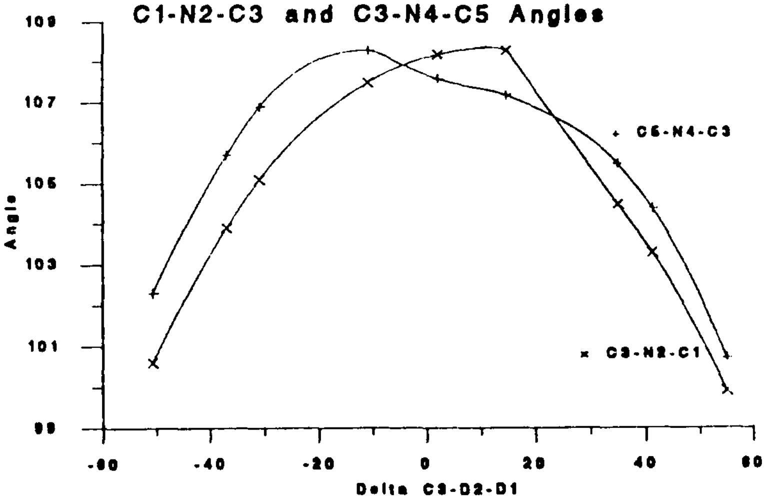

Figure 8-16
N4-C3-N2 Angle

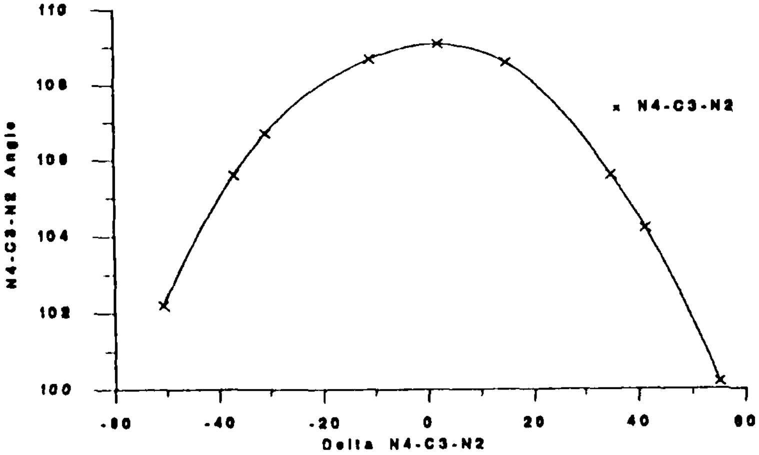

Figure 8-17
C5-C1-N2 and N4-C5-C1 Angles

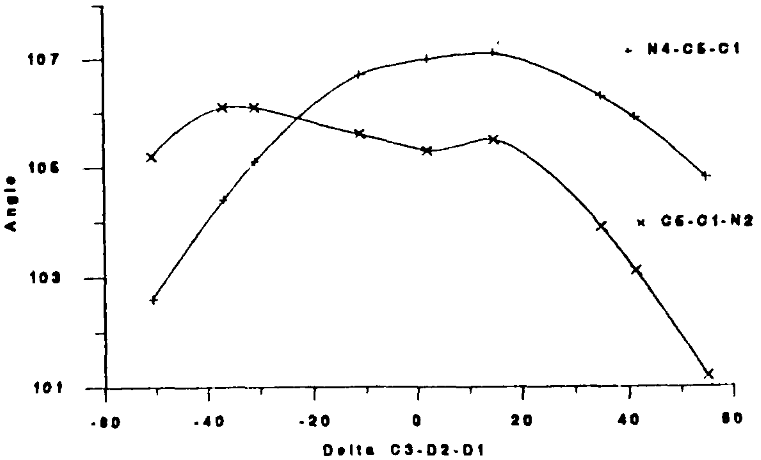

Figure 8-18
C7-N6-C5 and C7-N8-C1 Angles

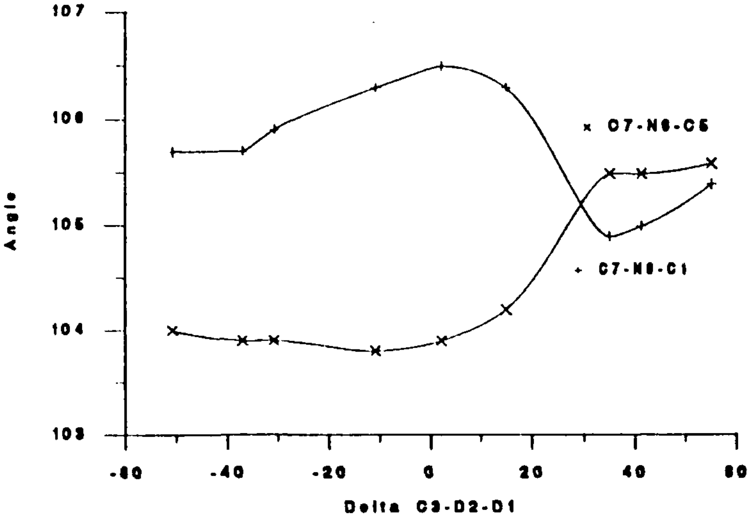

Figure 8-19
N8-C7-N6 Angle

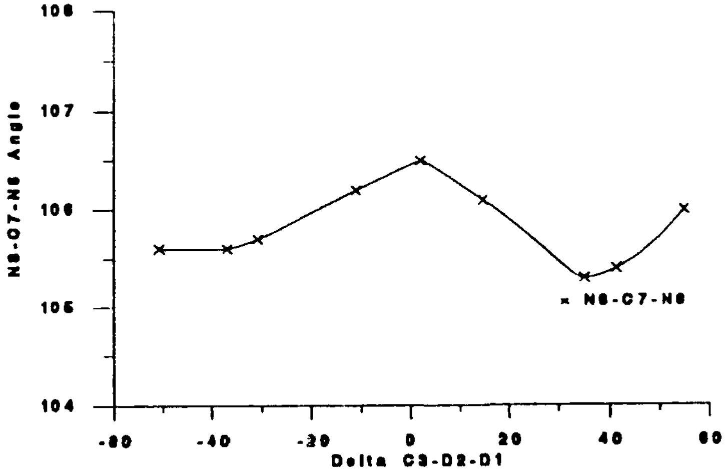

Figure 8-20
C5-C1-N8 and C1-C5-N6 Angles

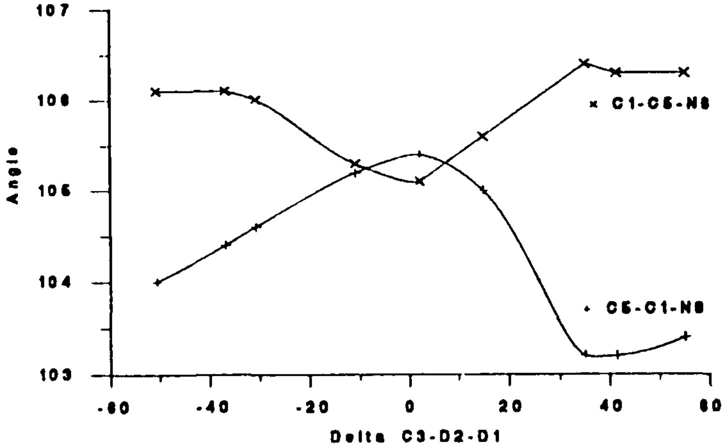

Figure 8-21
Theoretical Fundamental Vibration
Spectrum

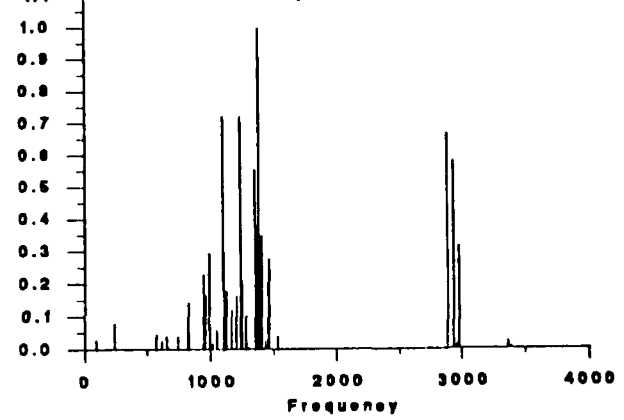

Chapter Nine

Introduction

The molecule 1,2,3-oxidiazolo-1,2,3-oxadiazole-1,1-dioxide, shown in Figure 9-1, is one the target molecules of the Navy's Energetic Materials Research Program. An empirical calculation has indicated this molecule should have a density greater than 2.0 g/cm^3 [137]. The molecule has not yet been synthesized and a literature search did not reveal any previous theoretical studies. The numbering scheme used in this work for 1,2,3-oxadiazolo-1,2,3-oxadiazole-1,1-dioxide is shown in Figure 9-1.

The scope of this Chapter follows the general pattern of Chapters Six, Seven, and Eight. Unless stated otherwise, all of the calculations reported in this chapter were completed with the 4-21NO*(D6) basis set. The chapter opens with a discussion of the optimized ab initio geometry. Next the ab initio geometry is corrected for the basis set offset to yield an approximation of the r_e geometry and then the ab initio and Scaled Quantum Mechanical force fields are discussed. The fundamental frequencies of vibration are calculated from the Scaled Quantum Mechanical force field and these frequencies are then used to calculate thermodynamic functions for 1,2,3-oxadiazolo-1,2,3-oxadiazole-1,1-dioxide. The chapter closes with the calculation of the E_0 energy

Optimum Ab Initio Geometry

The geometry of 1,2,3-oxadiazolo-1,2,3-oxadiazole-1,1-dioxide was optimized with both the 4-21NO*(P) and 4-21NO*(D6) basis sets using the gradient method [25] and the optimization criteria presented in Chapter Two. The 4-21NO*(D6) optimum geometry is shown in Table 9-1 and is almost identical to the 4-21NO*(P) geometry, the bond lengths differ by less than 0.002 Å and the bond angles differ by less than 0.2°. The optimum ab initio geometry is planar and belongs to the C_{2h} symmetry group.

To ensure the planar structure is the true equilibrium configuration, the geometry was optimized starting with a non-planar structure, one of the ring oxygen atoms was moved approximately 0.5 Å out of the molecular plane. During this series of calculations the forces on the atoms always tended to return the molecule to a planar geometry. The structure converged to the geometry given in Table 9-1, conclusively showing the planar configuration is the equilibrium geometry.

The bonding in 1,2,3-oxadiazolo-1,2,3-oxadiazole-1,1-dioxide does not appear to follow a classical bonding pattern. Orbitals localized according to Boys criterion [142] were calculated for 1,2,3-oxadiazolo-1,2,3-oxadiazole-1,1-dioxide, but the localization procedure did not converge. Thus, we cannot study the ring bonding structure with the localized orbitals and must rely on inferences drawn from the molecular geometry. For simplicity in the following discussion, only the bonding between the O8, C1, C5, N2, O9, N3, and N4 atoms will be discussed. The bonding between the other atoms is related to this discussion by simple symmetry considerations.

Comparing the 1,2,3-oxadiazolo-1,2,3-oxadiazole-1,1-dioxide bond lengths to the to the bond length data derived in Chapter Three provides insight into the degree of delocalization of each bond. The C1-C5 bond length is a classical CC double bond length indicating this bond is not delocalized. The C1-O8 bond length is at the short end of the bond length range spanned by delocalized CO bonds. The C1-N2 bond length is shorter than the typical CN single bond length, but longer than the typical delocalized CN bond length, indicating the C1-N2 bond is very weakly delocalized. The N3-O4 bond length is longer than the typical NO single bond length implying electron density is transferred from this bond to other bonds in the ring. The N2-O9 bond length is longer than the typical NO double bond length suggesting the electron density from this bond is transferred into the ring. The N2-N3 bond length is shorter than the typical delocalized NN bond length, but longer than the typical double NN bond length inferring the N2-N3 bond is very weakly delocalized. The above data indicate the C1-O8, C1-N2, N2-O9, and N2-N3 bonds participate in a weakly delocalized bonding network. The C1-C5 and N3-O4 bonds appear to be localized bonds.

1,2,3-Oxadiazolo-1,2,3-Oxadiazole-1,1-Dioxide Force Field

The 1,2,3-oxadiazolo-1,2,3-oxadiazole-1,1-dioxide force field was calculated using the finite difference method outlined in Chapter Two. The theoretical r_e geometry, shown in the second column of Table 9-1, was derived by correcting the optimized ab initio geometry for the basis set offset via the appropriate correction formulae from Chapter Three and was used as the reference geometry for the force field calculation. The constraints imposed by ring closure cause the minor differences between the ab initio and r_e ring bond angles. Internal coordinates were defined as suggested by Pulay [5, 25] and are shown in Table 9-2.

The molecular C_{2h} symmetry permits strict separation of the force constants associated with the 17 in-plane internal coordinates from the force constants associated with the seven out-of-plane internal coordinates. The ab initio in-plane force field is given as Table 9-3 and the ab initio out-of-plane force field is given as Table 9-4. Scaled Quantum Mechanical (SQM) force fields [5, 20] were calculated from the ab initio force fields using the scale factors given in Table 9-5; see Chapter Four for the derivation of these scale factors. Scale factors for internal coordinates 16, 17, and 24 were not derived in Chapter Four and they are assumed to be equal to 0.8. The SQM in-plane force field is given as Table 9-6 and the SQM out-of-plane force field is given as Table 9-7.

The theoretical force fields show extensive coupling between the ring stretching and bending coordinates, as one would expect for a ring system. Stretching of the N2-O9 bond, internal coordinate 10, couples with stretching of the C1-N2 and N2-O3 bonds, internal coordinates 1 and 2. The asymmetrical ring torsional internal coordinates, 19 and 21, couple with the NO wag coordinates, 22 and 23. The symmetrical ring torsional coordinates, 18 and 20, and the ring-ring torsional motion, internal coordinate 24, do not couple with other internal coordinates.

1,2,3-Oxadiazolo-1,2,3-Oxadiazole-1,1-Dioxide Vibrational Frequencies

Table 9-8 gives the ab initio and Scaled Quantum Mechanical fundamental vibration frequencies and symmetries, frequency assignments, and infrared intensities. The vibrational frequencies were calculated from the appropriate force field by Wilson's GF method [141]. The frequency assignments are based on the main contributors to the M matrix. The molecular C_{2h} symmetry splits the fundamental transitions into 9 A_g, 3 B_g, 4 A_u, and 8 B_u transitions. The A_g and B_g transitions are Raman active, while the A_u and B_u transitions are infrared active. The 1,2,3-oxadiazolo-1,2,3-oxadiazole-1,1-dioxide infrared vibration spectrum, therefore, consists of just 12 fundamental lines. The B_g and A_u transitions are the out-of-plane normal coordinates. Theoretical intensities were calculated from the theoretical dipole moment derivatives and transition integrals. The theoretical intensities suggest the ring-ring torsional transition, at 230 cm^{-1}, may be difficult to observe experimentally. The transitions at 754 cm^{-1} (a NO stretching and ring deformation mode), 1300 cm^{-1} (a CO stretching, NO stretching, and ring deformation mode), and 1364 cm^{-1} (a CN, NN, and CO stretching mode) should be characterized as very strong transitions in the experimental vibrational spectrum.

1,2,3-Oxadiazolo-1,2,3-Oxadiazole-1,1-Dioxide Thermodynamic Functions

Thermodynamic functions for 1,2,3-oxadiazolo-1,2,3-oxadiazole-1,1-dioxide were calculated using the rigid-rotor-harmonic-oscillator approximation and the method outlined in Chapter 2. The inputs for this calculation were the Scaled Quantum Mechanical vibrational frequencies, the rotational constants calculated from the r_e geometry (I_a=3205.34 Mhz, I_b=1226.61 Mhz, and I_c=887.13 Mhz), the molecular weight (143.99 gm/mole), and the rotational symmetry number (2). Table 9-9 gives the specific heat at constant volume (C_v), entropy, free energy, and enthalpy for 1,2,3-oxadiazolo-1,2,3-oxadiazole-1,1-dioxide from 200 K to 1500 K.

The 1,2,3-oxadiazolo-1,2,3-oxadiazole-1,1-dioxide may be calculated with the atomic equivalent method outlined in Chapter 2. The isodesmic reaction method cannot be used because accurate fundamental frequencies are not available for NH_2OH. In this study, the ab initio energy was calculated with the 4-21NO*(P) basis set, E=-591.399426 H, and with the 4-21NO*(D6) basis set, E=-591.416117 H. Subtracting the appropriate atomic equivalents determined in Chapter Five from these energies yields the heat of formation at 298 K. A value of 137 kcal/mole is derived the 4-21NO*(P) energy and a value of 140 kcal/mole is derived from the 4-21NO*(D6) energy. The average value of these two heats of formation was used to calculate E_0. The 298 K heat of formation was corrected to 0 K using the H_0^{298}-E_0 energy calculated from Table 9-9 and the H_0^{298}-E_0 energies for the standard states of carbon, nitrogen, and oxygen, see Table 7-12, to yield the a priori E_0 energy, 142 kcal/mole.

Table 9-1[a]

1,2,3-Oxadiazolo-1,2,3-oxadiazole-1,1-dioxide Geometries

Parameter	Ab initio	r_e[b]
N2-C1	1.400	1.402
N3-N2	1.281	1.298
O4-N3	1.398	1.460
C5-C1	1.304	1.327
C5-N4	1.328	1.336
N6-C5	1.400	1.402
N7-N6	1.281	1.298
O8-C1	1.328	1.336
O8-N7	1.398	1.460
O9-N2	1.219	1.251
O10-N6	1.219	1.251
N3-N2-C1	108.5	108.8
O4-N3-N2	109.1	108.3
C5-C1-N2	105.8	106.8
C5-O4-N3	104.8	104.0
O4-C5-C1	111.9	112.1
N6-C5-C1	105.8	106.8
N6-C5-O4	142.4	141.1
N7-N6-C5	108.5	108.8
O8-C1-N2	142.4	141.1
O8-C1-C5	111.9	112.1
O8-N7-N6	109.1	108.3
N7-O8-C1	104.8	104.0
O9-N2-C1	126.7	126.5
O9-N2-N3	124.8	124.7
O10-N6-C5	126.7	126.5
O10-N6-N7	124.8	124.7

a. Bond lengths in angstroms. Bond angles in degrees. The molecule is planar.

b. Estimated r_e geometry derived from the ab initio geometry.

Table 9-2[a]

Definition of 1,2,3-Oxadiazolo-1,2,3-oxadiazole-1,1-dioxide Internal Coordinates

Q	Definition
1	R(1,2)
2	R(2,3)
3	R(3,4)
4	R(4,5)
5	R(5,1)
6	R(5,6)
7	R(6,7)
8	R(7,8)
9	R(8,1)
10	R(2,9)
11	R(6,10)
12	(2,3,4)+a*[(5,4,3)+(1,2,3)]+b*[(4,5,1)+(5,1,2)]
13	(a-b)*[(5,4,3)-(1,2,3)]+(1-a)*[(4,5,1)-(5,1,2)]
14	(6,7,8)+a*[(1,8,7)+(5,6,7)]+b*[(8,1,5)+(1,5,6)]
15	(a-b)*[(1,8,7)-(5,6,7)]+(1-a)*[(8,1,5)-(1,5,6)]
16	(1,2,9)-(9,2,3)
17	(5,6,10)-(10,6,7)
18	b*[T(2,3,4,5)+T(1,2,3,4)]+a*[T(3,4,5,1)+T(5,1,2,3)] +T(4,5,1,2)
19	(a-b)*[T(5,1,2,3)-T(3,4,5,1)]+(1-a)*[T(1,2,3,4)-T(2,3,4,5)]
20	b*[T(6,7,8,1)+T(5,6,7,8)]+a*[T(7,8,1,5)+T(1,5,6,7)] +T(8,1,5,6)
21	(a-b)*[T(1,5,6,7)-T(7,8,1,5)]+(1-a)*[T(5,6,7,8)-T(6,7,8,1)]
22	D(9,3,1,2)
23	D(10,7,5,6)
24	T(6,5,1,2)-T(4,5,1,8)

a. a = cos(144°). b = cos(72°). T(a,b,c,d) is the angle between the (a,b,c) plane and the (b,c,d) plane. D(a,b,c,d) is the deformation angle between the a,b line segment and the b,c,d plane.

TABLE 9-3[a]

1,2,3 Oxadiazolo-1,2,3-Oxadiazole-1,1-Dioxide AB INITIO IN-PLANE FORCE FIELD

Q	1	2	3	4	5	6	7	8	9	10	11	12	13	14	15	16	17
1	5.904																
2	0.963	7.682															
3	0.054	0.077	3.034														
4	-0.483	0.779	0.329	7.446													
5	0.477	-0.442	0.017	0.550	10.730												
6	0.047	-0.155	-0.080	0.206	0.477	5.904											
7	-0.155	0.164	0.002	-0.154	-0.442	0.963	7.682										
8	-0.080	0.002	0.225	-0.221	0.017	0.054	0.077	3.034									
9	0.206	-0.154	-0.221	0.491	0.550	-0.483	0.779	0.329	7.446								
10	1.037	1.783	0.556	-0.195	-0.240	0.024	0.023	-0.052	0.178	7.200							
11	0.024	0.023	-0.052	0.178	-0.240	1.037	1.783	0.556	-0.195	0.040	7.200						
12	-0.335	0.260	0.196	-0.517	0.298	0.018	0.095	0.062	-0.005	0.219	-0.017	2.252					
13	-0.462	0.246	-0.517	0.683	-0.008	-0.209	-0.002	-0.125	0.180	-0.094	0.053	-0.069	2.025				
14	0.018	0.095	0.062	-0.005	0.298	-0.335	0.260	0.196	-0.517	-0.017	0.219	0.171	0.033	2.252			
15	-0.209	-0.002	-0.125	0.180	-0.008	-0.462	0.246	-0.517	0.683	0.053	-0.094	0.033	-0.345	-0.069	2.025		
16	0.087	-0.287	0.001	0.217	-0.140	-0.028	0.037	0.015	-0.088	0.008	0.016	-0.130	-0.035	0.022	0.011	0.961	
17	-0.028	0.037	0.015	-0.088	-0.139	0.087	-0.287	0.001	0.217	0.016	0.008	0.022	0.011	-0.130	-0.035	0.012	0.961

TABLE 9-4[a]

1,2,3-Oxadiazolo-1,2,3-Oxadiazole-1,1-Dioxide AB INITIO OUT-OF-PLANE FORCE FIELD

Q	18	19	20	21	22	23	24
18	0.322						
19	0.035	0.317					
20	0.086	0.002	0.322				
21	0.002	-0.001	0.035	0.317			
22	-0.099	-0.234	0.004	-0.002	0.894		
23	-0.004	0.002	-0.099	-0.234	0.008	0.894	
24	-0.023	0.067	-0.023	-0.067	0.028	0.028	0.238

[a] Energy in aJ. Coordinates in Å and radians.

Table 9-5

Scale Factors[a]

Q	Scale Factor
1	0.866
2	0.888
3	0.785
4	0.844
5	0.920
6	0.866
7	0.888
8	0.785
9	0.844
10	0.785
11	0.785
12	0.828
13	0.828
14	0.828
15	0.828
16	0.8[b]
17	0.8[b]
18	0.745
19	0.745
20	0.745
21	0.745
22	0.820
23	0.820
24	0.8[b]

a. See Chapter 5 for the derivation of the scale factors.

b. Assumed value.

TABLE 9-6[a]

1,2,3-Oxadiazolo-1,2,3-Oxadiazole-1,1-Dioxide SCALED QUANTUM MECHANICAL IN-PLANE FORCE FIELD

Q	1	2	3	4	5	6	7	8	9	10	11	12	13	14	15	16	17
1	5.113																
2	0.845	6.822															
3	0.045	0.065	2.382														
4	-0.413	0.674	0.267	6.284													
5	0.425	-0.400	0.015	0.485	9.872												
6	0.041	-0.136	-0.066	0.176	0.425	5.113											
7	-0.136	0.146	0.002	-0.134	-0.400	0.0845	6.822										
8	-0.066	0.002	0.176	-0.180	0.015	0.045	0.065	2.382									
9	0.176	-0.134	-0.180	0.414	0.485	-0.413	0.674	0.267	6.284								
10	0.855	1.488	0.437	-0.159	-0.204	0.020	0.019	-0.041	0.145	5.652							
11	0.020	0.019	-0.041	0.145	-0.204	0.855	1.488	0.437	-0.159	0.032	5.652						
12	-0.284	0.223	0.158	-0.432	0.260	0.015	0.081	0.050	-0.005	0.177	-0.014	1.865					
13	-0.391	0.211	-0.417	0.571	-0.007	-0.177	-0.002	*-0.101*	*0.150*	*-0.076*	0.043	-0.057	1.677				
14	0.015	0.081	0.050	-0.005	0.260	-0.284	0.223	0.158	-0.432	-0.014	0.177	0.141	0.028	1.865			
15	-0.177	-0.002	-0.101	0.150	-0.007	-0.391	0.211	-0.417	0.571	0.043	-0.076	0.028	-0.285	-0.057	1.677		
16	0.072	-0.242	0.000	0.179	-0.120	-0.023	0.031	0.012	-0.072	0.006	0.013	-0.106	-0.028	0.018	0.008	0.769	
17	-0.023	0.031	0.012	-0.072	-0.120	0.072	-0.242	0.000	0.179	0.013	0.006	0.018	0.009	-0.106	-0.028	0.010	0.769

TABLE 9-7[a]

1,2,3-Oxadiazolo-1,2,3-Oxadiazole-1,1-Dioxide SCALED QUANTUM MECHANICAL OUT-OF-PLANE FORCE FIELD

Q	18	19	20	21	22	23	24
18	0.240						
19	0.026	0.236					
20	0.064	0.001	0.240				
21	0.001	-0.001	0.026	0.236			
22	-0.077	-0.183	0.003	-0.001	0.733		
23	-0.003	0.001	-0.077	-0.183	0.007	0.733	
24	-0.018	-0.052	-0.018	-0.052	0.023	0.023	0.190

a. Energy in aJ. Coordinates in Å and radian.

TABLE 9-8[a]

FUNDAMENTAL VIBRATIONAL FREQUENCIES FOR

1,2,3-Oxadiazolo-1,2,3-Oxadiazole-1,1-Dioxide

N	AB INITIO FREQUENCY	SQM FREQUENCY	ASSIGNMENT[b]	IR INTENSITY	SYMMETRY
1	150	132	Sym. Ring Tors.	1076	A_u
2	260	230	Ring-Ring Tors.	364	A_u
3	260	236	Sym. Ring Def.	866	B_u
4	371	324	Asym. Ring Tors	0	B_g
5	391	355	NO Rock, CN Stre	0	A_g
6	463	400	Ring Tors.	603	A_u
7	612	539	Ring Tors, NO Wag	0	B_g
8	669	602	NO Stre, Ring Def	0	A_g
9	686	624	Asym Ring Def. NO Rock	13654	B_u
10	687	628	Symm. Ring Def. CN Stre, CO Stre	0	A_g
11	729	652	NO Stre, Ring Def	2345	B_u
12	730	657	NO Wag	2543	A_u
13	819	730	Ring Tors, NO Wag	0	B_g
14	831	736	NO Stre, Ring Def	0	A_g
15	843	754	NO Stre, Ring Def	28171	B_u
16	961	873	CO Stre	0	A_g
17	1147	1046	CN Stre, NO Stre Ring Def	11010	B_u
18	1288	1196	CN Stre, NN stre	7401	B_u
19	1307	1220	NN Stre	0	A_g
20	1414	1277	NO Stre	0	A_g
21	1435	1300	CO Stre, NO Stre Ring Def.	30143	B_u
22	1474	1364	CN Stre, NN Stre CO Stre	38704	B_u
23	1588	1467	CN Stre, CO Stre	0	A_g
24	1840	1746	CC Stre	0	A_g

a. Frequencies in cm^{-1}. Intensities in cm/mmole.

b. Assignments reflect the primary contributions to the M matrix and may not correspond to the experimental assignment.

Table 9-9

Thermodynamic Functions for

1,2,3-Oxadiazolo-1,2,3-Oxadiazole-1,1-dioxide

T[a]	C_v[b]	Entropy[b]	$-(G_0-E_0)/T$[b]	$(H_0-E_0)/T$[b]
200	18.49	72.47	59.68	12.79
300	26.32	82.30	65.60	16.70
400	32.54	91.33	70.92	20.41
500	37.25	99.57	75.84	23.73
600	40.74	107.0	80.43	26.62
700	43.33	113.8	84.73	29.11
800	45.27	120.0	88.76	31.27
900	46.74	125.7	92.55	33.13
1000	47.87	130.9	96.13	34.75
1100	48.75	135.7	99.50	36.16
1200	49.46	140.1	102.7	37.41
1300	50.03	144.3	105.7	38.51
1400	50.49	148.1	108.6	39.49
1500	50.87	151.8	111.4	40.37

a. Temperature in degrees Kelvin.

b. Units equal to cal/mole/K.

Figure 9-1
Atom Numbering Scheme

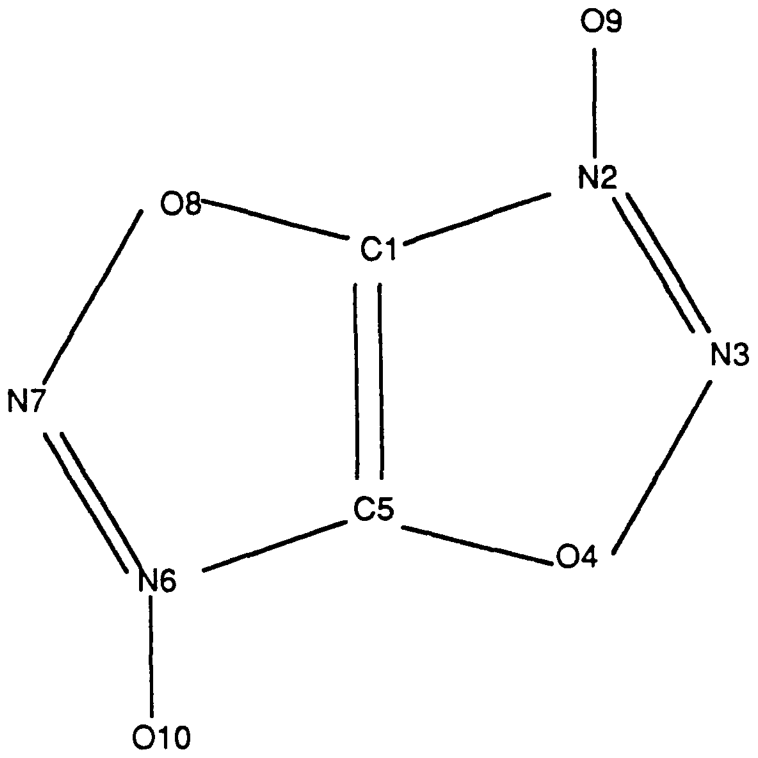
O9
N2
O8
C1
N3
N7
C5
O4
N6
O10

CHAPTER TEN

CONCLUDING REMARKS

The focus of this work has been the development and validation of a method for calculating a priori thermodynamic functions. Empirical formulae to correct a 4-21NO* ab initio geometry to an approximation of the r_e geometry were developed from carefully selected experimental data and the corresponding theoretical data. Force field scale factors and atomic energy equivalents were developed in a similar manner. The various correction formulae correct the ab initio data for errors caused by truncation of the basis set and the neglect of electron correlation.

The corrected vibrational frequencies are usually within 15 cm^{-1} of the corresponding experimental frequency [5]. A priori thermodynamic functions are calculated with standard statistical mechanical methods using the Scaled Quantum Mechanical vibration frequencies, rotational constants calculated from the r_e geometry, and molecular weight as input and applying the rigid rotor harmonic oscillator approximation. The a priori thermodynamic functions are compatible with current tabulations of thermodynamic functions and should have an accuracy comparable to experimentally derived thermodynamic functions that employ the rigid rotor harmonic oscillator approximation. The entropy and specific heat should be determined to an accuracy of ±2 per cent and the free energy and enthalpy should be determined to an accuracy of ±5 kcal/mole. The a priori thermodynamic functions are, in general, easier to determine than thermodynamic functions derived from experimental methods. In particular, the fundamental vibration frequencies are unambiguously assigned, eliminating a potential source of gross errors.

From a theoretical point of view this approach is not entirely satisfactory. Using correction formulae derived from experimental data to empirically correct ab initio geometries and force fields is somewhat arbitrary and one would prefer solving the problem only with theoretical methods and data. This type of approach requires large basis sets, 6-31G** or larger, and inclusion of electron correlation effects at a minimum level equivalent to MP4 [18, 19]. The cost associated with calculations of this sophistication is prohibitively expensive for molecules containing more than about ten second row atoms, assuming the molecule is asymmetric. The more pragmatic approach adopted in this work permits the study of larger molecules.

COMPUTATIONAL REMARKS

During the course of this work, the ab initio gradient program TEXAS was modified to execute on the CRAY XMP supercomputer. Execution speed was increased by 30 to 50 per cent by vectorizing sections of the integral and force packages, but the resulting program still did not take full advantage of the CRAY environment. Further execution speed increases for the TEXAS program will be difficult to obtain because the program structure is optimized for the scalar processing environment and is not amenable to multitasking. Obtaining maximum performance from scalar and vector computers will probably require the development of two different classes of ab initio gradient programs; one optimized for the scalar environment and the other optimized for the vector and multitasking environment. This approach will tend to limit the portability of the resulting programs, but using standard mathematical libraries, e.g. IMSLIB, optimized for a specific computer can ameliorate this problem.

The programming efforts conducted during this work identified three major areas of concern. The availability of computer memory no longer appears to be a major constraint on the development of new ab initio gradient codes. Matrices should, therefore, be written in full form, increasing memory requirements, but allowing more efficient vectorization. The method for calculating electron repulsion integrals should be revisited. The Rys polynomial method [46, 47, and 48] is extremely efficient in the scalar environment, particularly for high angular momentum functions, but the method's recursion structure prevents efficient vectorization of the algorithm. A major constraint on the maximum size of an ab initio calculation is the length of the largest disk file that can be created on any given system, which imposes an upper bound to number of integrals that can be stored. Almlöf has developed an efficient method for recalculating electron integrals as they are needed during the SCF calculation [51] eliminating the requirement for disk storage of the integrals and this permits the completion of very large calculations. Developing an efficient multitasking vectorized ab initio gradient code that eliminates disk storage of integrals is necessary if one is going to significantly increase the size of molecular systems that can be studied with ab initio methods.

TOPICS FOR FURTHER STUDY

As the final part of this work, it is appropriate to identify areas for further study that will extend or complement this work. Geometry correction formulae and force field scale factors should be calculated for the more widely used 3-21G and 6-31G* basis sets. The causes of the differences between the MNDO and ab initio N-methyl-hydroxy-hydroxyl-amine structures should be studied more carefully. The two methods should produce roughly similar structures, i.e. the torsion and bond angles should agree to within a few degrees, not structures that are completely different. Studies of large flexible molecules require a fast method for examining a large number of different conformations and then selecting a small number of the most stable structures, perhaps no more than four, that span the equilibrium geometry for additional study with more sophisticated theoretical methods. Molecular mechanics, semi-empirical calculations, or minimal basis set ab initio calculations may be able to meet this requirement, but the N-methyl-hydroxy-hydroxyl-amine results clearly show that further study is required to identify the most effective method.

The discrepancies between experimental and ab initio rotational potential functions and the corresponding energy levels merits further study. Hopefully, a simple correction scheme similar to the scale factors adopted in the Scale Quantum Mechanical force field formalism can be developed to correct the deficiencies that appear to be present in ab initio rotational potential functions.

Finally, the method of calculating a priori thermodynamic functions developed in this work should be extended to include anharmonic vibrational effects and centrifugal distortion effects. Including correction terms for these two effects should provide a priori thermodynamic functions that show much closer agreement with experimentally derived thermodynamic functions, particularly at high temperatures, by correcting two of the primary breakdowns in the rigid rotor harmonic oscillator approximation.

BIBLIOGRAPHY

1. F. Daniels and R. A. Alberty, PHYSICAL CHEMISTRY, Fourth Edition. John Wiley and Sons, New York, 1975.

2. D. A. McQuarrie, STATISTICAL MECHANICS. Harper and Row, New York, 1976.

3. D. R. Stull and H. Prophet, JANAF THERMOCHEMICAL TABLES, NBS-37, 1982.

4. G. Fogarasi and P. Pulay, "Ab Initio Calculation of Force Fields and Vibrational Spectra" in Vibrational Spectra and Structure, vol. 14, Ed. J. R. Durig, Elsevier Science Publishers, Amsterdam, 1985.

5. D. R. Stull, E. F. Westrum, Jr. and G. C. Sinke, THE CHEMICAL THERMODYNAMICS OF ORGANIC COMPOUNDS, John Wiley and Sons, New York, 1969.

6. See Thermodynamic Tables compiled in J. Phys. Chem. Ref. Data by numerous authors.

7. N. R. Davidson, STATISTICAL MECHANICS, McGraw-Hill Book Company, Inc. New York, 1962.

8. R. C. Tolman, THE PRINCIPLES OF STATISTICAL MECHANICS, Oxford University Press, London, 1938.

9. A. Szabo and N. S. Ostlund. MODERN QUANTUM CHEMISTRY: INTRODUCTION to ADVANCED ELECTRONIC STRUCTURE THEORY. MacMillan Publishing Co., New York.

10. W. J. Hehre, L. Radom, P. v. R. Schleyer and J. A. Pople, AB INITIO MOLECULAR ORBITAL THEORY, John Wiley and Sons, New York, 1986.

11. C. E. Blom and C. Altona, Mol. Phys. 1377 (31) 1976.

12. P. W. Atkins. MOLECULAR QUANTUM MECHANICS (Second Ed.), Oxford University Press, London.

13. H. C. Allen, Jr. and P. C. Cross. MOLECULAR VIB-ROTORS, John Wiley and Sons, New York, 1963.

14. C. H. Townes and A. L. Schalow, MICROWAVE SPECTROSCOPY, McGraw-Hill Book Co., Inc., New York, 1955.

15. I. N. Levine, MOLECULAR SPECTROSCOPY, John Wiley and Sons, New York, 1975.

16. Levine, J. Chem. Ed., 53 (62) 1985.

17. K. Dunn, Doctoral Dissertation, The University of Texas at Austin, 1986.

18. Y. Xie, Doctoral Dissertation, The University of Texas at Austin, 1988.

19. P. Pulay, G. Fogarsi, G. Pongor, J. E. Boggs and A. Vargha. J. Am. Chem. Soc. 7037 (105) 1983.

20. P. Pulay and F. Torok, Mol. Phys., 1153 (25) 1973.

21. M. J. S. Dewar and W. Thiel, J. Amer. Chem. Soc., 4899 and 4907, (99) 1977.

22. M. J. S. Dewar, G. P. Ford, M. L. McKee, H. S. Rzepa, W. Thiel, and Y. Yamaguchi, J. Mol. Struct., 135 (43) 1978..

23. J. E. Boggs and F. R. Cordell, J. Mol Struct. (Theochem), 329 (78) 1981.

24. P. Pulay, G. Fogarasi, F. Pang and J. E. Boggs, J. Am. Chem. Soc., 2550 (101) 1979.

25. J. S. Binkley, J. A. Pople, and W. J. Hehre, J. Amer. Chem. Soc., 939 (102) 1980.

26. J. E. Boggs, J. Mol. Struct. 1 (97) 1983.

27. F. R. Cordell, Masters Thesis, The University of Texas at Austin, 1987.

28. G. Pfafferott, H. Oberhammer, and J. E. Boggs, J. Amer. Chem. Soc. 2305 (107) 1985.

29. P. Pulay, Theoret. Chim. Acta (Berl.) 299 (50) 1979.

30. W. J. Hehre, R. Ditchfield and J. A. Pople, J. Chem. Phys., 2257 (56) 1972.

31. P. Pulay. "Direct Use of the Gradient for Investigating Molecular Energy Surfaces" in APPLICATIONS OF ELECTRONIC STRUCTURE THEORY, Modern Theoretical Chemistry Vol 4. Ed. H. F. Schaefer III. Plenum Press, New York, 1977.

32. H. Millendal, MB06 FORTRAN PROGRAM, University of Oslo, Norway..

33. H. Schlegel, S. Wolfe and F. Bernardi, J. Chem. Phys., 4181 (67) 1977.

34. E. B. Wilson, Jr., J. C. Decius, and P. C. Cross, MOLECULAR VIBRATIONS "The Theory of Infrared and Raman Spectra", McGraw-Hill Book Company, N.Y. 1955.

35. G. Banhegyi, G. Fogarasi and P. Pulay, J. Mol. Struct. 1 (89) 1982.

36. G. Banhegyi, P. Pulay and G. Fogarasi, Spectrochim. Acta, 761 (39A) 1983.

37. H. Sellers, P. Pulay and J. E. Boggs, J. Am. Chem. Soc. 6487 (107) 1985.

38. P. Pulay and W. Sawodny, J. Mol. Spectrosc. 150 (26) 1968.

39. W. J. Hehre, R. Ditchfield, L. Radom and J. A. Pople, J. Amer. Chem. Soc., 4796 (92) 1970.

40. K. B. Wiberg, J. Comp. Chem., 197 (5) 1984.

41. M. R. Ibrahim and P. R. Schleyer, J. Comp. Chem., 157 (6) 1985.

42. J. E. Boggs, M. Altman, F. R. Cordell and Y. Dai, J. Mol. Struct. (THEOCHEM), 373 (94) 1983.

43. W. Gordy and R. L. Cook, MICROWAVE MOLECULAR SPECTRA, TECHNIQUE OF ORGANIC CHEMISTRY, Vol. 9, A. Weissberger Ed., Wiley-Interscience, NY, 1970.

44. P. Pulay, G. Fogarasi and J. E. Boggs. J. Chem. Phys. 3999 (74) 1981.

45. L. Schafer, C. Van Alsenoy and J. N. Scarsdale. J. Mol. Struct. (Theochem) 349 (86) 1982.

46. S. A. Clough, Y. Beers, G. P. Klein and L. S. Rothman, J. Chem. Phys. 2254 (59) 1973.

47. J. D. Swalen and J. A. Ibers, J. Chem. Phys., 1914 (36) 1962.

48. G. Fogarasi and P. Pulay, Ann. Rev. Phys. Chem., 191 (35) 1984.

49. G. Pongor, P. Pulay, G. Fogarasi and J. E. Boggs, J. Am. Chem. Soc., 2765 (106) 1984.

50. H. Sellers, P. Pulay and J. E. Boggs, J. Am. Chem. Soc., 6487 (107) 1985.

51. K. Fan and J. E. Boggs, J. Mol. Struct. (Theochem), 401 (138) 1986.

52. M. C. L. Gerry, R. M. Lees and G. Winnewisser, J. Mol. Spectrosc., 231 (61) 1976.

53. A. Serrallach, R. Meyer and Hs. H. Gunthard, 28th Symposium on Molecular Structure and Spectroscopy 1973, paper Z 10.

54. K. Takagi and T. Kohma, J. Phys. Soc. Jpn., 1145 (30) 1971.

55. A. Yamaguchi, J. Chem. Soc. Japan, 1105 (80) 1959.

56. E. L. Wu, G. Zerbi, S. Califano and B. Crawford, Jr., J. Chem. Phys., 2060 (35) 1961.

57. G. Dellepiane and G. Zerbi, J. Chem. Phys., 3573 (48) 1968.

58. A. P. Gray and R. C. Lord, J. Chem. Phys., 690 (26) 1957.

59. A. Y. Hirakawa, M. Tsuboi and T. Shimanouchi, J. Chem. Phys., 1236 (57) 1972.

60. J. R. Durig, S. F. Bush and F. G. Baglin, J. Chem. Phys., 2106 (49) 1968.

61. C. J. Purnell, A. J. Barnes, S. Suzuki, O. F. Ball and W. J. Orville-Thomas, Chem. Phys. 77 (12) 1976.

62. J. E. Stewart, J. Chem. Phys., 1259 (30) 1959.

63. H. Wolff and H. Ludwig, Ber. Bunsenges. Phys. Chem. 474 (70) 1966.

64. P. Pulay and F. Torok, J. Mol. Struct. 239 (29) 1975.

65. Y. Hamada, N. Tanaka, Y. Sugawara, A. Y. Hirakawa and M. Tsuboi, J. Mol. Spectrosc. 313 (96) 1982.

66. E. Tannenbaum, R. J. Myers and W. D. Gwinn, J. Chem. Phys., 42 (25) 1956.

67. D. C. McKean and R. A. Watt, J. Mol. Spectrosc. 184 (61) 1976.

68. K. I. Rezchikova and V. A. Shlyapochnikov, Izvest. Akad. Nauk SSSR, Ser. Khim., 947 (4) 1985.

69. M. L. McKee, J. Am. Chem. Soc., 1900 (107) 1985.

70. C. W. Bock, S. V. Krasnoshchiokov, L. V. Khristenko, Y. N. Panchenko and Yu. A. Pentin, J. Mol. Struct. (Theochem) 1986.

71. A. P. Cox and J. M. Riveros, J. Chem. Phys., 3106 (42) 1965.

72. G. E. McGraw, D. L. Bernitt and I. C. Hisatsune, J. Chem. Phys., 237 (42) 1965.

73. A. Palm, A. Castelli and C. Alexander, Spectrochim. Acta Part A, 1658 (24) 1968.

74. P. N. Ghosh, C. E. Blom and A. Bauder, J. Mol. Spectrosc., 159 (89) 1981.

75. L. Nygaard, D. Christen, J. T. Nielsen, E. J. Pedersen, O. Snerling, E. Vestergaard and G. O. Sorensen, J. Mol. Struct., 401 (22) 1974.

76. A. Zecchina, L. Cerruti, S. Coluccia and E. Borello, J. Chem. Soc., B: 1363 (1967).

77. S. T. King, J. Phys. Chem., 2133 (74) 1970.

78. D. Cremer, J. Comp. Chem., 165 (3) 1982.

79. F. D. Rossini, K. S. Pitzer, R. L. Arnett, R. M. Braun and G. C. Pimentel, SELECTED VALUES OF PHYSICAL AND THERMODYNAMIC PROPERTIES OF HYDROCARBONS AND RELATED COMPOUNDS, Carnegie Press, Pittsburgh, PA, 1953.

80. S. S. Chen, S. A. Kudchadker and R. C. Wilhoit, J. Phys. Chem. Ref. Data, 527 (8) 1979.

81. J. Lielmezs, F. Bennett Jr. and D. G. McFee, Termochimica Acta, 287 (47) 1981.

82. Y. Yamaguchi and H. F. Schaefer III, J. Chem. Phys., 2310 (73) 1980.

83. W. S. Benedict, N. Gailar and E. K. Pylar, J. Chem. Phys., 1139 (24) 1956.

84. M. G. Bucknell and N. C. Handy, Mol. Phys., 777 (28) 1974.

85. J. D. Cox and G. Pilcher, THERMOCHEMISTRY OF ORGANIC AND ORGANOMETALLIC COMPOUNDS, Academic Press, London and New York, 1970.

86. D. B. Scully and D. H. Whiffen, Spectro chim. Acta, 1409 (16) 1960.

87. D. E. Freeman and I. G. Ross, Spectrochim. Acta, 1393 (16) 1960.

88. J. R. Scherer, J. Chem. Phys., 3308 (36) 1962.

89. E. P. Krainov, Opt. Spectrosc., 415 (16) 1964.

90. N. Neto, M. Scrocco and S. Califano, Spectrochm. Acta, 1981 (22) 1966.

91. G. Hagen and S. J. Cyvin, J. Chem. Phys., 1446 (72) 1968.

92. K. H. Michaelian and S. M. Ziegler, Appl. Spectrosc., 13 (27) 1973.

93. A. L. McClellan and G. C. Pimentel, J. Chem. Phys., 245 (23) 1955.

94. R. P. Sharma and R. S. Singh, Ind. J. Appl. Phys., 618 (11) 1973.

95. M Suzuki, T. Yokoyama and M. Ito, Spectrochim. Acta, Part A, 1091 (24) 1968.

96. D. M. Hanson and A. R. Gee, J. Chem. Phys., 5052 (51) 1969.

97. F. Stenman, J. Chem. Phys., 4217 (54) 1971.

98. A. Karonen, J. Rasanen and F. Stenman, Commentat. Phys. Math. Soc. Sci. Fenn., 69 (46) 1976.

99. A. Karonen and F. Stenman, Commentat. Phys. Math. Soc. Sci. Fenn., 85 (46) 1976.

100. F. M. Behlen, D. B. McDonald, B. Sethuraman and S. A. Rice, J. Chem. Phys., 5685 (75) 1981.

101. N. Rich and D. Dows, Mol. Cryst. Liq. Cryst., 111 (5) 1968.

102. K. Ohno, J. Mol. Spectrosc., 238 (72) 1978.

103. G. M. Barrow, and A. L. McClellan, J. Amer. Chem. Soc, 573 (73) 1951.

104. G. A. Miller, J. Chem. Eng. Data, 69 (8) 1963.

105. A. A. Vedneskii and D. M. Maiorov, J. Gen. Chem. USSR, 2106 (27) 1957.

106. G. C. Sinke, J. Chem. Thermodyn. 311 (6) 1974.

107. H. Sellers and J. E. Boggs, J. Mol. Struct., 137 (74) 1981.

108. S. N. Ketkar and M. Fink, J. Mol. Struct., 139 (77) 1981.

109. R. D. Bardo and W. H. Jones, "A Theoretical Calculation of the 0 K Isotherm for Shocked Nitromethane," in Shock Waves in Condensed Matter - 1983, J. R. Asay, et al., Eds., Elsevier, Chapter XIII:4.

110. R. H. Guirguis, "Investigation of the Thermal Initiation of Detonation in Nitromethane," NRL Rpt. J206-83-011/6223, October 21, 1983.

111. D. R. Hardesty, Comb. and Flame, 229 (27) 1976.

112. D. L. Omellas, "Calorimetric Determinations of the Heat and Products of Detonation for Explosives: October 1961 to April 1982," LLNL Rpt. UCRL-52821, April 5, 1982, pp. 55.

113. A. W. Campbell, W. C. Davis, and J. R. Travis, Phys. Fluids, 498 (4) 1961.

114. F. E. Walker and R. J. Wasley, Comb. and Flame, 233 (15) 1970.

115. J. W. Nunziato, J. e. Kennedy, and D. R. Hardesty, "Modes of Shock Wave Growth in the Initiation of Explosives," Proceedings Sixth Symposium (Int.) on Detonation, Office of Naval Research, ACR-221, p. 47, 1976.

116. R. D. Bardo, "Rate-Determining Steps for Ignition of Shocked Nitromethane," Shock Waves in Condensed Matter, Y. M. Gupta, Ed., pg. 843, Plenum Press, New York, 1986.

117. R. D. Bardo, "Calculated Reaction Pathways for Nitromethane and Their Role in the Shock Initiation Process," PROCEEDINGS OF THE EIGHTH SYMPOSIUM (INT) ON DETONATION, Office of Naval Research, Washington, D.C.

118. S. J. Cole, K. Szalewicz, and R. J. Bartlett, Int. J. Quantum Chem. Symp., 217 (19) 1985.

119. S. J. Cole, K. Szalewicz, G. D. Purvis III, and R. J. Bartlett, J. Chem. Phys. 6833 (84) 1986.

120. J. N. Macdonald, C. Plant, Private communication.

121. J. M. Short, Private communication.

122. W. M. Koppes, M. Chaykovsky, H. G. Adolph, R. Gilardi, and C. George, J. Org. Chem., 1113 (52) 1987.

123. R. Gilardi and C. George, ONR Annual Report, Oct 1, 1983 to Oct 1, 1984. Laboratory for the Structure of Matter, Code 6030, The Naval Research Labratory, Washington D.C. 20375.

124. R. Gilardi, C. George, and J. L. Flippen-Anderson, ONR Annual Report, Oct 1, 1983 to Oct 1, 1984. Laboratory for the Structure of Matter, Code 6030, The Naval Research Labratory, Washington D.C. 20375.

125. S. F. Boys, , in P. O. Lowdin (Ed.), Quantum Theory of Atoms, Molecules and the Solid State, Academic Press, 1968, pp. 253-262.

126. H. F. King and M. Dupuis, J. Comp. Phys. 144 (21) 1976.

127. J. Rys, M. Dupuis, and H. F. King, J. Comp. Chem. 154 (4) 1983.

128. J. Almlöf, K. Faegri, Jr. and K. Korsell, J. Computat. Chem., 385 (3) 1982.

VITA

Floyd Richard Cordell was born Floyd Richard Bull in Wiesbaden, West Germany on December 5, 1958. His mother, Roberta Diane Adams, married Glenn Alwin Cordell on May 2, 1964. As an Army Brat, he attended several different elementary, junior high, and high schools. He graduated from Mary Carroll High School, Corpus Christi, Texas in May 1976. He entered the University of Texas at Austin in August 1976 and graduated with Special Honors in August 1980 with a Bachelor of Science degree in Chemistry. Coincident with his graduation, he was commissioned an Ensign in the United States Navy.

Ensign Cordell was ordered to the Naval Aviation Schools Command for Naval Flight Officer training and subsequently received orders to Training Squadron Ten and Training Squadron Eighty-Six. He was awarded his "Wings" September 30, 1981 and was the highest rated graduate during Fiscal Year 1981.

Ensign Cordell was ordered to Attack Squadron One Two Eight for graduate level training in the A-6E Intruder. He completed the syllabus in October 1982 and was ordered to *Attack Squadron One Nine Six.* In July 1983 LT(jg) Cordell was selected as the 1983 "Student B/N of the Year" for his performance while onboard VA-128. While assigned to VA-196, LT Cordell completed a World Cruise onboard USS Coral Sea (CV-43) and an Indian Ocean Cruise onboard USS Constellation (CV-64).

In August 1985, LT Cordell was ordered to the University of Texas at Austin and entered the Graduate School. He received his Master of Arts degree in Chemistry in August 1987. LT Cordell returned to VA-128 for refresher training in the A-6E and in January 1988 reported to the Swordsmen of Attack Squadron One Four Five. On January 22, 1990, LCDR Cordell joined the Martin Baker Silk Tie Club. While assigned to VA-145, he completed an Indian Ocean Cruise onboard USS Ranger (CV-61) and was awarded the Navy Achievement Medal for his work during the introduction of the Systems Weapons Improvement Program (SWIP) version of the A-6E.

In May 1990, LCDR Cordell was ordered to the Naval Air Systems Command as the A-12 Avenger Assistant Class Desk Officer. During this assignment, he completed the requirements for the Doctor of Philosophy Degree in Physical Chemistry, much to the relief of his wife, and finally graduated from the University of Texas in August 1991. In November 1991 LCDR Cordell will return to VA-128 for refresher training in the Intruder and will subsequently receive orders to a Fleet Squadron. LCDR Cordell has accumulated 1850 flight hours and 501 carrier arrested landings in the Intruder.

Floyd Cordell married Sandra Lou Blalock on March 17, 1978. They have two daughters, Rebecca, born October 20, 1981 and Elizabeth, born October 4, 1983.

Permanent address: 5037 Cascade Drive
Corpus Christi, Texas
78413

This dissertation was typed by the author.